

**The University of
Nottingham**

Division of Drug Delivery and Tissue Engineering
School of Pharmacy

**Supercritical Fluid Technology for
Gastroretentive Formulations**

Elizabeth Hannah Ahmed
BSc (Hons)

**Thesis submitted to the University of Nottingham for
the degree of Doctor of Philosophy**

September 2012

Abstract

The oral route for drug administration offers an efficient and convenient method for drug delivery. However, there is an assortment of drugs which exhibit narrow absorption windows in the upper small intestine and as a result demonstrate limited bioavailabilities. One approach in the improvement of bioavailability in these cases is to retain the delivery system proximal to the absorption window for a prolonged period of time. Although controlled release products are widely available on the market, marketed gastroretentive systems remain elusive.

This work explores the manufacture and characterisation of a multi-unit gastroretentive system utilising the biocompatible polymer poly (lactic-co-glycolic acid). The novel PGSS technique enables the production of PLGA particles whilst omitting the use of volatile organic solvents. Morphological and microCT analyses of the particles revealed a highly porous matrix with porosity values in the order of 30-40%. The relationship between porosity, density and *in vitro* floating ability for particles with sizes between 100-2000 μm revealed that particle size plays an important role; larger microparticles possess decreased density, higher porosity and increased buoyancy.

Encapsulation of two model drugs, riboflavin and furosemide, was carried out during the processing step with high encapsulation efficiencies (80-100%) being revealed. Release of the drugs in PBS (pH7.4) was found to be sustained over a period of 24 hours with a decrease in cumulative release in simulated

gastric fluid (pH1.2). The introduction of the hydrophilic polymer poly (ethylene glycol) was found to modulate release rate; PEG with a molecular weight ≥ 3 KDa increased the rate of release in PBS media up to 20% over 24 hrs, however this was not observed for release in SGF. A comparison of morphology prior to and following exposure to the release media confirms that the emergence of intricate porous channels on exposure to the release medium is related to an increase in release rate.

In order to augment the gastroretentive potential of the system the mucoadhesive polymer, chitosan was incorporated both as a post processing surface modification and as part of the initial formulation. ToF-SIMS surface analysis confirmed the presence of chitosan at the surface of the particles in both cases. Initially the potential for the particles to interact with mucus was evaluated utilising *in vitro* tests. The presence of chitosan significantly improved adsorption of mucin to particles, as well as enhancing adhesion of particles to a mucus producing epithelial cell layer. The thiolated chitosan derivative chitosan-*N*-acetyl-cysteine demonstrated an increase in adhesion of mucin solution; however the modified chitosan resulted in a decrease in adhesion to a mucus producing cell line which was considered to be a result of the mucolytic actions it may exert on the mucus layer.

Oral administration of buoyant particles to a rat model improved the pharmacokinetics of the anti-hypoglycaemia drug metformin, with addition of mucoadhesive properties providing further improvement. This study demonstrates that introduction of buoyancy and mucoadhesion functionalities to particles prepared by the PGSS method could improve delivery of drugs demonstrating narrow absorption windows in the upper small intestine.

Acknowledgements

During the completion of the work presented in this thesis I have incurred the debt of many people, I would like to express the greatest gratitude to all the individuals who have contributed to this work.

Firstly, I would like to offer my sincere gratitude to my supervisors, Dr Snow Stolnik and Dr Andy Lewis for offering me this opportunity and whose support, advice and guidance. Their wisdom and enthusiasm for the project has been a great encouragement throughout. I would like to thank both my supervisors for providing me with the freedom to explore the project in my own way. I would also like to extend my appreciation to my internal assessor Dr Martin Garnett for his professional opinions and advice.

Special thanks must be given to the technical staff at the university, in particular Christine Grainger-Boulby for her expertise in SEM and for kindly answering my incessant questions, her help went a long way to ensuring (as much as possible) this journey was as smooth as possible. Also, Theresa Marshall for her assistance with the time-lapse microscope, and Sue Dodson for help with the X-ray microtomography.

I want to offer my appreciation for the professional advice of Dave Scurr without whom ToF-SIMS analysis would no doubt still remain a complex mystery. The contributions of Luca Casettari have proven invaluable in my understanding of the chemistry presented in Chapter 6.

To the staff at Critical pharmaceuticals I thank for the patience and advice throughout my PhD. Faron Jordan, and Kirk Jeffries for their time and efforts with the *in vivo* investigations and help with the pharmacokinetic analysis, and Tamsin Gamble and Clare Upton for training and their continued support on the high pressure equipment. The help of all the staff has been invaluable towards the completion of this project.

The key to surviving the PhD process is a supportive network of friends and I have been extraordinarily fortunate to have found life-long friends among my colleagues in Boots Science Building. These people have shared not only their help and advice throughout my PhD but also provided moral support, and an understanding ear which went a long way during the more difficult times. In particular I would like to thank Robyn, Jennie, Driton, Manali, Emilia, and Dimitra, and all the members of D19 not least for providing a means for procrastination.

I would like to express my particular appreciation to Paulina Cygan who is always there when I am in need of advice (or a beer) and for being there to share my woes during the final weeks. For all the good times (and the introduction to GTL) I would like to thank Martin Redhead. Meera Vijay and Marie Warren have been indispensable in their help with the PGSS work, not to mention the memorable Christmas parties.

Although there have been times when it seems just a fantasy, for reminding me of a life beyond my PhD I wish to thank those people who have been in the background for many years and hopefully for many years to come.

To Ruth, for her 'kindness, patience, and understanding' during my write up period, and for remaining 'calm' when I was incapable of social interaction.

The past year was made all the more endurable as a result of her support, the red wine, and so much decorating there were times when this thesis was (almost) a distant memory. My fellow pack members, Alfie and Frankie, I thank for providing entertainment when writing was driving me to the brink of sanity.

I have been blessed with a large and supportive family who have always been there for me; it is their love, kindness, and support that have helped me along the long, but fulfilling path to completion of this thesis. There are no words to express my gratitude to my parents Sally and Brian and my sister Sarah who have supported me selflessly throughout my university studies, not to mention helping move my stuff across most of the country and between count-less addresses! They have been a source of encouragement and inspiration as well as providing emotional, and at times financial, support when I needed it most, this thesis would not exist without them.

Table of Contents

Abstract.....	i
Acknowledgements.....	iii
Table of Contents.....	vi
List of Figures.....	xv
List of Tables.....	xxii
Abbreviations.....	xxiii

Chapter 1: Introduction

1.1	Oral Drug Delivery.....	1
1.2	The Gastrointestinal Tract.....	2
1.2.1	Structure and Function.....	3
1.2.1.1	The Oesophagus.....	4
1.2.1.2	The Stomach.....	4
1.2.1.3	The Small Intestine.....	8
1.2.1.4	The Large Intestine.....	10
1.2.2	Physiological Barriers to Oral Delivery.....	10
1.2.2.1	pH.....	10
1.2.2.2	Gastric Motility.....	13
1.2.2.3	Absorption Windows.....	15
1.3	Controlled Release Systems.....	16
1.4	Gastroretention.....	17
1.4.1	Overview.....	17
1.4.2	Expanding Systems.....	18

1.4.3	Mucoadhesive Systems.....	19
1.4.4	High Density Systems.....	22
1.4.5	Floating Systems.....	23
1.4.5.1	Effervescent.....	23
1.4.5.2	Non-effervescent.....	25
1.5	Methods for Particle Production.....	26
1.5.1	Conventional Methods for Particle Production.....	26
1.5.2	Supercritical Fluid Technology.....	28
1.5.2.1	Supercritical Carbon Dioxide Technology.....	28
1.5.2.2	Rapid Expansion of Supercritical Solutions Method.....	32
1.5.2.3	Gas Anti-Solvent Method.....	34
1.5.2.4	Supercritical Anti-Solvent Method.....	35
1.5.2.5	Solution Enhanced Dispersion by Supercritical Fluids Method.....	36
1.5.2.6	Particles from Gas Saturated Solutions (PGSS) Method.....	36
1.6	Project Aims.....	38
1.7	References.....	39

Chapter 2: Experimental Methods

2.1	Particles from Gas Saturated Solutions (PGSS) Method.....	52
2.2	Scanning Electron Microscopy.....	55
2.3	X-ray microtomography.....	55
2.4	Fluorescent Microscopy.....	56
2.5	Particle Size Analysis.....	57

2.6	Helium Air Pycnometry.....	58
2.7	<i>In vitro</i> Buoyancy Analysis of Porous Particles.....	59
2.8	Differential Scanning Calorimetry.....	59
2.9	Determination of Drug Encapsulation Efficiency.....	61
2.10	Preparation of Simulated Gastric Fluid.....	62
2.11	Drug Release Studies.....	62
2.12	Time of Flight Secondary Ion Mass Spectrometry (ToF-SIMS).....	63
2.13	Depth Profiling.....	64
2.14	References.....	65

Chapter 3: Particle Manufacture and Optimisation for

Gastroretention

3.1	Introduction.....	67
3.2	Materials and Methods.....	71
3.2.1	Materials.....	71
3.2.2	Methods.....	72
3.2.2.1	Particle Production.....	72
3.2.2.2	Scanning Electron Microscopy.....	72
3.2.2.3	Particle Size Analysis.....	72
3.2.2.4	Helium Air Pycnometry.....	72
3.2.2.5	<i>In vitro</i> Buoyancy Analysis.....	73
3.2.2.6	X-ray Microtomography.....	73
3.3	Results.....	73
3.3.1	Effect of Myristic Acid Content on Particle Morphology.....	73

3.3.2	Effect of Myristic Acid Content on Gastroretentive Potential.....	77
3.3.3	Changing Formulation.....	78
3.3.4	Effect of Particle Size on Potential Gastroretentive Behaviour.....	80
3.4	Discussion.....	83
3.5	Conclusions.....	89
3.6	References.....	90

Chapter 4: Incorporation of Active Pharmaceutical Ingredient into Particles Produced using the PGSS Method

4.1	Introduction.....	93
4.2	Materials and Methods.....	99
4.2.1	Materials.....	99
4.2.2	Methods.....	99
4.2.2.1	Incorporation of Active Pharmaceutical Ingredient into Particulate Formulation.....	99
4.2.2.2	Encapsulation Efficiency and <i>In vitro</i> Drug Release.....	100
4.2.2.3	Time-of-Flight Secondary Ion Mass Spectrometry.....	100
4.2.2.4	Scanning Electron Microscopy.....	100
4.2.2.5	Freeze Drying of Particles.....	100
4.2.2.6	X-ray Microtomography.....	100
4.2.2.7	Differential Scanning Calorimetry.....	101

4.3	Results.....	101
4.3.1	Encapsulation of Active Pharmaceutical Ingredients.....	101
4.3.2	Surface Analysis of Drug Loaded Particles.....	102
4.3.3	Release Profile of Furosemide and Riboflavin from Different Size PLGA Particles in PBS Medium at pH 7.4.....	104
4.3.4	Release Profile of Riboflavin and Furosemide from Different Sized Particle Fractions in SGF Medium at pH 1.2.....	107
4.3.5	Morphology of Particles Following Exposure to Release Media.....	109
4.3.6	Thermal Analysis of Particles Following Exposure to Release Media.....	111
4.3.7	Analysis of Mechanism of Drug Release.....	111
4.4	Discussion.....	113
4.5	Conclusions.....	118
4.6	References.....	119

Chapter 5: Modulation of Release Rate by the Incorporation of a Hydrophilic Excipient

5.1	Introduction.....	124
5.2	Materials and Methods.....	125
5.2.1	Materials.....	125
5.2.2	Methods.....	126
5.2.2.1	Production of Riboflavin Loaded Particles Containing Various Molecular Weights of PEG.....	126

5.2.2.2	<i>In vitro</i> Riboflavin Release from Various Formulations.....	126
5.2.2.3	Scanning Electron Microscopy.....	126
5.2.2.4	X-ray Microtomography.....	126
5.3	Results.....	127
5.3.1	Release of Drug from PEG Modified Particles into PBS Medium.....	127
5.3.2	Release of Drug from PEG Modified Particles in SGF Medium.....	129
5.3.3	Morphological Examination Following Exposure of PLGA Particles to Release Media.....	131
5.3.4	Mechanism of Drug Release from Particles.....	135
5.4	Discussion.....	140
5.5	Conclusions.....	147
5.6	References.....	148

Chapter 6: Surface Modification for the Introduction of Novel Properties

6.1	Introduction.....	151
6.2	Materials and Methods.....	157
6.2.1	Materials.....	157
6.2.2	Methods.....	157
6.2.2.1	Preparation of <i>N</i> -Acetyl Cysteine Modified Chitosan.....	157
6.2.2.2	Preparation of FITC Labelled Chitosan.....	159

6.2.2.3	Nuclear Magnetic Resonance (NMR) Spectroscopy.....	159
6.2.2.4	Ellman's Assay.....	159
6.2.2.5	Post-Processing Surface Modification of PLGA Particles.....	160
6.2.2.6	Introduction of Mucoadhesive Polymer into Formulation and Preparation of Particles Using PGSS Processing.....	161
6.2.2.7	Scanning Electron Microscopy.....	162
6.2.2.8	X-ray Microtomography.....	162
6.2.2.9	Fluorescent microscopy.....	162
6.2.2.10	Time-of-Flight Secondary Ion Mass Spectroscopy.....	162
6.2.2.11	Mucous Glycoprotein Assay.....	163
6.2.2.12	Adhesion of Particles to a Mucus Producing Cell Line.....	163
6.3	Results.....	164
6.3.1	Preparation of NAC Modified Chitosan.....	164
6.3.2	Morphological Analysis of Particles Following Post-Processing Surface Modification.....	167
6.3.3	ToF-SIMS Surface Analysis.....	169
6.3.4	Mucous Glycoprotein.....	175
6.3.5	Adhesion to a Mucus Producing Cell Culture Model.....	176
6.4	Discussion.....	179
6.5	Conclusion.....	182

6.6	References.....	182
Chapter 7: Pharmacokinetic Analysis of Metformin		
Hydrochloride Following Administration of Gastroretentive		
PLGA Particles		
7.1	Introduction.....	186
7.2	Materials and Methods.....	190
7.2.1	Materials.....	190
7.2.2	Methods.....	190
7.2.2.1	Incorporation of Metformin into PLGA Particles.....	190
7.2.2.2	Preparation of Non-Buoyant Particles.....	191
7.2.2.3	<i>In vitro</i> Metformin Release.....	191
7.2.2.4	High Performance Liquid Chromatography (HPLC) Analysis.....	192
7.2.2.5	Pharmacokinetic Analysis of Metformin in a Rat Model.....	192
7.2.2.6	Deproteinisation of Rat Serum Samples for HPLC.....	193
7.3	Results.....	193
7.3.1	Encapsulation and <i>In Vitro</i> Release of Metformin.....	193
7.3.2	Development of HPLC Method for Quantitative Analysis of Metformin in Rat Serum.....	196

7.3.3	Analysis and Quantification of Metformin Hydrochloride in Rat Serum Following Oral Application of Different Formulations.....	199
7.4	Discussion.....	201
7.5	Conclusions.....	205
7.6	References.....	206

Chapter 8: Summary and Future Directions

8.1	Overall Summary.....	210
8.2	Future Directions.....	215
8.3	References.....	216

List of Figures

Chapter 1

Figure 1.1. Structure of the Human Gastrointestinal Tract [9].....	3
Figure 1.2. The four anatomical regions of the stomach.....	5
Figure 1.3. Diagram depicting the gastric pit and the arrangement of its constituent cell types [12].....	6
Figure 1.4 The pH changes in the postprandial stomach. Administration of the meal is shown by the arrow [22].....	11
Figure 1.5. The basal acidity in the stomach over a course of 24 hours. A circadian rhythm exists with the stomach being more acidic early morning and late evening [19].....	12
Figure 1.6. Emptying rates of solid food (●) and liquids (○) from the stomach. Liquid is empties significantly faster than solid food [10].....	14
Figure 1.7. Pressure-temperature phase diagram for a pure component showing the triple point (T) and the critical point (C). The supercritical region (SCF) is demonstrated past the critical point. The density of the component is illustrated by the grey circles [140].....	29

Chapter 2

Figure 2.1. Simplified diagram of the high pressure equipment used to fabricate particles.....	53
---	----

Figure 2.2. Labelled photograph of the mixing chamber attached to the collection chamber.....	53
Figure 2.3. Transmission image demonstrating how the particles are loaded into the microCT instrument.....	56
Figure 2.4. Example of a DSC thermograph illustrating a glass transition, a crystallisation, and a melting point.....	60
Figure 2.5. Schematic diagram of the ToF-SIMS process illustrating the liberation of secondary ions from the sample surface.....	64
Figure 2.6. Diagram illustrating the depth profiling process. The analysis is carried out by the Bi^{3+} primary ion with the C^{60+} revealing a new surface layer.....	65
Chapter 3	
Figure 3.1. Schematic of the PGSS process [29].....	70
Figure 3.2. Percentage yield of particles as myristic acid content increases. (n=1).....	74
Figure 3.3. SEM images of particles prepared with different ratios of PLGA: Myristic acid. Scale bars in upper row 50 μm in middle and bottom row 100 μm	75
Figure 3.4. i) Cumulative Size distribution profile of particles prepared with various PLGA: myristic acid ratios ii) corresponding differential curve for the formulations.....	76
Figure 3.5. Density of particles produced with increasing PLGA polymer content. (n=6 \pm SD).....	77

Figure 3.6. Photographs illustrating the behaviour of particles with different PLGA: myristic acid ratios.....	78
Figure 3.7. SEM images showing particles prepared with PLGA(12KDa):PLGA(5KDa):SPAN80 (ratio 70:25:5) of different size fractions a) 1mm (scale bar 200 μ m) b) 800 μ m (scale bar 200 μ m) c) 500 μ m (scale bar 500 μ m)d) 250 μ m (scale bar 200 μ m) e) 100 μ m (scale bar 100 μ m).....	80
Figure 3.8. Porosity of microparticles with increasing size as measured using microCT (n=6 \pm SD).....	81
Figure 3.9. The relationship between particle density (n=6 \pm SD) and in vitro buoyancy (n=3 \pm SD) behavior for a range of particles sizes. Density determined as described in section 3.2.2.4 and buoyancy determined as described in section 3.2.2.5.....	82
Figure 3.10. In vitro buoyancy test for different sized particles (i) 100 μ m ii) 250 μ m iii) 500 μ m iv) 800 μ m v) 1000 μ m vi) 2000 μ m in a simulated gastric medium.....	82
Figure 3.11. Illustration of how the grinding procedure results in a number of smaller particles (b)) with lower porosity than the original larger particle (a)).....	88
 Chapter 4	
Figure 4.1. Chemical structures for a) furosemide and b) riboflavin.....	96
Figure 4.2. Encapsulation efficiency of furosemide and riboflavin for different size fractions of the PLGA particles prepared by the PGSS method (n=3 \pm SD).....	101

Figure 4.3. a) ToF-SIMS mass spectrum revealing the intensity of the SNO_2H and SNO_2H_2 peaks in i) drug loaded microparticles ii) blank microparticles and iii) Furosemide powder and b) the corresponding ion images which illustrate the distribution of the SNO_2H ion in i) drug loaded particles and ii) blank microparticles.....	103
Figure 4.4. ToF-SIMS depth profile analysis demonstrating the intensity of the SNO_2H ion as it is found through the layers of the microparticle. The intensity is plotted over time with each time point representing a new layer through the sample. The average of intensity for every 10 seconds was calculated and averaged.....	104
Figure 4.5. Cumulative release of a) riboflavin and b) furosemide from different sized microparticles using PBS pH 7.4 as the release medium ($n=3\pm\text{SEM}$).....	106
Figure 4.6. Cumulative release of a) riboflavin and b) furosemide from particles sized 1000 μm and 250 μm in SGF. ($n=3 \pm\text{SEM}$).....	108
Figure 4.7. SEM images of different size fractions of PLGA particles loaded with riboflavin following 24 h exposure to PBS pH7.4. Particle sizes and scale bars indicated on individual images (scale bar values i), ii) 500 μm iii), iv), v) 200 μm , and vi) 100 μm).....	110
Figure 4.8. SEM images of different size fractions of PLGA particles loaded with riboflavin following 24 h exposure to SGF pH1.2. Particle sizes and scale bars indicated on individual images (scale bar values i),ii),v) 500 μm and iii) and iv) 200 μm	110
Figure 4.9. 3D reconstruction of microCT data 1000 μm sized particles: following production and prior to the exposure (a) following exposure to PBS	

(b) and following exposure to SGF (c). In each case i) represents the polymer matrix, ii) represents the open pore space within the matrix allowing a visual comparison of the porosity to be made.....	110
Figure 4.10. DSC thermograph of PLGA particles before (green) exposure to release media and following exposure to PBS (blue) and SGF (Red).....	111
Figure 4.11. Release data fitted to the Higuchi model for release in PBS for i) riboflavin loaded particles and ii) furosemide loaded particles and for release in SGF for iii) riboflavin loaded particles and iv) furosemide loaded particles..	112
Chapter 5	
Figure 5.1. Release of riboflavin from the 1000 μm size fraction of PLGA particle incorporating 10% PEG of various molecular weight PBS pH 7.4 used as the release medium. (n=3 \pm SD).....	128
Figure 5.2. Release of riboflavin from 250 μm size fraction of PLGA particles incorporating 10% PEG of various molecular weights. PBS pH 7.4 used as the release medium (n=3 \pm SD).....	129
Figure 5.3. Release of riboflavin from 1000 μm size fraction of PLGA particles incorporating 10% PEG of various molecular weights. SGF pH 1.2 used as the release medium (n=3 \pm SD).....	130
Figure 5.4. Release of riboflavin from 250 μm size fraction of PLGA particles incorporating 10% PEG of various molecular weights. SGF pH 1.2 used as the release medium (n=3 \pm SD).....	131
Figure 5.5. Porosity data obtained by microCT analysis Blue-prior to exposure, Red- following exposure to PBS pH 7.4, Green- following exposure to SGF pH 1.2 (n=6 \pm SD) Corresponding 3D reconstruction ‘models’ shown as	

images next to the bar. The image on the left illustrates the matrix space within the particle and the image on the right illustrates open pore space.....	133
Figure 5.6. Scanning Electron Microscopy micrographs showing the appearance of the microparticles with incorporation of different molecular weight PEGs before and following the completion of the release studies i.e. exposure to PBS pH 7.4 of SGF pH 1.2.....	134
Figure 5.7. Data for the release of riboflavin from PLGA particles with various PEG molecular weights fitted to the Higuchi kinetic model for release data in PBS pH 7.4 for i) 1 mm sized and ii) 250 μ m sized particles.....	138
Figure 5.8. Data for the release of riboflavin from PLGA particles with various PEG molecular weights fitted to the Higuchi kinetic model for release data in SGF pH 1.2 for i) 1 mm sized and ii) 250 μ m sized particles.....	139
 Chapter 6	
Figure 6.1. The structures of i) Chitosan-NAC ii) Chitosan-TBA and iii) Chitosan-TGA.....	156
Figure 6.2. The synthesis of chitosan-NAC.....	157
Figure 6.3. ^1H NMR spectra of N-acetyl cysteine in DCl.....	165
Figure 6.4. ^1H NMR of the unmodified chitosan polymer in DCl.....	166
Figure 6.5. ^1H NMR spectra of the chitosan-NAC conjugate in DCl.....	166
Figure 6.6. Morphological analysis of i) control (uncoated), ii) chitosan coated post processing iii) chitosan-NAC coated post processing iv) chitosan incorporated into formulation (10%(w/w)) Both SEM and microCT images are presented.....	167

Figure 6.7. Fluorescent images of particles containing FITC-chitosan as a post processing coating (i) and ii) alongside chitosan incorporated into coumarin-6 labeled particles (iii) iv)).....	168
Figure 6.8. ToF-SIMS mass spectra showing the intensity of the CNO peak in the different formulations. The spectra confirm the increased intensity of CNO which is the chitosan associated ion in the coated samples.....	169
Figure 6.9. ToF-SIMS ion images demonstrating the distribution of the CN ⁻ , CNO ⁻ , and HS ⁻ ions in the different formulations.....	170
Figure 6.10. Depth profile demonstrating the intensity of the PLGA (red) ions and the chitosan ions (blue) as the analysis is carried out through the depth of the sample after post production coating.....	172
Figure 6.11. Depth profile demonstrating the intensity of the PLGA (red) ions and the chitosan ions (blue) as the analysis is carried out through the depth of the sample after the chitosan has been incorporated into the formulation.....	172
Figure 6.12. ToF-SIMS ion images demonstrating the distribution of the CN ⁻ , CNO ⁻ , and HS ⁻ ions in the z view following depth profiling.....	174
Figure 6.13. Chart comparing the amount of mucin which adheres to microparticles following incubation in a mucin solution (n=3±SD).....	175
Figure 6.14. Fluorescent and bright field images showing the particles adhered to the surface of the cell monolayer i) distribution of fluorescently labelled particles prior to washing ii) FITC-chitosan coated particles iii) FITC-chitosan-NAC coated particles iv) chitosan incorporated particles labelled with coumarin-6 v) control particles labelled with coumarin-6.....	177

Chapter 7

Figure 7.1. Chemical structure of metformin.....	190
Figure 7.2. In vitro release profile of metformin hydrochloride from 250-500µm sized particles following an initial drug loading of 5%. (n=3±SEM).....	194
Figure 7.3. In vitro release profile of metformin hydrochloride from 250-500µm sized particles following an initial drug loading of 10%. (n=3±SEM).....	194
Figure 7.4. Release data applied to the Higuchi kinetic model for 10% metformin.....	196
Figure 7.5. Linearity of peak area in the given concentration range for metformin in rat serum and mobile phase (n=6±SEM).....	197
Figure 7.6. Typical chromatograms showing the resolution of the metformin peak (demonstrated by the pointer) in i) mobile phase (0.05µg/ml) ii) blank serum iii) spiked serum sample (0.05µg/ml) and iv) typical chromatogram for a group 4 animal at 60mins.....	198
Figure 7.7. The log plasma concentration profile for metformin following oral administration of a 100mg/kg dose from the different formulations. I.V data is also provided for absolute bioavailability calculations (n=6±SEM).....	199

List of tables

Table 1.1. The improvement in mucoadhesive strength of various thiolated polymers [100].....	22
Table 1.2. Critical conditions P_c , T_c , ρ_c for selected substances.....	30
Table 3.1. Investigation of polymer blends and processing parameters in order to find a suitable candidate formulation for gastroretention using particle density values obtained from helium air pycnometry.....	79
Table 4.1. The regression parameters obtained for PLGA particles sized 1mm with in PBS for the different kinetic models.....	112
Table 5.1. The regression parameters obtained for particles sized 1mm with various PEG molecular weights in PBS for the different kinetic models.....	136
Table 5.2. The regression parameters obtained for particles sized 1mm with various PEG molecular weights in SGF for the different kinetic models.....	137
Table 7.1. The regression parameters obtained for release data for metformin loaded particles (10% w/w) for the different kinetic models.....	195
Table 7.2. Relative Standard Deviation (RSD) values given for peak area over a large concentration range of metformin in rat serum.....	197
Table 7.3. Pharmacokinetic parameters of metformin following oral administration.....	200

Abbreviations

%	Percentage
% w/w	% Weight
°C	Degrees Celsius
µm	Micrometer
ρ _c	Critical Density
ANOVA	Analysis of Variance
ASES	Aerosol Solvent Extraction System
AUC	Area Under the Curve
BSA	Bovine Serum Albumin
CDCl ₃	Deuterated Chloroform
CO ₂	Carbon Dioxide
DCl	Deuterated Hydrochloric Acid
dH ₂ O	Distilled Water
DMSO	Dimethyl Sulphoxide
D ₂ O	Deuterated Water
DSC	Differential Scanning Calorimetry
DTNB	5,5'-dithiobis-(2-nitrobenzoic acid)
EDAC	N-(3-Dimethylaminopropyl)-N'-ethylcarbodiimide hydrochloride
FITC	Fluorescein Isothiocyanate
GAS	Gas Antisolvent

GI	Gastrointestinal
GIT	Gastrointestinal Tract
H	Hour
H ⁺	Hydrogen ions
HCl	Hydrochloric Acid
hGH	Human Growth Hormone
HPLC	High Performance Liquid Chromatography
HPMC	Hydroxypropylmethyl cellulose
H ₂ O	Water
K	Kelvin
K ⁺	Potassium ions
KDa	KiloDalton
microCT	X-ray Microtomography
mins	Minutes
mg	Miligrams
ml	Mililitre
mm	Milimeter
MMC	Migrating Motor Complex
Mw	Molecular Weight
NAC	N-acetylcysteine
NaOH	Sodium Hydroxide
NMR	Nuclear Magnetic Resonance
o/w	Oil-in-Water
PBS	Phosphate Buffered Saline
P _c	Critical Pressure

PCA	Precipitation with a Compressed Antisolvent
PEG	Poly(ethylene glycol)
PGSS	Particles from Gas Saturated Solutions
PLA	Poly(lactic acid)
PLG	Poly(glycolic acid)
PLGA	Poly(lactic-co-glycolic acid)
PMMA	Poly(methyl methacrylate)
psi	Pounds per Square Inch
PVDF	Poly(vinylidene)
RESS	Rapid Expansion of Supercritical Solutions
SAS	Supercritical Antisolvent
SD	Standard Deviation
scCO ₂	Supercritical Carbon Dioxide
SEDS	Solution Enhanced Dispersion by Supercritical Fluids
SEM	Standard Error of the Mean
SEM	Scanning Electron Microscopy
SGF	Simulated Gastric Fluid
T _c	Critical Temperature
TEER	Transepithelial Electrical Resistance
T _g	Glass Transition Temperature
T _m	Melting Point
ToF-SIMS	Time of Flight- Secondary Ion Mass Spectrometry
UV/Vis	Ultra Violet / Visible Light
w/o/o	Water-in-Oil-in-Water

Chapter 1

Introduction

1.1 Oral Drug Delivery

In order to be effective, drugs must reach their target site of action in an adequate and therapeutically beneficial concentration. However, limitations in drug delivery may arise as a result of poor solubility [1-3], low absorption [3], inadequate distribution or insufficient selectivity [4]. The field of drug delivery aims to improve the pharmacological properties of the drug, allowing for more effective therapy.

For reasons including convenience for both patient and healthcare professionals, oral administration of drugs has emerged as one of the preferred routes for drug delivery [5, 6]. The majority of commercially available pharmaceutical products are designed for oral administration; in the US oral products represented approximately 70% of pharmaceutical sales in 2010 [7]. Therefore, considerable efforts in pharmaceutical development concentrate on the design and identification of active compounds readily deliverable through the oral route, as well as the fabrication of delivery devices designed to improve oral delivery of drugs.

Patient compliance is an important consideration when developing any pharmaceutical product as, without adequate dosing, the therapeutic aim of the dosage form will not be achieved. There is an inverse relationship between the amount of doses per day and patient compliance [8]; consequently, in the development of novel oral therapy the design of a dosage form should be such to minimize the dose frequency. Owing to the ability of the majority of patients to easily self-administer the drugs, patient compliance is often relatively higher for oral dosage forms.

There are many different formulations which serve to reduce oral dosing frequency. These systems often prolong drug release from the dosage form over an extended period decreasing dosage frequency and improving the therapeutic efficiency. Such systems will be described in more detail in the later sections.

1.2 The Gastrointestinal Tract

The gastrointestinal tract (GIT) includes all the anatomical structures from the mouth to the anus (Figure 1.1) and comprises of specialist sections capable of digesting food products, allowing the extraction of useful nutrients ending in the removal of waste products.

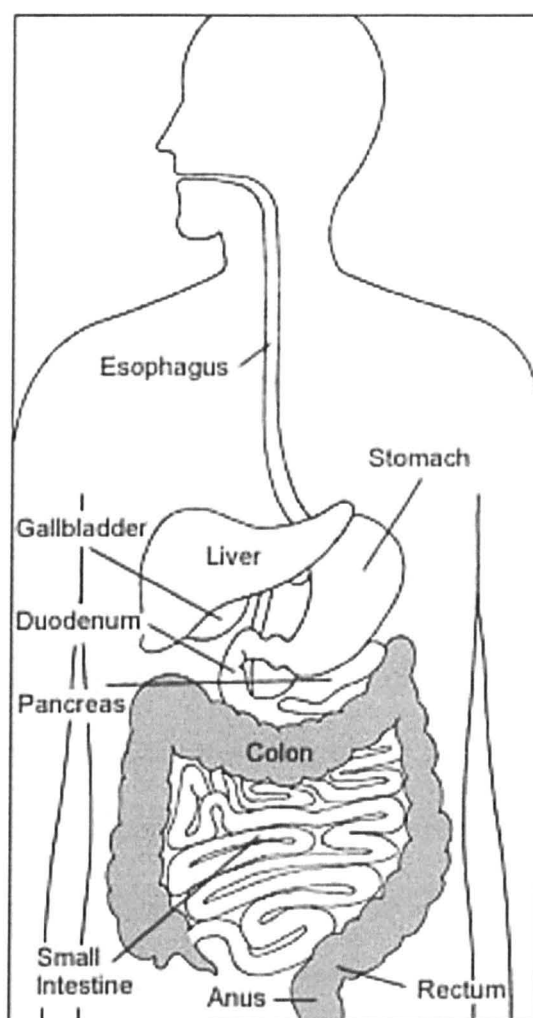


Figure 1.1 Structure of the Human Gastrointestinal Tract [9]

1.2.1 Structure and Function

The gastrointestinal tract measures around 5 meters in the average adult male. It is separated into two parts: upper and lower GIT (based on the function, and arterial supply), or into three parts: fore-, mid-, and hind-gut (based on embryological development). The digestion process begins in the mouth with the addition of saliva and the chewing of food materials; this semi-solid mass is carried down the oesophagus to the stomach.

The histological arrangement of the various sections of the GIT is similar, with variations allowing for specialized functions of the different anatomical sections.

1.2.1.1 The Oesophagus

The oesophagus, like much of the GIT, is a muscular tube allowing muscular contractions, or peristaltic waves, to push food along it. The oesophageal lumen is lined by thick stratified squamous epithelial cells ('squamous' refers to the flattened morphology of these cells). These cells are easily shed and the layer demonstrates a high turnover rate, providing protection from trauma and from the high volume transit of food, saliva, and mucus.

The submucosal layer contains the mucous glands which are responsible for the secretion of mucus. This viscous secretion serves a dual function in both protection and digestion, aiding the transit of food materials down into the stomach. Below the submucosal layer, the lumen of the oesophagus is surrounded by a layer of muscle which is divided into three sections. Voluntary muscle is located in the upper third, allowing conscious control over swallowing, with involuntary muscles in the lower third which are autonomically controlled. The final third possesses both types of muscle.

1.2.1.2 The Stomach

Food is moved along the oesophagus by peristaltic waves into the stomach. The stomach receives and temporarily stores ingested food. The several functions of the stomach include: acting as a reservoir; processing food products for easier absorption of nutrients; and regulating emptying rates of

chyme into the small intestine. The exposure to the external environment leaves the GIT vulnerable to pathogens and therefore, the stomach plays an integral role in defence from such threats. Parietal cells present in the gastric epithelium, serve to secrete gastric acid. The low pH in the stomach acts as a defence to pathogenic organisms, and also enables pepsin to function. The stomach itself is divided into four anatomical regions (Figure 1.2).

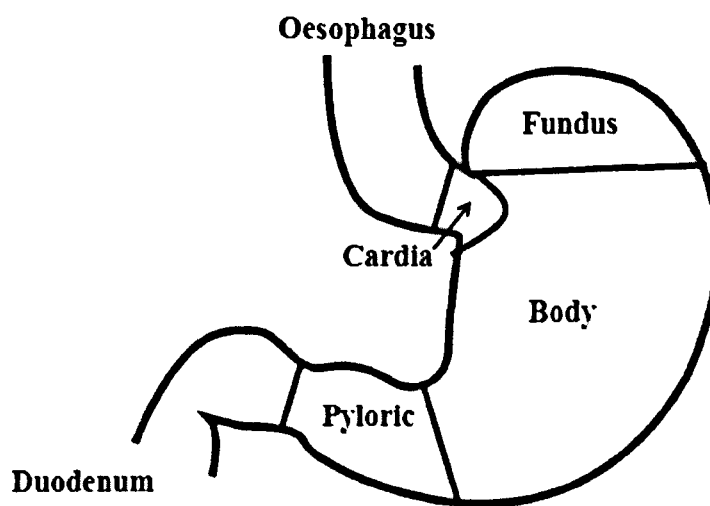


Figure 1.2 The four anatomical regions of the stomach

The different regions of the stomach are distinguished by specific cell types of the mucosal lining, each region with specialised functions. From the cardia region, food empties into the fundus, the top region of the stomach. The muscular contractions in this region are slow and sustained, gradually moving the stomach contents towards the small intestine. The largest part of the stomach is the body, where the ingested material is stored. Finally, the pyloric region is the funnel shaped region connected to the pyloric sphincter. The stomach can be subdivided into 2 areas with distinct roles in digestion. The

corpus (body) and the fundus are known as the cephalad and this is where the ingested materials are stored. The majority of the motility occurs in the area known as the caudad, which comprises the distal corpus and the pyloric region (or antrum). This is where mixing of the contents and gastric enzymes takes place and the food stuff is ground into a more digestible state.

Gastric secretions are essential for adequate digestion. The stomach secretes 2-3 litres of gastric juice *per* day [10, 11], and is capable of storing volumes from 0.5 litres to 5 litres. The majority of this fluid originates from various glands within the stomach wall. In the fundus, corpus and parts of the pylorus, invaginations extending into the gastric wall, known as gastric pits, house various cell types secreting an assortment of substances. Different cell types with different functions can be found at different layers of the pits (Figure 1.3).

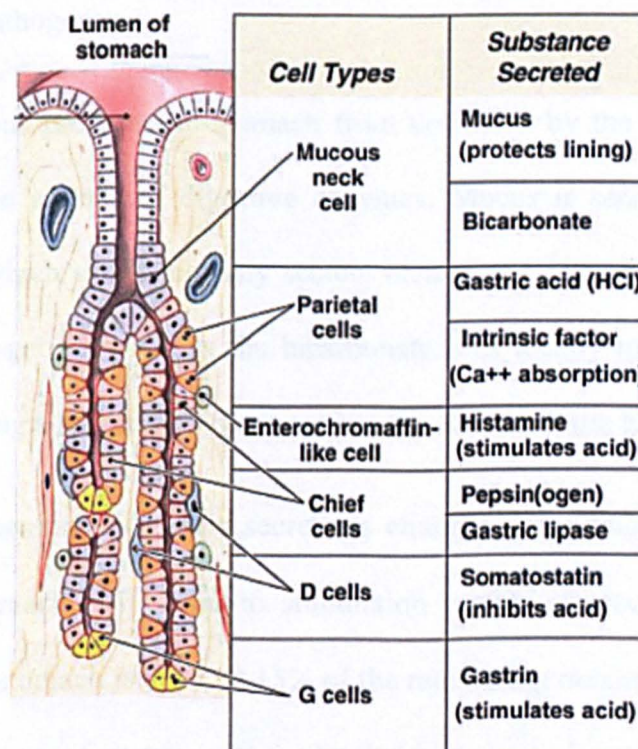


Figure 1.3 Diagram depicting the gastric pit and the arrangement of its constituent cell types [12].

There are four main constituents of gastric secretions - hydrogen ions, pepsin, mucus and intrinsic factors [13]. Each of these secretions plays an important role in GI physiology.

Hydrogen ions (H^+) are actively pumped into the stomach in exchange for potassium (K^+) by the H^+/K^+ ATPase proton pump. The movement of H^+ out of the cell results in an accumulation of OH^- in the cell, which undergoes catalysis by carbonic anhydrase to form the bicarbonate ion (HCO_3^-). The presence of HCO_3^- allows chloride ions to move against the gradient from the blood into the lumen of the stomach. HCl secretion into the stomach, although not essential for life, greatly aids digestion through the activation of pepsinogen which allows the activation of pepsin, as well as initial digestion of connective tissues and muscle fibres present in food. Although not related to digestion, the low pH HCl acts as a good non-specific defence mechanism against many pathogens.

A layer of mucus protects the stomach from corrosion by the low pH of its contents and the actions of digestive enzymes. Mucus is secreted from the mucosal cells which simultaneously secrete bicarbonate ions. The mucus is a water-insoluble gel which traps the bicarbonate ions locally to the epithelial surface, providing a buffering system against the H^+ within the lumen.

The exact composition of gastric secretions changes depending on the filling state of the stomach [14]. Prior to stimulation (empty stomach), basal acid secretion in the stomach is low (10-15% of the rate during maximal stimulation [13]). The secretion of gastric juice is divided into three phases [15, 16]. The cephalic phase occurs before food has entered the stomach, which is governed

by neuronal signals which arise following stimuli such as tasting, smelling, chewing, and swallowing food. It is the vagal nerve that relays the information from the cerebral cortex directly to the parietal cells and stimulates the release of HCl. The second phase is the gastric phase which is responsible for at least half of gastric secretion. This is a response to both the mechanical actions on the stomach walls, and the chemical actions through raising the pH. Following extensive mixing and grinding, the chyme (partially digested food products) passes through the pyloric sphincter which sieves the stomach contents into the duodenum. This is where the third and final phase of digestion, the intestinal phase, takes place. The digestion products of protein entering the duodenum stimulate this phase, initially increasing gastrin production and accounting for around 5% of gastric secretions. However, after the initial increase in stimulus for gastric secretion, the duodenum sends inhibitory signals via the enterogastric reflex. This inhibits the vagal stimulation and stimulates the sympathetic neurons sending inhibitory signals to the secretory cells.

1.2.1.3 The Small Intestine

The small intestine is where the majority of absorption takes place and is therefore of great interest in drug delivery. The small intestine itself is sectioned into three divisions. The lumen of the small intestine contains areas where the mucosa projects into the lumen to create finger like structures known as *villi*. These projections increase the surface area and the absorptive abilities of the small intestine. Among the specialised cell types present in the mucosa of the *villi* are the two secretory cell types: goblet cells (which secrete mucin, a major constituent of mucus, into the lumen) and neuroendocrine cells (which release hormones into the blood allowing communication to take place

between the nervous system and the endocrine system). Within the spaces between the villi, (the Crypts of Lieberkühn) additional cells are present, including paneth cells which secrete defensive molecules, stem cells which allow epithelial growth, and the intraepithelial lymphocytes which also play a key role in gastrointestinal defence. The submucosa connects the mucosa to layers of smooth muscle and provides mechanical strength to the small intestine.

The smooth muscle fibres are arranged in circular and longitudinal layers, an arrangement which allows the generation of peristaltic waves to push food along the GIT. Gap junctions between muscle cells enable the spreading of contractions along the GIT, and result in the smooth waves of peristalsis.

The upper small intestine, the duodenum, contains the longest villi projections and a high number of goblet cells; this is the site of most absorption. Within the Crypts of Lieberkühn lie submucosal glands, known as Brunner's glands, which secrete bicarbonate containing mucus. The high pH of these secretions serves to neutralise and protect the duodenum from the highly acidic chyme which is arriving from the stomach. The higher pH levels (reported to be pH 6.4 [17]) are also necessary for the activation of intestinal digestive enzymes. The duodenum also regulates the emptying of chyme from the stomach, the release of digestive enzymes from the pancreas, and bile secretion from the gall bladder.

Following the duodenum is the jejunum, the middle section of the small intestine, and, as in the duodenum, it provides a good absorptive surface for carbohydrates. The jejunum contains the Valves of Kerckring - circular folds,

which increase surface area for absorption as well as providing obstacles which slow the passage of food materials, allowing more time for absorption to occur. The final section of the small intestine is the ileum where the remaining nutrients are absorbed. Peyer's patches are abundant in the ileum and the large quantity of these lymphoid nodules play a key role in the generation of an immune response in the small intestine to the presence of pathogens.

1.2.1.4 The Large Intestine

The large intestine follows on from the small intestine. This region of the GIT lacks the abundant villi present in the highly absorptive small intestine and as a result relatively little absorption of nutrients (or drugs) takes place here. The large intestine functions to absorb water and transport waste from the body.

1.2.2 Physiological Barriers to Oral Delivery

The environment within the GIT is variable and may provide physical, biological and chemical obstructions for adequate drug delivery as well as opportunity to explore in designing oral drug formulations.

1.2.2.1 pH

Gastric secretions tend to be highly acidic as a result of the hydrochloric acid content. pH is an important factor when considering the performance of a drug delivery system due to the influence pH has over drug solubility and delivery system stability [18].

Keeping in mind the complexity of the gastric secretions and the importance of the pH levels on the delivery system and the drug itself, the contents of the upper GI tract have been characterised with the aim of developing a more

appropriate media for *in vitro* investigations [19]. In one such study, aspirates were withdrawn from the stomach for analysis following administration of 500 ml of Ensure Plus®; a model meal that has the equivalent nutritive value and composition as the FDA's recommended meal [20]. The results showed that there are substantial differences in the composition of the gastric fluid following the consumption of the meal. pH can increase up to 6.4 and the buffer capacity increases. The pH then gradually decreases over time back to the 'normal' range (reaching pH 2.7 after 210 mins), obviously dependent on content/constituents of the meal. This phenomenon has also been reported in other recent studies [21] as illustrated in Figure 1.4 (taken from [22]).

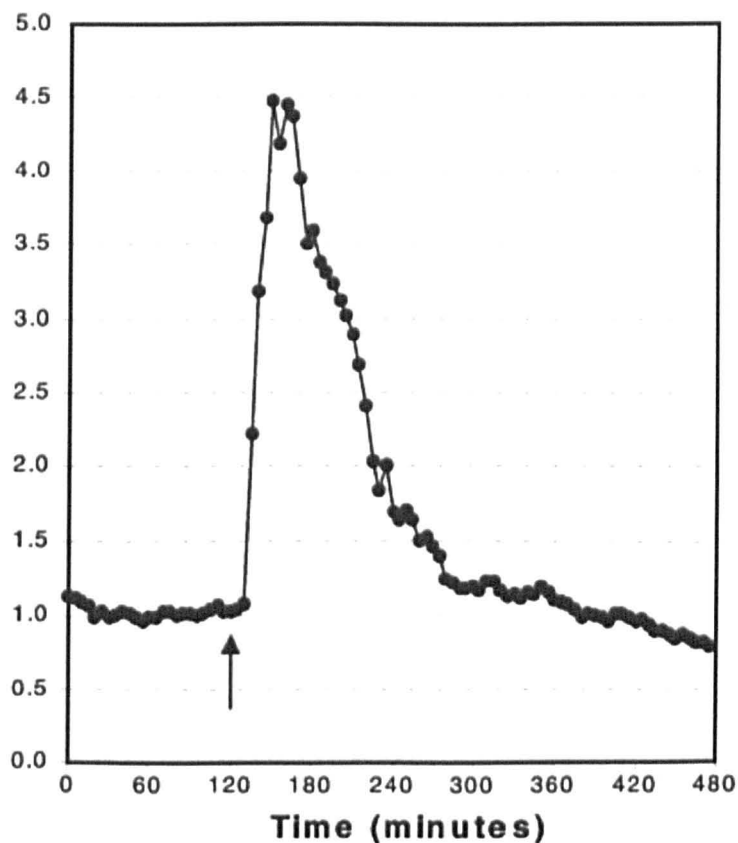


Figure 1.4 The pH changes in the postprandial stomach. Administration of the meal is shown by the arrow [22].

It is the gastric phase of digestion which is responsible for the majority of the pH changes in the post-prandial stomach. However, there is also a circadian rhythm of the basal hydrogen ion flow, resulting in a cyclical rise and fall of stomach pH over a 24 h period (Figure 1.5) [19].

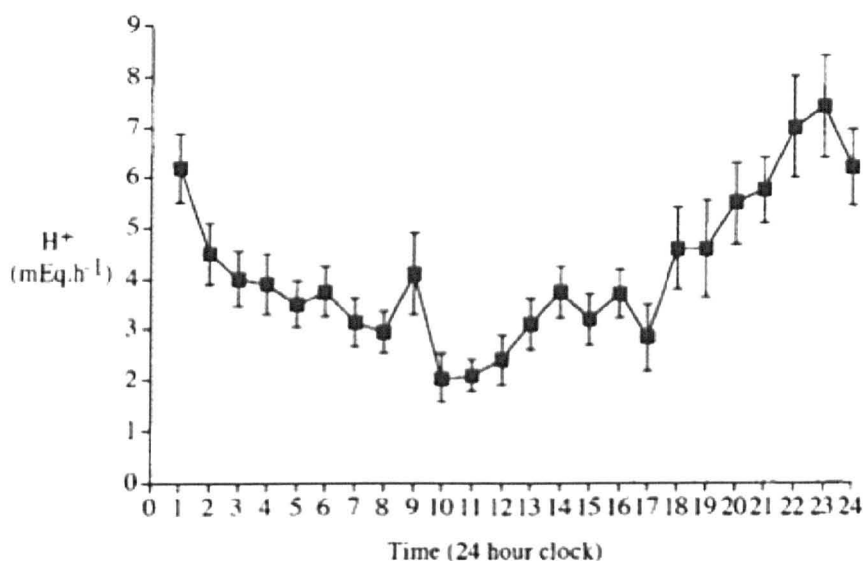


Figure 1.5 The basal acidity in the stomach over a course of 24 h. A circadian rhythm exists with the stomach being more acidic early morning and late evening [19].

The potential negative impact of the low pH on the incorporated drug and/or delivery system may be overcome through the use of pH responsive polymers [23]. These polymers respond to changes in pH levels, and exhibit dissolution only at pH levels higher than those in the stomach, usually pH 5.5 and above. A widely investigated example is Eudragit [24, 25] which has been utilised in oral formulations for improving delivery of drugs such as ibuprofen [26], insulin [27, 28] or, furosemide [29].

The Eudragit[®] polymers are copolymers derived from esters of acrylic and methacrylic acids. The family of different Eudragit[®] polymers, has been

exploited for enteric coating of oral drug delivery systems to protect the incorporated drug in the stomach and achieve their release in the intestines [30].

1.2.2.2 Gastric Motility

Motility in the stomach is important for digestion, it is essential for proper nutrition, as well as reliable drug delivery. The stomach in essence acts as a mixer and a grinder, a storage chamber, and a sophisticated pump, with gastric motility following pre-determined patterns [31]. The motility originates from contraction of GI smooth muscle, and it is used to move food along the GIT, as well as in the stomach, contributing to the mechanical 'digestion' of food.

There are distinctly different patterns of stomach motility in the fed and fasted states. On fasting, the motility is continuous and shows a near constant force of 15-20 mm Hg [32]. The fasting state is also characterised by the regular occurrence of the migrating motor complex (MMC) which is the main pattern of contraction [33]. The MMC is also known as the 'housekeeper wave' and serves to remove debris from the stomach [34].

The post-prandial stomach demonstrates a different pattern of contractions, with two distinct patterns. Peristalsis is where the contractions occur in waves along the GIT, forcing the food along the tract towards the anus. The majority of contractile activity in the stomach however is segmentation. These relatively weak contractions ensure thorough mixing of ingested material with the gastric secretions to produce chyme.

The contractile activity within the stomach not only ensures thorough mixing of the contents for digestion, but the motility is also synchronised in such a way to empty the contents into the duodenum. Gastric emptying is a highly regulated event. In fact, the stomach will demonstrate distinct emptying patterns for liquids, digestible solids, and indigestible solids [35]. As a result solids and liquids do not empty from the stomach at the same rate. Figure 1.6 illustrates that a comparison of the gastric emptying rates for healthy volunteers following administration of either a solid or liquid meal reveals liquids empty faster than solids [10].

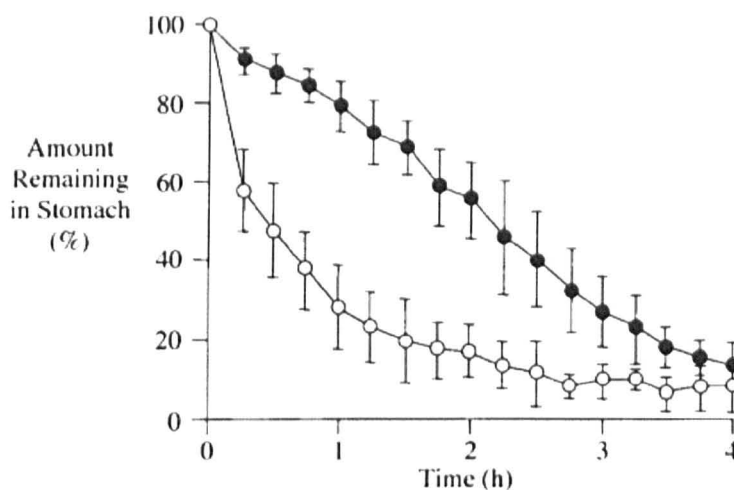


Figure 1.6 Emptying rates of solid food (●) and liquids (○) from the stomach. Liquid is emptied significantly faster than solid food [10].

In addition to the rate of gastric emptying being dependent on the consistency of the ingested material [36], the nature of the meal components also impact gastric emptying. For instance the presence of fatty acids, monoglycerides, and diglycerides has been shown to delay gastric emptying [37-39]; the phenomenon known as the ‘ileal brake’ [40, 41]. It occurs both because the fat will separate and ‘lay’ on top of the stomach content due to its low density [42,

43] to be consequently emptied last, as well as due to the fact that the presence of the fat causes inhibition of antral contractile activity [44].

Other 'external' influences over gastric emptying rate include alcohol consumption [45, 46], disease state [47], gender [48], body mass index [49], and anxiety [50].

1.2.2.3 Absorption Window

It has been demonstrated that some drugs are only absorbed at specific sections/sites along the GIT [51]. This may be a result of their poor solubility at certain pH levels along the GIT [52, 53], their degradation by digestive enzymes, or specific mechanisms required for their uptake [51]. As previously discussed, the anatomical characteristics of the small intestine are designed to achieve an ideal surface for absorption, with the upper small intestine being particularly relevant. As a result the absorption of many drugs is confined, to this section of intestinal tract, a so called absorption window [51, 54-56]. This presents a problem for drug delivery for different reasons. The variable nature of gastric transit time may lead to rapid transit of the delivery system (containing drug) past the site of drug absorption. In such an event, any subsequent drug release will be redundant and the delivered dose will simply pass through the remaining GIT. The presence of absorption windows is thought to limit the bioavailability of drugs [51].

Often, the rapid release and rapid absorption of conventional oral delivery systems [57] results in peaks and troughs in plasma drug concentrations. These fluctuations present problems with the emergence of side effects due to toxicity or, on the other side of the spectrum, inadequate therapy due to low drug

concentrations. The design of systems to overcome the limitations of narrow absorption windows focuses on increasing the time period that the drug is exposed to this area.

1.3 Controlled Release Systems

The coating of oral delivery systems has been common practice for purposes relating to taste [58] for many years. However, in 1884, a coating was developed which was designed to delay disintegration until the system reached the small intestine [59]. As early as 1952, Smith Kline & French were employing the concept of time-release in a formulation they named the Spansule [60]. Since the introduction of the Spansule, numerous controlled release products are now widely available on the market.

Various designs for these controlled-release drugs have been proposed, these include matrix-controlled systems [61, 62] in which the drug is distributed throughout a polymeric matrix through which the drug may diffuse out into the surrounding medium. The diffusion controlled reservoir systems work in a similar way to matrix-controlled systems, where the drug is found in the core and must diffuse out into the surrounding medium. In the reservoir systems, the drug is found in the core and must diffuse through a membrane in order to be released. Finally, osmotically controlled devices are governed by osmotic pressure. These systems consist of an osmotic core, containing the drug and usually an osmagent, which is coated with a semi permeable membrane [63]. The influx of water into the system occurs at a rate determined by the osmotic pressure of the core of the system and the permeability of the membrane to

water. These osmotically controlled devices have proven to be relatively successful as the release is independent of many physiological parameters.

Controlled-release systems span a huge spectrum of release rates which may be as long as months such as the case of Depo-Provera which is a progestogen-only contraceptive injection administered every 3 months, or as short as systems developed for once a day oral dosing such as the extended release diclofenac and naproxen.

1.4 Gastroretention

1.4.1 Overview

A controlled release of drug over time from a dosage form may minimise the peaks and troughs found in plasma drug concentrations and improve bioavailability of drugs [64]. In certain cases, controlled release alone may not however provide adequate improvements in pharmacokinetics. For drugs exhibiting absorption windows in a small area in the proximal GIT, when the delivery system has travelled past this narrow window any subsequent drug released will not be absorbed into the circulation. In such a case, alternative modifications to the delivery system may enable more efficient absorption and more desirable pharmacokinetic properties of the drug.

Retention of the delivery system at or proximal to the site of absorption for a prolonged period of time might provide conditions in which presence of the released drug at the absorption window will improve the level of drug absorption. There are numerous drug candidates for this type of system which could be grouped into; (i) drugs reported to have an absorption window in the upper small intestine [51] such as calcium, Atenolol, Levodopa, and

Riboflavin; (ii) drugs which have a pH-dependant absorption [65] such as barbital [66]; and (iii) drugs for local action in the stomach such as antacids, anti-ulcer drugs, and antibiotics for *H.pylori* infections [65, 67].

The various methods employed to achieve gastroretention have been reviewed previously [68-71] and will be considered in the following sections.

1.4.2 Expanding Systems

Expanding, or unfolding, delivery systems work on the principle that on contact with the gastric contents, the size of the system will increase to a diameter greater than that of the pylorus, thus delaying movement from the stomach to the small intestine. Once expanded, these systems must achieve a size appropriate for retention, whereby the size of 13mm has been proposed [72]. The very concept of this design however, immediately presents problems; for instance, premature expansion, which could result in the system unfolding in the oesophagus, causing discomfort for the patient. Moreover, after the expanding dosage form has served its purpose, there must be a mechanism of its removal from the stomach to avoid accumulation.

Klausner et al 2003 [73] investigated a novel levodopa dosage form based on an unfolding polymeric membrane packed into a gelatine capsule. In this case, the rigidity and increasing size, up to 2.1 cm or larger, allowed prolonged gastric residence time in man reaching 5 h. Another method of creating a size increasing dosage form is to use a hydrogel which swells on contact with the gastric fluid. A hydrogel is a three-dimensional cross-linked network which swells but does not dissolve in an aqueous environment [74]. The swelling is often dependent on the particular conditions of the environment. Enzyme-

digestible hydrogels have demonstrated high gastric residence times of up to 24 h in dogs [75].

1.4.3 Mucoadhesive Systems

Mucoadhesive delivery systems are those which act by adhering to the mucosal surfaces in the body. The gastrointestinal tract is potentially an appropriate site for mucoadhesive systems. Bioadhesion was first explored by Park and Robinson in 1984 [76] who reported a delay in gastric transit time in rats on introduction of either poly (acrylic acid-divinyl glycol) or poly (methacrylic acid-divinylbenzene). Mucin is a major constituent of mucus and it is one of the principle targets for mucoadhesion. Mucin is a heavily glycosylated protein with terminal groups rich in cysteine residues which allow mucin to form disulfide interactions with materials. This is exploited in mucoadhesive delivery systems with many materials capable of forming disulphide bridges with these cysteine groups.

Polyanions are polymers which demonstrate good adhesion to mucus; an example is polyacrylic acid [77-79]. These polymers adhere to mucus through hydrogen bonds between the carboxyl groups of the polymer and the hydroxyl groups present in the carbohydrate region of the mucin. Polyacrylic acid with a high charge density has been found to demonstrate good tensile stress (mucoadhesive strength) *in vitro* [80]. The Carbopol[®] polymers are polyacrylic acids with varying degrees of cross-linking and have been used widely in mucoadhesive drug delivery [81-84]. Studies show that the degree of cross-linking within the Carbopol[®] polymers is an important factor in mucoadhesion [85], with greater crosslinking improving mucoadhesion.

As well as the polyanions, cationic polymers such as chitosan exhibit good bioadhesion properties as a result of their overall positive charge and the ability to form electrostatic interactions with the negatively charged mucin. The use of chitosan as a mucoadhesive agent has been explored extensively with good mucoadhesion being demonstrated *in vitro* [86, 87]. Chitosan microspheres are one of the most widely studied drug delivery systems for the controlled release of many types of drugs [88]. Interactions between chitosan and mucin have been measured using various *in vitro* techniques with the conclusion that the interactions are strong and dependent on the positive zeta potential of chitosan [86]. Much promise has been found with chitosan in animal studies. However, the evidence is less convincing for its use in humans [89].

Other polysaccharides with proven mucoadhesive abilities include: alginic acid, sodium salts of carboxymethylcellulose, hyaluronic acid, and carrageenan [85]. Alginic acid microspheres have been manufactured for use in nasal administration of carvedilol [90], as well as gastroretentive systems for acyclovir. In the latter application, 66% *in vitro* mucoadhesion was revealed with gastric residence time surpassing 4 h. [91]. Sodium alginate and sodium carboxymethylcellulose are capable of demonstrating good sustained release of metformin hydrochloride in a gastric environment, with sodium alginate demonstrating the most effective mucoadhesion [92].

The aforementioned mucoadhesive polymers may improve delivery of drugs through enhancing the contact with the mucosal surface. However, such systems have not yet amounted to commercially successful products [93]. This has led to the development of derivatives of these polymers capable of

improving mucoadhesive properties. These improvements aim to introduce covalent bonding to constituents of mucus which should increase the integrity of the interaction between delivery system and mucosal surface. Polymers containing thiol groups (thiolated polymers, or thiomers) should be able to form strong disulfide bonds with the cysteine rich regions in mucin [94], and should therefore demonstrate more effective mucoadhesion than the non-thiolated counterparts [85].

Various thiolated derivatives of chitosan have been explored, including: chitosan-*N*-acetyl cysteine (chitosan-NAC), Chitosan-4-thio-butyl-amidine (chitosan-TBA), and chitosan-thioglycolic acid (chitosan-TGA) [95-97]. In comparison with unmodified chitosan, and other mucoadhesive polymers, the thiolated chitosans demonstrate superior mucoadhesion in gastroretentive microspheres for acyclovir [98]. Mucoadhesion was also improved by a thiolated chitosan in a gastroretentive particulate system for riboflavin-5' monophosphate sodium salt dehydrate [99]. It has been reported that thiolated derivatives can improve mucoadhesion by as much as 250 fold (see Table 1.1 modified from [100]).

It should be noted, however, that there are limitations to mucoadhesive systems, with the main disadvantage being the turnover rate of mucus in the stomach and intestine. This is relatively high but also variable [101]. Peristaltic waves may also force the delivery system further along the GI tract. Finally, the adhesion of the system is not gastro-specific, and there is a chance that adhesion will occur earlier in the GI tract, in the oesophagus, or even past the absorption window.

Table 1.1 The improvement in mucoadhesive strength of various thiolated polymers [100]

Polymer	Improvement in mucoadhesiveness
Chitosan–iminothiolane	250-fold improved mucoadhesive properties
Poly(acrylic acid)–cysteine	100-fold improved mucoadhesive properties
Poly(acrylic acid)–homocysteine	20-fold improved mucoadhesive properties
Chitosan–thioglycolic acid	10-fold improved mucoadhesive properties
Chitosan–thioethylamidine	9-fold improved mucoadhesive properties
Alginate–cysteine	4-fold improved mucoadhesive properties
Poly(methacrylic acid)–cysteine	Improved cohesive and mucoadhesive properties
Sodium carboxymethylcellulose– cysteine	Improved mucoadhesive properties

1.4.4 High Density Systems

As a result of the anatomy of the stomach, ingested high density material ingested will often ‘sink’ into the greater curvature at the base of the stomach. In this position, a dosage form could release drug undisturbed by the aggressive mixing occurring in the stomach. It has been suggested that by sedimenting within the folds at the base of the stomach, it is possible for ‘heavy’ particles to remain in the stomach for periods of up to 24 h [102]. It has been proposed that ‘heavy particles’ such as dense pellets must demonstrate a density of 3 gcm^{-3} or greater [54]. Such systems have not yet been widely investigated, presumably due to difficulties in producing systems with such a high density from acceptable materials.

1.4.5 Floating Systems

Conversely to the high density systems described above, systems designed to remain buoyant on the gastric contents have shown great promise as a means for achieving gastroretention [71, 103, 104]. Floating drug delivery systems first appeared in 1968 when Davis proposed a method to overcome difficulties when swallowing a pill by decreasing the density of the pill to below that of water [105]. Drug delivery systems may achieve buoyancy on the gastric contents through two different mechanisms as effervescent and non-effervescent systems.

1.4.5.1 Effervescent Gastroretentive Formulations

Effervescent delivery systems incorporate carbon dioxide generating agents in the formulation, which will lower the density of the system on contact with the gastric contents. The gas can be produced through two means, the first being the use of volatile liquid systems. In this case, a liquid which turns to a gas at body temperature is used to fill the delivery system lowering the overall density [106]. Secondly, the gas may be produced through a gas generating system whereby effervescent reactions are used to liberate amounts of CO₂.

A tablet formulation incorporating sodium bicarbonate and anhydrous citric acid demonstrated floating for around 24 h in an *in vitro* test [107]. A major drawback of this type of system, however, is a lag time between the initial contact with the gastric contents and the generation of gas. In the above study, the lag time exceeded 100 seconds for some formulations [107]. A similar effervescent mixture of sodium bicarbonate and citric acid incorporated into a gastroretentive formulation demonstrated floating *in vitro* for 24 h, with a

markedly higher lag time of 10 mins [108]. This may present a problem, as the peristaltic waves within the stomach could result in the system being emptied before the gas generation has allowed sufficient floating. There have been efforts to decrease this lag time to reduce the risk of premature emptying. For example, it has been demonstrated that the ratio of sodium bicarbonate in the formulation can affect the lag time, and through formulation optimization, it has been reduced to 8 s for formulations containing 20% sodium bicarbonate [109]. These formulations were retained in the human stomach for 5.50 h.

There are two ways in which the effervescent agents may be incorporated into the system. In a single-layered tablet, the effervescent compounds are combined with the components of the tablet [110]. Bilayer effervescent tablets have also been described [111] whereby two distinct layers are present. One of these layers is for the polymer and the drug. This layer may be able to convey sustained drug release within the stomach, and the second layer contains the carbon dioxide generating components. Triple layered systems have also been developed, where the extra layer consists of bismuth salt. The bismuth layer rapidly dissolves in the gut, giving immediate release following which the matrix will swell [112].

As well as tablet based effervescent formulations, sodium alginate beads have also been studied and developed using effervescent compounds [113]. The alginate microspheres are prepared by ionotropic gelation with the gas forming calcium carbonate. The benefit of this method is that the dose delivered composes of numerous alginate beads, and so poor lag time and the loss of a fraction of the dose would not have as great an impact as the loss of a monolithic device.

1.4.5.2 Non-Effervescent Gastroretentive Systems

Non-effervescent floating dosage systems demonstrate buoyancy as a result of their inherent low density. The density of the gastric fluid has been measured to be around 1.004 gcm^{-3} [114], thus, any formulation with a density less than this should exhibit floating properties in the gastric environment.

Buoyancy has been achieved through the incorporation of materials with a low density, such as polypropylene foam powder [115]. The foam powder-containing tablets have revealed floating times of 8 h *in vitro* [114]. This system was capable of demonstrating sustained release with control over the rate being exerted through altering the ratios of matrix polymers and foam forming polymers. As an alternative to incorporating low density materials into the formulation, microparticles containing a hollow core (known as 'microballoons') [116] have been prepared, demonstrating potential for sustained pharmacological action *in vivo*. Hollow polycarbonate microspheres demonstrated good floating behaviour and a corresponding improvement in bioavailability in rabbits for piroxicam loaded microspheres [117].

Similarly to microballoons, microparticles demonstrating highly porous morphologies may demonstrate buoyancy. Calcium silicate based porous microparticles with porosity values in excess of 70% demonstrated good buoyancy, with over 80% of the particles remaining buoyant *in vitro* after 10 h [118]. This was despite true density values of the microparticles higher than 1 gcm^{-3} . Porous calcium silicate formulations have also been applied as a porous carrier for the delivery of glipizide with similar floating behaviours observed [119]. Particles with 34% porosity and a bulk density of less than 1 gcm^{-3} prepared with calcium pectinate have been shown to remain floating *in vitro*

for up to 12 h [120]. Furthermore, the low density allowed the system to remain in the rabbit stomach for 5 h [120]. Porous particles of ethyl cellulose were capable of floating on a simulated gastric fluid for over 12 h *in vitro*, translating to good *in vivo* performance in rabbits with improvements in ranitidine bioavailability [121].

Although these floating systems have demonstrated potential for successful gastroretention in *in vivo* studies, there are very few systems available on the market which exhibit gastroretention through buoyancy on the gastric media [122].

A wide variety of delivery systems has arisen from the research into gastroretentive delivery systems. The single-unit formulations such as tablets have a disadvantage as they demonstrate an all-or-nothing gastric emptying behaviour. In this case if the dose does not demonstrate adequate gastroretention the entire dose will be emptied into the small intestine prematurely. Multi-unit systems such as microparticles offer a solution, as it is less likely that the entire dose will fail, this improves therapeutic performance.

1.5 Methods for Particle Production

1.5.1 Conventional Methods for Particle Production

Microparticulate systems have attracted much interest in recent years and have been employed in various successful products [123]. There are different methods available to achieve production of microparticles. There are also many different manufacturing methods for use in microencapsulation of an API. Several of these technologies include:

-
- Coacervation [124]
 - Emulsions [125]
 - Supercritical fluid techniques [126]
 - Spray drying [127]

Emulsification methods are most frequently used for the production of polymeric microparticles [128]. This technique is extensively studied and is highly versatile to allow the production of a variety of systems. The process can either be conducted in a single oil-in-water (o/w) emulsion or as a double water-in-oil-in-water (w/o/w) emulsion. In the single emulsion, a polymer that forms the microparticles is dissolved in a volatile organic solvent which is immiscible within water, typically used as continuous phase. The organic phase also contains the drug, dissolved or dispersed. Evaporation of the organic solvent results in hardening of microparticles which physically incorporate drug. This technique can efficiently encapsulate a range of water insoluble drugs such as chlorpromazine [129], doxorubicin, and hydrocortisone [130]. However, incorporation of water soluble drugs is not efficient and the preferred method may be the double-emulsion method [131] where the hydrophilic drug is dissolved in an aqueous phase, which is added to the polymer containing, organic phase before emulsification into the outer water phase. The double-emulsion technique has been applied in the encapsulation of water soluble drugs, in particular, proteins and peptides [132-134].

These techniques have been applied in the creation of oral sustained release microparticles containing the drug nitrofurantoin [135]. In this case a modified solvent evaporation method [136] was employed, which allowed the introduction of an enteric coating of the nitrofurantoin microparticles. A

gastroretentive, sustained release system for ketoprofen was produced using the emulsion method [137] with good encapsulation and a high percentage of particles demonstrating buoyancy following 6 h in simulated gastric fluid. Although well characterised, the emulsion techniques require complex multi-step processes which are difficult to scale up economically. The use of volatile organic solvents is a major limitation as any toxic residues must be removed from the final product.

1.5.2 Supercritical Fluid Technology

A recent novel method of processing polymers has been developed using supercritical fluids. A supercritical fluid has been described as ‘any substance, the temperature and pressure of which are higher than their critical values, and which has a density close to or higher than its critical density’. Publications in the area appearing from 1991 [138, 139] have described a technique which may evade the use of toxic organic solvents (‘green technology’) and complex multi-step procedures.

1.5.2.1 Supercritical Carbon Dioxide Technology

Supercritical fluid refers to a phase of material which is an intermediary phase between gaseous and liquid. By increasing the temperature and pressure of substances to beyond the thermodynamic critical point, a phase boundary is broken and a new single phase is revealed. Supercritical fluids have the diffuse abilities of a gas and can dissolve materials like a liquid.

Carbon dioxide (CO_2) is an ideal choice as it is cheap, nontoxic, non-inflammable, recyclable and has a mild critical temperature ($T_c=304.2\text{K}$, $P_c=7.3\text{MPa}$). A typical phase diagram is illustrated in Figure 1.7 [140].

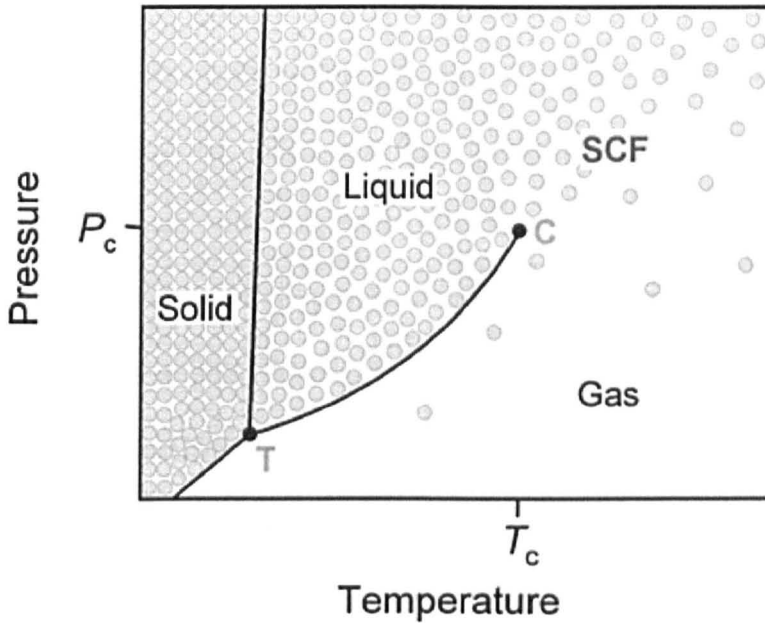


Figure 1.7 Pressure-temperature phase diagram for a pure component showing the triple point (T) and the critical point (C). The supercritical region (SCF) is demonstrated past the critical point. The density of the component is illustrated by the grey circles [140].

The phase diagram demonstrates the boundaries between the three conventional states of matter. As temperature and pressure of a liquid increase, the liquid will expand and therefore the density will decrease. Conversely, as the temperature and pressure of a gas is increased the density will increase. Eventually, as the critical temperature and pressure is reached, the densities of the gas and the liquid are identical and there is no longer any distinction between the two phases. The disappearance of the phase boundary is indicative of the supercritical fluid [140, 141]. A supercritical fluid is therefore denser

than a gas and with the ability to dissolve solids while simultaneously demonstrating diffusivity. Furthermore, it is possible to make minute changes to the processing conditions which will in turn have a large impact on the properties of the fluid enabling control over the processing of polymers.

The use of supercritical CO₂ (scCO₂) in particle formation has been around for a couple of decades with various reviews emerging in this area [142-146]. However CO₂ is not the only option for supercritical fluid technology as there are many substances with obtainable critical points (Table 1.2). Water is an example of a substance with no toxicity and flammability issues. However, its critical temperatures and pressures are high and introduces processing issues which render water less viable [147]. Substances with more ambient critical points such as sulphur hexafluoride (SF₆) although non inflammable encounter other limitations such as the concerns over SF₆ as a greenhouse gas.

Table 1.2 Critical conditions P_c , T_c , ρ_c for selected substances

Substance	P_c (bar)	T_c (°C)	ρ_c (gcm ⁻³)
CO ₂	73.8	31.1	0.47
N ₂ O	72.5	36.5	0.45
SF ₆	37.1	45.5	0.74
Xe	58.4	16.6	1.10
CH ₃ OH	78.9	240.5	0.27
CH ₃ CH(OH)CH ₃	47.0	235.3	0.27
H ₂ O	218	374	0.32

scCO₂ is widely used in extraction: for example, in the food industry, for the extraction of fat from meat products [148], the production of decaffeinated coffee [149, 150], the extraction of cholesterol from dried egg yolk [151]. The extraction process requires the extracted substance to be soluble in scCO₂. scCO₂ can also be used for the recovery of and separation of organic products [152]. The plasticisation effect of scCO₂ on polymers is well established [153] and may be utilised to achieve high polymerisation rates using various methods.

As well as polymer synthesis, scCO₂ has been applied in polymer processing to form various structures. scCO₂ has been applied in the production of polymer foams, including the production of poly(methyl methacrylate) (PMMA) foams to generate a microcellular core surrounded by a non-porous skin [154]. Such microcellular structures have applications in adsorbants, controlled release, separation media, and catalyst supports. Foams prepared of a PMMA and poly(vinylidene) (PVDF) blend, have demonstrated improved morphologies, compared to foams composed solely of the highly crystalline polymer PVDF [155]. It is possible to tailor the properties of these foams by manipulating the molecular weight of the polymer [156], or the processing parameter [154].

scCO₂ has also been applied in the production of particles of various biocompatible polymers for the encapsulation of therapeutic agents [146, 157]. There are a number of techniques that have been adapted to use scCO₂ in the production of particles for pharmaceutical applications. In each method, scCO₂ demonstrates a different function depending on its solvent properties or its solubility in polymers. CO₂ is a good solvent for non polar and low molecular

weight compounds and certain polymers such as amorphous, fluoropolymers, and siloxane-based polymers [158, 159]. scCO_2 may also diffuse within a liquefied polymer, the extent of the solubility depends upon the molecular structure and the morphology of the polymer [126]. The dissolved scCO_2 in the polymer may reduce the glass transition temperature (T_g), allowing plasticisation to occur at lower temperatures [160]. scCO_2 has been shown to interact with polycarbonate (PC) and polysulfonate (PSF) [161], as well as poly(ethylene glycol) (PEG, and polyphenylene oxide (PPO) [162].

Owing to the poor solubility of many compounds, in some supercritical fluid techniques, scCO_2 has been used as an antisolvent where the compound is dissolved in a conventional organic solvent which will dissolve in scCO_2 . On introduction of scCO_2 to the organic solvent, compound mixture will increase in density and therefore crystallization of the compound can take place.

1.5.2.2 Rapid Expansion of Supercritical Fluid Solutions Method

There has been development of a number of modified processes for the application of scCO_2 . Rapid expansion of supercritical solutions (RESS) [163] utilises scCO_2 as a solvent (in which the compound is dissolved) and therefore the polymer must have a degree of solubility in scCO_2 . When the solution is depressurized through a nozzle, the temperature change decreases the solvent power, leading to precipitation of the solute. The governing principle of RESS is pressure induced phase separation [146]. RESS has previously been used in coatings [164, 165] and was first applied in the production of drug loaded microparticles in 1993 [166]. Since this time, RESS has been used to produce microstructures of a poly(styrene)-*b*-(poly(methyl methacrylate))-*co*-poly

(glycidyl methacrylate)) copolymer [167], poly (lactic acid) [168], polystyrene [169], and PGA [170]. It has also been used with encapsulation of drugs such as the non-steroidal anti-inflammatory drugs naproxen [168], and ibuprofen [171]. In the latter study, ATR-IR spectroscopy was used to study the films produced, with a molecular interaction between the ibuprofen and the polymeric matrix (poly (vinylpyrrolidone)) being revealed. This was confirmed using Raman spectroscopy. The proteins lipase [172] and BSA [173] have both been encapsulated using RESS with good sustained release of BSA over 24 h being achieved.

A major drawback with the RESS method is that the drug and polymer must be soluble in scCO₂, which few compounds are, and therefore modifications to the process have emerged in an attempt to widen the scope of applications. Co-solvents are a common addition to the process; suitable co-solvents include: ethanol [167], which allowed the processing of polymers such as poly(styrene)-*b*-(poly(methyl methacrylate)-*co*-poly (glycidyl methacrylate)) copolymer, PEG and PMMA. These polymers demonstrate poor solubility in CO₂ and ethanol but the two solvents combined allowed adequate processing into microparticles. Co-solvents such as acetone [174], chlorodifluoromethane [175], and methanol [176] have been used successfully to improve processing. However, the use of co-solvents introduces problems with drug stability for protein drugs, as well as solvent removal and residues in the final product.

1.5.2.3 Gas Anti-Solvent (GAS) Method

Owing to the problems of processing biodegradable polymers, an alternative processes where scCO_2 is used as an anti-solvent has been developed. This system is more suitable for several polymers, as the process uses a conventional organic solvent in which the drug/polymer is dissolved, before scCO_2 is used to supersaturate the solvent. The GAS process recrystallizes solid compounds that are not soluble in supercritical fluids [177, 178]. It is therefore especially appropriate for polymers.

GAS is the scCO_2 technique often used to encapsulate protein drugs [179, 180] but has also been applied in the production of carbamazepine loaded PEG particles [181], and hydrocortisone/PVP composites [182]. scCO_2 has been applied as an anti-solvent in the processing of poly(L-lactic acid) to create a porous scaffold [183]. In this case, the use of scCO_2 is particularly advantageous for the creation of pores, as they will simply occur from the dispelling CO_2 from within the matrix on particle formation.

scCO_2 can be used as an anti-solvent, and techniques utilising this include GAS, SAS, PCA, ASES and SEDS. All these techniques use a traditional organic solvent to dissolve the solute and then the scCO_2 is used to supersaturate the solution and precipitate the solute. This works, as when the dense CO_2 is introduced to the organic solvent, the liquid phase is expanded and the solvent power of the solvent decreases, leading to particle formation.

The choice of solvent for dissolving the drug/ polymer components must allow the drug and polymer to be dissolved, while simultaneously being soluble in scCO_2 itself. However, as with the application of a co-solvent in the RESS

technique, there are issues arising from the use of a conventional organic solvent.

1.5.2.4 Supercritical Anti-solvent (SAS) Method

This technique is similar to GAS, whereby the supercritical fluid acts as an anti-solvent for polymers. However, the contacting mechanism is different. It has been modified for both batch and continuous processes and used in the processing of explosives, polymers, and pharmaceutical products, superconductors and catalysts [184]. Rifampicin micro- and nano-particles have been produced, using DMSO as the organic solvent [185]. Similarly DMSO was the solvent of choice for the micronization of salbutamol [186]. The co-precipitation of PLA and paclitaxel used a modified SAS process, which introduces ultra-sonic vibrations for the production of more uniform particles with a narrower size distribution. Paclitaxel was encapsulated at 83.5% and release was sustained over 30 days [187].

Similar techniques to SAS include aerosol solvent extraction system (ASES), where the $scCO_2$ flows in a counter current against the solution, or precipitation with a compressed antisolvent (PCA). In this method, the polymer is dissolved in a liquid solvent, it is then sprayed into a chamber where the supercritical fluid antisolvent already exists. These two techniques have also been used in pharmaceutical processing [188, 189].

1.5.2.5 Solution Enhanced Dispersion by Supercritical Fluids (SEDS)

Method

This is a similar technique to SAS, although the liquid solution and supercritical fluid are sprayed together using a specially designed coaxial nozzle [146]. The two high-speed streams of the solution and the supercritical fluid are able to generate a finely dispersed mixture and give particle precipitation. It is possible to use three processing components, such as two different supercritical fluids and one organic solvent which can convey versatility on the system. Advantages of this process include the ability to process aqueous solutions allowing the formation of particles from proteins and sugars. Biodegradable microparticles can be prepared using this system [190, 191]. 5-Fluorouracil was micronized and used to produce microparticles with PLA utilising dichloromethane as a solvent [192]. The preparation of particles without the use of organic solvent have been attempted using this technique, however, without an organic solvent the resultant product is wet with a suitable dry powder very difficult to obtain [193].

1.5.2.6 Particles from Gas Saturated Solutions (PGSS) Method

The PGSS method differs from the above methods as scCO_2 is not being relied upon as a solvent or an anti-solvent. The high solubility of CO_2 in some materials is exploited in this method and may lead to a gas saturated solution. It is often the case that the interaction of scCO_2 with a polymer reduces the glass transition temperature, allowing plasticization to occur at more ambient temperatures [153]. A key advantage of this technique is that the polymer and drug do not need to be soluble in scCO_2 , but it does require the polymer to be

plasticized by the scCO₂. The polymer and therapeutic agent are placed in a chamber where the temperature is increased and CO₂ is pumped in up to a set pressure. As the temperature and pressure increase, the polymer will plasticise. The stirring of the polymer and drug particles creates a homogenous mixture which upon depressurisation will solidify trapping the drug particles.

The PGSS method was originally developed for the production of powder coatings [194] and has also been applied in the food industry [195]. More recently the process has been used in the production of pharmaceutical products. The T_g lowering effect of the scCO₂ in this process has enabled the encapsulation of protein drugs. Human growth hormone was encapsulated in PLGA/PLA microparticles with high encapsulation efficiencies and good sustained release over 14 days [196]. Ribonuclease A and lysozyme have also been incorporated into PLA microparticles [197] with no significant loss of protein activity.

Porous scaffolds for applications in tissue engineering have been prepared using the PGSS technique [198, 199]. However, by implementing a spraying step in the process, various structures can be prepared. Fibres or microparticles can be manufactured by introducing a back pressure in the collection chamber [153]. The back pressure is usually created using nitrogen gas as it is relatively inert and will not plasticise polymers under the operating conditions allowing solidification. It also exerts control over product morphology, by regulating the diffusion of carbon dioxide out of the solidifying polymer. The viscosity of the polymer mixture can impact the atomisation step in this process [153, 200].

Benefits of this technique over the other methods of particle formation include the absence of conventional solvents during processing, by-passing the problems with toxic products in the dosage form. It also does not require the polymer or the drug to be soluble in $scCO_2$, and so mild processing conditions are used.

1.6 Project Aims

The introduction of gastroretentive delivery systems have enabled more efficient delivery of candidate drugs which demonstrate narrow absorption windows in the upper GIT, however, very few systems have proven successful enough to reach the market. Although there has been poor *in vitro-in vivo* correlation with these systems, a combination of buoyancy and mucoadhesion may improve oral bioavailability.

The supercritical fluid method, PGSS, is a novel polymer processing technique which enables the production of highly porous microparticles without the use of volatile organic solvents, or high temperatures. This thesis aims to apply the PGSS technique to the design of highly porous biodegradable polymeric particles capable of gastric retention. The process parameters, and specific particle properties required to achieve gastroretention thus improving oral delivery of 'problematic' drugs will be investigated.

In vitro analysis, aims to establish a fundamental understanding of a correlation between the buoyancy of particles and their physicochemical properties (including size, density, and morphology). Buoyant particles will be loaded with suitable candidate drugs (furosemide, metformin, riboflavin) and the drug loading potential and release profile of the formulation will be determined and optimized to correlate with the potential gastric retention time.

The choice of these three therapeutics was justified as all three are characterised by narrow absorption windows in the upper small intestine. The three drugs exhibit differing solubilities enabling comparisons to be made of their release properties. The mucoadhesive polymer chitosan and its derivative chitosan-NAC will be introduced to the system with the aim of introducing mucoadhesive properties to the buoyant particles, potentially augmenting gastroretention. *In vitro* analysis of mucoadhesion will be investigated.

The success of selected formulations will be evaluated *in vivo* and plasma concentration profiles prepared in order to allow conclusions to be drawn upon the success of the system as a potential new drug delivery system for the oral route.

1.7 References

1. Kawabata, Y., et al., *Formulation design for poorly water-soluble drugs based on biopharmaceutics classification system: Basic approaches and practical applications*. International Journal of Pharmaceutics. **420**(1): p. 1-10.
2. Heimbach, T., D. Fleisher, and A. Kaddoumi, *Overcoming Poor Aqueous Solubility of Drugs for Oral Delivery*, in *Prodrugs: Challenges and Rewards, Part 1*. 2007. p. 157-215.
3. Lipinski, C.A., *Drug-like properties and the causes of poor solubility and poor permeability*. Journal of Pharmacological and Toxicological Methods, 2000. **44**(1): p. 235-249.
4. Allen, T.M. and P.R. Cullis, *Drug delivery systems: Entering the mainstream*. Science, 2004. **303**(5665): p. 1818-1822.
5. Kogan, A., et al., *Premedication with midazolam in young children: a comparison of four routes of administration*. Paediatric Anaesthesia, 2002. **12**(8): p. 685-689.
6. Shojaei, A.H., *Buccal mucosa as a route for systemic drug delivery: a review*. Journal of pharmacy & pharmaceutical sciences : a publication of the Canadian Society for Pharmaceutical Sciences, Societe canadienne des sciences pharmaceutiques, 1998. **1**(1): p. 15-30.
7. Colombo, P., et al., *Novel Platforms for Oral Drug Delivery*. Pharmaceutical Research, 2009. **26**(3): p. 601-611.
8. Claxton, A.J., J. Cramer, and C. Pierce, *A systematic review of the associations between dose regimens and medication compliance*. Clinical Therapeutics, 2001. **23**(8): p. 1296-1310.

9. <http://www.ncbi.nlm.nih.gov/books/NBK22183/>. 1998 .
10. Washington, N., *Physiological Pharmaceutics: barriers to Drug Absorption*. 2000: CRC Press.
11. G.R. Agarwal, O.P.A., K. Agarwal, *Text Book of Biochemistry*. 14th ed. 2007: GOEL Publishing House. 711.
12. Parsa, S. <http://anatomytopics.wordpress.com/tag/gastric-pits/>. 2012 [cited 2012 10th July 2012].
13. Johnson, L.R., *Gastrointestinal physiology* Fifth ed, ed. L.R. Johnson. 1997: Mosby. 179.
14. Brooks, F.P., *Effect of diet on gastric-secretion*. American Journal of Clinical Nutrition, 1985. **42**(5): p. 1006-1019.
15. Dragstedt, L.R., et al., *Quantitative studies on the mechanism of gastric secretion in health and disease*. Transactions of the ... Meeting of the American Surgical Association. American Surgical Association. Meeting, 1950. **68**: p. 305-19.
16. Wolfe, M.M. and A.H. Soll, *The physiology of gastric-acid secretion*. New England Journal of Medicine, 1988. **319**(26): p. 1707-1715.
17. Fallingborg, J., et al., *pH-profile and regional transit times of the normal gut measured by a radiotelemetry device*. Alimentary Pharmacology & Therapeutics, 1989. **3**(6): p. 605-613.
18. Horter, D. and J.B. Dressman, *Influence of physicochemical properties on dissolution of drugs in the gastrointestinal tract*. Advanced Drug Delivery Reviews, 2001. **46**(1-3): p. 75-87.
19. Kalantzi, L., et al., *Characterization of the human upper gastrointestinal contents under conditions simulating bioavailability/bioequivalence studies*. Pharmaceutical Research, 2006. **23**(1): p. 165-176.
20. Gajjar, D.A., et al., *Effect of a high-fat meal on the pharmacokinetics of the des-F(6)-quinolone BMS-284756*. Pharmacotherapy, 2002. **22**(2): p. 160-165.
21. Klein, S., et al., *Media to simulate the postprandial stomach I. Matching the physicochemical characteristics of standard breakfasts*. Journal of Pharmacy and Pharmacology, 2004. **56**(5): p. 605-610.
22. Gardner, J.D., A.A. Ciociola, and M. Robinson, *Measurement of meal-stimulated gastric acid secretion by in vivo gastric autotitration*. Journal of Applied Physiology, 2002. **92**(2): p. 427-434.
23. McConnell, E.L., H.M. Fadda, and A.W. Basit, *Gut instincts: Explorations in intestinal physiology and drug delivery*. International Journal of Pharmaceutics, 2008. **364**(2): p. 213-226.
24. Khan, M.Z.I., Z. Prebeg, and N. Kurjakovic, *A pH-dependent colon targeted oral drug delivery system using methacrylic acid copolymers: I. Manipulation of drug release using Eudragit(R) L100-55 and Eudragit(R) S100 combinations*. Journal of Controlled Release, 1999. **58**(2): p. 215-222.
25. Mehta, K.A., et al., *Release performance of a poorly soluble drug from a novel: Eudragit (R)-based multi-unit erosion matrix*. International Journal of Pharmaceutics, 2001. **213**(1-2): p. 7-12.
26. Perumal, D., *Microencapsulation of ibuprofen and Eudragit (R) RS 100 by the emulsion solvent diffusion technique*. International Journal of Pharmaceutics, 2001. **218**(1-2): p. 1-11.

27. Lowman, A.M., et al., *Oral delivery of insulin using pH-responsive complexation gels*. Journal of Pharmaceutical Sciences, 1999. **88**(9): p. 933-937.
28. Jain, D., D.K. Majumdar, and A.K. Panda, *Insulin loaded Eudragit L100 microspheres for oral delivery: Preliminary in vitro studies*. Journal of Biomaterials Applications, 2006. **21**(2): p. 195-211.
29. Aceves, J.M., R. Cruz, and E. Hernandez, *Preparation and characterization of Furosemide-Eudragit controlled release systems*. International Journal of Pharmaceutics, 2000. **195**(1-2): p. 45-53.
30. Trenkrog, T., et al., *Enteric coated insulin pellets: Development, drug release and in vivo evaluation*. European Journal of Pharmaceutical Sciences, 1996. **4**(6): p. 323-329.
31. Pal, A., et al., *Gastric flow and mixing studied using computer simulation*. Proceedings of the Royal Society of London Series B-Biological Sciences, 2004. **271**(1557): p. 2587-2594.
32. Kong, F. and R.P. Singh, *Disintegration of solid foods in human stomach*. Journal of Food Science, 2008. **73**(5): p. R67-R80.
33. Stanghellini, V., et al., *Fasting and postprandial gastrointestinal motility in ulcer and nonulcer dyspepsia*. Gut, 1992. **33**(2): p. 184-190.
34. Sarna, S.K., *Cyclic motor-activity- Migrating motor complex - 1985*. Gastroenterology, 1985. **89**(4): p. 894-913.
35. Kelly, K.A., *Gastric-emptying of liquids and solids- ROles of proximal and distal stomach*. American Journal of Physiology, 1980. **239**(2): p. G71-G76.
36. Santangelo, A., et al., *Physical state of meal affects gastric emptying, cholecystokinin release and satiety*. British Journal of Nutrition, 1998. **80**(6): p. 521-527.
37. Stacher, G., et al., *Slow gastric-emptying induced by high-fat content of a meal accelerated by cisapride administered rectally*. Digestive Diseases and Sciences, 1991. **36**(9): p. 1259-1265.
38. French, S.J. and N.W. Read, *Effect of guar gum on hunger and satiety after meals of differing fat-content-Relationship with gastric-emptying*. American Journal of Clinical Nutrition, 1994. **59**(1): p. 87-91.
39. Meyer, J.H., et al., *Gastric processing and emptying of fat*. Gastroenterology, 1986. **90**(5): p. 1176-1187.
40. Van Citters, G.W. and H.C. Lin, *The ileal brake: a fifteen-year progress report*. Current gastroenterology reports, 1999. **1**(5): p. 404-9.
41. Brown, N.J., et al., *Characteristics of lipid substances activating the ileal brake in the rat*. Gut, 1990. **31**(10): p. 1126-1129.
42. Chang, C.A., R.D. McKenna, and I.T. Beck, *Gastric emptying rate of water and fat phases of a mixed test meal in man*. Gut, 1968. **9**(4): p. 420-&.
43. Schulze, K., *Imaging and modelling of digestion in the stomach and the duodenum*. Neurogastroenterology and Motility, 2006. **18**(3): p. 172-183.
44. McLaughlin, J., et al., *Fatty acid chain length determines cholecystokinin secretion and effect on human gastric motility*. Gastroenterology, 1999. **116**(1): p. 46-53.
45. Jian, R., et al., *Effect of ethanol ingestion on postprandial gastric-emptying and secretion biliopancreatic secretions, and duodenal*

- absorption in man*. Digestive Diseases and Sciences, 1986. 31(6): p. 604-614.
46. Barboria.Jj and R.C. Meade, *Effect of alcohol on gastric-emptying in man*. American Journal of Clinical Nutrition, 1970. 23(9): p. 1151-&.
 47. Chaudhuri, T.K. and S. Fink, *Gastric-emptying in human disease states*. American Journal of Gastroenterology, 1991. 86(5): p. 533-538.
 48. Mojaverian, P., et al., *Effects of gender, posture, and age on gastric residence time of an indigestible solid- Pharmaceutical considerations*. Pharmaceutical Research, 1988. 5(10): p. 639-644.
 49. Madsen, J.L., *Effects of gender, age, and body-mass index on gastrointestinal transit times*. Digestive Diseases and Sciences, 1992. 37(10): p. 1548-1553.
 50. Lorena, S.L.S., et al., *Gastric emptying and intragastric distribution of a solid meal in functional dyspepsia - Influence of gender and anxiety*. Journal of Clinical Gastroenterology, 2004. 38(3): p. 230-236.
 51. Davis, S.S., *Formulation strategies for absorption windows*. Drug Discovery Today, 2005. 10(4): p. 249-257.
 52. Hoerter, D. and J.B. Dressman, *Influence of physicochemical properties on dissolution of drugs in the gastrointestinal tract*. Advanced Drug Delivery Reviews, 2001. 46(1-3): p. 75-87.
 53. Pouton, C.W., *Formulation of poorly water-soluble drugs for oral administration: Physicochemical and physiological issues and the lipid formulation classification system*. European Journal of Pharmaceutical Sciences, 2006. 29(3-4): p. 278-287.
 54. Garg, R. and G.D. Gupta, *Progress in Controlled Gastroretentive Delivery Systems*. Tropical Journal of Pharmaceutical Research, 2008. 7(3): p. 1055-1066.
 55. Rouge, N., P. Buri, and E. Doelker, *Drug absorption sites in the gastrointestinal tract and dosage forms for site-specific delivery*. International Journal of Pharmaceutics, 1996. 136(1-2): p. 117-139.
 56. Kagan, L. and A. Hoffman, *Systems for region selective drug delivery in the gastrointestinal tract: biopharmaceutical considerations*. Expert Opinion on Drug Delivery, 2008. 5(6): p. 681-692.
 57. Urquhart, J., *Controlled drug delivery: therapeutic and pharmacological aspects*. Journal of Internal Medicine, 2000. 248(5): p. 357-376.
 58. Sohi, H., Y. Sultana, and R.K. Khar, *Taste masking technologies in oral pharmaceuticals: Recent developments and approaches*. Drug Development and Industrial Pharmacy, 2004. 30(5): p. 429-448.
 59. Wen H., P.K., *Oral Controlled Release Formulation Design and Drug Delivery: Theory to Practice*. 2010: John Wiley & Sons, Inc.
 60. Helfand, W.H. and D.L. Cowen, *Evolution of pharmaceutical oral dosage forms*. Pharmacy in history, 1983. 25(1): p. 3-18.
 61. Grassi, M. and G. Grassi, *Mathematical modelling and controlled drug delivery: Matrix systems*. Current Drug Delivery, 2005. 2(1): p. 97-116.
 62. Huang, X. and C.S. Brazel, *On the importance and mechanisms of burst release in matrix-controlled drug delivery systems*. Journal of Controlled Release, 2001. 73(2-3): p. 121-136.

63. Verma, R.K., D.M. Krishna, and S. Garg, *Formulation aspects in the development of osmotically controlled oral drug delivery systems*. *Journal of Controlled Release*, 2002. **79**(1-3): p. 7-27.
64. Dmochowski, R.R. and D.R. Staskin, *Advances in drug delivery: improved bioavailability and drug effect*. *Current urology reports*, 2002. **3**(6): p. 439-44.
65. Charman, W.N., et al., *Physicochemical and physiological mechanisms for the effects of food on drug absorption: The role of lipids and pH*. *Journal of Pharmaceutical Sciences*, 1997. **86**(3): p. 269-282.
66. Croutham.Wg, et al., *Drug absorption. 4. Influence of pH on absorption kinetics of weakly acidic drugs*. *Journal of Pharmaceutical Sciences*, 1971. **60**(8): p. 1160-&.
67. Ishak, R.A.H., et al., *Preparation, in vitro and in vivo evaluation of stomach-specific metronidazole-loaded alginate beads as local anti-Helicobacter pylori therapy*. *Journal of Controlled Release*, 2007. **119**(2): p. 207-214.
68. Parikh, D.C. and A.F. Amin, *In vitro and in vivo techniques to assess the performance of gastro-retentive drug delivery systems: a review*. *Expert Opinion on Drug Delivery*, 2008. **5**(9): p. 951-965.
69. Pawar, V.K., et al., *Industrial perspective of gastroretentive drug delivery systems: Physicochemical, biopharmaceutical, technological and regulatory consideration*. *Expert Opinion on Drug Delivery*. **9**(5): p. 551-565.
70. Prinderre, P., C. Sauzet, and C. Fuxen, *Advances in gastro retentive drug-delivery systems*. *Expert Opinion on Drug Delivery*. **8**(9): p. 1189-1203.
71. Kotreka, U.K. and M.C. Adeyeye, *Gastroretentive Floating Drug-Delivery Systems: A Critical Review*. *Critical Reviews in Therapeutic Drug Carrier Systems*. **28**(1): p. 47-99.
72. Streubel, A., J. Siepmann, and R. Bodmeier, *Drug delivery to the upper small intestine window using gastroretentive technologies*. *Current Opinion in Pharmacology*, 2006. **6**(5): p. 501-508.
73. Klausner, E.A., et al., *Novel gastroretentive dosage forms: Evaluation of gastroretentivity and its effect on levodopa absorption in humans*. *Pharmaceutical Research*, 2003. **20**(9): p. 1466-1473.
74. Swarnalatha, S., et al., *A novel amphiphilic nano hydrogel using ketene based polyester with polyacrylamide for controlled drug delivery system*. *Journal of Materials Science-Materials in Medicine*, 2008. **19**(9): p. 3005-3014.
75. Shalaby, W.S.W., W.E. Blevins, and K. Park, *Gastric retention of enzyme-digestible hydrogels in the canine stomach under fasted and fed conditions- Preliminary analysis using new analytical techniques*. *Acs Symposium Series*, 1991. **469**: p. 237-248.
76. Park, K. and J.R. Robinson, *Bioadhesive Polymers as Platforms for Oral-Controlled Drug Delivery - Method to Study Bioadhesion*. *International Journal of Pharmaceutics*, 1984. **19**(2): p. 107-127.
77. Lehr, C.M., *Bioadhesion technologies for the delivery of peptide and protein drugs to the gastrointestinal-tract*. *Critical Reviews in Therapeutic Drug Carrier Systems*, 1994. **11**(2-3): p. 119-160.

78. Leung, S.H.S. and J.R. Robinson, *Polyanionic polymers in bioadhesive and mucoadhesive drug delivery*. ACS Symposium Series, 1992. **480**: p. 269-284.
79. Park, H. and J.R. Robinson, *Mechanisms of mucial adhesion of poly(acrylic acid) hydrogels*. *Pharmaceutical Research*, 1987. **4**(6): p. 457-464.
80. Leung S-H, S. and J.R. Robinson, *The contribution of anionic polymer structural features to mucoadhesion*. *Journal of Controlled Release*, 1988. **5**(3): p. 223-232.
81. Smart, J.D., *An in vitro assessment of some mucosa-adhesive dosage forms*. *International Journal of Pharmaceutics*, 1991. **73**(1): p. 69-74.
82. Patel, J.K. and J.R. Chavda, *Formulation and evaluation of stomach-specific amoxicillin-loaded carbopol-934P mucoadhesive microspheres for anti-Helicobacter pylori therapy*. *Journal of Microencapsulation*, 2009. **26**(4): p. 365-376.
83. Takeuchi, H., et al., *Mucoadhesive properties of carbopol or chitosan-coated liposomes and their effectiveness in the oral administration of calcitonin to rats*. *Journal of Controlled Release*, 2003. **86**(2-3): p. 235-242.
84. Bonacucina, G., S. Martelli, and G.F. Palmieri, *Rheological, mucoadhesive and release properties of Carbopol gels in hydrophilic cosolvents*. *International Journal of Pharmaceutics*, 2004. **282**(1-2): p. 115-130.
85. Grabovac, V., D. Guggi, and A. Bernkop-Schnurch, *Comparison of the mucoadhesive properties of various polymers*. *Advanced Drug Delivery Reviews*, 2005. **57**(11): p. 1713-1723.
86. He, P., S.S. Davis, and L. Illum, *In vitro evaluation of the mucoadhesive properties of chitosan microspheres*. *International Journal of Pharmaceutics*, 1998. **166**(1): p. 75-88.
87. Lehr, C.M., et al., *In vitro evaluation of mucoadhesive properties of chitosan and some other natural polymers*. *International Journal of Pharmaceutics*, 1992. **78**(1): p. 43-48.
88. Sinha, V.R., et al., *Chitosan microspheres as a potential carrier for drugs*. *International Journal of Pharmaceutics*, 2004. **274**(1-2): p. 1-33.
89. Sakkinen, M., et al., *Are chitosan formulations mucoadhesive in the human small intestine? An evaluation based on gamma scintigraphy*. *International Journal of Pharmaceutics*, 2006. **307**(2): p. 285-291.
90. Patil, S.B. and K.K. Sawant, *Development, optimization and in vitro evaluation of alginate mucoadhesive microspheres of carvedilol for nasal delivery*. *Journal of Microencapsulation*, 2009. **26**(5): p. 432-443.
91. Shadab, et al., *Gastroretentive drug delivery system of acyclovir-loaded alginate mucoadhesive microspheres: formulation and evaluation*. *Drug Delivery*. **18**(4): p. 255-64.
92. Piao, J., et al., *Development of novel mucoadhesive pellets of metformin hydrochloride*. *Archives of Pharmacal Research*, 2009. **32**(3): p. 391-397.
93. Bernkop-Schnurch, A. and S. Steininger, *Synthesis and characterisation of mucoadhesive thiolated polymers*. *International Journal of Pharmaceutics*, 2000. **194**(2): p. 239-247.

94. Gum, J.R., et al., *The human MUC2 intestinal mucin has cysteine-rich subdomains located both upstream and downstream of its central repetitive region*. Journal of Biological Chemistry, 1992. **267**(30): p. 21375-21383.
95. Langoth, N., et al., *Thiolated chitosans: Design and in vivo evaluation of a mucoadhesive buccal peptide drug delivery system*. Pharmaceutical Research, 2006. **23**(3): p. 573-579.
96. Bernkop-Schnurch, A., D. Guggi, and Y. Pinter, *Thiolated chitosans: development and in vitro evaluation of a mucoadhesive, permeation enhancing oral drug delivery system*. Journal of Controlled Release, 2004. **94**(1): p. 177-186.
97. Sreenivas, S.A. and K.V. Pai, *Thiolated Chitosans: Novel Polymers for Mucoadhesive Drug Delivery - A Review*. Tropical Journal of Pharmaceutical Research, 2008. **7**(3): p. 1077-1088.
98. Dhaliwal, S., et al., *Mucoadhesive microspheres for gastroretentive delivery of acyclovir: In vitro and in vivo evaluation*. Aaps Journal, 2008. **10**(2): p. 322-330.
99. Senyigit, Z.A., et al., *Gastroretentive particles formulated with thiomers: development and in vitro evaluation*. Journal of Drug Targeting, 2010. **18**(5): p. 362-372.
100. Bernkop-Schnurch, A., et al., *Thiomers: potential excipients for non-invasive peptide delivery systems*. European Journal of Pharmaceutics and Biopharmaceutics, 2004. **58**(2): p. 253-263.
101. E. Touitou, B.W.B., *Enhancement in Drug Delivery*. 2006: CRC Press. 633.
102. Bechgaard, H. and K. Ladefoged, *Distribution of pellets in gastrointestinal tract- Influence on transit time exerted by density or diameter of pellets*. Journal of Pharmacy and Pharmacology, 1978. **30**(11): p. 690-692.
103. Bhadouriya, P., M. Kumar, and K. Pathak, *Floating Microspheres - to Prolong the Gastric Retention Time in Stomach*. Current Drug Delivery. **9**(3): p. 315-324.
104. Sathish, D., et al., *Floating Drug Delivery Systems for Prolonging Gastric Residence Time: A Review*. Current Drug Delivery. **8**(5): p. 494-510.
105. Davis, W.D., *Method of swallowing a pill*, US, Editor. 1968.
106. Singh, B.N. and K.H. Kim, *Floating drug delivery systems: an approach to oral controlled drug delivery via gastric retention*. Journal of Controlled Release, 2000. **63**(3): p. 235-259.
107. Elkhesheh, S.A., et al., *In vitro and in vivo evaluation of floating controlled release dosage forms of verapamil hydrochloride*. Pharmazeutische Industrie, 2004. **66**(11): p. 1364-1372.
108. Rahman, Z., M. Ali, and R. Khar, *Design and evaluation of bilayer floating tablets of captopril*. Acta Pharmaceutica (Zagreb), 2006. **56**(1): p. 49-57.
109. Tadros, M.I., *Controlled-release effervescent floating matrix tablets of ciprofloxacin hydrochloride: Development, optimization and in vitro-in vivo evaluation in healthy human volunteers*. European Journal of Pharmaceutics and Biopharmaceutics, 2010. **74**(2): p. 332-339.

110. Hashim, H. and A.L.W. Po, *Improving the release characteristics of water-soluble drugs from hydrophilic sustained-release matrices by in situ gas generation*. International Journal of Pharmaceutics, 1987. **35**(3): p. 201-209.
111. Oth, M., et al., *The bilayer floating capsule- A stomach directed drug delivery system for misoprostol*. Pharmaceutical Research, 1992. **9**(3): p. 298-302.
112. Yang, L.B., J. Eshraghi, and R. Fassihi, *A new intragastric delivery system for the treatment of Helicobacter pylori associated gastric ulcer: in vitro evaluation*. Journal of Controlled Release, 1999. **57**(3): p. 215-222.
113. Ma, N.N., et al., *Development and evaluation of new sustained-release floating microspheres*. International Journal of Pharmaceutics, 2008. **358**(1-2): p. 82-90.
114. Streubel, A., J. Siepmann, and R. Bodmeier, *Floating matrix tablets based on low density foam powder: effects of formulation and processing parameters on drug release*. European Journal of Pharmaceutical Sciences, 2003. **18**(1): p. 37-45.
115. Streubel, A., J. Siepmann, and R. Bodmeier, *Multiple unit gastroretentive drug delivery systems: a new preparation method for low density microparticles*. Journal of Microencapsulation, 2003. **20**(3): p. 329-347.
116. Sato, Y., et al., *In vitro and in vivo evaluation of riboflavin-containing microballoons for a floating controlled drug delivery system in healthy humans*. International Journal of Pharmaceutics, 2004. **275**(1-2): p. 97-107.
117. Joseph, N.J., S. Lakshmi, and A. Jayakrishnan, *A floating-type oral dosage form for piroxicam based on hollow polycarbonate microspheres: In vitro and in vivo evaluation in rabbits*. Journal of Controlled Release, 2002. **79**(1-3): p. 71-79.
118. Jain, S.K., et al., *Calcium silicate based microspheres of repaglinide for gastroretentive floating drug delivery: Preparation and in vitro characterization*. Journal of Controlled Release, 2005. **107**(2): p. 300-309.
119. Pandya, N., M. Pandya, and V.H. Bhaskar, *Preparation and in vitro Characterization of Porous Carrier-Based Glipizide Floating Microspheres for Gastric Delivery*. Journal of young pharmacists : JYP, 2011. **3**(2): p. 97-104.
120. Badve, S.S., et al., *Development of hollow/porous calcium pectinate beads for floating-pulsatile drug delivery*. European Journal of Pharmaceutics and Biopharmaceutics, 2007. **65**(1): p. 85-93.
121. Mastiholimath, V.S., et al., *In vitro and in vivo evaluation of ranitidine hydrochloride ethyl cellulose floating microparticles*. Journal of Microencapsulation, 2008. **25**(5): p. 307-314.
122. Gangadharappa, H.V., K.T.M. Pramod, and K.H.G. Shiva, *Gastric floating drug delivery systems: A review*. Indian Journal of Pharmaceutical Education and Research, 2007. **41**(4): p. 295-305.
123. Tao, S.L. and T.A. Desai, *Microfabricated drug delivery systems: from particles to pores*. Advanced Drug Delivery Reviews, 2003. **55**(3): p. 315-328.

124. Moreira, C., et al., *Improving chitosan-mediated gene transfer by the introduction of intracellular buffering moieties into the chitosan backbone*. Acta Biomaterialia, 2009. 5(8): p. 2995-3006.
125. McClements, D.J. and Y. Li, *Structured emulsion-based delivery systems: Controlling the digestion and release of lipophilic food components*. Advances in Colloid and Interface Science, 2010. 159(2): p. 213-228.
126. Davies, O.R., et al., *Applications of supercritical CO₂ in the fabrication of polymer systems for drug delivery and tissue engineering*. Advanced Drug Delivery Reviews, 2008. 60(3): p. 373-387.
127. Chow, A.H.L., et al., *Particle engineering for pulmonary drug delivery*. Pharmaceutical Research, 2007. 24(3): p. 411-437.
128. Odonnell, P.B. and J.W. McGinity, *Preparation of microspheres by the solvent evaporation technique*. Advanced Drug Delivery Reviews, 1997. 28(1): p. 25-42.
129. Suzuki, K. and J.C. Price, *Microencapsulation and dissolution properties of a neuroleptic in a biodegradable polymer, poly(D,L-lactide)*. Journal of Pharmaceutical Sciences, 1985. 74(1): p. 21-24.
130. Giunchedi, P., H.O. Alpar, and U. Conte, *PDLLA microspheres containing steroids: spray-drying, o/w and w/o/w emulsifications as preparation methods*. Journal of Microencapsulation, 1998. 15(2): p. 185-195.
131. Lee, J.H., T.G. Park, and H.K. Choi, *Effect of formulation and processing variables on the characteristics of microspheres for water-soluble drugs prepared by w/o/o double emulsion solvent diffusion method*. International Journal of Pharmaceutics, 2000. 196(1): p. 75-83.
132. Yang, Y.Y., T.S. Chung, and N.P. Ng, *Morphology, drug distribution, and in vitro release profiles of biodegradable polymeric microspheres containing protein fabricated by double-emulsion solvent extraction/evaporation method*. Biomaterials, 2001. 22(3): p. 231-241.
133. Pistel, K.F. and T. Kissel, *Effects of salt addition on the microencapsulation of proteins using W/O/W double emulsion technique*. Journal of Microencapsulation, 2000. 17(4): p. 467-483.
134. Nihant, N., et al., *Polylactide microparticles prepared by double emulsion/evaporation technique. 1. Effect of primary emulsion stability*. Pharmaceutical Research, 1994. 11(10): p. 1479-1484.
135. Liu, J.T., S.Y. Chan, and P.C. Ho, *Polymer-coated microparticles for the sustained release of nitrofurantoin*. Journal of Pharmacy and Pharmacology, 2002. 54(9): p. 1205-1212.
136. Maharaj, I., J.G. Nairn, and J.B. Campbell, *Simple Rapid Method for the Preparation of Enteric-Coated Microspheres*. Journal of Pharmaceutical Sciences, 1984. 73(1): p. 39-42.
137. El-Kamel, A.H., et al., *Preparation and evaluation of ketoprofen floating oral delivery system*. International Journal of Pharmaceutics, 2001. 220(1-2): p. 13-21.
138. Tom, J.W. and P.G. Debenedetti, *Particle formation with supercritical fluids- A review*. Journal of Aerosol Science, 1991. 22(5): p. 555-584.

139. Darr, J.A. and M. Poliakoff, *New directions in inorganic and metal-organic coordination chemistry in supercritical fluids*. Chemical Reviews, 1999. **99**(2): p. 495-541.
140. Cooper, A.I., *Polymer synthesis and processing using supercritical carbon dioxide*. Journal of Materials Chemistry, 2000. **10**(2): p. 207-234.
141. Clifford, T., *Fundamentals of Supercritical Fluids*. 1999: Oxford University Press.
142. Brunner, G., *Applications of Supercritical Fluids*, in *Annual Review of Chemical and Biomolecular Engineering, Vol 1*. 2010. p. 321-342.
143. Hakuta, Y., H. Hayashi, and K. Arai, *Fine particle formation using supercritical fluids*. Current Opinion in Solid State & Materials Science, 2003. **7**(4-5): p. 341-351.
144. Jung, J. and M. Perrut, *Particle design using supercritical fluids: Literature and patent survey*. Journal of Supercritical Fluids, 2001. **20**(3): p. 179-219.
145. Knez, Z. and E. Weidner, *Particles formation and particle design using supercritical fluids*. Current Opinion in Solid State & Materials Science, 2003. **7**(4-5): p. 353-361.
146. Yeo, S.D. and E. Kiran, *Formation of polymer particles with supercritical fluids: A review*. Journal of Supercritical Fluids, 2005. **34**(3): p. 287-308.
147. Kritzer, P., *Corrosion in high-temperature and supercritical water and aqueous solutions: a review*. Journal of Supercritical Fluids, 2004. **29**(1-2): p. 1-29.
148. King, J.W., J.H. Johnson, and J.P. Friedrich, *Extraction of fat tissue from meat-products with supercritical carbon-dioxide*. Journal of Agricultural and Food Chemistry, 1989. **37**(4): p. 951-954.
149. Icen, H. and M. Guru, *Extraction of caffeine from tea stalk and fiber wastes using supercritical carbon dioxide*. Journal of Supercritical Fluids, 2009. **50**(3): p. 225-228.
150. Peker, H., et al., *Caffeine extraction rates from coffee beans with supercritical carbon-dioxide*. Aiche Journal, 1992. **38**(5): p. 761-770.
151. Froning, G.W., et al., *Extraction of cholesterol and other lipids from dried egg-yolk using supercritical carbon-dioxide*. Journal of Food Science, 1990. **55**(1): p. 95-98.
152. Blanchard, L.A. and J.F. Brennecke, *Recovery of organic products from ionic liquids using supercritical carbon dioxide*. Industrial & Engineering Chemistry Research, 2001. **40**(1): p. 287-292.
153. Hao, J.Y., et al., *Plasticization and spraying of poly (DL-lactic acid) using supercritical carbon dioxide: Control of particle size*. Journal of Pharmaceutical Sciences, 2004. **93**(4): p. 1083-1090.
154. Goel, S.K. and E.J. Beckman, *Generation of microcellular polymeric foams using supercritical carbon-dioxide. 1. Effect of pressure and temperature on nucleation*. Polymer Engineering and Science, 1994. **34**(14): p. 1137-1147.
155. Siripurapu, S., et al., *Generation of microcellular foams of PVDF and its blends using supercritical carbon dioxide in a continuous process*. Polymer, 2002. **43**(20): p. 5511-5520.

156. Stafford, C.M., T.P. Russell, and T.J. McCarthy, *Expansion of polystyrene using supercritical carbon dioxide: Effects of molecular weight, polydispersity, and low molecular weight components*. *Macromolecules*, 1999. **32**(22): p. 7610-7616.
157. Subramaniam, B., R.A. Rajewski, and K. Snavely, *Pharmaceutical processing with supercritical carbon dioxide*. *Journal of Pharmaceutical Sciences*, 1997. **86**(8): p. 885-890.
158. Taylor, D.K., R. Carbonell, and J.M. DeSimone, *Opportunities for pollution prevention and energy efficiency enabled by the carbon dioxide technology platform*. *Annual Review of Energy and the Environment*, 2000. **25**: p. 115-146.
159. Rindfleisch, F., T.P. DiNoia, and M.A. McHugh, *Solubility of polymers and copolymers in supercritical CO₂*. *Journal of Physical Chemistry*, 1996. **100**(38): p. 15581-15587.
160. Shieh, Y.T., et al., *Interaction of supercritical carbon dioxide with polymers .2. Amorphous polymers*. *Journal of Applied Polymer Science*, 1996. **59**(4): p. 707-717.
161. Tang, M., W.-H. Huang, and Y.-P. Chen, *Comparisons of the sorption and diffusion of supercritical carbon dioxide into polycarbonate and polysulfone*. *Journal of the Chinese Institute of Chemical Engineers*, 2007. **38**(5-6): p. 419-424.
162. Nalawade, S.P., et al., *The FT-IR studies of the interactions of CO₂ and polymers having different chain groups*. *Journal of Supercritical Fluids*, 2006. **36**(3): p. 236-244.
163. Davies, O.R., et al., *Applications of supercritical CO₂ in the fabrication of polymer systems for drug delivery and tissue engineering*. *Advanced Drug Delivery Reviews*, 2008. **60**(3): p. 373-387.
164. Tsutsumi, A., et al., *A novel fluidized-bed coating of fine particles by rapid expansion of supercritical-fluid solutions*. *Powder Technology*, 1995. **85**(3): p. 275-278.
165. Chernyak, Y., et al., *Formation of perfluoropolyether coatings by the rapid expansion of supercritical solutions (RESS) process. Part 1: Experimental results*. *Industrial & Engineering Chemistry Research*, 2001. **40**(26): p. 6118-6126.
166. Tom, J.W., et al., *Applications of supercritical fluids in the controlled release of drugs*. *Acs Symposium Series*, 1993. **514**: p. 238-257.
167. Matsuyama, K., et al., *Environmentally benign formation of polymeric microspheres by rapid expansion of supercritical carbon dioxide solution with a nonsolvent*. *Environmental Science & Technology*, 2001. **35**(20): p. 4149-4155.
168. Kim, J.H., T.E. Paxton, and D.L. Tomasko, *Microencapsulation of naproxen using rapid expansion of supercritical solutions*. *Biotechnology Progress*, 1996. **12**(5): p. 650-661.
169. Petersen, R.C., D.W. Matson, and R.D. Smith, *The formation of polymer fibers from the rapid expansion of supercritical fluid solutions*. *Polymer Engineering and Science*, 1987. **27**(22): p. 1693-1697.
170. Mishima, K., et al., *Production of polyethylene glycol and polyoxyalkylenealkylphenyl ether microspheres using supercritical*

- carbon dioxide, in *Advances in Chemical Conversions for Mitigating Carbon Dioxide*. 1998. p. 661-664.
171. Kazarian, S.G. and G.G. Martirosyan, *Spectroscopy of polymer/drug formulations processed with supercritical fluids: in situ ATR-IR and Raman study of impregnation of ibuprofen into PVP*. International Journal of Pharmaceutics, 2002. **232**(1-2): p. 81-90.
 172. Matsuyama, K., et al., *Microencapsulation of proteins with polymer-blend by rapid expansion of supercritical carbon dioxide*. Kagaku Kogaku Ronbunshu, 2001. **27**(6): p. 707-713.
 173. Dos Santos, I.R., et al., *Microencapsulation of protein particles within lipids using a novel supercritical fluid process*. International Journal of Pharmaceutics, 2002. **242**(1-2): p. 69-78.
 174. Tom, J.W. and P.G. Debenedetti, *Formation of bioerodible polymeric microspheres and microparticles by rapid expansion of supercritical solutions*. Biotechnology Progress, 1991. **7**(5): p. 403-411.
 175. Debenedetti, P.G., et al., *Rapid expansion of supercritical solutions (RESS) - FUndamentals and applications*. Fluid Phase Equilibria, 1993. **82**: p. 311-321.
 176. Pathak, P., et al., *Nanosizing drug particles in supercritical fluid processing*. Journal of the American Chemical Society, 2004. **126**(35): p. 10842-10843.
 177. Gallagher, P.M., et al., *Gas Antisolvent recrystallization- New process to recrystallize compounds insoluble in supercritical fluids*. Acs Symposium Series, 1989. **406**: p. 334-354.
 178. Krukonis, V.J., Gallagher, P.M., *Gas Anti-solvent recrystallization process*. 1994.
 179. Caliceti, P., et al., *Effective protein release from PEG/PLA nanoparticles produced by compressed gas anti-solvent precipitation techniques*. Journal of Controlled Release, 2004. **94**(1): p. 195-205.
 180. Bustami, R.T., et al., *Generation of micro-particles of proteins for aerosol delivery using high pressure modified carbon dioxide*. Pharmaceutical Research, 2000. **17**(11): p. 1360-1366.
 181. Moneghini, M., et al., *Processing of carbamazepine PEG 4000 solid dispersions with supercritical carbon dioxide: preparation, characterisation, and in vitro dissolution*. International Journal of Pharmaceutics, 2001. **222**(1): p. 129-138.
 182. Corrigan, O.I. and A.M. Crean, *Comparative physicochemical properties of hydrocortisone-PVP composites prepared using supercritical carbon dioxide by the GAS anti-solvent recrystallization process, by coprecipitation and by spray drying*. International Journal of Pharmaceutics, 2002. **245**(1-2): p. 75-82.
 183. Tsvintzelis, I., E. Pavlidou, and C. Panayiotou, *Porous scaffolds prepared by phase inversion using supercritical CO₂ as antisolvent - I. Poly(L-lactic acid)*. Journal of Supercritical Fluids, 2007. **40**(2): p. 317-322.
 184. Reverchon, E., *Supercritical antisolvent precipitation of micro- and nano-particles*. Journal of Supercritical Fluids, 1999. **15**(1): p. 1-21.
 185. Reverchon, E., I. De Marco, and G. Della Porta, *Rifampicin microparticles production by supercritical antisolvent precipitation*. International Journal of Pharmaceutics, 2002. **243**(1-2): p. 83-91.

186. Reverchon, E., G. Della Porta, and P. Pallado, *Supercritical antisolvent precipitation of salbutamol microparticles*. Powder Technology, 2001. **114**(1-3): p. 17-22.
187. Lee, L.Y., C.H. Wang, and K.A. Smith, *Supercritical antisolvent production of biodegradable micro- and nanoparticles for controlled delivery of paclitaxel*. Journal of Controlled Release, 2008. **125**(2): p. 96-106.
188. Falk, R., et al., *Controlled release of ionic compounds from poly (L-lactide) microspheres produced by precipitation with a compressed antisolvent*. Journal of Controlled Release, 1997. **44**(1): p. 77-85.
189. Young, T.J., et al., *Encapsulation of lysozyme in a biodegradable polymer by precipitation with a vapor-over-liquid antisolvent*. Journal of Pharmaceutical Sciences, 1999. **88**(6): p. 640-650.
190. Ghaderi, R., P. Artursson, and J. Carlfors, *Preparation of biodegradable microparticles using solution-enhanced dispersion by supercritical fluids (SEDS)*. Pharmaceutical Research, 1999. **16**(5): p. 676-681.
191. Kang, Y., et al., *Preparation of PLLA/PLGA microparticles using solution enhanced dispersion by supercritical fluids (SEDS)*. Journal of Colloid and Interface Science, 2008. **322**(1): p. 87-94.
192. Chen, A.-Z., et al., *Preparation of 5-fluorouracil-poly(L-lactide) microparticles using solution-enhanced dispersion by supercritical CO₂*. Macromolecular Rapid Communications, 2006. **27**(15): p. 1254-1259.
193. Nesta, D.P., J.S. Elliott, and J.P. Warr, *Supercritical fluid precipitation of recombinant human immunoglobulin from aqueous solutions*. Biotechnology and Bioengineering, 2000. **67**(4): p. 457-464.
194. Weidner, E., R. Steiner, and Z. Knez, *Powder generation from polyethyleneglycols with compressible fluids*, in *High Pressure Chemical Engineering*. 1996. p. 223-228.
195. Skerget, M., A. Perva-Uzunalic, and Z. Knez, *Improvement of Food Product Properties Using Supercritical Fluids*, in *Proceedings of the 2008 Joint Central European Congress, Vol 1*. 2008, Croatian Chamber Economy: Zagreb. p. 225-231.
196. Jordan, F., et al., *Sustained release hGH microsphere formulation produced by a novel supercritical fluid technology: In vivo studies*. Journal of Controlled Release, 2010. **141**(2): p. 153-160.
197. Whitaker, M.J., et al., *The production of protein-loaded microparticles by supercritical fluid enhanced mixing and spraying*. Journal of Controlled Release, 2005. **101**(1-3): p. 85-92.
198. Howdle, S.M., et al., *Supercritical fluid mixing: preparation of thermally sensitive polymer composites containing bioactive materials*. Chemical Communications, 2001(01): p. 109-110.
199. Tai, H., et al., *Control of pore size and structure of tissue engineering scaffolds produced by supercritical fluid processing*. European Cells & Materials, 2007. **14**: p. 64-76.
200. Kelly, C.A., et al., *Supercritical CO₂: A Clean and Low Temperature Approach to Blending PDLA and PEG*. Advanced Functional Materials, 2012. **22**(8): p. 1684-1691.

Chapter 2

Experimental Methods

This chapter describes the general methods used throughout this thesis which cover the production and characterisation of PLGA particles produced using the PGSS method. Chapter specific methods will be described in the appropriate chapters.

2.1 Particles from Gas Saturated Solutions Method

Microparticles were prepared using the Particles from Gas Saturated Solutions system (PGSS) as described previously [1-3]. The basis of this process is the ability of supercritical carbon dioxide to decrease the glass transition temperature of many biodegradable polymers suitable for applications in drug delivery. Poly(lactic-co-glycolic acid) (PLGA) is a widely used polymer in drug delivery and is highly compatible with this process [4]. The components of the formulation and are mixed together before being introduced to a 10 ml cone shaped mixing chamber which is then attached to the head of the apparatus which contains the stirrer and sealed using a clamp and a viton 42 x 2 mm o-ring. A schematic of the high pressure equipment can be found in Figure 2.1 along with a labelled photograph illustrating the main components (Figure 2.2).

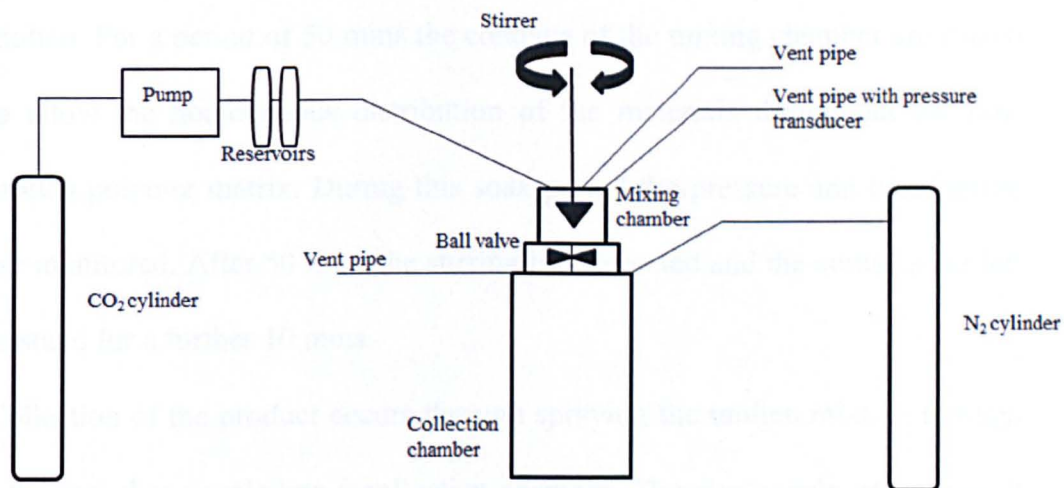


Figure 2.1 Simplified diagram of the high pressure equipment used to fabricate particles

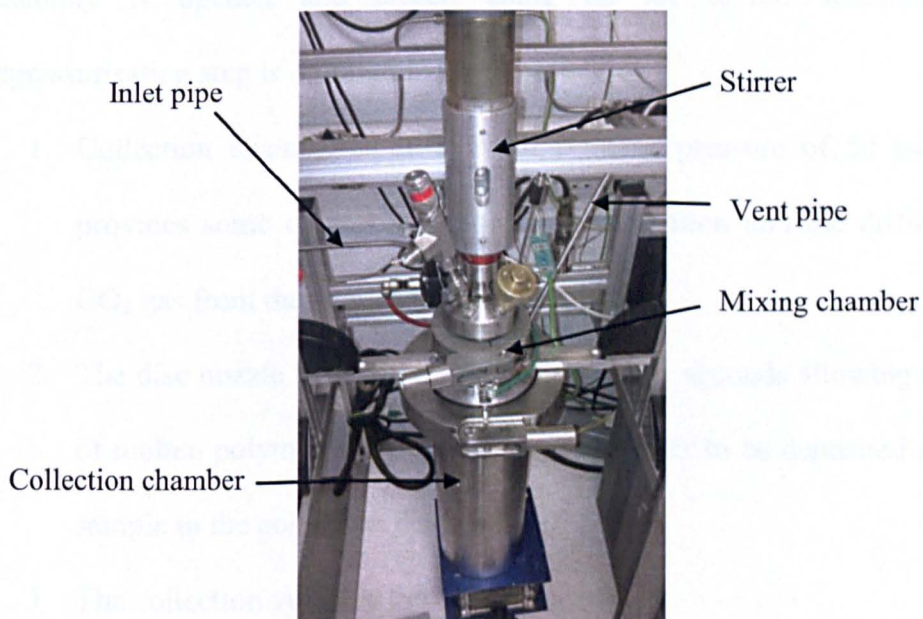


Figure 2.2 Labelled photograph of the mixing chamber attached to the collection chamber.

The temperature is increased initially to 40°C by a heating band around the mixing chamber. CO₂ is introduced to the system through the inlet port to a pressure of 140 bar and the mixing chamber is finally heated up to 60°C. At

this point the carbon dioxide is in the supercritical state and the PLGA will be molten. For a period of 50 mins the contents of the mixing chamber are stirred to allow the homogenous distribution of the materials throughout the now molten polymer matrix. During this soak period the pressure and temperature are monitored. After 50 mins the stirring is terminated and the contents are left to stand for a further 10 mins.

Collection of the product occurs through spraying the molten mixture through a 0.5 mm disc nozzle into a collection chamber. The disc nozzle sits on top of the collection chamber with a 15 x 2 mm o-ring, the ball valve is mounted on top of the disc nozzle, sealed using a 14 x 2 mm viton o-ring, between the ball valve mount and the mixing chamber there is a 10 x 2 mm o-ring. This nozzle assembly is opened and closed using an air driven actuator. This depressurisation step is outlined in the steps below:

1. Collection chamber is filled with N₂ to a pressure of 50 bar. This provides some control over the depressurisation and the diffusion of CO₂ gas from the solidifying polymer matrix
2. The disc nozzle is opened for a period of 0.5 seconds allowing a spray of molten polymer to exit the mixing chamber to be deposited as solid sample in the collection chamber.
3. The collection vessel is then depressurised.
4. The process (steps 1-3) is repeated eight times before the product is collected from the collection chamber.

The depressurisation is carried out eight times as it was found to facilitate the most efficient collection. The product is collected and ground (Cookworks coffee and herb grinder) before sieving through sieves of aperture size 2000

μm , 1000 μm , 800 μm , 500 μm , 250 μm , and 100 μm (Fisher Scientific) using a Retsch/Copley AS300 shaker to separate the different size fractions. Sieving was carried out for 30 mins at an amplitude of 90 mm.

2.2 Scanning Electron Microscopy

The morphology of the particles was evaluated by scanning electron microscopy (SEM) using a Jeol 6060LV (Tokyo, Japan) variable pressure instrument. Prior to analysis samples were mounted on aluminium stubs using adhesive double-sided carbon discs. A Balzers SCD030 gold sputter coater (AG, Liechtenstein) was used for coating the samples. Coating occurred in an argon atmosphere for 4 mins before the SEM analysis was carried out. Image analysis was carried out using the in-built SEM control and user interface software (version 6.57) and digital imaging system.

2.3 X-ray Microtomography

A detailed internal analysis of the particles was carried out using a SkyScan 1174-V2 X-ray Microtomography System. Micro-computed tomography (micro-CT) is a non-invasive technique which creates 2D cross-sections of a 3D object. It is then possible to reconstruct a 3D image of the object to allow a representation of the internal structure to be built.

This technique found applications in drug delivery as it allows the relationship between delivery system structure and its function to be determined [5]. MicroCT enables visualisation and quantification of matrix porosity and density. Details such as pore size, shape, connectivity, and distribution can be revealed [5, 6]. Although microCT has established applications in

determination of porosity in polymeric scaffolds for tissue engineering [7], microCT in matrix based drug delivery devices is less well reported [8].

In the present thesis particles were mounted on a carbon disc which was attached to a small microCT holder (Figure 2.3) and placed in the scanner. Analysis of raw data was carried out using NRecon and CTAN. Scanning was carried out at 50 kV and 800 mA current. Thresholding of the 2D images allowed a distinction between polymeric matrix and porous space.

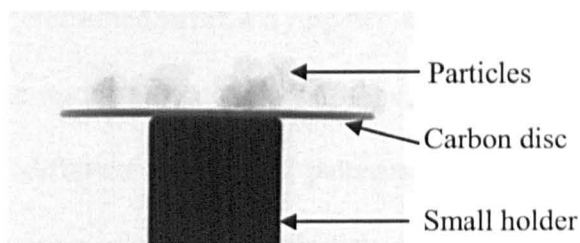


Figure 2.3 Transmission image demonstrating how the particles are loaded into the microCT instrument.

2.4 Fluorescent Microscopy

Fluorescence microscopy provides images of a sample based on its fluorescent or phosphorescent properties. The microscope operates by illuminating a sample with light of a wavelength known to cause excitation of the fluorophores. This energy is manifested as emitted light which is much weaker and of a longer wavelength than the illumination light allowing it to be distinguished and imaged. In this study particles were imaged using a Gx fluorescent microscope (GTVision) equipped with a QImaging Qi camera (Fast1394). Fluorescent materials were introduced to the samples for imaging in two different methods. Firstly, PLGA particles produced using the PGSS

method were loaded with coumarin 6 (0.5% w/w) during manufacture (with the same mass of PLGA (Resomer, RG502H) being removed. Alternatively the mucoadhesive polymer chitosan was fluorescently modified through covalent attachment of fluorescein isothiocyanate (FITC) and used to coat the particles post processing (process described in Chapter 6). Following imaging analysis was carried out using QCapture (version 6).

2.5 Particle Size Analysis

The size of the particles was determined using a Sympatec HELOS/BF particle size analyser. In this technique laser light interacts with the particles causing it to diffract and as there are different diffraction patterns for different size particles, it is possible to determine the size distribution of the sample being analysed. The pattern of diffraction can be described using the Fraunhofer theory which states that the diffraction angle for a small particle is larger than the diffraction angle for a larger particle. This is a result of the small particle having a relatively more curved surface. The angle at which the light is scattered is inversely proportional to the size of that particle.

The light that is scattered from the particles is focused onto a detector by a lens. A photo-detector acquires an intensity distribution of the diffracted light. The data is compared to an optical model.

In this thesis particles were mixed with 1% Tween 20 and then added to a cuvette containing de-ionised water in the Sympatec HELOS to be analysed. The cuvette is $\frac{3}{4}$ filled with de-ionised water and 10 drops of tween20 1%. The stirrer is switched on at 1200 rpm and the cuvette added to the laser diffracter. Approximately 50 mg of sample is mixed into a paste with tween20 1%. The

surfactant is added in small amounts until the required consistency is reached. Using a small spatula the paste is added to the cuvette until the HIELOS detector elements box reads an obscuration percentage of 5-35%. The measurements are now taken. The instrument is set up to take 3 measurements and an average is taken and reported.

2.6 Helium Air Pycnometry

The density of the microparticles was measured using a Micromeritics AccuPyc 1330 helium pycnometer. The apparatus consists of two chambers, one is the sample chamber and the second is a standard chamber with a known internal volume. The equipment operates by detecting a pressure change resulting from the displacement of gas in the chamber by the solid sample. A sample of known mass is introduced to the sample chamber and helium gas is introduced up to a fixed pressure. The gas is then transferred to the reference chamber where the pressure is measured allowing the volume of the sample to be calculated using Boyle's law which states that for a confined gas pressure x volume is constant. The calculated volume is then used to determine density using the following equation:

$$\text{Density (g/cm)} = \text{Mass particles (g)} \div \text{Volume (cm)}$$

The pycnometer was calibrated with an iron sphere of known volume and the method was validated prior to sample analysis. Approximately 0.7 g of the sample was loaded into the sample chamber. Each measurement involved

purging with helium 5 times up to a fill pressure of 19.5 psig at a rate of 0.05 psig / min. Density analysis was carried out five times for each sample.

2.7 *In vitro* Buoyancy Analysis of Porous Particles

To determine how effective particles produced using the PGSS method are at remaining buoyant in a simulated gastric environment, *in vitro* buoyancy analysis was carried out. 10 mg of particles were weighed out and suspended on 10 ml simulated gastric fluid (SGF) (see Section 2.10) in a glass scintillation vial. The vials were then placed in a shaking water bath (Fisher Scientific) at 120 shakes / min and 37°C for 8 h. Following this time the vials were photographed (using a Nikon Coolpix S3000 compact camera) and any particles which remain floating on the surface of the media were removed and frozen in liquid nitrogen before freeze drying (Edwards Modulyo freeze drier). After 3 days dried particles were weighed allowing an approximate percentage for amount of particles which remain buoyant using the following equation:

Percentage of buoyant particles (%)

$$= \left(\frac{\text{Mass of particles which remain buoyant}}{\text{Initial mass of particles}} \right) \times 100$$

2.8 Differential Scanning Calorimetry

Differential scanning calorimetry (DSC) measures heat flows associated with temperature-induced transitions in materials. It allows the determination of specific temperatures associated with thermal events, as when the sample undergoes a temperature related physical change more or less heat will need to flow to it than a calibrated standard in order to maintain the sample and

standard at the same temperature. Whether the heat flow increases or decreases determines whether the change is endothermic or exothermic.

As an amorphous substance is heated it undergoes a transition from a glassy state to a rubbery state and this is known as a glass transition temperature (T_g). Figure 2.4 illustrates the T_g on a DSC trace as a downward step, indicating that it is an endothermic event. As it moves through its T_g , a material dramatically increases in viscosity and undergoes a transition from the hard and brittle 'glassy' state to the elastic and flexible 'rubbery' state. The second thermal event in Figure 2.4 is crystallisation. This exothermic event occurs when the molecules within a material undergo partial alignment into a crystalline form. The third and final peak on the DSC trace is the melting point (T_m). As heating is continued the material will undergo a state change from solid to liquid, this is an endothermic event.

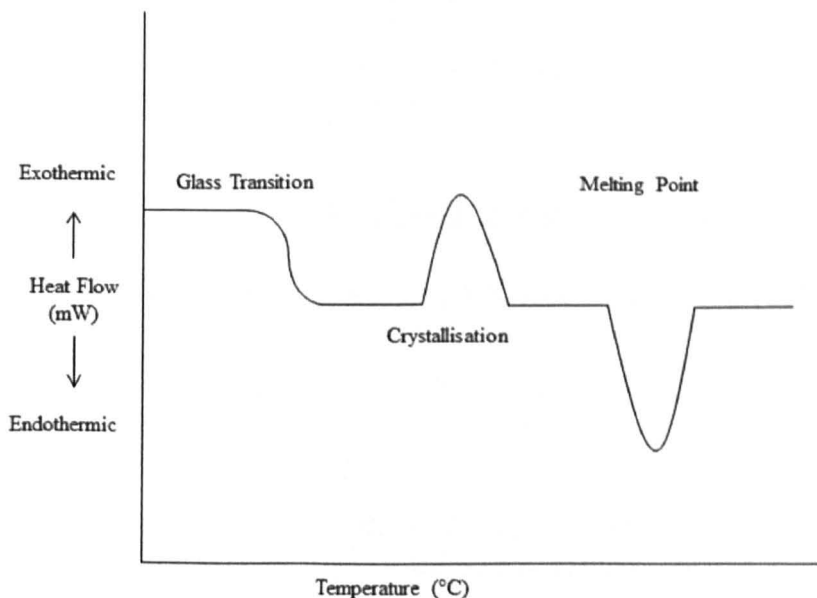


Figure 2.4 Example of a DSC thermograph illustrating a glass transition, a crystallisation, and a melting point.

In this study thermal events were analysed using a TA-Q2000 differential scanning calorimeter (TA Instruments), calibrated with an indium standard. Typically, 4-5 mg of particles were weighed into aluminium pans (Tzero DSC pans) and were hermitically sealed with a Tzero DSC lid using a Tzero press containing a Black Tzero lower die and a flat die. Samples were heated at 10°C per minute and temperature was ramped from 0°C to 150°C followed by a cooling cycle back down to 0°C the samples undergo two temperature ramp cycles.

2.9 Determination of Drug Encapsulation Efficiency

5mg of drug loaded porous particles were suspended in 10 ml 1M NaOH and left to dissolve completely. Following this the solutions were analysed using UV/VIS spectrophotometry (Beckman coulter DU800) for absorbance at 450 nm for riboflavin and 277 nm for furosemide. 300 µl of sample was pipette into a Tm cuvette 14 mm high (Beckman instruments, inc. USA. Part number 517481).

Concentration of drug was determined against a standard curve.

Drug loading was calculated as a percentage of drug using the following formula:

$$\text{Drug loading (\%)} = \left(\frac{\text{Mass of drug in particles (mg)}}{\text{Mass of particles (mg)}} \right) \times 100\%$$

The encapsulation efficiency was then calculated using the following formula:

$$\text{Encapsulation efficiency (\%)} = \left(\frac{\text{Actual drug loading}}{\text{Theoretical loading}} \right) \times 100\%$$

2.10 Preparation of Simulated Gastric Fluid

Initial drug release studies were carried out in phosphate buffer solution (PBS) (Fisher Scientific PBS tablets made up to 100 ml/tablet) at pH7.4 which allows a comparison of the drug release properties with similar systems already in the literature, however the system described in this thesis is destined for the GIT where conditions are not adequately replicated using PBS at pH7.4. Therefore, a more physiologically relevant media was prepared and used for drug release studies. The composition of the gastric fluid (as described in detail in Section 1.2.1 is highly variable and complex however a simplified 'simulated gastric fluid' (SGF) was prepared in line with the US pharmacopoeia [9] and consists of 2.0 g sodium chloride and 3.2 g pepsin dissolved in 7.0 ml hydrochloric acid (HCl) (5M) and sufficient deionised water to make 1000 ml. The final solution is made to pH1.2 using 5M HCl.

2.11 Drug Release studies

The release of the drugs furosemide, riboflavin, and metformin from the drug loaded particles was investigated over a period of 24 hours. 10 mg of drug loaded particles weighed out in triplicate were introduced to 20 ml scintillation vials. 10 ml of release media was added to the vials and they were placed in a shaking water bath (Fisher Scientific) at 37°C and 120 shakes / minute. Three different release media were prepared, phosphate buffer solution (pH7.4),

phosphate buffer solution adjusted to pH2.0 using 5M HCl, and Simulated Gastric Fluid (SGF) (Section 2.10). 500 μ l samples were pipetted out of the release media and replaced with fresh media at 10, 20, 40, 80, 160, 320, 600, 1440 mins. Each sample was analysed using UV/VIS (as described above (Section 2.9)) at the following wavelengths; furosemide loaded samples were analysed at 277 nm, riboflavin samples were analysed at 450 nm, and metformin samples at 233 nm.

2.12 Time of Flight Secondary Ion Mass Spectrometry

A surface analysis of particles was carried out using Time-of-Flight secondary ion mass spectrometry (ToF-SIMS) IV instrument (ION-TOF GmbH Münster, Germany) equipped with a liquid metal ion gun (LMIG) with a Bi_3^+ cluster primary ion source. This technique allows detailed analysis of the composition of the surface material in a sample, usually to a depth of approximately 1 nm [10], however the individual nature of samples makes it difficult to accurately estimate the depth of analysis.

In this technique an area of the sample is bombarded with primary ions, in this case Bi_3^+ , the impact of the primary ions on the sample surface results in the fragmentation of ion species from the surface material which, in turn, results in the emission of secondary ions (Figure 2.5). Both negative and positive secondary ions are emitted from the sample. The ions will then travel through an ultra-high vacuum towards a detector along an electric field of known strength which allows all ions of the same charge to have the same kinetic energy which is important as it is the mass of each ion which is of interest and at the same kinetic energy it is the mass/charge ratio which determines the

velocity of the ion so the heavier ions will travel more slowly and reach the analyser later. The time it takes to reach the detector and the known operating conditions make it possible to separate out the ions.

The operating conditions involved primary ion energy of 25 kV and a pulsed target current of approximately 1.0 pA. Low energy electrons (20 eV) were used to compensate for surface charging which is a result of the primary ion bombardment on insulator surfaces. A raster area of typically $500 \mu\text{m}^2$ was analysed and data analysis was carried out using IonSpec and IonImage (version 4.1).

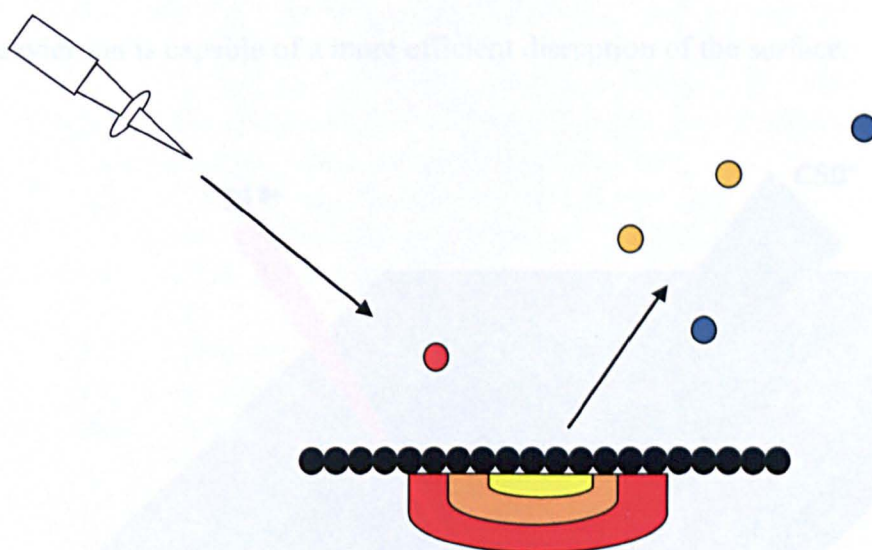


Figure 2.5 Schematic diagram of the ToF-SIMS process illustrating the liberation of secondary ions from the sample surface.

ToF-SIMS has been applied in the analysis of controlled-drug delivery systems [11] exposing the distribution of active pharmaceutical ingredients within a delivery system.

2.13 Depth Profiling

As a surface technique ToF-SIMS does not provide information on any material below the initial layers. Depth profiling acquires this data by analysing the surface of the sample followed by erosion of the surface to reveal a new layer of material (Figure 2.6). The new surface layer is then analysed and the cycle is repeated.

As described above, the ToF-SIMS technique detects secondary ions liberated from the sample following disruption of the surface by a primary ion beam, the technique itself is therefore causing disruption to the surface. Depth profiling exploits this and the relatively heavier ion $C60^+$ is used in place of Bi^{3+} as the heavier ion is capable of a more efficient disruption of the surface.

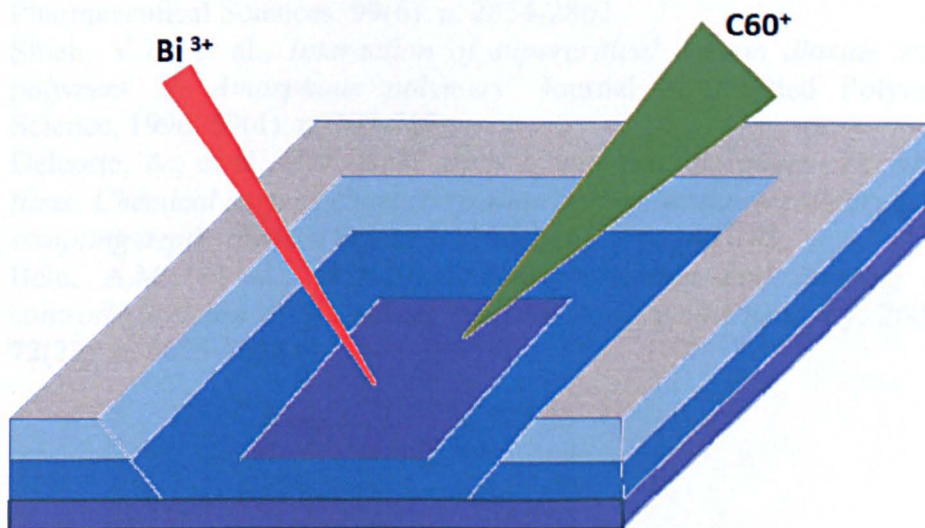


Figure 2.6 Diagram illustrating the depth profiling process. The analysis is carried out by the Bi^{3+} primary ion with the C^{60+} revealing a new surface layer.

2.14 References

1. Hao, J.Y., et al., *Supercritical fluid assisted melting of poly(ethylene glycol): a new solvent-free route to microparticles*. Journal of Materials Chemistry, 2005. **15**(11): p. 1148-1153.
2. Jordan, F., et al., *Sustained release hGH microsphere formulation produced by a novel supercritical fluid technology: In vivo studies*. Journal of Controlled Release. **141**(2): p. 153-160.
3. Casettari, L., et al., *Surface Characterisation of Bioadhesive PLGA/Chitosan Microparticles Produced by Supercritical Fluid Technology*. Pharmaceutical Research. **28**(7): p. 1668-1682.
4. Kelly, C.A., *Supercritical CO₂: A Clean and Low Temperature Approach to Blending PLA and PEG*. Advanced Functional Materials, 2010. **22**: p. 8.
5. Wang, Y., et al., *Micro-CT in drug delivery*. European Journal of Pharmaceutics and Biopharmaceutics. **74**(1): p. 41-49.
6. Jones, J.R., et al., *Non-destructive quantitative 3D analysis for the optimisation of tissue scaffolds*. Biomaterials, 2007. **28**(7): p. 1404-1413.
7. Barbetta, A., et al., *Role of X-ray microtomography in tissue engineering*. Annali Dell Istituto Superiore Di Sanita. **48**(1): p. 10-18.
8. Wang, Y., et al., *Micro-CT Analysis of Matrix-Type Drug Delivery Devices and Correlation With Protein Release Behaviour*. Journal of Pharmaceutical Sciences. **99**(6): p. 2854-2862.
9. Shieh, Y.T., et al., *Interaction of supercritical carbon dioxide with polymers .2. Amorphous polymers*. Journal of Applied Polymer Science, 1996. **59**(4): p. 707-717.
10. Delcorte, A., et al., *ToF-SIMS study of alternate polyelectrolyte thin films: Chemical surface characterization and molecular secondary ions sampling depth*. Surface Science, 1996. **366**(1): p. 149-165.
11. Belu, A.M., et al., *TOF-SIMS characterization and imaging of controlled-release drug delivery systems*. Analytical Chemistry, 2000. **72**(22): p. 5625-5638.

Chapter 3

Particle Manufacture and Optimisation for Gastroretention

3.1 Introduction

In the literature, floating formulations are separated into two distinct groups. The first being the effervescent systems, these produce gas on contact with the gastric media [1, 2]. The entrapment of produced gas within effervescent systems leads to a buoyancy effect through a decrease in density. As previously discussed (Chapter 1, Section 1.4.5), a major limitation of this type of delivery system is the lag time between the initial contact with the gastric media and the time the floating behaviour is exhibited. If this lag time is extended for too long there is the potential for the loss of the entire dose. The second group of floating systems includes those which do not effervesce, but possess characteristics which convey buoyancy in the gastric media. These characteristics include low density, with low density systems demonstrating good promise in the improvement of bioavailability of orally delivered drugs [3-5].

Buoyant (low density) microparticulate systems can include porous microparticles [6] or hollow microspheres [7, 8]. Instances where such systems have demonstrated promise in gastroretention include porous polypropylene microparticles loaded with ibuprofen, which were successfully optimised for gastroretention. The system achieved a time-dependant delivery for the treatment of arthritis symptoms [6]. Hollow polymeric microballoons of >500 μm size, loaded with riboflavin (6% (w/w)), possessed promising buoyancy following dispersal in a simulated gastric fluid [7] with 97% of the formulation remaining buoyant after 4 h. Riboflavin excretion half-life with the floating formulation was observed to correlate to the buoyancy of the system [7]. This correlation between buoyancy and extended urinary excretion indicated the importance of low density of the formulation. In another study, promising *in vivo* performance of rosiglitazone loaded Eudragit based multi-unit floating microparticles was reported [8]. The microparticles demonstrated 65-96% buoyancy following 24 h in SGF, in addition to high rosiglitazone entrapment efficiencies (78-97%) and sustained release behaviours over 12 h [8], this formulation demonstrated good glycaemic control in a rat model. The above studies confirm that low density systems improve therapeutic potential of formulations. This chapter focuses on the optimisation of a low density oral delivery system using a novel supercritical fluid technology.

Multi-unit systems, such as microparticles, may have a greater potential for success in gastroretention when compared to their single unit counterparts. Single-unit systems are limited by an 'all or nothing' principle, whereby if the gastroretention effect fails, the therapeutic performance will be compromised [2]. The production of microparticles for a variety of drug delivery purposes

has been subjected to much research and has been reviewed previously [9-12]. The different techniques in particle production are discussed in further detail in Chapter 1 (Section 1.5).

Recently, supercritical fluid techniques have provided a solvent free route to the production of particulate formulations. Due to favourable critical conditions ($P_c=73.9$ bar $T_c=31.1^\circ\text{C}$), as well as low cost, and low toxicity, scCO_2 is often used in these techniques. There are several reviews in this area discussing the different approaches to particle development applying supercritical fluids, in particular CO_2 [13-17] and have been discussed in this thesis in detail in Chapter 1 (Section 1.5). The PGSS technique in particular holds great promise in the preparation of particles for drug delivery, as it requires no organic solvent and it does not rely on the solvent or anti-solvent capabilities of scCO_2 instead exploiting the ability of scCO_2 to act as a plasticiser [18-20].

The PGSS method was originally designed for powder coatings [21], however it has since been applied in the food industry [22] and, more recently, in the development of pharmaceutical products [23-27]. This technique utilises scCO_2 as a plasticiser for biodegradable polymers, by dissolving into materials and reducing their glass transition temperature (T_g) to allow plasticisation to occur at relatively low temperatures and pressures. Drug, in the form of solid particles, can then be mixed into such a polymer melt. When plasticisation occurs at low temperatures (often more than 10°C below the polymers usual T_g [28]) the method offers a possibility to encapsulate thermally unstable drugs, including proteins [27]. The homogenous mixture of liquefied polymer and drug particles is rapidly depressurised through a nozzle into a collection

chamber, upon depressurization the CO_2 returns to the gaseous state and the polymer solidifies producing drug encapsulated polymer particles. This process is illustrated in figure 3.1.

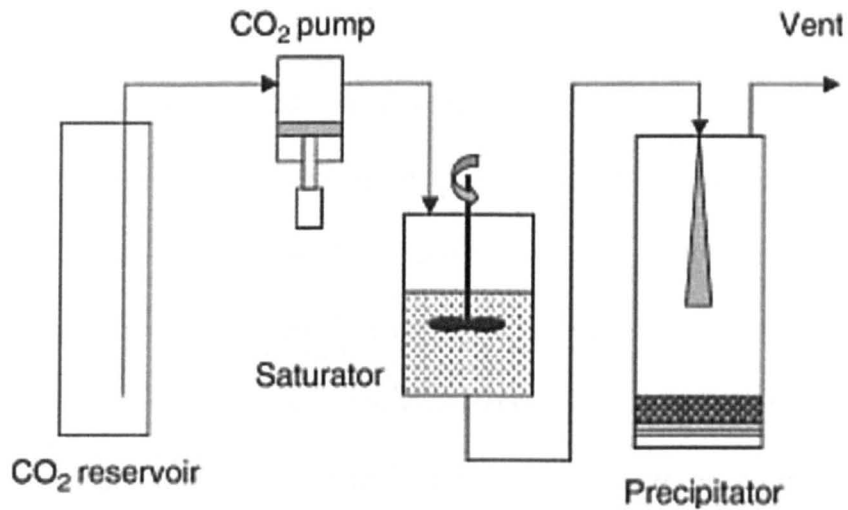


Figure 3.1 Schematic of the PGSS process [29]

The depressurisation step is integral to the success of the PGSS in fabrication of gastroretentive systems. As the CO_2 returns to the gaseous state, it diffuses out of the solidifying polymer leaving behind a porous, network within the matrix. This property is behind the formation of porous scaffolds aimed for tissue engineering applications [30]. This porous, matrix may possess decreased density properties, the fundamental characteristic which conveys gastroretention.

Biocompatible polymers such as PEG [26, 31] and PLGA [27] are often selected for processing in the PGSS method. These polymers are approved for use in medical preparations such as drug delivery systems, implants, and sutures. The selection of material used in PGSS processing has a profound effect on the morphology of the product [32]. It has been reported that the

viscosity of the polymer melt impacts the morphology of the final product [33]. More viscous polymers undergo atomisation during the depressurisation less efficiently than less viscous polymers, resulting in little or no yield, or a fibrous product [34].

Size of delivery systems has previously demonstrated to impact gastric residence time, an increase in size up to 5 mm in diameter has been reported to increase gastric residence time [35], and solids may only empty from the stomach if they are smaller than 2 mm [36]. It has been reported that particles larger than this do not demonstrate any difference in gastric residence [37]. A comparison of the GI transit of small (0.5 mm) and large (4.75 mm) pellets was examined using gamma scintigraphy and although gastric emptying was found not to be affected by size, small intestinal residence time was prolonged by the larger pellets [38]. This chapter considers the effect of particle size on potential particle buoyancy enabling optimisation of gastroretention.

3.2 Materials and Methods

3.2.1 Materials

PLGA (Resomer[®] RG502H ~12KDa free carboxylic acid end group and RG503 ~25KDa ester end group) was supplied by Boeringher Ingleheim. Myristic acid, SPAN80 was purchased from Sigma Aldrich. CO₂ (pharmaceutical grade 99.9%) and Nitrogen were supplied by BOC. All reagents were used as received. All water used for the preparation of solutions, and subsequent dilutions, throughout this thesis was deionized and purified. Produced using an Elgastat system (Elga, High Wycombe, UK) (15 MΩcm resistivity).

3.2.2 Methods

3.2.2.1 Particle Production

Particles were prepared using the PGSS method as described in detail in Chapter 2 (Section 2.1). In this chapter no drug was introduced to the particles and each 2 g batch contained a combination (as described) of PLGA and processing aids.

3.2.2.2 Scanning Electron Microscopy

SEM was used to assess the morphology of particles as described in Chapter 2 (Section 2.2).

3.2.2.3 Particle Size Analysis

Laser diffraction was used to determine the size distribution of the microparticles prepared. This method is described in detail in Section 2.5).

3.2.2.4 Helium Air Pycnometry

Density was determined using helium air pycnometry as described in Chapter 2 (Section 2.6). The method allows the density to be assessed from a known mass of the sample and a determined volume of the sample. The volume of the sample is determined by the amount of space in a calibrated volume the sample occupies, with helium gas being used to make a comparison of space occupied in an empty sample holder and the holder containing the sample.

3.2.2.5 *In vitro* Buoyancy Analysis

Ability of the different formulations to exhibit adequate buoyancy in a simulated gastric environment was carried out as described in Chapter 2 (Section 2.7).

3.2.2.6 X-ray Microtomography

Porosity was determined both quantitatively and qualitatively using microCT as described in Chapter 2 (Section 2.3)

3.3 Results

3.3.1 Effect of Myristic Acid Content on Particle Morphology

Particles were initially produced using PLGA (Resomer[®] RG502II) with an approximate molecular weight of 12 KDa. This polymer has previously been well characterised in the PGSS method in the production of controlled release drug delivery particles [27]. Initially, processing 100% (2g) PLGA produced a very low yield (see Figure 3.2) and therefore the fatty acid, myristic acid, was incorporated into the formulation as a processing aid. The presence of myristic acid in the formulation was found to improve processing of the mixture. Figure 3.1 confirms the increasing myristic acid content in the particles improves the yield with particles made solely of myristic acid having a yield of 65%.

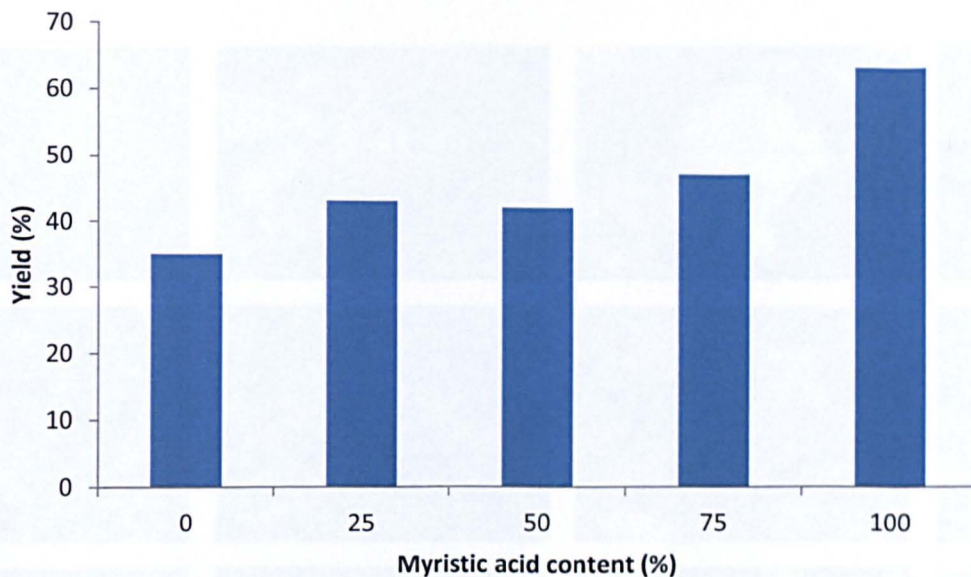


Figure 3.2 Percentage yields of particles as myristic acid content increases. (n=1)

The changing morphologies of particles, as the PLGA: myristic acid ratio was investigated using SEM, are illustrated in Figure 3.3. With increasing myristic acid content the particles assume a more ‘fluffy’ appearance and appear to form aggregates. Formulations possessing higher PLGA contents reveal larger, more discrete structures.

The particle size analysis, using laser diffraction as described in Section 2.5, does not appear to conclude a specific trend in PLGA content effect on particle size (Figure 3.4). SEM images (Figure 3.3) demonstrate that myristic acid particles form aggregates and it is likely that aggregation of the particles containing myristic acid may confound the results.

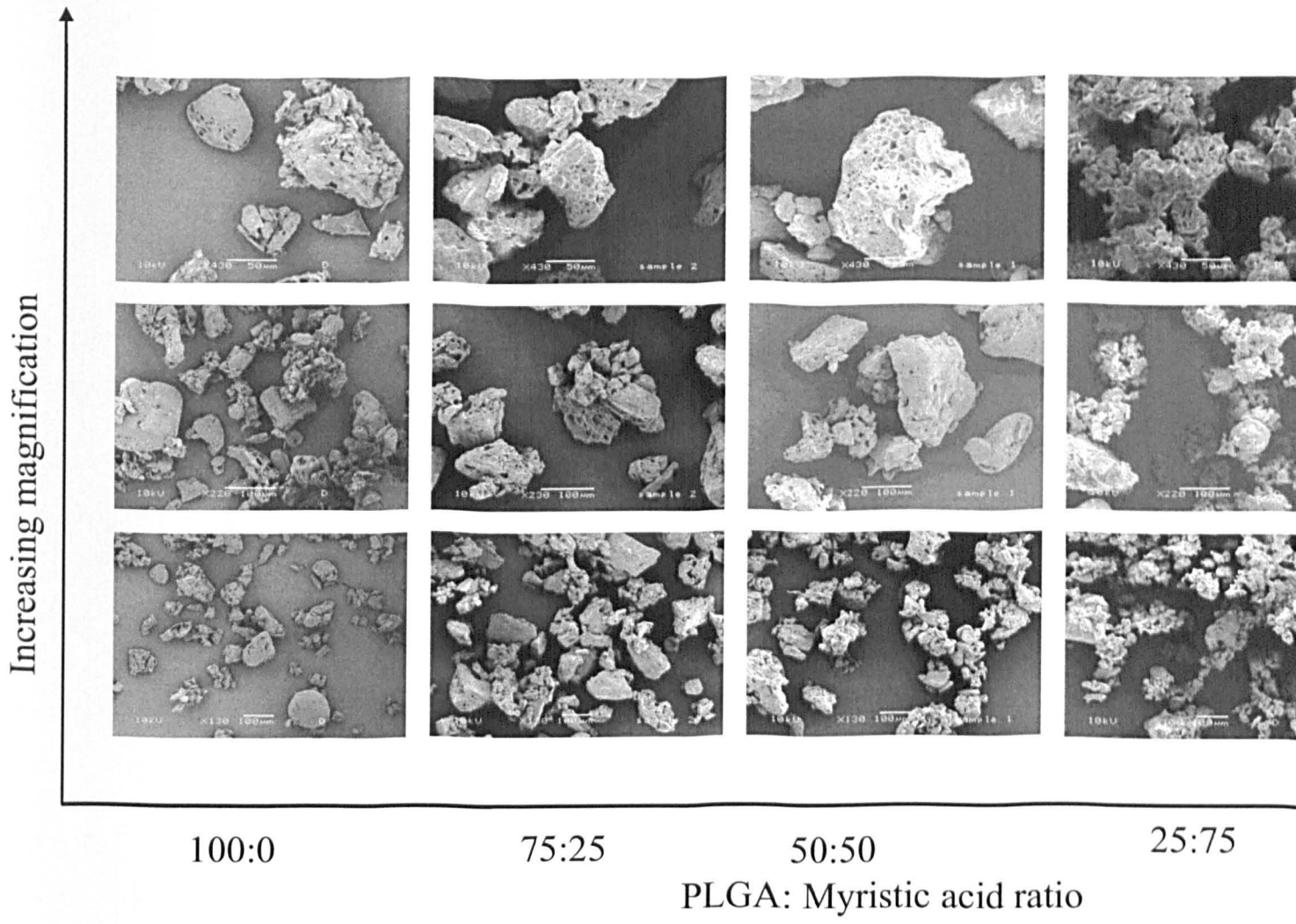


Figure 3.3 SEM images of particles prepared with different ratios of PLGA: Myristic acid. Scale bars in and bottom row 100µm

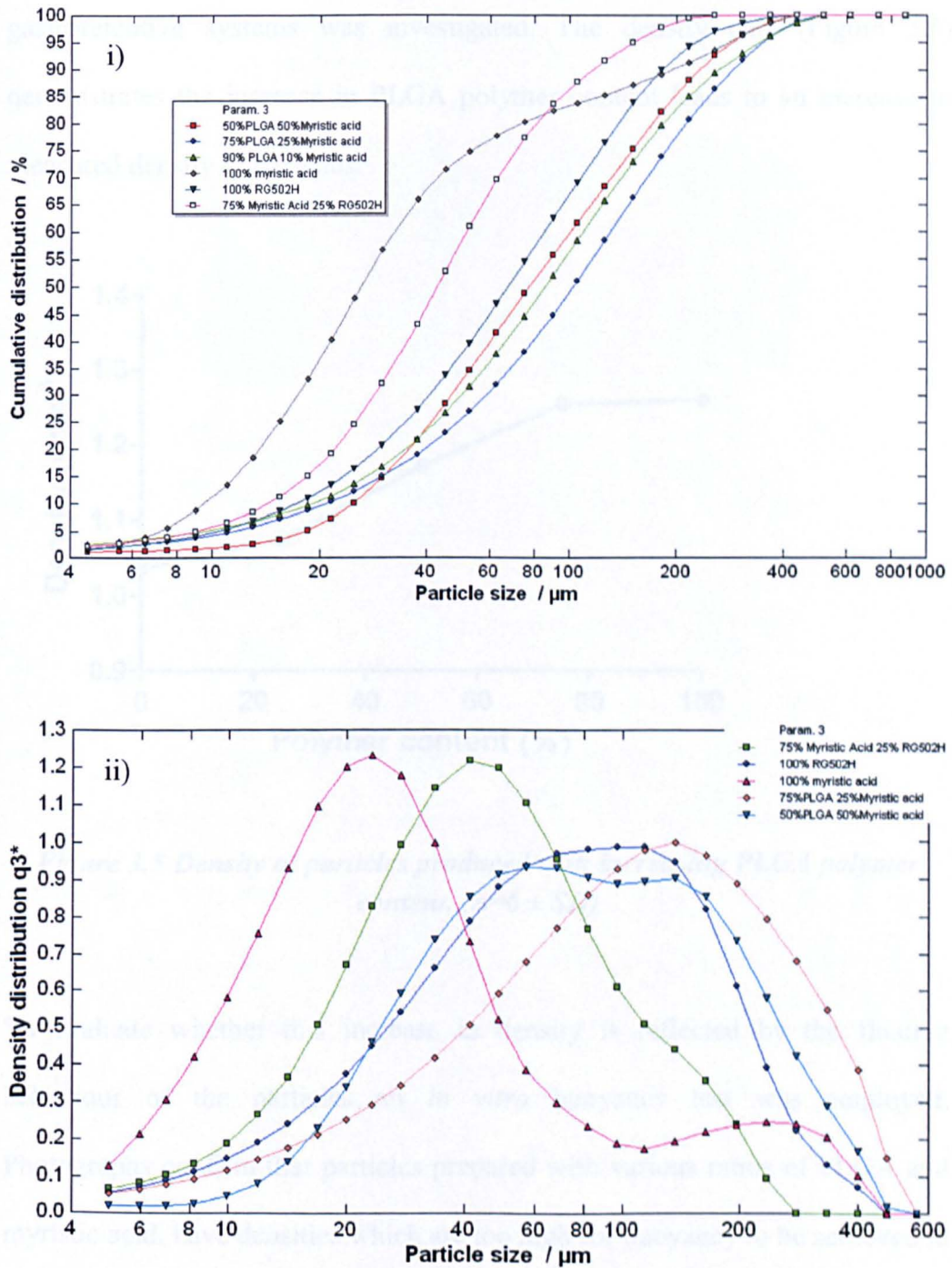


Figure 3.4 i) Cumulative Size distribution profile of particles prepared with various PLGA: myristic acid ratios ii) corresponding differential curve for the formulations

3.3.2 Effect of Myristic Acid Content on Gastroretentive Potential

Following analysis of the morphology of the microparticles their suitability as gastroretentive systems was investigated. The density data (Figure 3.5) demonstrates the increase in PLGA polymer content leads to an increase in measured density of particles.

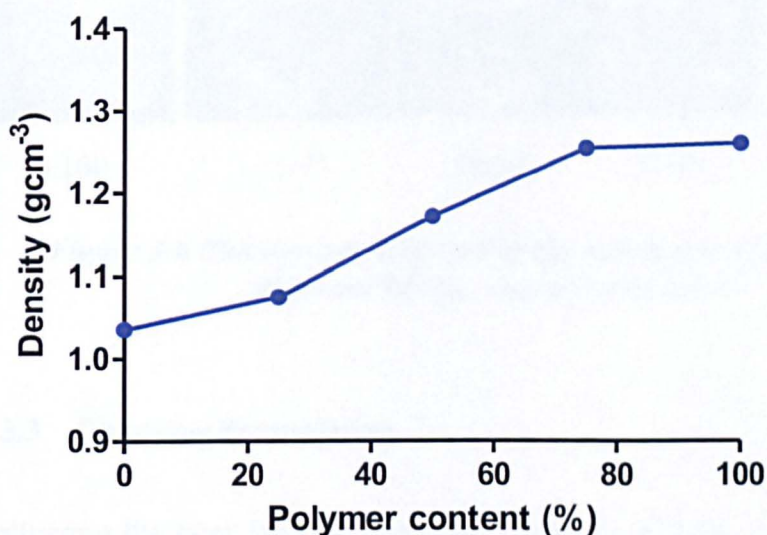


Figure 3.5 Density of particles produced with increasing PLGA polymer content. (n=6 ± SD)

To evaluate whether this increase in density is reflected by the floating behaviour of the particles an *in vitro* buoyancy test was employed. Photographs confirm that particles prepared with various ratios of PLGA and myristic acid, have densities which are too high for buoyancy to be achieved in the gastric media (Figure 3.6). The photographs show a large proportion of particles remaining in suspension with the suspending buffer to appearing turbid. The images do show a fraction of particles at each formulation present

towards the surface of the media this may be due to the surface tension and the hydrophobicity of the myristic acid component of the particles.

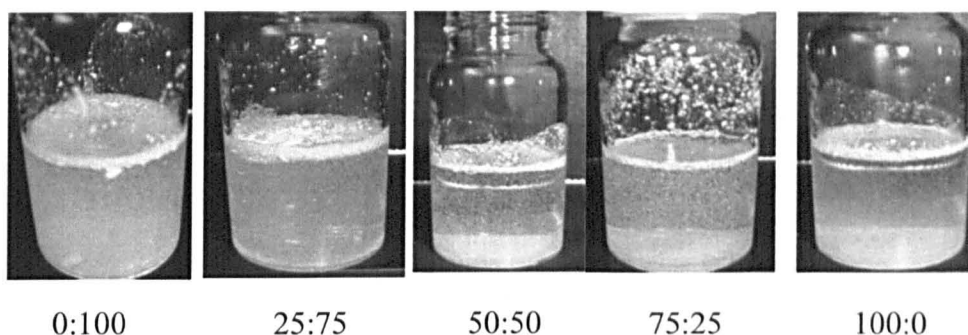


Figure 3.6 Photographs illustrating the behaviour of particles with different PLGA: myristic acid ratios

3.3.3 Changing Formulation

Following the poor buoyancy obtained with the PLGA: myristic acid blends alternative processing aids and polymers were incorporated into the formulation. The higher molecular weight PLGA (Resomer[®] RG503) was introduced along with the myristic acid as the higher intrinsic viscosity (0.32-0.44 dl/g compared to 0.16-0.24 dl/g with the RG502H PLGA) may result in a larger product capable of containing more pores. However the high viscosity reduces the likelihood that the mixture will be sprayed through the 0.5mm disc nozzle, this is confirmed in Table 3.1 and as a result a new processing aid SPAN[™] 80 was introduced and various combinations of the excipients were processed using PGSS and the density of any product collected evaluated.

IMAGING SERVICES NORTH

Boston Spa, Wetherby

West Yorkshire, LS23 7BQ

www.bl.uk

MISSING PRINT



Table 3.1 Investigation of polymer blends and processing parameters in order to find a suitable gastroretention using particle density values obtained from helium air pycno.

Polymer	%(w/w) of polymer	Processing aid	%(w/w) of Processing aid	Temperature (°C)
RG503	50	Myristic acid	50	40
RG503	58	SPAN80	42	40
RG503	75	SPAN80	25	40
RG502H	50	SPAN80	50	40
RG502H	80	SPAN80	20	40
RG502H	85	SPAN81	15	40
RG502H / RG503	65% / 10%	Myristic acid	25	40
RG502H / RG503	70% / 25%	SPAN80	5	40
RG502H / RG503	50% / 20%	Myristic Acid	30	60
RG502H / RG503	55% / 30%	SPAN80	15	60
RG502H / RG503	65% / 10%	SPAN80	25	60
RG502H / RG503	75% / 20%	SPAN80	5	60

3.3.4 Effect of Particle Size on Potential Gastroretentive Behaviour

A formulation was selected based on yield and density, and was sieved to produce discrete size fractions from 100 μm to 2000 μm . These particles were then analysed for morphology, density, and porosity. The effect of size on porosity and subsequent density was assessed.

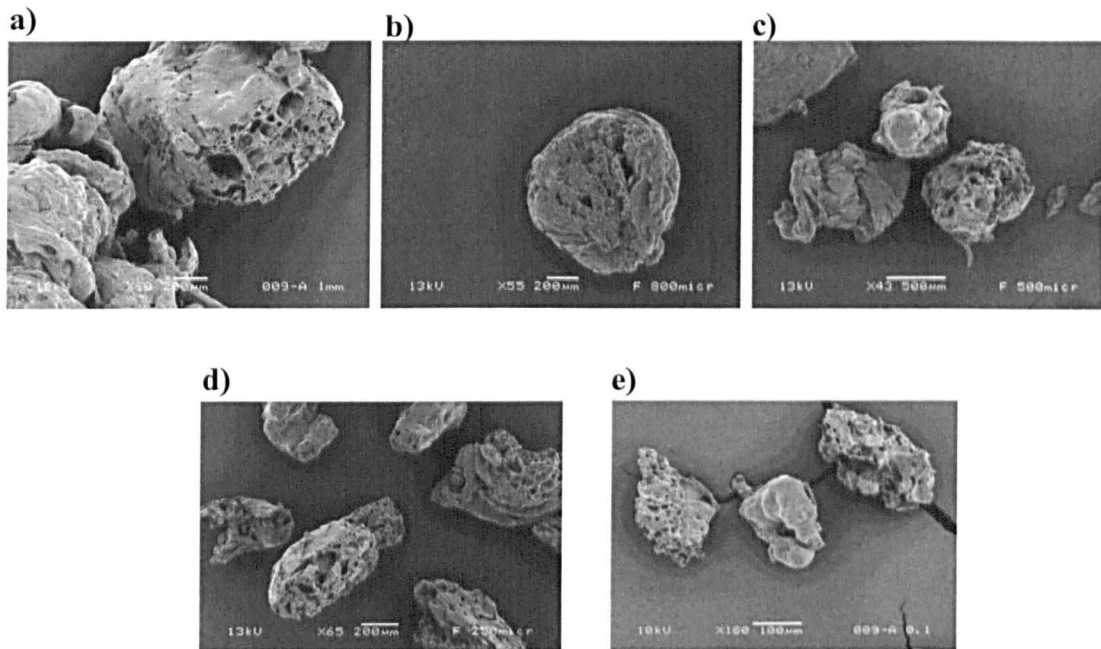


Figure 3.7 SEM images showing particles prepared with PLGA (12KDa): PLGA (5KDa):SPAN80 (ratio 70:25:5) of different size fractions a) 1 mm (scale bar 200 μm) b) 800 μm (scale bar 200 μm) c) 500 μm (scale bar 500 μm) d) 250 μm (scale bar 200 μm) e) 100 μm (scale bar 100 μm).

The SEM (Figure 3.7) images provide evidence for the surface morphology of particles; x-ray microtomography (microCT) allowed a more detailed exploration of the microarchitecture of the particles to be carried out.

Figure 3.8 shows the porosity (given as a percentage of total particle space) for the different size ranges from 100 μm up to 2000 μm as determined using microCT. The profile shows that the larger particles have a greater percentage

porosity and there appears to be a large jump between those particles $<500 \mu\text{m}$ and those which are $>500 \mu\text{m}$. The larger sized particles express extremely high porosity values of around 60%.

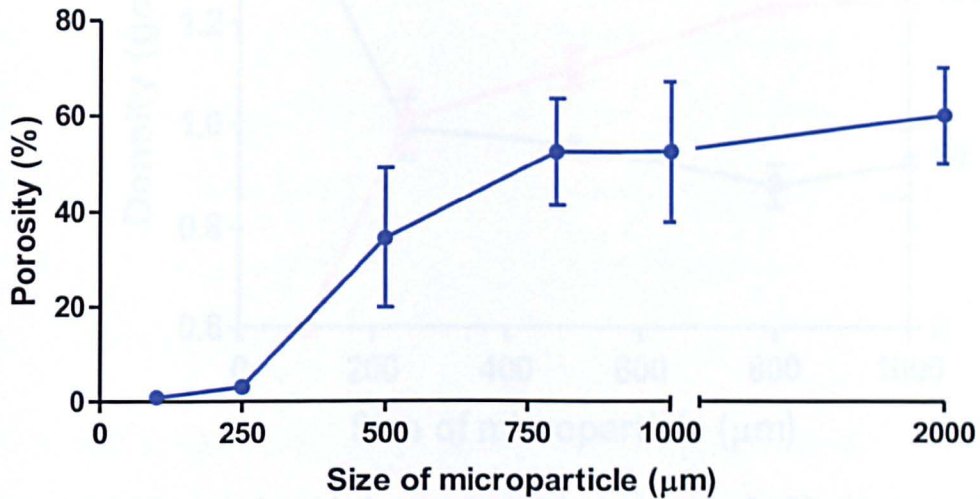


Figure 3.8 Porosity of microparticles with increasing size as measured using microCT ($n=6 \pm SD$)

Both density data and *in vitro* buoyancy data are presented in Figure 3.9 confirming that the smaller, less porous (as determined by microCT), particles possess higher densities and subsequently demonstrate poorer performance in the *in vitro* buoyancy investigation. Photographs were taken of the particles following 6 h suspension in SGF and are presented in Figure 3.10. The photographs confirm the conclusion provided by Figures 3.8 and 3.9 as particles larger than 500 μm remain buoyant following 6 h exposure to simulated gastric media. However particles smaller than 500 μm begin to lose buoyancy and particles smaller than 250 μm do not demonstrate successful buoyancy over the time period (6 h).

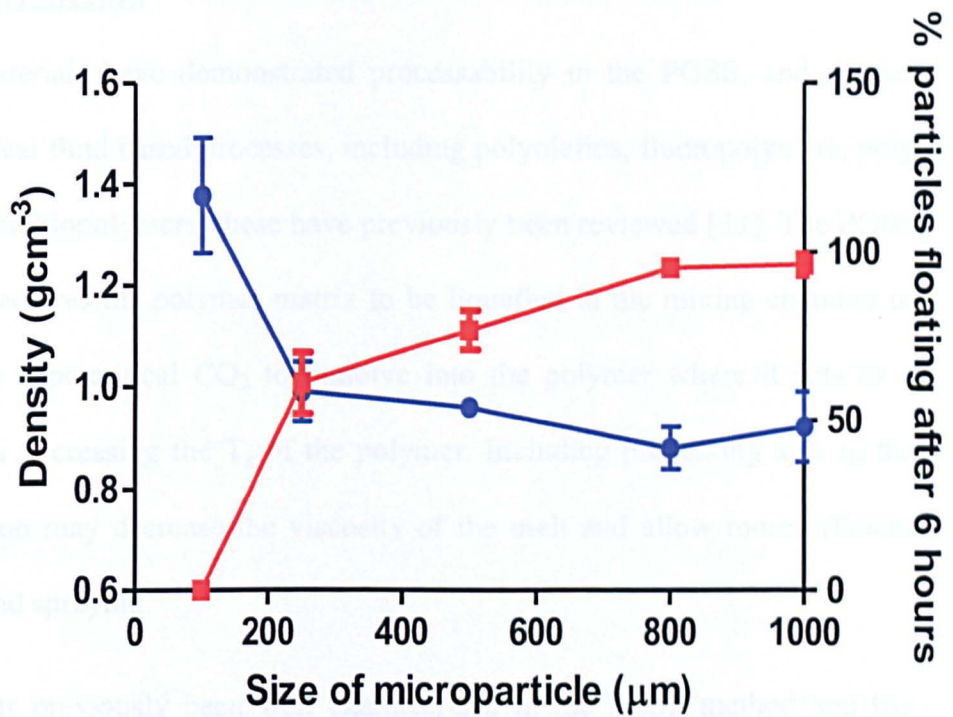


Figure 3.9 The relationship between particle density ($n=6 \pm SD$ (blue)) and *in vitro* buoyancy ($n=3 \pm SD$) (red) behaviour for a range of particles sizes. Density determined as described in section 3.2.2.4 and buoyancy determined as described in section 3.2.2.5

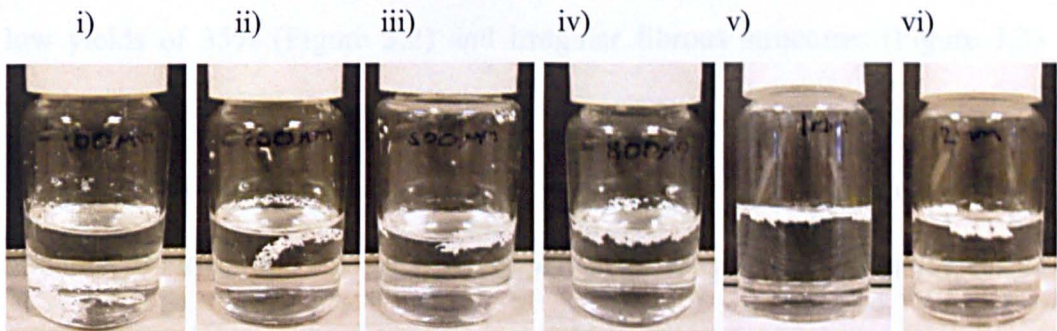


Figure 3.10 *In vitro* buoyancy test for different sized particles i) 100 µm ii) 250 µm iii) 500 µm iv) 800 µm v) 1000 µm vi) 2000 µm in a simulated gastric medium.

3.4 Discussion

Many materials have demonstrated processability in the PGSS, and similar supercritical fluid based processes, including polyolefins, fluoropolymers, polyamides and biopolymers, these have previously been reviewed [32]. The PGSS process requires the polymer matrix to be liquefied in the mixing chamber to allow the supercritical CO₂ to dissolve into the polymer where it acts as a plasticiser decreasing the T_g of the polymer. Including processing aids in the formulation may decrease the viscosity of the melt and allow more efficient mixing and spraying.

PLGA has previously been well characterised in the PGSS method and has been shown to produce microparticles suitable for controlled release drug delivery [27]. PLGA was therefore selected as the polymer in this study to form the microparticle matrix. However, the high viscosity of the PLGA (inherent viscosity 0.16-0.24 dl/g) led to processing difficulties and relatively low yields of 35% (Figure 3.2) and irregular fibrous structures (Figure 3.3) being obtained. As a consequence to the low yields achieved with formulations containing 100% PLGA the fatty acid myristic acid was incorporated with the intention of lowering the viscosity of the polymer melt allowing for easier processing and the production of higher yields.

The changing morphologies of particles as the PLGA: myristic acid ratio is altered as revealed by SEM imaging is shown in Figure 3.3. The presence of myristic acid resulted in particles which appeared smaller, with an increased tendency to form aggregates with an almost 'fluffy' morphology. The use of fatty acids has previously been reviewed in the production of solid lipid nanoparticles [39]. Specifically, myristic acid has been successfully processed

using the PGSS method as the supercritical conditions depress the melting point of myristic acid from 54.3°C to 39-40°C [40]. As the ratio of PLGA in the formulation increases the particles become more discrete and appear larger. On scrutiny of the SEM images porosity is also apparent in the particles.

Particle yield data presented in Figure 3.2 demonstrates that although increasing the myristic acid content in the particles the yield can be improved from 35% to 65%. However as the myristic acid content increases other properties of the system such as controlled release may be compromised. The myristic acid may act as a processing aid improving yield in a similar way to poloxamer 407 and 188 and Solutol HS15 which have been introduced as processing aids in the PGSS method [27]. These processing aids were employed to improve the drug release characteristics of human growth hormone (hGH) loaded PLGA microparticles which demonstrated maintenance of hGH in rat serum for 3 days. The addition of PEG to PLA in the PGSS process has been observed to decrease the viscosity of the melt. A decrease in viscosity was measured as the two materials became increasingly miscible. This miscibility was also found to have a direct effect on the processing of the blend of the two polymers [28]. In the present work, myristic acid may be acting in a similar way improving particle production though a decrease in viscosity of the polymer melt.

As the PLGA content increases relative to myristic acid the density of the microparticles was found to increase (Figure 3.5). Helium air pycnometry was selected to measure density as it allows a measure of the true volume of the system to be determined, taking into account the porous space. Due to its small size, helium gas is used to diffuse into the smallest pores and may also diffuse

between the polymer chains. This provides a true measure of the exact volume of polymer matrix which is then used along with a known mass to determine density of the particles. The results confirmed that the lowest densities found in particles prepared with 100% myristic acid exhibit densities higher than 1 gcm^{-3} . The reported density of myristic acid as a pure material is 0.8622 gcm^{-3} indicating that during processing the density of myristic acid actually may increase. This is not the case for PLGA as the pre-processing density was measured as $1.4793(\pm 0.0199) \text{ gcm}^{-3}$ with a decrease to $1.2611(\pm 0.0016) \text{ gcm}^{-3}$ being measured following processing.

Reports in the literature state that the density of the gastric fluid is in the region of 1.004 gcm^{-3} [41] therefore a system suitable for gastroretention in this environment must demonstrate a density of less than this value. Figure 3.5 shows photographs of the particles in suspension in a simulated gastric fluid offering an illustration as to how successful these particles will be as floating drug delivery systems. Whilst all formulations show a fraction of particles appear to remain buoyant the majority of the particles are in suspension or simply sink to the bottom of the vial suggesting these formulations may not be appropriate for gastroretention. Nevertheless the decrease in PLGA density following processing indicates the potential of the PGSS method to reduce density of starting materials and therefore produce particles with low densities. Porosity data, as measured using microCT (Figure 3.8) reveals porosity can exceed 50% supporting the claim that the PGSS method has the capacity to produce a highly porous product. In order to achieve the appropriate low densities a highly porous product must be fabricated. In the PGSS method the pores are formed during the depressurization step, the supercritical carbon

dioxide is dissolved into the plasticised polymer which on depressurisation will return to the gaseous state and diffuse out. Simultaneously the plasticised polymer will be solidifying and therefore the gaseous carbon dioxide will leave behind open spaces the introduction of a nitrogen back pressure enables this step to be controlled as the presence of a back pressure slows down the diffusion of CO₂ from the product allowing the production of microparticles [34].

Due to the high densities of particles produced with the PLGA / myristic acid blend these particles were deemed to be unsuitable for gastroretention (Figure 3.5 and Figure 3.6) subsequently other materials were investigated with the aim of producing particles with lower densities. Table 3.1 demonstrates the various formulations attempted in the pursuit to produce particles with high yields and low densities. Initially, the surfactant SPANTM80 was introduced in place of myristic acid; by changing the processing aid the particles produced may be more suitable in terms of yield and density for the aims of this project. The SPANTM80 has a lower melting point than myristic acid (-20.3°C compared to 54.4°C) and demonstrates a lower viscosity than myristic acid. Such properties may enhance the processing aids ability to improve PLGA processing. Nevertheless, the particles containing SPANTM80 and PLGA did not produce high yields and any product was soft and adhesive at room temperature and therefore could not be collected. As a next step a higher molecular weight PLGA polymer, which maintains the 50:50 lactide: glycolide ratio but has an approximate molecular weight of ~25 kDa was included. This polymer is more viscous, with an inherent viscosity of 0.32-0.44 dl/g compared to 0.16-0.24 dl/g of the PLGA with a lower molecular weight. As a result of

this increased viscosity this polymer does not produce any product following PGSS processing, however in combination with a processing aid such as SPAN™80 it is possible to produce a product with a yield of around 60% (Table 3.1).

The formulation demonstrating good yields ($61.4\% \pm 3.5$), with a highly porous product and the potential for buoyancy in the gastric medium has a composition of RG502H 75%, RG503 20%, SPAN 80 5%. This formulation was processed, and the product ground to produce a particulate product which was sieved into various size fractions.

Previously it has been reported that larger particles demonstrate longer gastric residence times [42], as the smaller particles are likely to get emptied from the stomach along with food particles during digestive processes. In the present work a wide range of size fractions were considered and analysed for prospective use as gastroretentive systems. The SEM images in Figure 3.7 show the morphologies of the different size fractions. Although the particles are irregular in shape the presence of pores at the surface appears to be conserved in all size fractions.

The density of the various size fractions was investigated using helium air pycnometry. As previously discussed, the density of a system suitable for gastroretention is $<1.004 \text{ gcm}^{-3}$. The relationship between size, density, and buoyancy was investigated with particles larger than $250 \mu\text{m}$ being revealed to remain buoyant in the gastric environment. This was verified using an *in vitro* buoyancy analysis in which the $>100 \mu\text{m}$ size fraction did not demonstrate adequate buoyancy and as the size is increased the percentage of particles

which remain buoyant also increased (Figure 3.8). In order to better understand the fundamental differences between particles of different sizes which may contribute to the changes in density, the detailed microarchitecture of the particles was examined using microCT. This data demonstrates that as the particle size increased the percentage porosity also increased, (Figure 3.10) this decreased the density of the particles. The presence of pores in the product is a result of the phase changes of the CO₂ and the polymer on depressurisation and is therefore difficult to control. The grinding of the product may be the basis of the decreased porosity of the smaller particles. Grinding and milling are common processes in many industries, in the food industry air holes present in material has been found to provide cleavage steps [43] influencing particle shape following milling. Fracturing is more likely to occur along lines of weakness, this would include existing pores. Smaller particles will contain fewer pores and the larger particles are able to harbour more and larger pores, this concept is illustrated below in Figure 3.11.

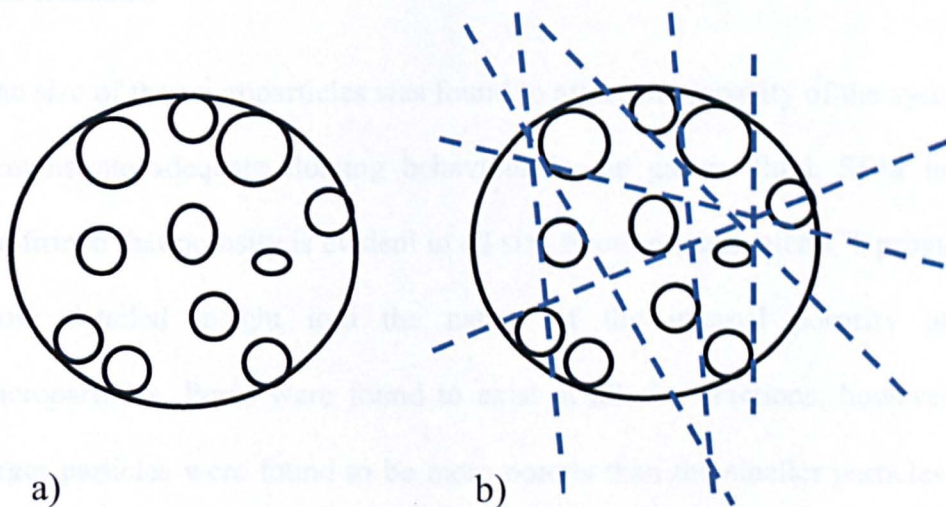


Figure 3.11 Illustration of how the grinding procedure results in a number of smaller particles (b) with lower porosity than the original larger particle (a).

3.5 Conclusions

The effect of material on the yield and morphology of the product was initially investigated, with the choice of polymer and the composition of the formulation being found to affect the yield and morphology of the product. Initially, particles prepared using PLGA and myristic acid were investigated, however helium air pycnometry quantitatively revealed that the density of these particles was not acceptable for gastroretention. Conclusions drawn from the density data was verified by investigating the floating ability of the particles in a simulated gastric fluid at 37°C under constant agitation in a shaking water bath for 6 h. This confirmed that none of the PLGA/ myristic acid formulations were suitable for gastroretention. New formulations were explored in an attempt to produce particles with lower densities. The most porous formulation tested was 75% RG502H (PLGA 12 kDa 505:50 LA:GA ratio) 20% RG503 (PLGA 24 kDa 50:50 LA: GA ratio) 5% SPAN80 and following production the product was ground and sieved to produce discrete size fractions.

The size of the microparticles was found to affect the capacity of the system to demonstrate adequate floating behaviour in the gastric fluid. SEM images confirmed that porosity is evident in all size fractions, and microCT provided a more detailed insight into the nature of the internal porosity of the microparticles. Pores were found to exist at all size fractions, however, the larger particles were found to be more porous than the smaller particles. The porosity data along with the *in vitro* buoyancy studies confirmed those size fractions which are suitable candidates for gastroretention are the particles >500 µm.

Large porous structures have previously been prepared using supercritical fluids in the area of tissue engineering, however the production of large, porous microparticles for gastroretention using this method, has not as far as the authors are aware previously been investigated.

3.6 References

1. Meka, L., et al., *Design and Evaluation of Polymeric Coated Minitablets as Multiple Unit Gastroretentive Floating Drug Delivery Systems for Furosemide*. Journal of Pharmaceutical Sciences, 2009. **98**(6): p. 2122-2132.
2. Goole, J., F. Vanderbist, and K. Amighi, *Development and evaluation of new multiple-unit levodopa sustained-release floating dosage forms*. International Journal of Pharmaceutics, 2007. **334**(1-2): p. 35-41.
3. Desai, S. and S. Bolton, *A floating controlled-release drug-delivery system in-vitro-in-vivo evaluation*. Pharmaceutical Research, 1993. **10**(9): p. 1321-1325.
4. Sher, P., et al., *Low density porous carrier based conceptual drug delivery system*. Microporous and Mesoporous Materials, 2007. **102**(1-3): p. 290-298.
5. Streubel, A., J. Siepmann, and R. Bodmeier, *Floating matrix tablets based on low density foam powder: effects of formulation and processing parameters on drug release*. European Journal of Pharmaceutical Sciences, 2003. **18**(1): p. 37-45.
6. Sher, P., et al., *Modulation and Optimization of Drug Release from Uncoated Low Density Porous Carrier Based Delivery System*. Aaps Pharmscitech, 2009. **10**(2): p. 547-558.
7. Sato, Y., et al., *In vitro and in vivo evaluation of riboflavin-containing microballoons for a floating controlled drug delivery system in healthy humans*. International Journal of Pharmaceutics, 2004. **275**(1-2): p. 97-107.
8. Kamila, M.M., et al., *Multiunit Floating Drug Delivery System of Rosiglitazone Maleate: Development, Characterization, Statistical Optimization of Drug Release and In Vivo Evaluation*. Aaps Pharmscitech, 2009. **10**(3): p. 887-899.
9. Maa, Y.-F. and S.J. Prestrelski, *Biopharmaceutical powders: Particle formation and formulation considerations*. Current Pharmaceutical Biotechnology, 2000. **1**(3): p. 283-302.
10. Dubey, R., T.C. Shami, and K.U.B. Rao, *Microencapsulation Technology and Applications*. Defence Science Journal, 2009. **59**(1): p. 82-95.
11. Uhrich, K.E., et al., *Polymeric systems for controlled drug release*. Chemical Reviews, 1999. **99**(11): p. 3181-3198.
12. Freiberg, S. and X. Zhu, *Polymer microspheres for controlled drug release*. International Journal of Pharmaceutics, 2004. **282**(1-2): p. 1-18.
13. Jung, J. and M. Perrut, *Particle design using supercritical fluids: Literature and patent survey*. Journal of Supercritical Fluids, 2001. **20**(3): p. 179-219.
14. Knez, Z. and E. Weidner, *Particles formation and particle design using supercritical fluids*. Current Opinion in Solid State & Materials Science, 2003. **7**(4-5): p. 353-361.
15. Shariati, A. and C.J. Peters, *Recent developments in particle design using supercritical fluids*. Current Opinion in Solid State & Materials Science, 2003. **7**(4-5): p. 371-383.

16. Nalawade, S.P., F. Picchioni, and L. Janssen, *Supercritical carbon dioxide as a green solvent for processing polymer melts: Processing aspects and applications*. Progress in Polymer Science, 2006. **31**(1): p. 19-43.
17. Reverchon, E. and G. Della Porta, *Supercritical fluids-assisted micronization techniques. Low-impact routes for particle production*. Pure and Applied Chemistry, 2001. **73**(8): p. 1293-1297.
18. Kwon, K.-T., et al., *Preparation of micro particles of functional pigments by gas-saturated solution process using supercritical carbon dioxide and polyethylene glycol*. Korean Journal of Chemical Engineering. **28**(10): p. 2044-2049.
19. Wendt, T., *Production of powder-shaped multiphase composite by means of the PGSS procedure*. Chemie Ingenieur Technik, 2007. **79**(3): p. 287-295.
20. Brion, M., et al., *The supercritical micronization of solid dispersions by Particles from Gas Saturated Solutions using experimental design*. Journal of Supercritical Fluids, 2009. **51**(1): p. 50-56.
21. Weidner, E., et al., *Manufacture of powder coatings by spraying of gas-enriched melts*. Chemical Engineering & Technology, 2001. **24**(5): p. 529-533.
22. Weidner, E., *High pressure micronization for food applications*. Journal of Supercritical Fluids, 2009. **47**(3): p. 556-565.
23. Davies, O.R., et al., *Applications of supercritical CO₂ in the fabrication of polymer systems for drug delivery and tissue engineering*. Advanced Drug Delivery Reviews, 2008. **60**(3): p. 373-387.
24. Tandy, A., et al., *Dense gas processing of polymeric controlled release formulations*. International Journal of Pharmaceutics, 2007. **328**(1): p. 1-11.
25. Subramaniam, B., R.A. Rajewski, and K. Snavely, *Pharmaceutical processing with supercritical carbon dioxide*. Journal of Pharmaceutical Sciences, 1997. **86**(8): p. 885-890.
26. Nalawade, S.P., F. Picchioni, and L.P.B.M. Janssen, *Batch production of micron size particles from poly(ethylene glycol) using supercritical CO₂ as a processing solvent*. Chemical Engineering Science, 2007. **62**(6): p. 1712-1720.
27. Jordan, F., et al., *Sustained release hGH microsphere formulation produced by a novel supercritical fluid technology: In vivo studies*. Journal of Controlled Release, 2010. **141**(2): p. 153-160.
28. Kelly, C.A., *Supercritical CO₂: A Clean and Low Temperature Approach to Blending PLA and PEG*. Advanced Functional Materials, 2010. **22**: p. 8.
29. Martin, A. and M.J. Cocero, *Micronization processes with supercritical fluids: Fundamentals and mechanisms*. Advanced Drug Delivery Reviews, 2008. **60**(3): p. 339-350.
30. Tai, H., et al., *Control of pore size and structure of tissue engineering scaffolds produced by supercritical fluid processing - Discussion with reviewers*. European Cells & Materials, 2007. **14**: p. 76-77.
31. Weidner, E., R. Steiner, and Z. Knez, *Powder generation from polyethyleneglycols with compressible fluids*, in *High Pressure Chemical Engineering*. 1996. p. 223-228.
32. Yeo, S.D. and E. Kiran, *Formation of polymer particles with supercritical fluids: A review*. Journal of Supercritical Fluids, 2005. **34**(3): p. 287-308.
33. Hao, J.Y., et al., *Supercritical fluid assisted melting of poly(ethylene glycol): a new solvent-free route to microparticles*. Journal of Materials Chemistry, 2005. **15**(11): p. 1148-1153.
34. Hao, J.Y., et al., *Plasticization and spraying of poly (DL-lactic acid) using supercritical carbon dioxide: Control of particle size*. Journal of Pharmaceutical Sciences, 2004. **93**(4): p. 1083-1090.

35. Itoh, T., et al., *Effect of particle-size and food on gastric residence time of nondisintegrating solids in Beagle dogs*. Journal of Pharmacy and Pharmacology, 1986. **38**(11): p. 801-806.
36. Khosla, R. and S.S. Davis, *The effect of tablet size on the gastric-emptying of nondisintegrating tablets*. International Journal of Pharmaceutics, 1990. **62**(2-3): p. R9-R11.
37. Khosla, R., L.C. Feely, and S.S. Davis, *Gastrointestinal transit of non-disintegrating tablets in fed subjects*. International Journal of Pharmaceutics, 1989. **53**(2): p. 107-117.
38. Clarke, G.M., J.M. Newton, and M.D. Short, *Gastrointestinal transit of pellets of differing size and density*. International Journal of Pharmaceutics, 1993. **100**(1-3): p. 81-92.
39. Muller, R.H., K. Mader, and S. Gohla, *Solid lipid nanoparticles (SLN) for controlled drug delivery - a review of the state of the art*. European Journal of Pharmaceutics and Biopharmaceutics, 2000. **50**(1): p. 161-177.
40. Vijayaraghavan, M., *A Supercritical Carbon Dioxide Route to Protein Loaded Microparticles for Pulmonary Drug Delivery*, in *School of Pharmacy*. 2010, University of Nottingham: Nottingham. p. 206.
41. Whitehead, L., et al., *Floating dosage forms: an in vivo study demonstrating prolonged gastric retention*. Journal of Controlled Release, 1998. **55**(1): p. 3-12.
42. Garg, R. and G.D. Gupta, *Progress in Controlled Gastroretentive Delivery Systems*. Tropical Journal of Pharmaceutical Research, 2008. **7**(3): p. 1055-1066.
43. Scanlon, M.G. and J. Lamb, *Fracture mechanisms and particle-shape formation during size-reduction of a model food material*. Journal of Materials Science, 1995. **30**(10): p. 2577-2583.

Chapter 4

Incorporation of Active Pharmaceutical Ingredient into Particles Produced using the PGSS Method

4.1 Introduction

Oral administration for therapeutics in many cases is highly desirable from the point of view of the patient and health care professional alike, however limitations of these systems often lie with poor bioavailability [1, 2]. The low bioavailability of drugs administered *via* the oral route can be a result of the barriers the drug must overcome from the intestinal lumen in order to reach the systemic circulation. In order to reach the circulation this journey involves the absorption through the intestinal wall. For many drugs, including furosemide, riboflavin, acyclovir, captopril, levodopa and metformin [3], the absorption occurs at a relatively narrow area of the upper small intestine, within a so called absorption window (as discussed in Section 1.2.2.3). This presents a problem when considering relatively rapid gastric transit times. The 'house keeper' wave (discussed in more detail in Section 1.2.2.2) occurs every 1-2 h in the fasted state [4] and serves to remove debris from within the stomach. Such peristaltic waves usually carry the delivery system past the absorption window. For instance, ranitidine has been reported to exhibit absorption in the

upper part of the small intestine and demonstrates an oral bioavailability of 50% of the administered dose [5]. Although 50% is considered an adequate value for oral bioavailability, the oral bioavailability has been improved 2.4 times using a gastroretentive floating formulation [6]. Similarly, an approximate 210% increase in oral bioavailability for riboflavin has been reported for a gastroretentive system, relative to a 'classical' immediate release formulation [7]. This was achieved through gastroretention over a period of approximately 10 h. The diuretic drug furosemide has a reported oral bioavailability of 40-60% [8]. This has been increased by a mucoadhesive formulation which demonstrated an AUC value 1.8 times larger in comparison with a non-adhesive formulation [3], once again indicating an improvement in bioavailability through gastroretention. These studies illustrate the potential that novel formulations may hold in improving oral bioavailability.

Gastroretentive delivery systems potentially increase drug bioavailability by retaining the delivery system in the stomach, above the drug absorption window, typically located in the upper small intestine. If the system is in the same time capable of exhibiting controlled release of the drug, it would provide a 'stable' supply of drug to the absorption window. Examples of gastroretentive delivery systems have been recently reviewed [9]. Although good success has been reported with different gastroretentive formulations, there are many factors that need to be considered for a formulation to be effective.

Gastrointestinal transit is a major factor when developing gastroretentive systems; it is the motility along the GIT which must be overcome in order for the delivery formulation to remain in the stomach. In an average human, the

time taken for stomach contents to pass into the intestines is around 4 h [10], although this value is highly variable and may be as fast as 10-15 mins for water or up to 6 h for a barium meal

A recent publication demonstrated a mean gastric retention period of 5.5 ± 0.8 h for a controlled release floating tablet [11]. A comparable period of gastric retention (5.50 ± 0.77 h) was reported for effervescent floating matrix tablets containing baclofen [12]. Other gastric-floating drug delivery systems based on bilayer tablets have reported gastric residence times of 6 h [13], and values in excess of 8 h have been reported for floating matrices of metronidazole [14]. However high intersubject variability in gastric residence times has been observed as well as day-day intrasubject variability [15, 16]. Physiological factors such as composition and volume of stomach content, gastric content transit times, pH levels, presence of food along with the specific composition of consumed material, gender and age all influence gastric emptying [17]. The presence of food in the stomach affects gastric transit time and therefore exerts an impact on drug bioavailability [18, 19] by influencing drug solubility, gastric transit, and delivery system disintegration.

Gastric pH is another important factor, which can impact both, the solubility of the drug and the stability of the delivery system [20, 21]; this is a particular concern with gastroretentive systems which remain resident in the stomach at a low pH for prolonged periods.

This chapter focuses on the development of the system previously described in Chapter 3 as a drug delivery system for the sustained release of active pharmaceutical compounds over the period of time the system will remain

resident in the stomach (~ 6 h). The model drugs selected for *in vitro* release studies, furosemide and riboflavin (chemical structures are presented in Fig. 4.2), both demonstrate narrow absorption windows in the upper small intestine and therefore could benefit from gastroretentive technology. Furosemide is a highly potent diuretic which inhibits chloride reabsorption in the loop of Henley in the kidney; this in turn prevents sodium reabsorption. It is used in the treatment of congestive heart failure and oedema. Various sustained release formulations for furosemide include hydroxypropylmethyl cellulose (HPMC) matrix tablets [22] which demonstrate good sustained release properties, however, as furosemide is absorbed in the upper small intestine, sustained release formulation is not an ideal solution, unless coupled with gastroretention. A prolonged release unfolding gastroretentive formulation of furosemide has shown improvements in pharmacokinetics in humans compared with immediate release, unfolding, counterpart [23]. Floating formulations of furosemide, based on gas generating sodium bicarbonate and an outer layer of polymethacrylates, have demonstrated sustained release over 10 h and a gastric residence time of 6 h [24].

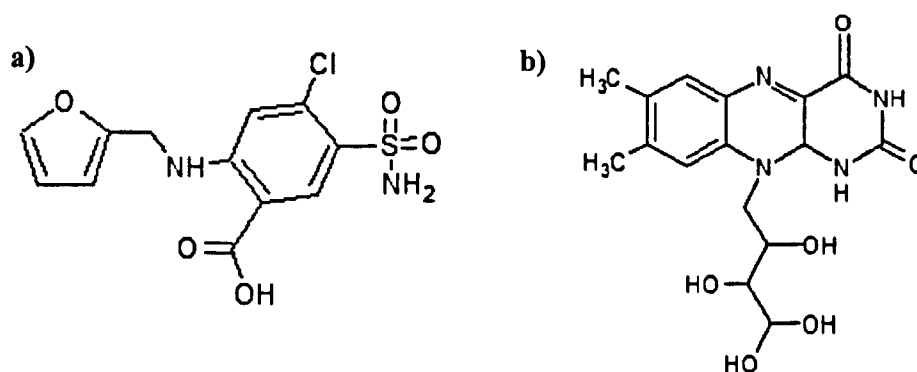


Figure. 4.1 Chemical structures for a) Furosemide and b) Riboflavin. Solubilities 0.006 and 0.01 mg/ml respectively

Riboflavin, also known as vitamin B₂, plays a key role in energy metabolism. Riboflavin is often used as a model drug for gastroretentive formulation development, as it is a suitable candidate with known absorption window and relative safety. Enhancement of bioavailability of riboflavin has been demonstrated in dogs [25], as well as humans [7], through the use of gastroretentive systems based on an unfolding formulation. Floating microballoons containing riboflavin have demonstrated good gastroretention in man [26] although this was found to be dependent on filling state of the stomach.

The release of the drug from a gastroretentive formulation should ideally be sustained for the duration of the formulation's presence above the absorption site in the intestinal tract for that particular drug. *In vitro* investigations into the release profiles of drugs from gastroretentive formulations have reported sustained release for approximately 9 [27], 8 [28], or up to 24 [29] h. These periods should correlate with the expected time the system will be resident in the stomach/above the absorption window. Otherwise, any subsequent release of the drug will not contribute to the absorption/bioavailability.

Regarding the drug release, the size of delivery formulation has been found to impact the release of drugs from PLGA microparticles [30]. For instance, the release of dexamethasone from PLGA microspheres of two different sizes, 1 μm and 20 μm , showed that, although the burst release from the smaller microspheres was high (around 20% of the encapsulated dose), the cumulative release over the course of the study (550 h) was only 30%. In contrast, 20 μm microspheres demonstrated an almost linear drug release up to 90% over 550 h

with very little initial burst [31]. 5-Fluorouracil-loaded, poly(lactic-co-glycolic acid)-based microparticles also demonstrated a trend for slower release with smaller particle sizes [32]. Although at the final time point (21 h) the release from all size fractions was at 100% the smaller particles (<36 μm) demonstrated a slower rate with only 50% released after 7 h, whereas the larger particles (125-72 μm) revealed approximately 80% release after 7 h.

The faster release rate from the larger particles in the above examples may be surprising as it is more common for PLGA microparticles to demonstrate a decrease in drug release rate with larger particles [33]. This decrease does not appear as pronounced in microparticles demonstrating high porosities [30]. In order to explain this release behaviour, changes in T_g of the small and large particles over the course of the release study were assessed. T_g decreased faster with time for the larger particles (reduction to 25°C for 73 μm particles and 45°C for 7.3 μm particles over 30 days) which may indicate an increased rate of polymer degradation in the larger particles. This increase in PLGA degradation rate in larger particles has been reported previously [34]. With the rate of drug release being influenced by the size of particle, this presents a parameter which should not be overlooked when optimising release rate from a novel system.

The release profiles of the two model drugs from particles of various sizes (prepared as detailed in Chapter 3) will be investigated in this chapter. The release profile will be discussed in the context of the morphological changes of the particles following exposure to the release media at different pH levels, PBS (at pH 7.4) and SGF (at pH 1.2).

4.2 Materials and methods

4.2.1 Materials

Furosemide was obtained from VWR International Ltd, and riboflavin was obtained from Calbochem[®]. Sodium chloride, pepsin, and 5M HCl to prepare the simulated gastric fluid was obtained from Fisher Scientific. The phosphate buffer solution was obtained from Fisher Scientific as tablets and prepared as *per* manufacturer instructions. Sodium hydroxide pellets were obtained from Fisher Scientific. Other materials used in particle preparation are described in Chapter 3 (Section 3.2.1).

4.2.2 Methods

4.2.2.1 Incorporation of Active Pharmaceutical Ingredient into Particulate Formulation

Initial drug loading for both drugs was 5 % (w/w) of the 2 g batch introduced to the PGSS apparatus. The following formulation was selected as it demonstrated the most appropriate characteristics for gastroretention, it consisted of:

- PLGA (RG502H ~12KDa) 70% (w/w)
- PLGA (RG503 ~25KDa) 20% (w/w)
- SPAN[™]80 5% (w/w)
- Active pharmaceutical ingredient 5% (w/w)

The materials were weighed out, introduced to the PGSS apparatus and formulations prepared as described in detail in Chapter 2 (Section 2.1).

4.2.2.2 Encapsulation Efficiency and *In Vitro* Drug Release

The encapsulation efficiency of drug loaded particles and the subsequent release patterns in both simulated gastric fluid (SGF) (preparation detailed in Chapter 2 Section 2.10) at pH 1.2 and in PBS at pH 7.4 was carried using UV/VIS as described in detail in Chapter 2 (Section 2.9).

4.2.2.3 Time-of-Flight Secondary Ion Mass Spectrometry (ToF-SIMS)

ToF-SIMS surface analysis was carried out to determine the distribution of drug related ionic species across the surface of the sample as described in detail in Chapter 2 (Section 2.12)

4.2.2.4 Scanning Electron Microscopy (SEM)

To assess the morphological characteristics of the particles prior to and following release studies SEM was carried out as described in Chapter 2 (Section 2.2)

4.2.2.5 Freeze Drying of Particles

In order to carry out microCT and SEM analysis of the particles following exposure to the release media the particles were filtered from the media and frozen in liquid nitrogen. The particles were then lyophilised in the freeze drier (Edwards Modulyo) for a period of 3 days.

4.2.2.6 X-ray Microtomography (microCT)

microCT was carried out to determine the porosity and internal morphology of the particles prior to and following the release study as described in detail in Chapter 2 (Section 2.3).

4.2.2.7 Differential Scanning Calorimetry (DSC)

Thermal analysis of particles was carried out as described in detail in Chapter 2 (Section 2.8).

4.3 Results

4.3.1 Encapsulation of Active Pharmaceutical Ingredients

Riboflavin, or furosemide, were introduced to the formulation at a ‘theoretical loading’ of 5% (w/w). Both drugs were encapsulated with high efficiencies of over 80% for all size fractions (Figure 4.2). A two-way ANOVA analysis carried out on the encapsulation data, confirms that there is no significant effect of particle size on encapsulation efficiency ($P=0.0671$), and that there is also no significant difference in the encapsulation efficiency between the two drugs ($P=0.0539$).

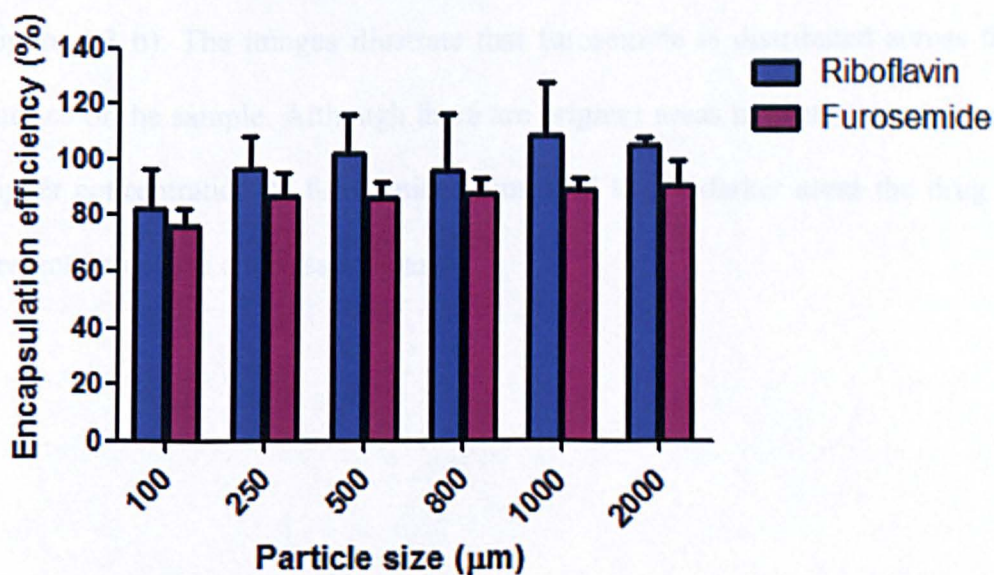


Figure 4.2. Encapsulation efficiency of furosemide and riboflavin for different size fractions of the PLGA particles, prepared by the PGSS method ($n=3 \pm SD$)

4.3.2 Surface Analysis of Drug Loaded Particles

ToF-SIMS surface analysis was applied to assess the distribution of the drug on the particles surface. Figure 4.3 a) shows the mass spectrum of the SNO_2H^- and SNO_2H_2^- peaks, which are characteristic of furosemide, in a furosemide loaded formulation, a blank PLGA formulation and furosemide powder. These peaks were selected to illustrate the presence of the drug due to the characteristic sulphur atom which is not found in other components of the formulation, enabling drug molecules to be distinguished from the other materials present. These peaks are higher in the furosemide powder sample than the formulation containing furosemide, which is expected due to the relatively higher amount of furosemide. The presence of the peaks in the furosemide loaded samples confirms that there is successful encapsulation within these particles. There is no 'contamination' with the drug of the control particles. The SNO_2H^- peak was used to prepare the ion images presented in Figure 4.3 b). The images illustrate that furosemide is distributed across the surface of the sample. Although there are brighter areas indicating a relatively higher concentration of furosemide, compared to the darker areas the drug is present across the entire sample area.

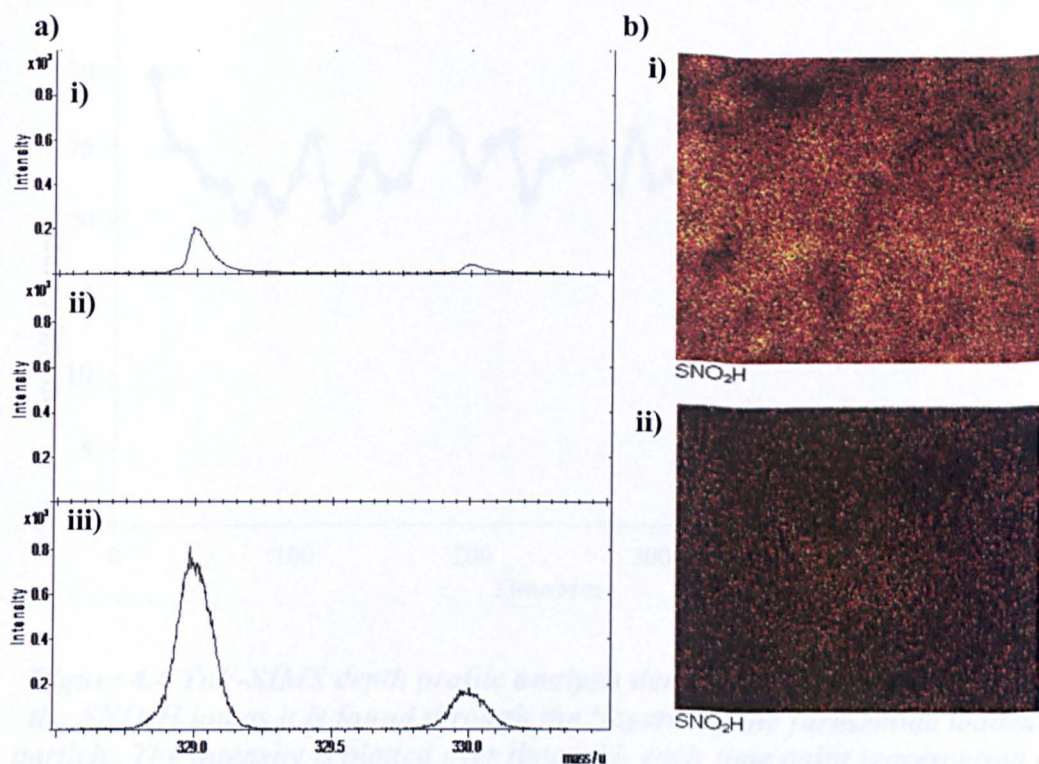


Figure 4.3 a) ToF-SIMS mass spectrum revealing the intensity of the SNO_2H (mass= 329) and SNO_2H_2 (mass= 330) peaks in i) drug loaded microparticles ii) blank microparticles and iii) furosemide powder. b) The corresponding ion distribution images which illustrate the distribution of the SNO_2H ion in i) drug loaded particles and ii) blank microparticles.

An application of ToF-SIMS known as depth profiling (explained in detail in section 2.13), allows the intensity of a specific ion fragment to be traced through a certain depth of a sample. This is, in essence, achieved by the sample surface being repeatedly ‘fired’ between the data acquisitions with heavy C_{60} ions which destroy a thin layer of ions close to the surface revealing a new layer below. This cycle of analysis followed by disruption of the surface was carried out every second for 500 seconds. Intensities for every ten seconds were averaged and plotted against time to explore any potential trends through the depth of the sample (Figure 4.4).

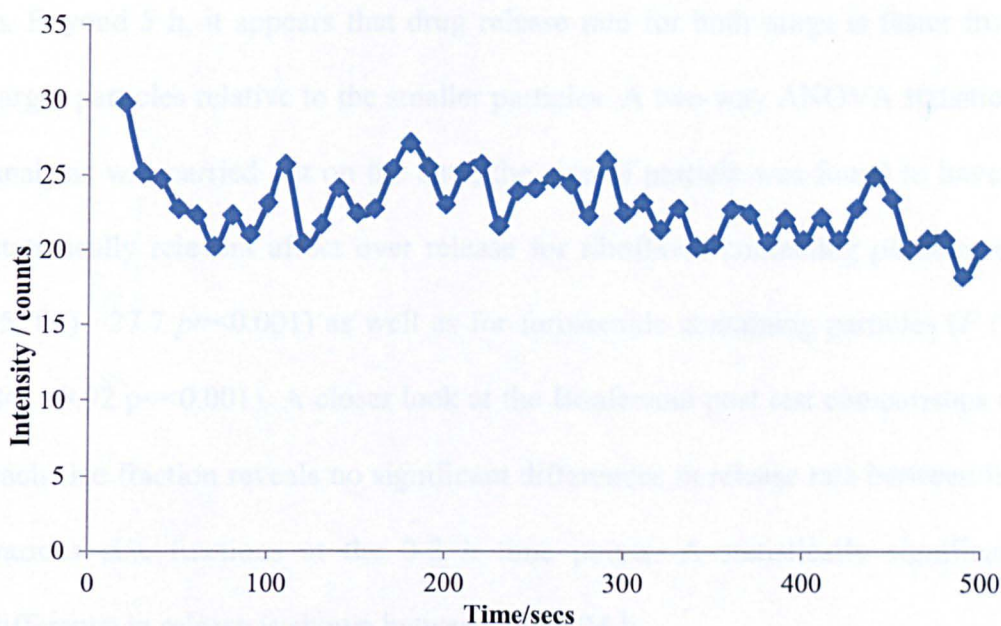


Figure 4.4 ToF-SIMS depth profile analysis demonstrating the intensity of the SNO_2H ion as it is found through the 'layers' of the furosemide loaded particle. The intensity is plotted over time with each time point representing a new layer through the sample. The average of intensity for every 10 seconds was calculated and averaged.

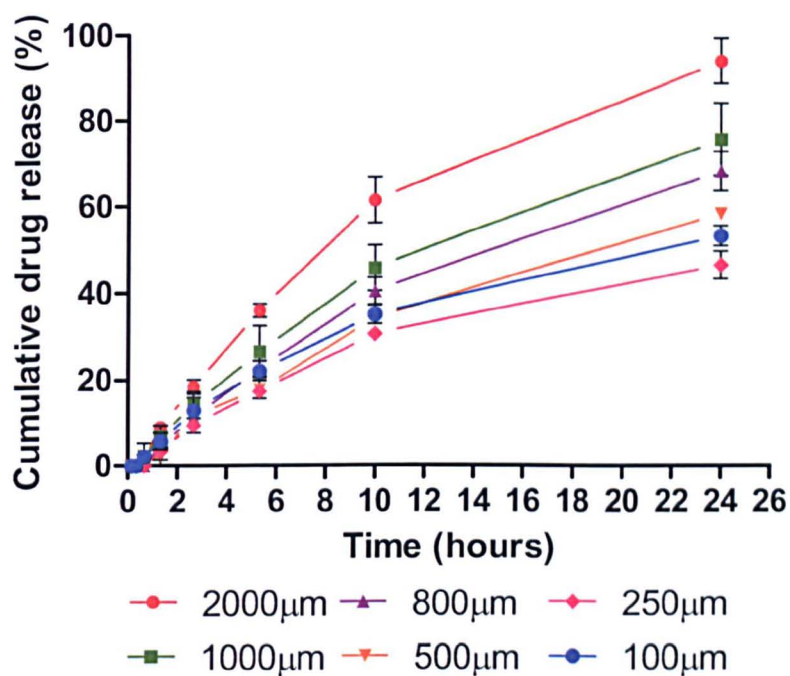
The depth profile appears to demonstrate that there is a higher intensity of furosemide originated ions on the very surface of the particles, followed by a decrease between the 10 and 20 second analyses. Penetrating deeper into the sample shows that the intensity generally remains about the same level, with a very shallow decrease in the intensity towards the deeper layers (300-500 seconds analyses).

4.3.3 Release Profile of Furosemide and Riboflavin from Different Size PLGA Particles in PBS Medium at pH7.4

The cumulative drug release profiles for furosemide and riboflavin from the PLGA formulation in *in vitro* conditions using PBS pH 7.4 as release medium are shown in Figure 4.5 a) and b). The release profiles do not reveal significant burst release of incorporated drugs, with gradual release up to approximately 5

h. Beyond 5 h, it appears that drug release rate for both drugs is faster from larger particles relative to the smaller particles. A two-way ANOVA statistical analysis was carried out on the data, the size of particle was found to have a statistically relevant affect over release for riboflavin containing particles ($F(5, 84) = 27.7$ $p < 0.001$) as well as for furosemide containing particles ($F(5, 84) = 9.92$ $p < 0.001$). A closer look at the Bonferroni post test comparisons of each size fraction reveals no significant differences in release rate between the various size fractions at the 0-3 h time points. A statistically significant difference in release is shown between 3 and 24 h.

a)



b)

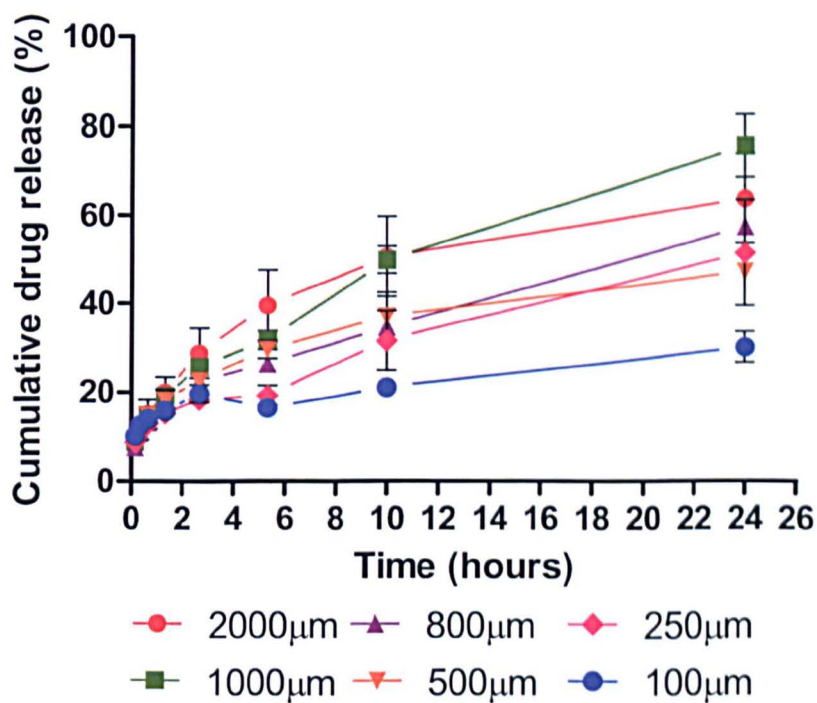
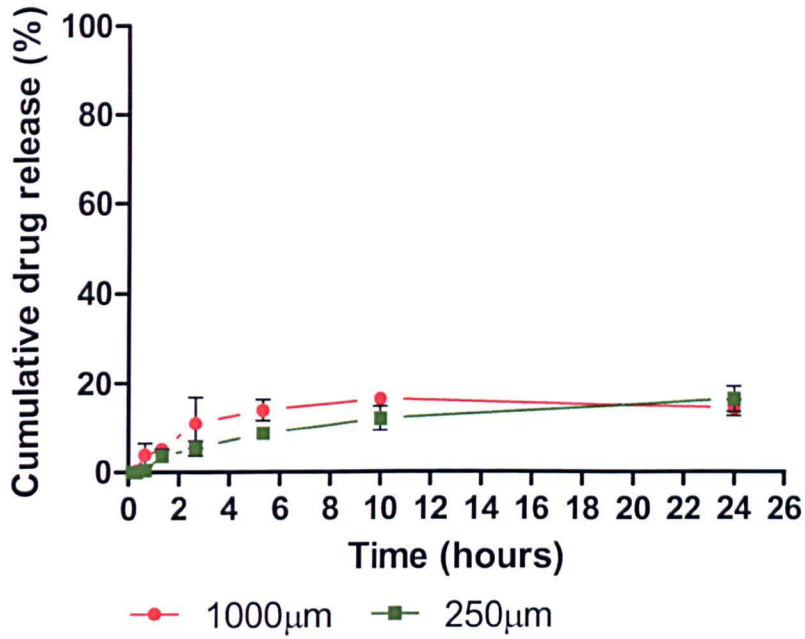


Figure 4.5 Cumulative release of a) riboflavin and b) furosemide from different sized microparticles using PBS pH7.4 as the release medium ($n=3\pm SEM$)

4.3.4 Release Profile of Riboflavin and Furosemide from Different Sized Particle Fractions in SGF Medium (pH1.2)

The previous section (4.2.3) describes the release studies using PBS as the release medium. This buffer is often used to simulate physiological conditions in drug release studies; however, it is not representative of the conditions in the stomach. Consequently release studies of an oral formulation need to be conducted in a more appropriate medium. The release studies were hence performed using particles with size of 1000 μm and 250-500 μm in a simulated gastric fluid (SGF) at pH 1.2 (Figure 4.6). The release profiles demonstrate that rate of drug release decreases in SGF medium relative to in PBS medium, with cumulative release not exceeding 20% for the two analysed size fractions over the course of 24 h. Statistical analysis of the data confirms a decrease in release rate in SGF, compared to in PBS at all time points for furosemide loaded particles sized 1000 μm ($p < 0.0001$) and at time points after 5 h for riboflavin loaded particles of the same size ($p = 0.001$).

a)



b)

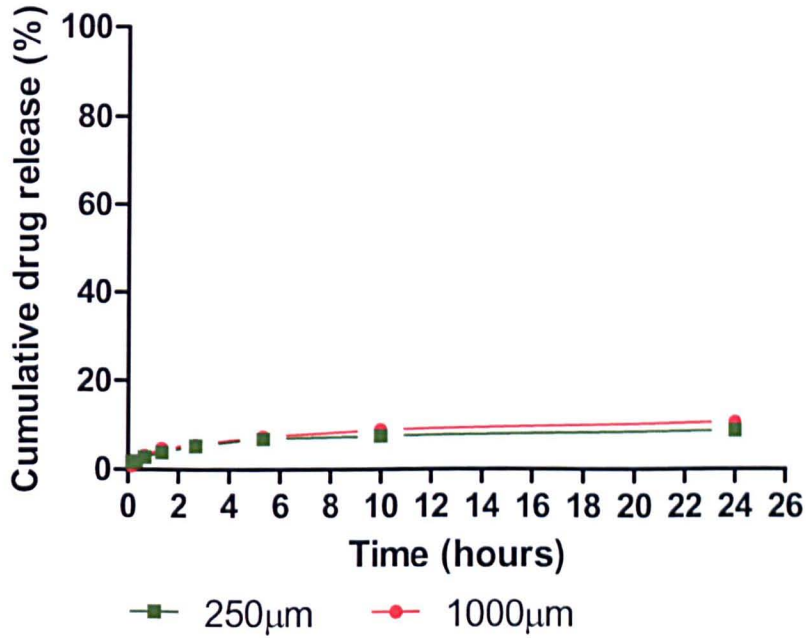


Figure 4.6 Cumulative release of a) riboflavin and b) furosemide from PLGA particle fractions sized 1000 μm and 250 μm in SGF. ($n=3 \pm\text{SEM}$)

4.3.5 Morphology of Particles Following Exposure to Release Media

Morphological analysis of formulations applying SEM and microCT was employed to determine possible changes in microarchitecture of the PLGA matrix following the *in vitro* release studies. Morphology of the formulation following the release study appears to be dependent on the medium used; for PBS pH 7.4 medium surface erosion is evident as *per* increased appearance of surface pores and sponge like structures (Figure 4.7), relative to the initial particles morphology. This contrasts with the morphology seen following exposure to SGF pH 1.2 (Figure 4.8) where the particles demonstrate smoother surfaces than is seen following exposure to PBS. This difference in morphology is complemented by the microCT analysis. The 3D models reconstructed from the data collected (Figure 4.9) show both the space occupied by polymeric matrix and the space within the particle which is 'open pore' space. Particles exposed to the low pH SGF show a decrease in porosity relative to their original porosity (Figure 4.9).

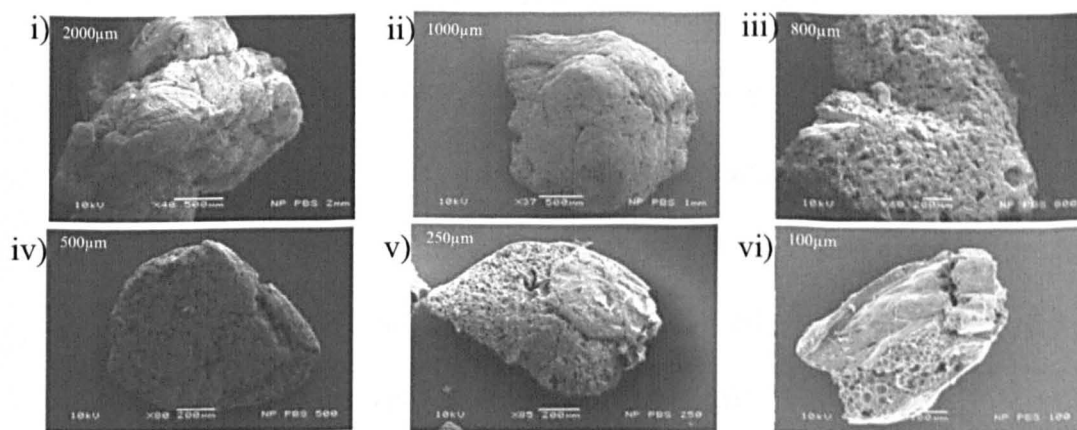


Figure 4.7 SEM images of different size fractions of PLGA particles loaded with riboflavin following 24 h exposure to PBS pH7.4. Particle sizes and scale bars indicated on individual images (scale bar values i), ii) 500 μm iii), iv), v) 200 μm , and vi) 100 μm)

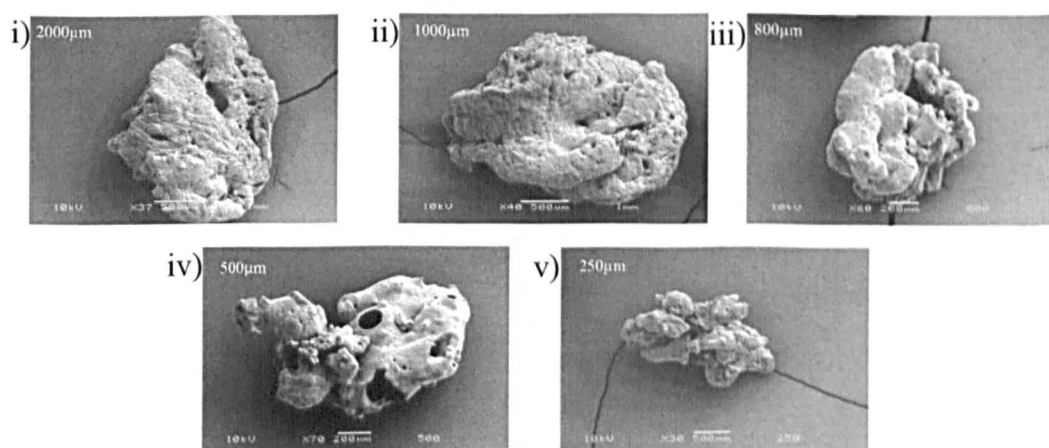


Figure 4.8 SEM images of different size fractions of PLGA particles loaded with riboflavin following 24 h exposure to SGF pH1.2. Particle sizes and scale bars indicated on individual images (scale bar values i),ii),v) 500 μm and iii) and iv) 200 μm)

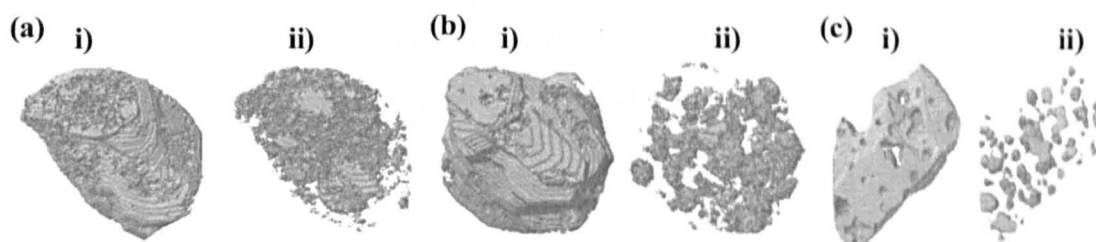


Figure 4.9 3D reconstruction of microCT data 1000 μm sized particles: following production and prior to the exposure (a) following exposure to PBS (b) and following exposure to SGF (c). In each case i) represents the polymer matrix, ii) represents the open pore space within the matrix allowing a visual comparison of the porosity to be made.

4.3.6 Thermal Analysis of Particles Following Exposure to Release Media

DSC analysis was carried out to determine the thermal characteristics of the PLGA particles loaded with riboflavin before and following the release studies. The thermograph (Figure 4.10) exposes a new thermal event following exposure of the formulations to both release media and somewhat decreased T_g temperatures following exposure to both PBS and SGF.

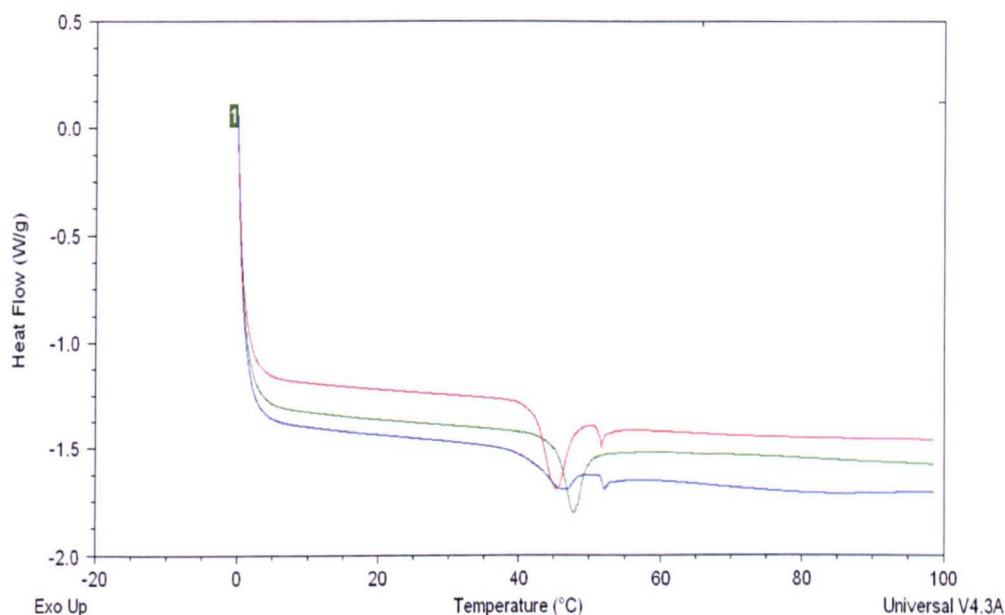


Figure 4.10 DSC thermograph of PLGA particles before exposure to release media (green) and following exposure to PBS (blue) and SGF (red).

4.3.7 Analysis of Mechanism of Drug Release

The release data obtained in section 4.4 and 4.5 were analysed by fitting the 24 h data obtained for the riboflavin release from 1000 μm sized particles fraction in PBS and SGF to typically used kinetic models (Table 4.1). Data demonstrated the best linearity with the Higuchi model. Hence release data for all size fractions of both the riboflavin and furosemide formulations were

subsequently fitted to the Higuchi model (Figure 4.11). Good linear regression is gained for all formulations.

Table 4.1 Regression parameters obtained for PLGA particles sized 1mm loaded with riboflavin in PBS for the different kinetic models.

Sample	Zero-order		First-order		Higuchi		Korsmeyer-Peppas	
	r^2	$K_0(h^{-1})$	r^2	$K_1(h^{-1})$	r^2	$K_H(h^{-1/2})$	r^2	n
No PEG PBS	0.9392	0.0162	0.6834	0.0463	0.9720	0.0868	0.8400	0.3026
No PEG SGF	0.4303	0.0028	0.2950	0.0244	0.6556	0.01821	0.4657	0.1741

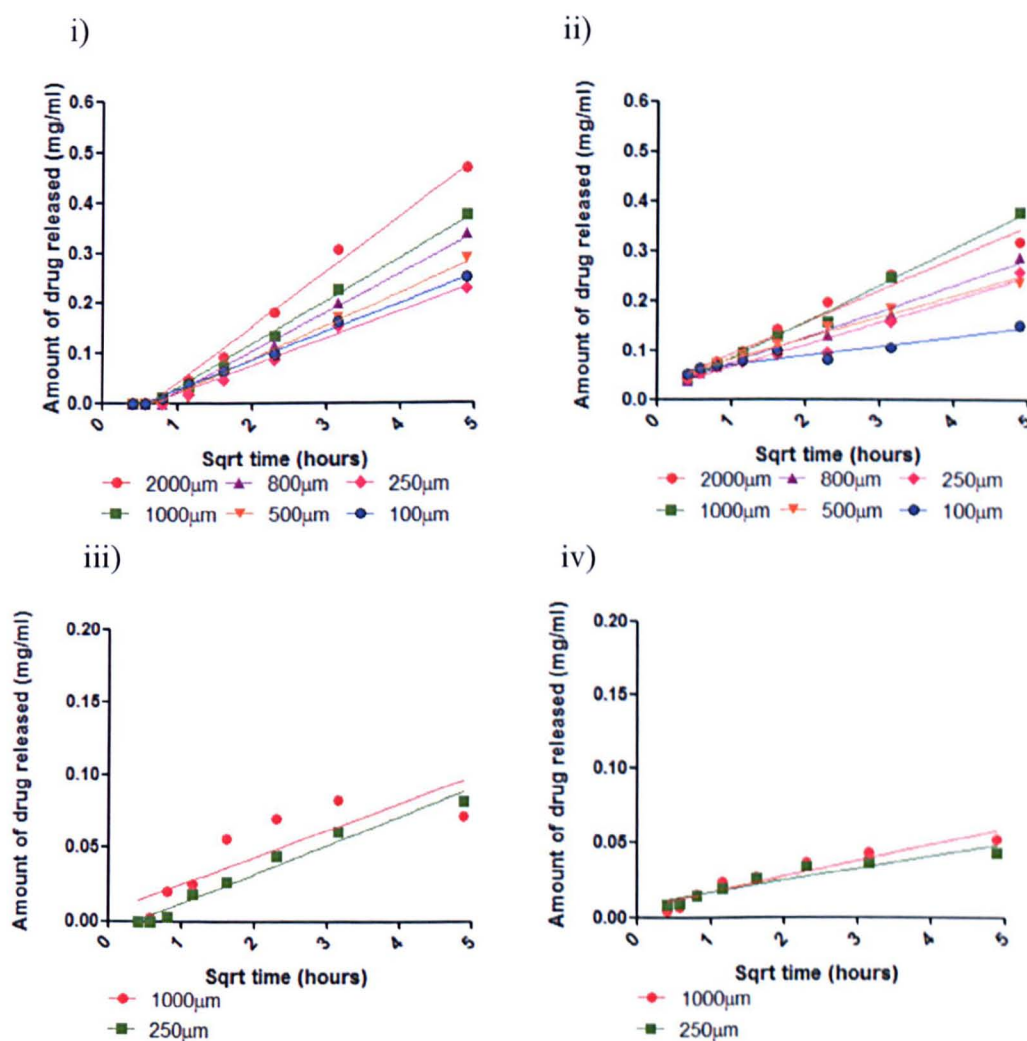


Figure 4.11 Release data fitted to the Higuchi model for release in PBS for i) riboflavin loaded particles and ii) furosemide loaded particles and for release in SGF for iii) riboflavin loaded particles and iv) furosemide loaded particles.

4.4 Discussion

Two candidate drugs for gastroretentive formulations, furosemide and riboflavin, were incorporated into the PLGA based matrices. The high encapsulation efficiency was achieved for all size fractions of the matrices, with values between 80 and 100%. These values are favourably comparable with conventional methods of small molecular drug encapsulation within PLGA microparticles where values may vary between 20 and 70% [35]. For instance, the encapsulation efficiency of rhodamine in PLG microparticles prepared by an acoustic excitation method (which involves spraying of the polymer mixture through a nozzle whilst an ultrasonic generator allows ultrasonic excitation to produce uniform droplets) was found to be around 63% for 20 μm particles and similar values of 61% were reported for larger particles of 65 μm [36]. Previously reported data from this group for incorporation of human growth hormone into PLGA based microparticles prepared by the PGSS method was 100% [37] this suggests that the PGSS method for drug encapsulation is comparable, and indeed favourable to other methods.

The mixing of the drug within the PLGA polymer matrix occurs during the soak period of the fabrication process (described in Section 2.1), where a stirrer enables the mixing of the solid drug particles within the plasticized polymer matrix under supercritical conditions [38, 39]. In the next stage of the process the mixture formed is sprayed through the nozzle from the mixing chamber into a collection chamber where conditions are no longer supercritical. The PLGA polymer rapidly solidifies, physically entrapping the drug particles within the polymeric matrix. Following production, the particles were analysed using ToF-SIMS to assess if the process provides a relatively

homogenous distribution of drug particles throughout the matrix, as this could have an impact on subsequent drug release profile. ToF-SIMS has recently been applied in the pharmaceutical sciences to allow detailed surface chemical analysis of carrier systems as well as providing an insight into the distribution of drugs within a certain depth of the carrier system [40, 41].

The ion images in Figure 4.3 b) show the intensity of the SNO_2H ion, representative of furosemide in drug loaded and blank samples. The relative homogeneity of intensity (or lack of extremely high and low intensity regions) confirms that the mixing of drug and polymer during the soak period creates a reasonably homogenous mixture of drug particles in the plasticised polymer melt. The distribution of drug particles in the polymer matrix is important when considering its release. Typically a uniform distribution of drug particles throughout the matrix will support sustained release while a heterogeneous distribution can lead to a pronounced burst release [42].

ToF-SIMS is a technique which provides molecular analysis of materials present in the shallow surface layers of a sample, and it should be noted that this data cannot be representative throughout the entire particle. PLGA based microparticulate systems have been reported to possess a relatively larger amount of drug present on the surface of the particles [43]. This surface bound drug contributes to the high burst release frequently reported for these systems [42, 44]. Unlike these reports, the release profiles for PLGA microparticles reported in this study (Figure 4.6) do not reveal any significant burst release; this may be explained by data obtained by ToF-SIMS depth profiling. Depth profiling allows the surface analysis to be continued through the 'layers' of the sample with the region of interest being 'deepened' between each analysis.

Conclusions can then be drawn upon the drug distribution through the certain depth of the system. The depth profile illustrates that there is a somewhat higher intensity of drug originated ions on the upper sub-micron layers of the particles (Figure 4.4), followed by a slight decrease moving through the sample. This demonstrates that the intensity generally remains at similar levels throughout the sample, again supporting PGSS process capabilities in the production of particles with a homogenous distribution of a therapeutic agent and potentially facilitating sustained release.

It has been reported that, although porous particles release drug rapidly and with a high burst release, it is possible, by closing these pores, to sustain release over a period of about a month [45]. The microCT data described in Chapter 3 (Figure 3.8) illustrates that the larger particles are more porous than smaller particles, which may explain the faster release from larger relative to smaller particle fraction (Figure 4.5). However, within all size fractions there are areas of solid matrix between the pores. In the larger particles these areas of solid matrix space can be larger in size than the smaller particles themselves. It is therefore surprising that the larger particles would exhibit faster release (provided that the drug is reasonably homogeneously distributed within these regions).

Release of drug from PLGA microparticulate systems has frequently been reported to be governed by Fickian diffusion [46-48], whereby the expected trend would be for large particles to release drug more slowly due to increased diffusion distances [36, 49]. However the majority of studies in the literature deal with particles in the micrometer / nanometre size range leaving it difficult to make direct comparisons with the far larger particles studied in this work.

The effect of longer diffusion pathway has been shown to be compensated for by the effect of 'auto-catalysis' of larger PLGA matrices [30]. This is the phenomenon whereby hydrolytic degradation of the ester bonds in the PLGA produces the acidic oligomers lactic acid and glycolic acid. The build up of these oligomers within the microparticles decreases pH [50]. As the rate of this hydrolysis is higher at lower pH, the build up of oligomers results in an increase in rate of degradation. This effect of auto-catalysis has been shown to be more profound in larger particles [51] and therefore may compensate for the increased diffusion distance in these systems. There is much literature on the effect of auto-catalysis [52, 53], however, the time scale for such experiments has previously been over a time scale far greater (around 35 days) than reported in the present study (24 h) [54, 55]. Autocatalysis is unlikely to have a great effect on release in this study due to the short time frame. Park 1994 [56] quantitated the decrease in molecular weight of PLGA of various lactic acid : glycolic acid ratios, the study revealed a sharp decrease in molecular weight of the 50:50 PLGA in the first couple of days therefore this hydrolytic breakdown of PLGA chains may impact release in the present work.

Another factor contributing to the release profile *via* its effect on the matrix degradation is the molecular weight of the PLGA material [57, 58]. DSC data (Figure 4.10) indicates that during the 24 h period of the *in vitro* release study some degradation of the PLGA polymer had occurred, with a decrease in T_g being apparent.

It has been demonstrated that the degradation of PLGA microspheres occurs more rapidly at low pH levels as a result of the catalytic effect of low pH on ester bond hydrolysis [59]. The increase in the rate of degradation of PLGA at

low pH is often followed by an increase in the rate of release, with the morphological analysis over the course of the release study confirming morphological changes [59]. The present study also reports on the effects of particles exposure to a release medium on their morphology and drug release (Figures 4.6 and 4.7), however the results are somewhat contradictory to the literature. Exposure of the particles to PBS pH 7.4 medium results in the emergence of surface erosion and increased surface porosity, whereas at pH 1.2 smooth polymeric matrix dominated. This was accompanied with significantly decreased drug release in SGF medium at pH 1.2 compared to release in PBS pH 7.4 (Figure 4.6).

A potential explanation for this phenomenon may be arising from the SEM and microCT data in Figures 4.7 and 4.8 which clearly show the presence of smooth almost pore-less surfaces following exposure to acidic release medium, and evidence of pores and surface pitting in the PLGA matrices after exposure to PBS pH 7.4 release medium. Similar pH dependent matrix morphology has previously been reported [21, 59]. As the release media moves into the porous microparticles it results in the hydrolytic degradation of PLGA chains and the build up of acidic oligomers, these oligomers contribute to the decrease in pH levels within the microparticle in what has been described as a pH 'microclimate' [50, 60]. At low pH (such as SGF) the oligomers are not soluble, whereas at more neutral pH (PBS) the oligomers will dissolve resulting in the emergence of porous channels explaining the emergence of surface porosity following exposure to PBS (pH7.4).

The time course of release profile obtained by gastroretentive delivery systems must complement the period of time the system will spend proximal to the

drug's absorption site. Previously reported systems are achieving gastric residence times of around 6-8 h [61, 62]. The amount of drug release over the period of 8 h for the largest size fraction is approximately only 50% in PBS medium (Figure 4.5). It was therefore important to modulate the release profile to enable optimal drug release over the period of gastric residence.

4.5 Conclusions

This chapter describes the potential of the gastroretentive particles investigated in Chapter 3 as sustained release systems. The release of two drugs, furosemide and riboflavin was explored in both PBS and SGF. These drugs were selected as potential candidates for gastroretentive systems as they both demonstrate narrow absorption windows in the upper small intestine, and both have demonstrated different levels of solubility in both the PBS (pH 7.4) and the SGF (pH 1.2) and therefore allows an insight into the effect of the drug solubility can be obtained. The encapsulation efficiencies obtained by the PGSS process has been shown to be reproducibly high and favourable compared to other conventional methods of drug encapsulation.

Chapter 3 concluded the larger particles are more suitable for gastroretention as they are more inherently buoyant due to their low densities. This chapter looked at the different release profiles found with different size fractions. The larger particles demonstrated the fastest rate of drug release. However, taking into account that previously reported systems are achieving gastric residence times of around 8 h, the amount of drug release in this period even for the largest size fraction is approximately 50%. In the next chapter improvements in the rate of release are explored in order to improve potential bioavailability.

4.6 References

1. Fasinu, P., et al., *Diverse approaches for the enhancement of oral drug bioavailability*. *Biopharmaceutics & Drug Disposition*, 2011. **32**(4): p. 185-209.
2. Gomez-Orellana, I., *Strategies to improve oral drug bioavailability*. *Expert opinion on drug delivery*, 2005. **2**(3): p. 419-33.
3. Davis, S.S., *Formulation strategies for absorption windows*. *Drug Discovery Today*, 2005. **10**(4): p. 249-257.
4. C.G., W.N.W.C.W., *Physiological pharmaceutics*. 2001, New York: Taylor and Francis inc.
5. Dave, B.S., A.F. Amin, and M.M. Patel, *Gastroretentive drug delivery system of ranitidine hydrochloride: Formulation and in vitro evaluation*. *AAPS PharmSciTech*, 2004. **5**(2).
6. Mastiholimath, V.S., et al., *In vitro and in vivo evaluation of ranitidine hydrochloride ethyl cellulose floating microparticles*. *Journal of Microencapsulation*, 2008. **25**(5): p. 307-314.
7. Kagan, L., et al., *Gastroretentive Accordion Pill: Enhancement of riboflavin bioavailability in humans*. *Journal of Controlled Release*, 2006. **113**(3): p. 208-215.
8. Lee, M.G. and W.L. Chiou, *Evaluation of potential causes for the incomplete bioavailability of furosemide-gastric 1st pass metabolism*. *Journal of Pharmacokinetics and Biopharmaceutics*, 1983. **11**(6): p. 623-640.
9. Garg, R. and G.D. Gupta, *Progress in Controlled Gastroretentive Delivery Systems*. *Tropical Journal of Pharmaceutical Research*, 2008. **7**(3): p. 1055-1066.
10. Bolondi, L., et al., *Measurement of gastric-emptying time by real-time ultrasonography*. *Gastroenterology*, 1985. **89**(4): p. 752-759.
11. Tadros, M.I., *Controlled-release effervescent floating matrix tablets of ciprofloxacin hydrochloride: Development, optimization and in vitro-in vivo evaluation in healthy human volunteers*. *European Journal of Pharmaceutics and Biopharmaceutics*, 2010. **74**(2): p. 332-339.
12. Gande, S. and Y.M. Rao, *Sustained-release effervescent floating matrix tablets of baclofen: development, optimization and in vitro-in vivo evaluation in healthy human volunteers*. *Daru-Journal of Pharmaceutical Sciences*, 2011. **19**(3): p. 202-209.
13. Ozdemir, N., S. Ordu, and Y. Ozkan, *Studies of floating dosage forms of furosemide: In vitro and in vivo evaluations of bilayer tablet formulations*. *Drug Development and Industrial Pharmacy*, 2000. **26**(8): p. 857-866.
14. Cedillo-Ramirez, E., L. Villafuerte-Robles, and A. Hernandez-Leon, *Effect of added pharmatose DCL11 on the sustained-release of metronidazole from methocel K4M and carbopol 971P NF floating matrices*. *Drug Development and Industrial Pharmacy*, 2006. **32**(8): p. 955-965.
15. Lartigue, S., et al., *Intersubject and intrasubject variability of solid and liquid gastric emptying parameters- A scintigraphic study in healthy subjects and diabetic patients*. *Digestive Diseases and Sciences*, 1994. **39**(1): p. 109-115.

16. Brophy, C.M., et al., *Variability of gastric-emptying measurements in man employing standardized radiolabeled meals*. Digestive Diseases and Sciences, 1986. **31**(8): p. 799-806.
17. McConnell, E.L., H.M. Fadda, and A.W. Basit, *Gut instincts: Explorations in intestinal physiology and drug delivery*. International Journal of Pharmaceutics, 2008. **364**(2): p. 213-226.
18. Toothaker, R.D. and P.G. Welling, *The effect of food on drug bioavailability*. Annual Review of Pharmacology and Toxicology, 1980. **20**: p. 173-199.
19. Melander, A., *Influence of food on bioavailability of drugs*. Clinical Pharmacokinetics, 1978. **3**(5): p. 337-351.
20. Faisant, N., et al., *Effects of the type of release medium on drug release from PLIGA-based microparticles: Experiment and theory*. International Journal of Pharmaceutics, 2006. **314**(2): p. 189-197.
21. Li, J., G. Jiang, and F. Ding, *The effect of pH on the polymer degradation and drug release from PLGA-mPEG microparticles*. Journal of Applied Polymer Science, 2008. **109**(1): p. 475-482.
22. Farshi, F.S., et al., *Formulation and comparative bioavailability of conventional and sustained release furosemide tablets*. Stp Pharma Sciences, 1995. **5**(5): p. 361-366.
23. Klausner, E.A., et al., *Furosemide pharmacokinetics and pharmacodynamics following gastroretentive dosage form administration to healthy volunteers*. Journal of Clinical Pharmacology, 2003. **43**(7): p. 711-720.
24. Meka, L., et al., *Design and Evaluation of Polymeric Coated Minitablets as Multiple Unit Gastroretentive Floating Drug Delivery Systems for Furosemide*. Journal of Pharmaceutical Sciences, 2009. **98**(6): p. 2122-2132.
25. Klausner, E.A., et al., *Novel gastroretentive dosage forms: Evaluation of gastroretentivity and its effect on riboflavin absorption in dogs*. Pharmaceutical Research, 2002. **19**(10): p. 1516-1523.
26. Sato, Y., et al., *In vivo evaluation of riboflavin-containing microballoons for floating controlled drug delivery system in healthy human volunteers*. Journal of Controlled Release, 2003. **93**(1): p. 39-47.
27. Rao, M.R.P., et al., *Development and in vitro evaluation of floating rosiglitazone maleate microspheres*. Drug Development and Industrial Pharmacy, 2009. **35**(7): p. 834-842.
28. Streubel, A., J. Siepmann, and R. Bodmeier, *Floating matrix tablets based on low density foam powder: effects of formulation and processing parameters on drug release*. European Journal of Pharmaceutical Sciences, 2003. **18**(1): p. 37-45.
29. Ma, N., et al., *Development and evaluation of new sustained-release floating microspheres*. International Journal of Pharmaceutics, 2008. **358**(1-2): p. 82-90.
30. Klose, D., et al., *How porosity and size affect the drug release mechanisms from PLIGA-based microparticles*. International Journal of Pharmaceutics, 2006. **314**(2): p. 198-206.

31. Dawes, G.J.S., et al., *Size effect of PLGA spheres on drug loading efficiency and release profiles*. Journal of Materials Science-Materials in Medicine, 2009. **20**(5): p. 1089-1094.
32. Siepmann, J., et al., *Effect of the size of biodegradable microparticles on drug release: experiment and theory*. Journal of Controlled Release, 2004. **96**(1): p. 123-134.
33. Acharya, G., et al., *A study of drug release from homogeneous PLGA microstructures*. Journal of Controlled Release, 2010. **146**(2): p. 201-206.
34. Grizzi, I., et al., *Hydrolytic degradation of devices based on poly(DL-lactic acid) size-dependence*. Biomaterials, 1995. **16**(4): p. 305-311.
35. Freitas, S., H.P. Merkle, and B. Gander, *Microencapsulation by solvent extraction/evaporation: reviewing the state of the art of microsphere preparation process technology*. Journal of Controlled Release, 2005. **102**(2): p. 313-332.
36. Berkland, C., et al., *Precise control of PLG microsphere size provides enhanced control of drug release rate*. Journal of Controlled Release, 2002. **82**(1): p. 137-147.
37. Jordan, F., et al., *Sustained release hGH microsphere formulation produced by a novel supercritical fluid technology: In vivo studies*. Journal of Controlled Release, 2010. **141**(2): p. 153-160.
38. Woods, H.M., et al., *Materials processing in supercritical carbon dioxide: surfactants, polymers and biomaterials*. Journal of Materials Chemistry, 2004. **14**(11): p. 1663-1678.
39. Hao, J.Y., et al., *Supercritical fluid assisted melting of poly(ethylene glycol): a new solvent-free route to microparticles*. Journal of Materials Chemistry, 2005. **15**(11): p. 1148-1153.
40. Belu, A.M., et al., *TOF-SIMS characterization and imaging of controlled-release drug delivery systems*. Analytical Chemistry, 2000. **72**(22): p. 5625-5638.
41. Barnes, T.J., I.M. Kempson, and C.A. Prestidge, *Surface analysis for compositional, chemical and structural imaging in pharmaceuticals with mass spectrometry: A ToF-SIMS perspective*. International Journal of Pharmaceutics, 2011. **417**(1-2): p. 61-69.
42. Yeo, Y. and K.N. Park, *Control of encapsulation efficiency and initial burst in polymeric microparticle systems*. Archives of Pharmacal Research, 2004. **27**(1): p. 1-12.
43. Wang, J., B.A. Wang, and S.P. Schwendeman, *Characterization of the initial burst release of a model peptide from poly(D,L-lactide-co-glycolide) microspheres*. Journal of Controlled Release, 2002. **82**(2-3): p. 289-307.
44. Yan, C.H., et al., *Characterization and morphological analysis of protein-loaded Poly(lactide-co-glycolide) microparticles prepared by water-in-oil-in-water emulsion technique*. Journal of Controlled Release, 1994. **32**(3): p. 231-241.
45. Kim, H.K., H.J. Chung, and T.G. Park, *Biodegradable polymeric microspheres with "open/closed" pores for sustained release of human growth hormone*. Journal of Controlled Release, 2006. **112**(2): p. 167-174.

46. Faisant, N., J. Siepmann, and J.P. Benoit, *PLGA-based microparticles: elucidation of mechanisms and a new, simple mathematical model quantifying drug release*. European Journal of Pharmaceutical Sciences, 2002. **15**(4): p. 355-366.
47. Soppimath, K.S. and T.M. Aminabhavi, *Ethyl acetate as a dispersing solvent in the production of poly(DL-lactide-co-glycolide) microspheres: effect of process parameters and polymer type*. Journal of Microencapsulation, 2002. **19**(3): p. 281-292.
48. D'Aurizio, E., et al., *Preparation and characterization of poly(lactic-co-glycolic acid) microspheres loaded with a labile antiparkinson prodrug*. International Journal of Pharmaceutics, 2011. **409**(1-2): p. 289-296.
49. Hadinoto, K., K. Zhu, and R.B.H. Tan, *Drug release study of large hollow nanoparticulate aggregates carrier particles for pulmonary delivery*. International Journal of Pharmaceutics, 2007. **341**(1-2): p. 195-206.
50. Ding, A.G. and S.P. Schwendeman, *Acidic Microclimate pH Distribution in PLGA Microspheres Monitored by Confocal Laser Scanning Microscopy*. Pharmaceutical Research, 2008. **25**(9): p. 2041-2052.
51. Klose, D., et al., *PLGA-based drug delivery systems: Importance of the type of drug and device geometry*. International Journal of Pharmaceutics, 2008. **354**(1-2): p. 95-103.
52. Brunner, A., K. Mader, and A. Gopferich, *pH and osmotic pressure inside biodegradable microspheres during erosion*. Pharmaceutical Research, 1999. **16**(6): p. 847-853.
53. Fu, K., et al., *Visual evidence of acidic environment within degrading poly(lactic-co-glycolic acid) (PLGA) microspheres*. Pharmaceutical Research, 2000. **17**(1): p. 100-106.
54. Park, T.G., *Degradation of poly(lactic-co-glycolic acid) microspheres-Effect of copolymer composition*. Biomaterials, 1995. **16**(15): p. 1123-1130.
55. Anderson, J.M. and M.S. Shive, *Biodegradation and biocompatibility of PLA and PLGA microspheres*. Advanced Drug Delivery Reviews, 1997. **28**(1): p. 5-24.
56. Park, T.G., *Degradation of poly(lactic-co-glycolic acid) microspheres-Effect of molecular weight*. Journal of Controlled Release, 1994. **30**(2): p. 161-173.
57. Mittal, G., et al., *Estradiol loaded PLGA nanoparticles for oral administration: Effect of polymer molecular weight and copolymer composition on release behavior in vitro and in vivo*. Journal of Controlled Release, 2007. **119**(1): p. 77-85.
58. Fu, X., Q. Ping, and Y. Gao, *Effects of formulation factors on encapsulation efficiency and release behaviour in vitro of huperzine A-PLGA microspheres*. Journal of Microencapsulation, 2005. **22**(1): p. 57-66.
59. Zolnik, B.S. and D.J. Burgess, *Effect of acidic pH on PLGA microsphere degradation and release*. Journal of Controlled Release, 2007. **122**(3): p. 338-344.

-
60. Li, L. and S.P. Schwendeman, *Mapping neutral microclimate pH in PLGA microspheres*. *Journal of Controlled Release*, 2005. **101**(1-3): p. 163-173.
 61. Md, S., et al., *Acyclovir-Loaded Chitosan Microspheres for Gastroretention: Development and Evaluation*. *Journal of Dispersion Science and Technology*, 2011. **32**(9): p. 1318-1324.
 62. Whitehead, L., et al., *Floating dosage forms: an in vivo study demonstrating prolonged gastric retention*. *Journal of Controlled Release*, 1998. **55**(1): p. 3-12.

Chapter 5

Modulation of Release Rate by the Incorporation of a Hydrophilic Excipient.

5.1 Introduction

The objective of gastroretentive drug delivery systems is to retain and deliver drug proximal to the absorption window where the drug will be released in a sustained manner and in this way allow for improved bioavailability and reduced dosing frequency.

PLGA based polymers have been widely and successfully used in production of controlled release formulations [1-3]. These systems often explore variations in molecular weight [4, 5], as well as lactide : glycolide ratio [6] in the optimisation of the release rate. Polymer blending has also been investigated as a means to improve or tailor formulation characteristics such as microparticle degradation properties [7, 8] and drug release rates [9, 10]. Hydrophilic excipients in particular, such as poly (ethylene glycol), have demonstrated potential in the improvement of drug loading as well as release rates in PLGA based microparticulate systems [11-13]. The hydrophilicity of the PEG is considered to improve the hydration of the matrix, in turn enhancing the penetration of release medium into matrix and consequently the diffusion of the drug into the medium. In the case of PEG, its presence not

only improves hydration of the microparticles but its high solubility in water results in the production of pores as the PEG dissolves, leaving behind an extensive network of water channels which enhance the diffusion of the drug out of the system. Other water soluble materials can be applied in this way to produce diffusion channels within a polymeric matrix, including sodium chloride, and sucrose [14]. These materials are typically introduced during the production of intended formulations and are subsequently extracted by dissolving in water. This pore formation has been reported to be followed by an increase in drug diffusion coefficients for vitamin B12 and proxyphyline [14]. PEG has also been applied as a porogen where the porosity will enhance not only the diffusion of therapeutic materials from within the system but also the movement of materials into the interior of systems [14].

This chapter describes the addition of hydrophilic PEG of different molecular weights into the PGSS processing of PLGA particles in order to exert control over the drug release. Moreover, the chapter explores the relationship between particles micro-architecture and rate of drug release.

5.2 Materials and methods

5.2.1 Materials

Poly (ethylene glycol) of molecular weights 1 KDa, 3 KDa, 6 KDa, and 35 KDa were obtained from Sigma Aldrich. Other materials used in the preparation of PLGA particles are described in Chapter 3.

5.2.2 Methods

5.2.2.1 Production of Riboflavin Loaded Particles Containing Various Molecular Weights of PEG

Particles were produced using the PGSS method as described in detail in Chapter 2 (Section 2.1). PEG was introduced to the formulation described in Chapter 4 at a loading of 10% (w/w) with the formulation containing:

- PLGA (RG502H ~12 KDa) 60% (w/w)
- PLGA (RG503 ~ 25 KDa) 20% (w/w)
- PEG 10% (w/w)
- SPANTM80 5% (w/w)
- Riboflavin 5% (w/w)

5.2.2.2 *In vitro* Drug Release from Various Formulations

Drug release studies were carried out as described in detail in Chapter 2 (Section 2.11). Quantification of drug release was carried out using UV/Vis analysis (Section 2.9).

5.2.2.3 Scanning Electron Microscopy (SEM)

SEM was carried out to determine morphological characteristics as described in detail in Chapter 2 (Section 2.2).

5.2.2.4 X-ray Microtomography (microCT)

The internal morphology was evaluated using microCT as described in detail in Chapter 2 (Section 2.3).

5.3 Results

5.3.1 Release of Drug from PEG Modified Particles into PBS Medium

Poly (ethylene glycol) of various molecular weights, at a theoretical loading of 10% (w/w), was incorporated into the formulation (To maintain overall batch mass the same, 10% (w/w) of PLGA was removed from the formulation described in Chapter 4). Microparticles of the size fractions 1000-2000 μm and 250-500 μm were selected for release studies in PBS pH 7.4 medium (Figure 5.1).

Statistical analysis applying two way ANOVA was carried out on the release data over the initial 4 h of the study. This indicated that at these early time points there is (i) no significant difference in the drug release on the addition of PEG and (ii) there is no significant effect on the release of different PEG molecular weights. However, statistical analysis carried out over the 24 h reveals that the overall effect of PEG incorporation is a statistically significant increase in the drug release rate with the exception of PEG 1 KDa. Moreover, the effect of molecular weight was found to be significant for both the larger particles ($F(4, 70) = 202.2$ $p < 0.0001$) (Figure 5.1) and the smaller particles ($F(4, 70) = 55.42$ $p < 0.0001$) (Figure 5.2).

Interestingly, PEG of 3 KDa molecular weight demonstrates the greatest increase in drug release in both size fractions tested. Unlike the higher molecular weight PEGs, PEG of 1 KDa does not increase rate of release for either size fraction; quite the contrary, for larger particles (1000 μm)

introducing PEG 1 KDa statistically decreases amount of released drug at the later time points.

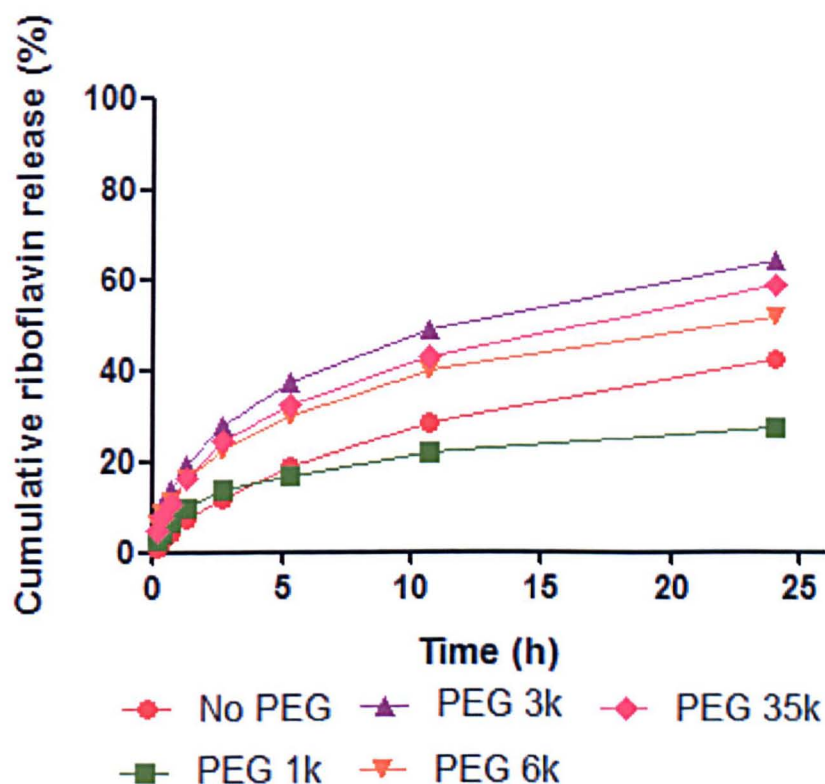


Figure 5.1. Release of riboflavin from the 1000 μm size fraction of PLGA particle incorporating 10% PEG of various molecular weight PBS pH 7.4 used as the release medium. ($n=3 \pm SD$)

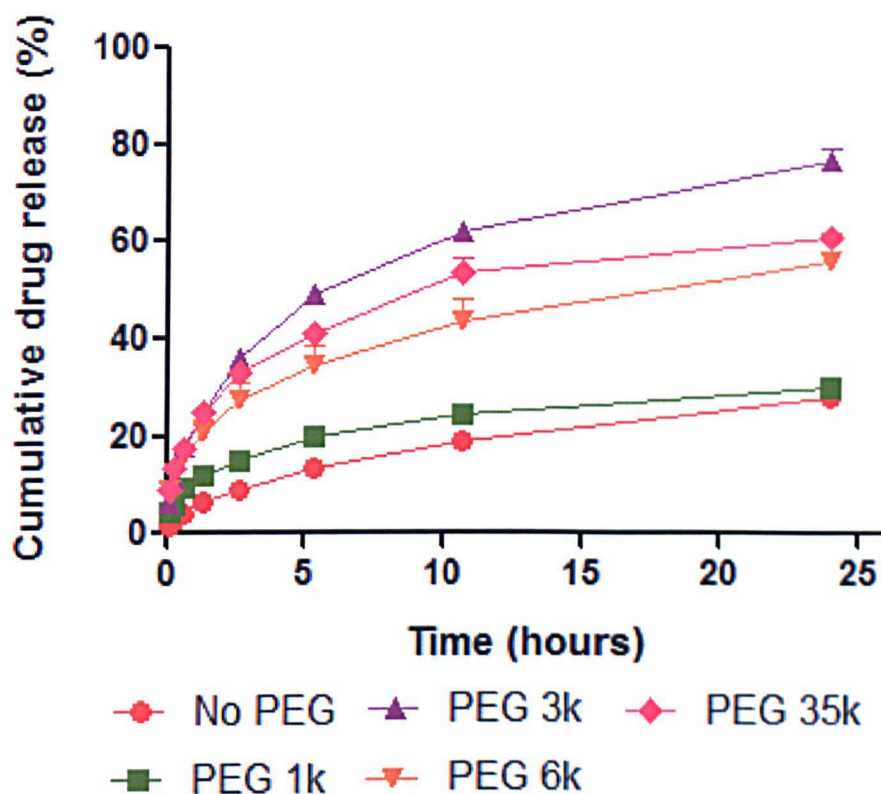


Figure 5.2. Release of riboflavin from 250 μm size fraction of PLGA particles incorporating 10% PEG of various molecular weights. PBS pH 7.4 used as the release medium ($n=3 \pm SD$)

5.3.2 Release of Drug from PEG Modified Particles in SGF Medium

As in chapter 4, the release studies were also conducted in SGF medium, as it is generally considered more representative of the gastric fluid [15-17]. In addition, a comparison of the release profiles in different media may provide some insight into the detailed mechanism of release.

In SGF pH 1.2 the release trend differs to that seen in PBS pH 7.4. The overall release of incorporated riboflavin within 24 h experiment is lower, being just over 30% for the highest performing system, relative to the value reported for release in PBS at around 70%. In SGF the two way ANOVA statistical

analysis provided evidence to confirm that PEG has an overall significant effect for the larger ($F(4,70)=28.15, p < 0.0001$) (Figure 5.3) particles, in which case the effect is negative and actually decreases release. There is also a significant effect of PEG introduction to increase release from the smaller particles ($F(4, 70) = 28.39 p < 0.0001$) (Figure 5.3).

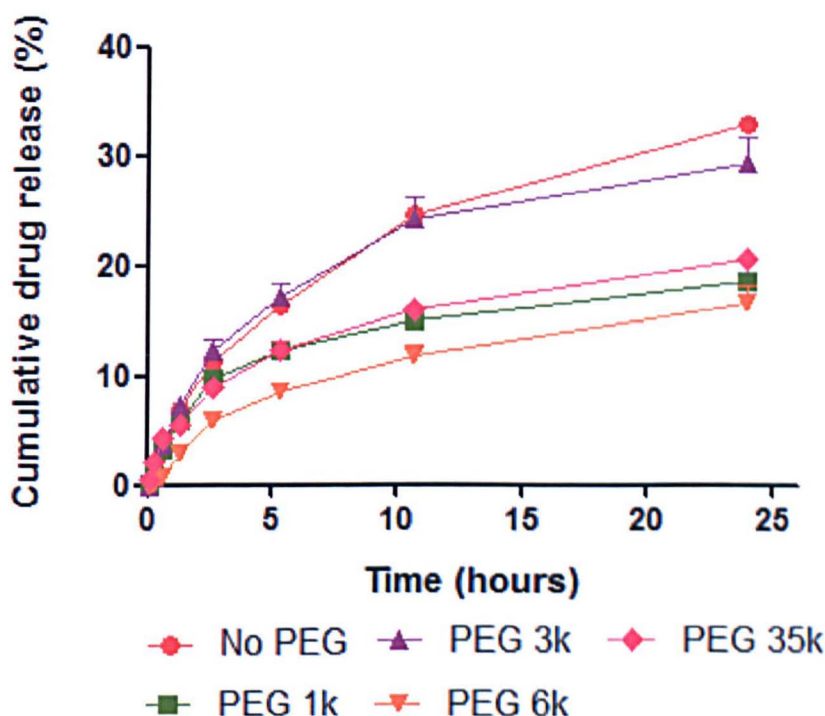


Figure 5.3 Release of riboflavin from 1000 μm size fraction of PLGA particles incorporating 10% PEG of various molecular weights. SGF pH 1.2 used as the release medium ($n=3 \pm \text{SD}$)

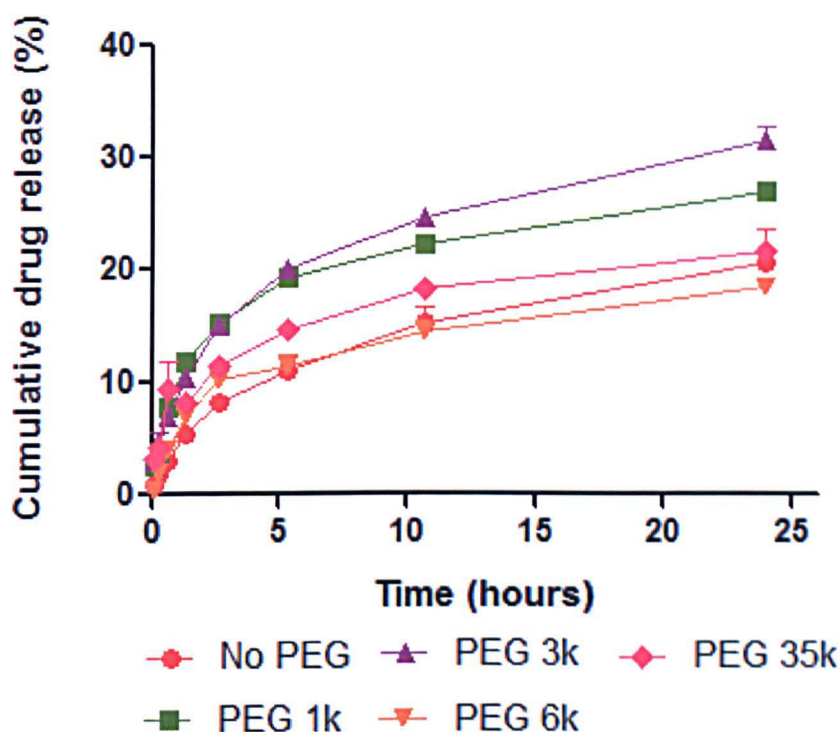


Figure 5.4 Release of riboflavin from 250 μm size fraction of PLGA particles incorporating 10% PEG of various molecular weights. SGF pH 1.2 used as the release medium ($n=3 \pm \text{SD}$)

5.3.3 Morphological Examination Following Exposure of PLGA Particles to Release Media

Following 24 h exposure to PBS or SGF release media, PLGA particles were collected and freeze dried for microCT analysis. This data was compared with that of the particles before exposure to the release media with the aim of investigating the relationship between potential morphological changes and the drug release. Although the quantitative microCT data for porosity (Figure 5.5) does not provide any statistically significant findings, the corresponding 3D models along with the SEM images (Figure 5.6) illustrate that exposure to the different release media indeed affect morphology at the surface of the particles. Interestingly, comparing models for the open pore space in the microCT models (Figure 5.5) for PEG MW > 3 KDa reveals a decrease in porosity on

introduction of PEG into the matrix. This, however following particles exposure to the PBS as the release media increases. This is likely due to the PEG solubilisation and diffusion out of the matrix which created a porous network. Particles containing PEG 1 KDa do not show such pronounced increases in porosity. Comparing the open pore space models for exposure to SGF with exposure to PBS media indicated that following exposure to the SGF the open space is typically less than in with PBS exposure.

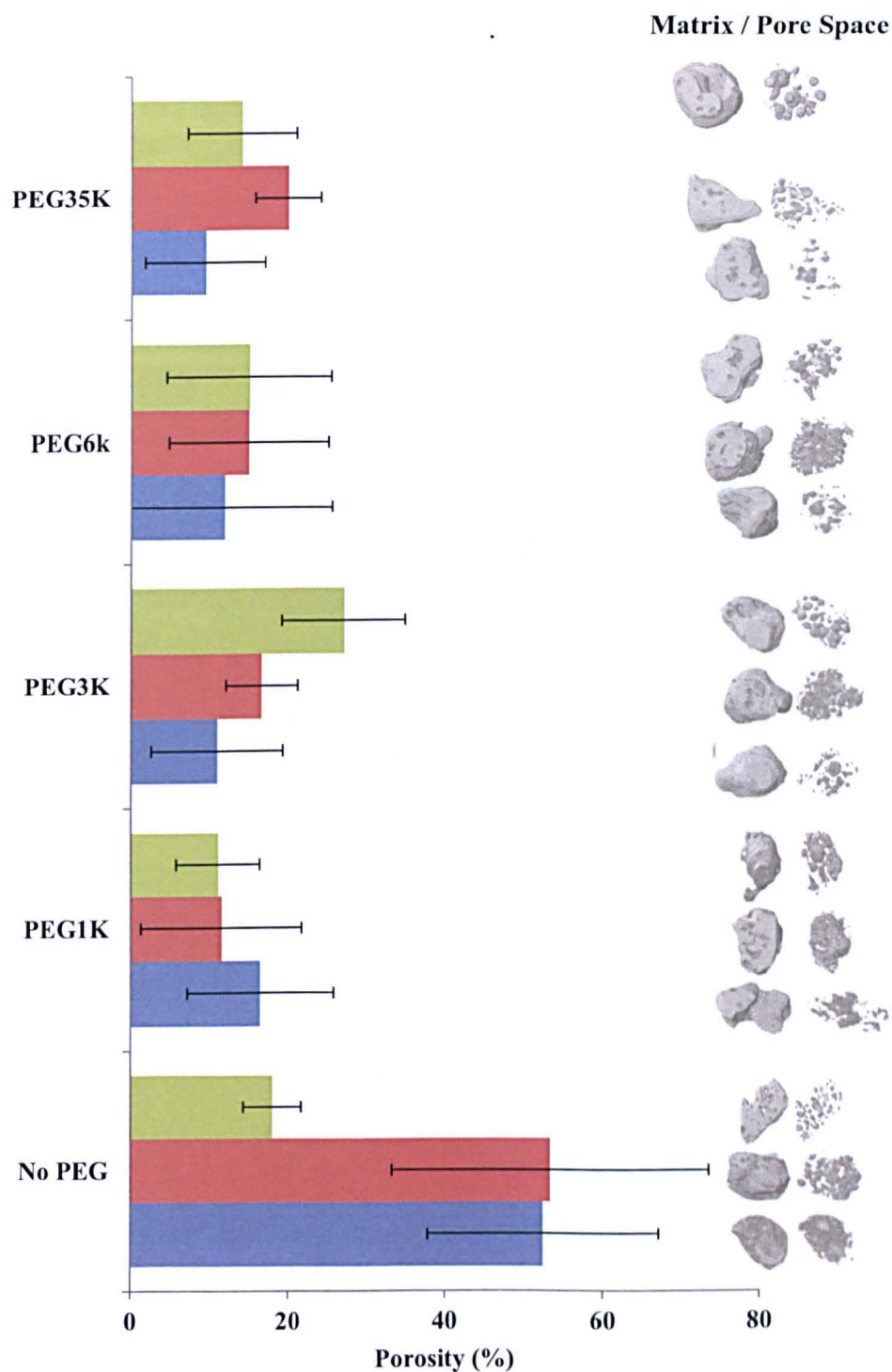


Figure 5.5 Porosity data obtained by microCT analysis Blue-prior to exposure, Red- following exposure to PBS pH 7.4, Green- following exposure to SGF pH 1.2 ($n=6\pm SD$) Corresponding 3D reconstruction 'models' shown as images next to the bar. The image on the left illustrates the matrix space within the particle and the image on the right illustrates open pore space.

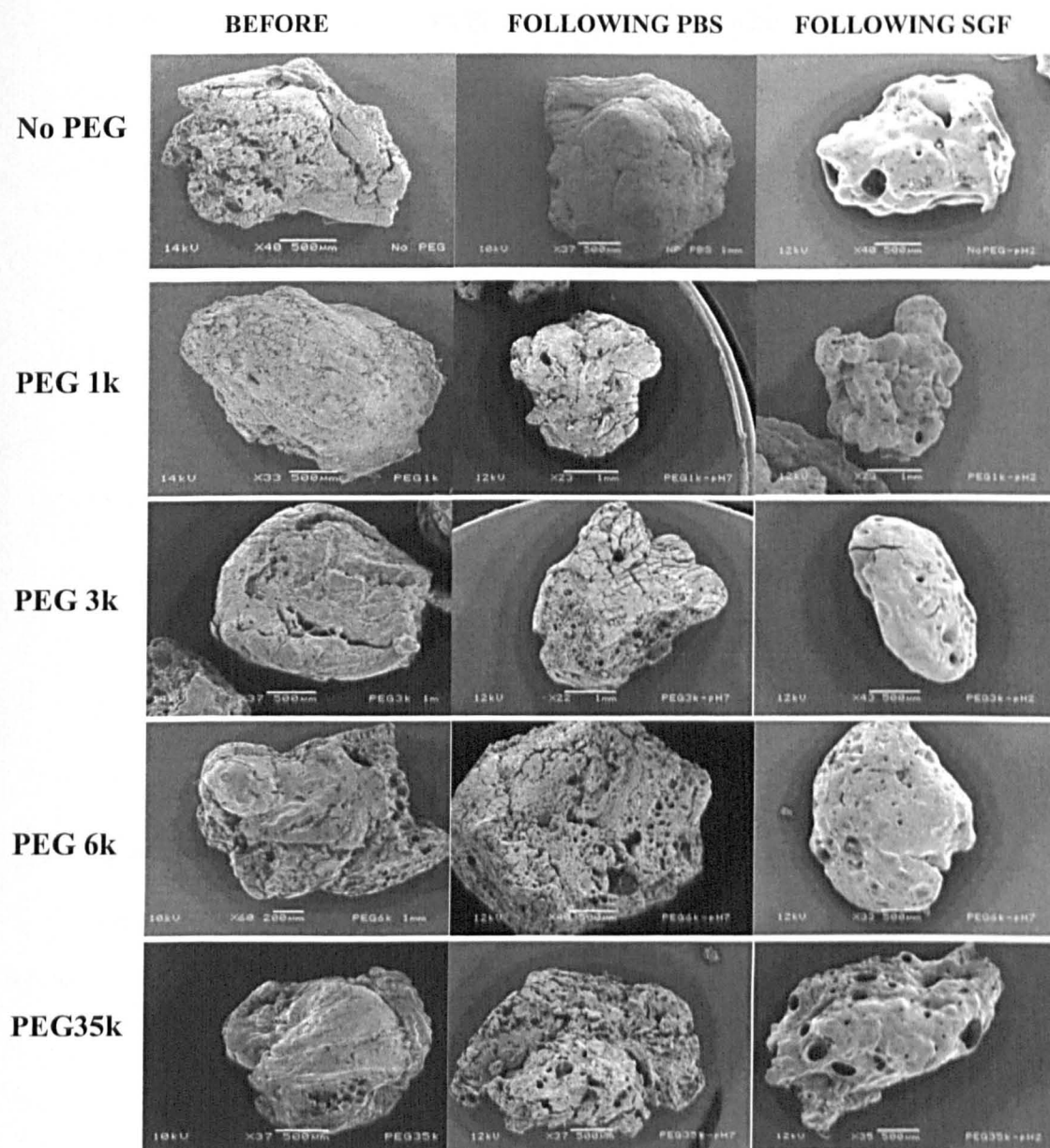


Figure 5.6 Scanning Electron Microscopy micrographs showing the appearance of the microparticles with incorporation of different molecular weight PEGs before and following the completion of the release studies i.e. exposure to PBS pH 7.4 of SGF pH 1.2.

SEM images (Figure 5.6) provide further evidence for the morphological changes at the surface following exposure to the different release media. Exposure to the two release media results in very different morphologies. Following exposure to PBS the particles show an increase in surface porosity

with a breakdown in matrix integrity, which contrasts greatly to the morphology revealed following exposure to SGF where there is evidence of surface porosity but the surfaces are generally smoother and there is far less surface porosity.

5.3.4 Mechanism of Drug Release from Particles

In order to understand the mechanism of release of the drug from the system, release data was fitted to several typically used kinetic models [18], as outlined below.

1) Zero Order:

$$Q_t = Q_0 + K_0 t$$

Where Q_t is the amount of drug dissolved at time t , Q_0 is the initial amount of drug in solution and K_0 is the zero order release constant. The zero order rate equation describes situations where the release rate is independent of concentration.

2) First Order:

$$Q = \log C_0 - \frac{Kt}{2.303}$$

Where C_0 is the initial concentration of drug, K is the release constant and t is time. First order release is concentration dependant.

3) Higuchi:

$$Q = K \sqrt{t}$$

Where K is the rate constant. The Higuchi model describes the rate of release based on Fickian diffusion of a dissolved drug through an insoluble matrix

4) Korsmeyer-Peppas:

$$\frac{M_t}{M_\infty} = kt^n$$

Where M_t / M_∞ is a fraction of drug released at time t and K is the release constant and n is the release exponent.

The regression parameters obtained for the release data in PBS and SGF following fitting to the various kinetic models are presented in Tables 5.1 and 5.2. The release data demonstrates the best fit with the Higuchi model for both release media (Tables 5.1 and 5.2).

Release data for $>1000 \mu\text{m}$ and $250 \mu\text{m}$ - $500 \mu\text{m}$ sized particles containing the various molecular weights of PEG in both release media were fitted to the Higuchi release model with consistently good linearity at all time points (Figure 5.7 and 5.8).

Table 5.1 The regression parameters for the different kinetic models obtained for release of riboflavin from PLGA particles with various PEG molecular weights. Size fraction of 1mm was used in PBS pH 7.4.

Sample	Zero-order		First-order		Higuchi		Korsmeyer-Peppas	
	r^2	$K_0(\text{h}^{-1})$	r^2	$K_1(\text{h}^{-1})$	r^2	$K_H(\text{h}^{-1/2})$	r^2	n
No PEG	0.8214	2.3101	0.5983	0.0321	0.9865	0.0470	0.7737	0.3244
PEG 1 KDa	0.8166	0.915	0.5786	0.0298	0.9625	0.0274	0.7944	0.1931
PEG 3 KDa	0.8511	2.3009	0.6201	0.0332	0.9821	0.0650	0.8355	0.2028
PEG 6 KDa	0.8538	1.8252	0.6431	0.0317	0.9803	0.0515	0.8545	0.1926
PEG 35 KDa	0.8538	1.85252	0.6141	0.036	0.9882	0.0604	0.8294	0.2201

Table 5.2 The regression parameters for the different kinetic models obtained for release of riboflavin from PLGA particles with various PEG molecular weights. Size fraction of 1mm was used in SGF pH 1.2 as the release medium.

Sample	Zero-order		First-order		Higuchi		Korsmeyer-Peppas	
	r^2	$K_0(\text{h}^{-1})$	r^2	$K_1(\text{h}^{-1})$	r^2	$K_H(\text{h}^{-1/2})$	r^2	n
No PEG	0.8626	1.3355	0.4551	0.0561	0.9831	0.0375	0.6839	0.3309
PEG 1 KDa	0.7241	0.7059	0.3241	0.054	0.9058	0.0209	0.5941	0.2713
PEG 3 KDa	0.7865	1.1882	0.468	0.0509	0.9286	0.0344	0.6376	0.2872
PEG 6 KDa	0.8533	0.6871	0.478	0.0589	0.9469	0.0194	0.7090	0.2946
PEG 35 KDa	0.8089	0.7758	0.4431	0.0432	0.9579	0.0223	0.6188	0.2826

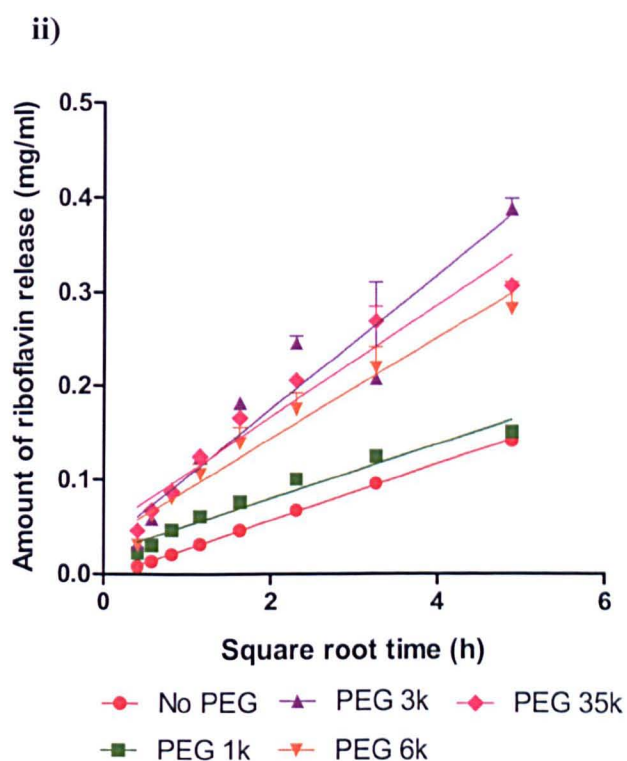
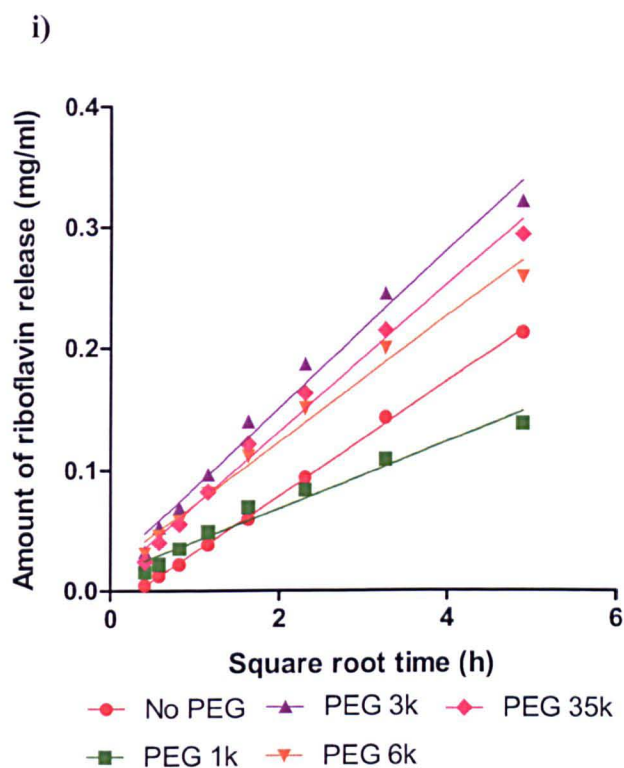


Figure 5.7 Data for the release of riboflavin from PLGA particles with various PEG molecular weights fitted to the Higuchi kinetic model for release data in PBS pH 7.4 for i) 1 mm sized and ii) 250 μ m sized particles

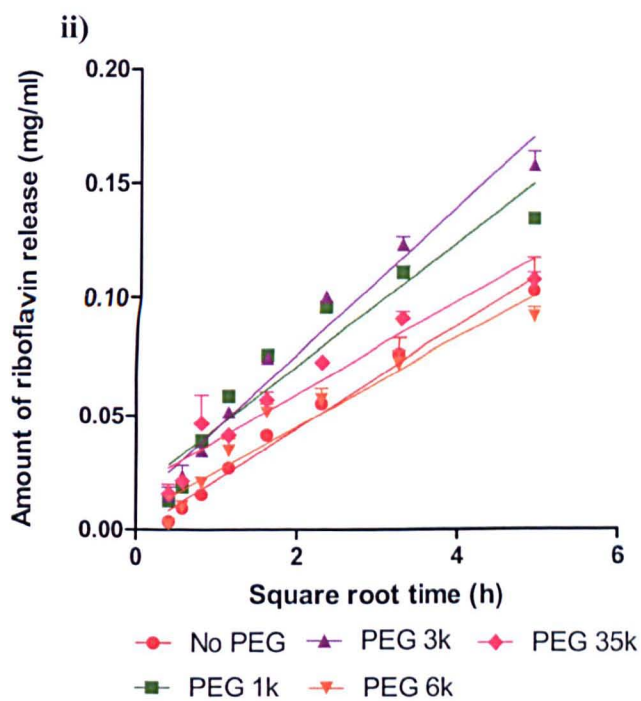
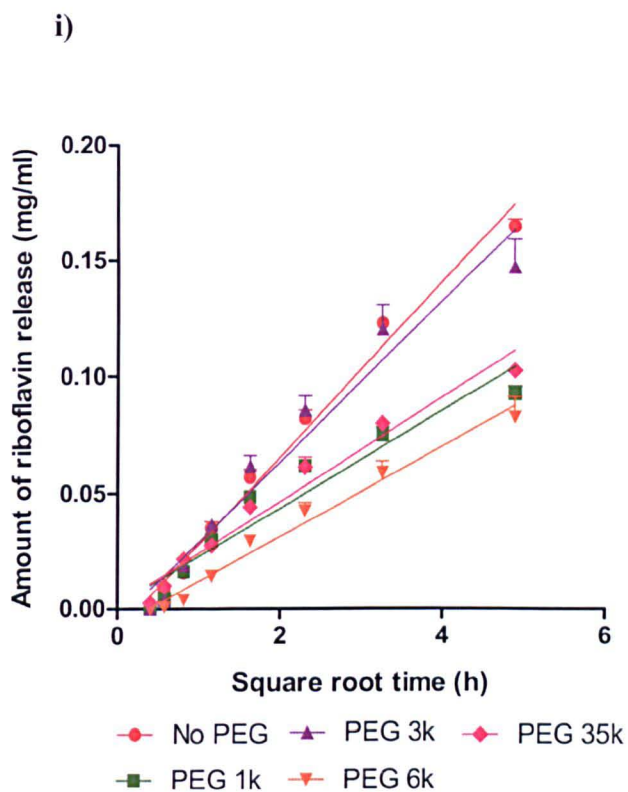


Figure 5.8 Data for the release of riboflavin from PLGA particles with various PEG molecular weights fitted to the Higuchi kinetic model for release data in SGF pH 1.2 for i) 1 mm sized and ii) 250 μ m sized particles

5.4 Discussion

In this thesis, porous microparticles have been successfully produced and loaded with model therapeutic agents using the novel supercritical fluid method, Particles from Gas Saturated Solutions. The potential for controlled release of a therapeutic agent has been confirmed and the modulation of this release to suit the aimed gastroretentive application was investigated by incorporation of the hydrophilic excipient PEG. This chapter presents a systematic study correlating drug release profiles in different media with a detailed insight into the matrix morphology provided by microCT and SEM.

Previously, it has been demonstrated that the morphology of microparticles prepared with poly (lactic acid) has an influence over somatostatin drug release [19]. The effect of porosity on somatostatin release was found to be greatest at the early time points, whereby, the release from porous matrices was faster. Similarly, a comparison of lidocaine release from porous and non-porous PLGA microparticles indicated an increase in drug motility in porous particles fundamentally changing the release profile and resulting in an increase in release rate [20].

The contrast between the rapid drug movement through fluid-filled pores and relatively slower movement through polymeric matrix is the root of these changes in release rate. In Chapter 4 the size of PLGA particles was found to affect rate of release. The microCT data (refer to Figure 3.8) indicated porosity within the PLGA particles is dependent upon the size of particle. The present chapter introduced the effect of PEG on the porosity of the particles and discusses the consequent effects on the drug release rate.

The introduction of PEG in the particles formulation was accompanied by an overall decrease in percentage porosity, typically decreasing from 53% for formulations with no PEG to as low as 11% on the addition of PEG 35 KDa (10% w/w) for similarly sized particles (Figure 5.5). This marked decrease is illustrated further by the 3D models, which additionally provide an insight into how this porosity is distributed through the particle. The decrease in porosity is in contrast to other methods of particle production where PEG or other hydrophilic materials are often used as porogens [21-23]. However, the mechanism of pore production in the PGSS method differs to that with conventional methods. On depressurisation of the plasticised mixture, the CO₂ gas leaves the rapidly solidifying matrix leaving behind an open pore network in its place. PEG is a crystalline polymer and supercritical CO₂ has been reported to infiltrate the polymer with more difficulty [24]. A smaller amount of CO₂ in the matrix will result in a decreased number of pore channels in the product.

Despite the decrease in initial porosity, the introduction of PEG to the system generally increases the rate of release (Figure 5.1 and 5.2). Introducing PEG into the system statistically increases release of riboflavin in PBS for PEG molecular weights greater than 3 KDa ($p < 0.001$), there is no specific trend seen in the molecular weight of the PEGs. In contrast, the PEG 1 KDa incorporation results in a decrease in release rate. Statistical analysis on the drug release data reports that in the 1 mm particles the presence of PEG has a statistically significant effect on the rate of drug release ($F(4, 70) = 28.15, p < 0.0001$). Similarly in the case of the 250 μ m particles it was revealed that the presence of PEG had a statistically significant effect on rate of release ($F(4,$

70) =28.39 $p<0.0001$). In Chapter 4 it was established that there is little burst release observed at the early time points for the PLGA particles of different size fractions. This is particularly surprising given the high porosity of the particles (up to 50% for particles with no incorporated PEG and 20% upon the incorporation of PEG). The inclusion of PEG in the formulation results in a somewhat increase in release at the early time points (0-3 h), although this is not a statistically significantly increase compared to particles with no PEG. Beyond 3 h, this is a different story with PEG mw greater than 3 KDa increasing the rate of release in PBS compared to particles of the same size with no PEG.

Typically, drug release from PLGA based microparticles demonstrates extensive burst release [25]. ToF-SIMS exposed the homogenous distribution of drug throughout the particle with relatively little, preferentially surface bound drug (refer to Figure 4.2 Chapter 4). This could explain the low burst release.

The shape of the release curves do not show any dramatic changes between particles with PEG and those without, it was therefore unlikely that there would be any change in mechanism of release and this was confirmed through the application of various kinetic models the release data (Tables 5.1 and 5.2). The Higuchi model demonstrates the best correlation with the drug release data (Figure 5.8) indicating that the release is diffusion dependent for all formulations, and further demonstrating that the mechanism of release does not change on the addition of PEG.

The pH of SGF (pH 1.2) significantly slows the release rate relative to release in PBS (pH 7.4) at all time points for particles prepared with PEG with molecular weight >3000 KDa ($p < 0.0001$). Chapter 4 reported a decrease in release rate for the different size fractions (1000 μm and 250 μm) in SGF relative to in PBS (Figures 4.4 and 4.5). A decrease in release rate at lower pH levels has been reported to be a result of a decrease in glass transition temperature for the PLGA polymer at the lower pH [26]. On contact with SGF medium the polymer moves through the transition of the glassy to rubbery state, the structure of the particles will consequently become compromised and there will be an element of breakdown in the porous network. Following this the polymer chains may reorganise to become more tightly packed resulting in the smoother particles shown in Figure 5.6. Particles prepared with no PEG and PEG 1 KDa do not show any statistically significant difference in release rate until the final time points where the rate is significantly decreased in SGF at 24 h ($p < 0.0001$). The significantly increased rate of drug release on PEG incorporation in PBS is in marked contrast to its effect in SGF.

Quantitative data corresponding to the porosity before and after the release along with the 3D reconstruction models allows a detailed look at this microstructure within the particles (Figure 5.5). The microCT data was subjected to a two-way ANOVA statistical analysis which revealed that the addition of PEG to the formulation significantly decreased porosity at all molecular weights ($p < 0.001$). Following exposure to PBS the porosity is also significantly higher in the case of particles with no PEG ($p < 0.001$). As previously stated, it is the diffusion of CO_2 from within the polymer matrix which results in the intricate porous network found in particles produced using

the PGSS process [27] and if less CO₂ is 'dissolved' in the material during PGSS [24] the porosity will be decreased when PEG is introduced to the matrix.

Following exposure to PBS the change in porosity was not found to be significant at any of the formulations. Although there appears to be a general trend for exposure to PBS to increase porosity (PEG 1 KDa being the exception to this) the variations between porosity measurements between the samples are too great to gain statistically significant difference. The mechanism of pore formation in the PGSS process is the result of the gaseous CO₂ diffusing from within the solidifying polymeric matrix, as these bubbles of gaseous CO₂ move around they will coalesce creating larger bubbles which leave behind large pore spaces. Variations in porosity are too great to form any statistically significant conclusions. The large variations may be because the sample size selected was far too small with only 10 particles being selected from each batch.

Exposure to the low pH of SGF does not reveal any significant changes in porosity. Never-the-less, a general trend in porosity may provide some information with regards to the differences in this microarchitecture following exposure to different release media. PBS, particularly for particles containing PEG, appears to increase surface porosity, whereas SGF appears to decrease porosity. A comparison of the microCT data with the SEM images confirms this trend. This microCT data is verified further by the SEM images which provide additional evidence to suggest an increase in porosity and surface degradation in particles containing PEG, this was anticipated considering the presence of PEG is known to improve the hydration of the matrix and has

previously been reported to form channels through the matrix [28]. Following production SEM images reveal irregular shaped particles with some surface roughness and porosity (Figure 5.6), following exposure to PBS there is an increase in this surface porosity with surface pitting becoming evident and some indication of degradation of structure at the surface. In the lower pH SGF the resultant morphology is very different, with SEM images demonstrating smoother surfaces without the extensive surface pitting and appearance of surface pores (Figure 5.6). The surface porosity seen in the particles following production is no longer present. Corresponding to the SEM images 3D reconstructions were prepared using the microCT data and illustrate how the internal porosity changes. With SGF, in contrast to the extensive pore network present following exposure to PBS, the 3D models show more discrete pores within the polymer matrix. The contrasting morphologies following exposure to media of different pH levels was reported previously by Zolnik et al [29] where the pH level did not appear to affect the mechanism of release, therefore the shape of the release profile remained the same it was moved down on the release plot, a similar phenomenon was revealed in this study with the release data both in PBS and in SGF fitting well to the Higuchi model. Previous studies however have found that altering the pH level of the media has an impact on the fundamental mechanism of release [30] this study investigated a range of pH levels from 10.8 to 1.3 and little difference in release profile shape was seen between low pH levels and those nearer neutral.

The smooth appearance of particles has been reported to be a result of homogeneity of pH levels within the particle as the diffusion of media into the particles results in degradation of the PLGA chains and a build up of oligomers

occurs. During release in PBS the acidic oligomers create a microclimate within the particles where the pH is low in comparison to the surrounding medium [31] this results in a heterogeneity in pH levels inside the particle and it is this which leads to the production of pores. In contrast, if the media has a low pH, then the presence of the oligomers will not alter the microclimate as significantly and the pH level within the microparticle remains homogenous. Thermal analysis in previous studies has demonstrated the difference in state of the polymer in the different pH levels which may provide an explanation for the difference in release [26] at low pH levels the polymer is in the glassy state whereas at more neutral pH levels the polymer is in the rubbery state. In the rubbery state the chains of the polymer are more mobile improving the motility of the drug particles within the polymer matrix.

The decrease in porosity and thus release rate from particles containing PEG 1 KDa may be a result of the melting temperature of PEG 1 KDa. This is approximately 35°C and it is unique amongst the PEGs selected for this study as this temperature is below that of the release media (37°C). This may have structural implications for the microparticles causing the intricate pore network to breakdown when the PEG 1 KDa becomes molten.

Polymer blends have previously been employed to modify characteristics of delivery systems, in particular in the modification of release rate. Mallardé et al [13] reported the release of teverelix from PLGA particles to be significantly increased when using a PLGA-PEG copolymer with the actions of PEG in the particles being described as a 'water-pump' inducing drug release. Reports of the enhancing effect of PEG on drug release are many in the literature [28] however this study has demonstrated that although the presence of PEG does

have an effect on the rate of release in this case, it is the impact PEG has on morphology which governs this.

5.5 Conclusions

The PGSS method was successfully applied in the preparation of large porous particles for application in controlled, gastroretentive drug release. Particles in the size range 2000 μm -100 μm were produced using a blend of PLGA (50:50) of two molecular weights (\sim 12 KDa and \sim 25KDa) and 10% (w/w) PEG of various molecular weights (1-35 KDa). It is reported here that the presence of PEG of molecular weight \geq 3 KDa increases rate of drug release over 24 h, this increase relates to the hydrophilicity of PEG and this polymer's actions as a porogen during the course of the release study. Although the particles prepared with no PEG incorporation demonstrated higher initial porosity, there is a markedly greater increase in porosity following exposure to PBS in particles with PEG, relative to the increase in particles with no PEG, which results in an increase in drug release for these particles.

PEG 1 KDa did not demonstrate a similar effect as the higher molecular weight PEGs although the explanation for this remains unclear it is likely to be a result of the lower melting temperature of PEG 1 KDa compared with PEG 3 KDa and above.

The data presented in this chapter demonstrates that modulation of drug release properties is possible through altering formulation parameters.

5.6 References

1. Cohen, S., et al., *Controlled deliovery systems for proteins based on poly(lactic glycolic acid) microspheres*. *Pharmaceutical Research*, 1991. **8**(6): p. 713-720.
2. Lim, T.Y., C.K. Poh, and W. Wang, *Poly (lactic-co-glycolic acid) as a controlled release delivery device*. *Journal of Materials Science-Materials in Medicine*, 2009. **20**(8): p. 1669-1675.
3. Varde, N.K. and D.W. Pack, *Microspheres for controlled release drug delivery*. *Expert Opinion on Biological Therapy*, 2004. **4**(1): p. 35-51.
4. Kang, B.K., et al., *Controlled release of paclitaxel from microemulsion containing PLGA and evaluation of anti-tumor activity in vitro and in vivo*. *International Journal of Pharmaceutics*, 2004. **286**(1-2): p. 147-156.
5. Mittal, G., et al., *Estradiol loaded PLGA nanoparticles for oral administration: Effect of polymer molecular weight and copolymer composition on release behavior in vitro and in vivo*. *Journal of Controlled Release*, 2007. **119**(1): p. 77-85.
6. Pillai, O. and R. Panchagnula, *Polymers in drug delivery*. *Current Opinion in Chemical Biology*, 2001. **5**(4): p. 447-451.
7. Dunn, A.S., P.G. Campbell, and K.G. Marra, *The influence of polymer blend composition on the degradation of polymer/hydroxyapatite biomaterials*. *Journal of Materials Science-Materials in Medicine*, 2001. **12**(8): p. 673-677.
8. Gopferich, A., *Polymer degradation and erosion: Mechanisms and applications*. *European Journal of Pharmaceutics and Biopharmaceutics*, 1996. **42**(1): p. 1-11.
9. Abraham J. Domb, M.M., Andrew S. T. Haffer, *Biodegradable polymer blends for drug delivery*. 1999, Massachusetts Institute of Technology: US.
10. Lao, L.L., S.S. Venkatraman, and N.A. Peppas, *Modeling of drug release from biodegradable polymer blends*. *European Journal of Pharmaceutics and Biopharmaceutics*, 2008. **70**(3): p. 796-803.
11. Yeh, M.K., et al., *Improving the delivery capacity of microparticle systems using blends of poly(DL-lactide co-glycolide) and poly(ethylene glycol)*. *Journal of Controlled Release*, 1995. **37**(1-2): p. 1-9.
12. Moneghini, M., et al., *Processing of carbamazepine PEG 4000 solid dispersions with supercritical carbon dioxide: preparation, characterisation, and in vitro dissolution*. *International Journal of Pharmaceutics*, 2001. **222**(1): p. 129-138.
13. Mallarde, D., et al., *PLGA-PEG microspheres of teverelix: influence of polymer type on microsphere characteristics and on teverelix in vitro release*. *International Journal of Pharmaceutics*, 2003. **261**(1-2): p. 69-80.
14. Badiger, M.V., M.E. McNeill, and N.B. Graham, *Porogens in the preparation of microporous hydrogels based on poly(ethylene oxides)*. *Biomaterials*, 1993. **14**(14): p. 1059-1063.

15. Jantratid, E., et al., *Dissolution media simulating conditions in the proximal human gastrointestinal tract: An update*. Pharmaceutical Research, 2008. **25**(7): p. 1663-1676.
16. Galia, E., et al., *Evaluation of various dissolution media for predicting in vivo performance of class I and II drugs*. Pharmaceutical Research, 1998. **15**(5): p. 698-705.
17. Marques, M.R.C., R. Loebenberg, and M. Almukainzi, *Simulated Biological Fluids with Possible Application in Dissolution Testing*. Dissolution Technologies, 2011. **18**(3): p. 15-28.
18. Ahuja, N., O.P. Katare, and B. Singh, *Studies on dissolution enhancement and mathematical modeling of drug release of a poorly water-soluble drug using water-soluble carriers*. European Journal of Pharmaceutics and Biopharmaceutics, 2007. **65**(1): p. 26-38.
19. Herrmann, J. and R. Bodmeier, *THE EFFECT OF PARTICLE MICROSTRUCTURE ON THE SOMATOSTATIN RELEASE FROM POLY(LACTIDE) MICROSPHERES PREPARED BY A W/O/W SOLVENT EVAPORATION METHOD*. Journal of Controlled Release, 1995. **36**(1-2): p. 63-71.
20. Klose, D., et al., *How porosity and size affect the drug release mechanisms from PLGA-based microparticles*. International Journal of Pharmaceutics, 2006. **314**(2): p. 198-206.
21. Lee, A.G., et al., *Development of Macroporous Poly(ethylene glycol) Hydrogel Arrays within Microfluidic Channels*. Biomacromolecules, 2010. **11**(12): p. 3316-3324.
22. Kim, H.K., H.J. Chung, and T.G. Park, *Biodegradable polymeric microspheres with "open/closed" pores for sustained release of human growth hormone*. Journal of Controlled Release, 2006. **112**(2): p. 167-174.
23. Lei, L., et al., *Zero-order release of 5-fluorouracil from PCL-based films featuring trilayered structures for stent application*. European Journal of Pharmaceutics and Biopharmaceutics, 2011. **78**(1): p. 49-57.
24. Kelly, C.A., *Supercritical CO₂: A Clean and Low Temperature Approach to Blending PLA and PEG*. Advanced Functional Materials, 2010. **22**: p. 8.
25. Wang, J., B.A. Wang, and S.P. Schwendeman, *Characterization of the initial burst release of a model peptide from poly(D,L-lactide-co-glycolide) microspheres*. Journal of Controlled Release, 2002. **82**(2-3): p. 289-307.
26. Faisant, N., et al., *Effects of the type of release medium on drug release from PLGA-based microparticles: Experiment and theory*. International Journal of Pharmaceutics, 2006. **314**(2): p. 189-197.
27. Tandy, A., F. Dehghani, and N.R. Foster, *Micronization of cyclosporine using dense gas techniques*. Journal of Supercritical Fluids, 2006. **37**(3): p. 272-278.
28. Cleek, R.L., et al., *Microparticles of poly(DL-lactic-co-glycolic acid)/poly(ethylene glycol) blends for controlled drug delivery*. Journal of Controlled Release, 1997. **48**(2-3): p. 259-268.
29. Zolnik, B.S. and D.J. Burgess, *Effect of acidic pH on PLGA microsphere degradation and release*. Journal of Controlled Release, 2007. **122**(3): p. 338-344.

30. Faisant, N., J. Siepmann, and J.P. Benoit, *PLGA-based microparticles: elucidation of mechanisms and a new, simple mathematical model quantifying drug release*. *European Journal of Pharmaceutical Sciences*, 2002. **15**(4): p. 355-366.
31. Ding, A.G. and S.P. Schwendeman, *Acidic Microclimate pH Distribution in PLGA Microspheres Monitored by Confocal Laser Scanning Microscopy*. *Pharmaceutical Research*, 2008. **25**(9): p. 2041-2052.

Chapter 6

Surface Modification for the Introduction of Novel Properties

6.1 Introduction

The introduction of bioadhesive properties to drug delivery systems is an intensively studied area for mucosal routes of drug delivery including oral, buccal, nasal and vaginal [1]. Mucosal surfaces are covering areas exposed to the external environment and provide both defences against external factors and are also involved in secretion and absorption. Features of mucosal surfaces such as the high surface area offer ideal conditions for localised site-specific delivery, and may enhance retention of the delivery system at the relevant site for optimal drug absorption.

Bioadhesion may be defined as ‘the state in which two materials, at least one of which is of a biological nature, are held together for an extended period of time by interfacial forces’ [2]. In the field of drug delivery this concept has been applied to the adhesion of a drug carrier system to a mucosal surface and the more specific term ‘mucoadhesion’ was coined. During the last two decades mucoadhesion concept has provided evidence for improved bioavailability of drugs from formulations applied to the buccal [3], nasal [4], respiratory [5], and intestinal [6] mucosa. Drug delivery to the oral cavity has

gained much interest due to the convenience of oral dosing. The introduction of mucoadhesive properties to oral dosage systems allows intimate contact to be formed between the system and the walls of the gastrointestinal tract (GIT) prolonging residence time [7]. There have been reports of different attempts to successfully create a system which will adhere to the mucus of the GIT [1, 7, 8].

In vitro mucoadhesion tests have demonstrated microparticles prepared with chitosan develop strong interactions with mucin in solution, the extent of the interactions was found to be proportional to the positive values for zeta potential of the microspheres indicating the importance of charge in these interactions [9]. The high surface area of microspheres compared with a single-unit tablet is likely to enhance the adhesion to the GIT lining. The PGSS method has previously been used in our group to prepare microparticles with mucoadhesive properties introduced through the incorporation of chitosan [10]. Interactions were found to exist between chitosan and mucin in solution, with the interactions increasing for increased amounts of chitosan (w/w) in the particles.

Although *in vitro* mucoadhesive tests have demonstrated successful adhesion of mucoadhesive systems to mucins in solutions [11], as well as in rat gut loop studies [12], it should be noted that the levels of mucoadhesive success seen in *in vitro* have rarely been replicated in *in vivo* studies. Gamma scintigraphic studies have revealed that compared with a control, bioadhesive formulations prepared using Carbopol 934P and polycarbophil did not significantly change the time taken for the system to arrive at the colon [13]. Similarly, chitosan based systems have also been analysed using gamma scintigraphy [14] and,

although *in vitro* investigations into the mucoadhesive properties of the microspheres demonstrate high levels of mucoadhesion, subsequent *in vivo* analysis did not replicate such successful adhesion with retention time being found to be short and not reproducible [14]. The major obstacles for mucoadhesive formulations include the high mucus turnover rate and strong peristaltic forces [15]. These limit the retention time of mucoadhesive systems, as a consequence to this in the present work a combination of mucoadhesion and buoyancy have been bestowed upon the drug delivery system in an effort to improve retention time.

Progress in the design of gastroretentive delivery formulations has brought about the emergence of systems which combine the gastroretentive potential of floating systems and mucoadhesive systems. A problem with the floating systems would be that as the stomach empties the delivery system would empty with the liquid. By introducing a mucoadhesive material, the delivery system would bind to the gastric walls during emptying. This will maintain the system within the stomach and enhance gastric residence time. Clarithromycin loaded microparticles prepared with chitosan-alginate-ethylcellulose enabling both floating and mucoadhesion, demonstrated a higher concentration of the clarithromycin at the gastric mucosa compared to a control [16]. *In vitro* analysis of a floating and bioadhesive system for sotalol HCl confirmed potential as a novel oral delivery system following analysis of characteristics such as controlled release, bioadhesiveness, and buoyancy in an acidic environment [17]. As a recent development in oral delivery these floating and bioadhesive systems are not as yet widely reported, however as outlined above

they do possess the potential to improve upon those systems which demonstrate only buoyancy or only mucoadhesion.

Mucous membranes are coated in a viscous secretion known as mucus, synthesised within the goblet cells. Mucus is composed of 95% water, >4% mucins, and <1% proteins, lipids, and mucopolysaccharides [7, 18]. Mucins are high molecular weight glycoproteins which play an instrumental role in defence [19], with their gelling properties contributing to the viscosity of the mucus layer [20]. Typically, mucins consist of two distinct regions, the first being a large central protein core to which numerous *O*-linked glycosaccharides are attached, secondly there are terminal peptide regions with little or no glycosylation but rich in cysteine residues. The cysteine residues provide thiol groups which give rise to disulphide bridges in and between mucin monomers allowing the formation of the intricate network of glycoproteins and the highly viscous nature of mucus [7].

Mucoadhesive polymers typically contain numerous hydrophilic groups such as hydroxyl, carboxyl, amide, and sulphides which enable the attachment of the material to mucus or the cell membrane itself [1]. When selecting suitable polymers for mucoadhesion various properties must be considered; it has been reported that the presence of certain functional groups, the degree of hydration, the molecular weight, charge, and the degree of cross linking are all important factors to consider [7]. Anionic polymers are often selected for mucoadhesion and may form strong interactions with mucin *via* hydrogen bonds. The presence of carboxyl and sulphate groups on these polymers leads to an overall negative charge. Poly (acrylic acid) and its related polymers Carbopol (Poly (acrylic acid) cross-linked with allyl sucrose), and polycarbophil (poly (acrylic

acid cross-linked with divinyl glycol) have been extensively tested in mucoadhesive systems with the cross-linked polymers performing better than the uncross-linked poly (acrylic acid) [21].

Cationic polymers, notably chitosan, have also been considered for their mucoadhesive properties. Chitosan is a polysaccharide produced by the deacetylation of chitin. Unlike poly (acrylic acid) which interacts with the mucus through hydrogen bonding, chitosan utilises ionic interactions between the amino groups in the chitosan and the sialic acid groups which are present as glycosidically bound branches in the mucin glycoproteins found in mucus [22]. Chitin, being the second most abundant polysaccharide in nature (following cellulose), is readily available and this, along with good biocompatibility has led to the popularity of chitosan for use in delivery systems [23]. Other polysaccharides such as alginic acid, hyaluronic acid, and carboxymethylcellulose have also been used in mucoadhesive systems.

The ionic and hydrogen based interactions with mucus are non-specific in nature. More recently second-generation mucoadhesives have made way for exploring specific covalent bonding. Introduction of thiol groups to polymers allows covalent disulphide interactions to occur with the cysteine rich areas within the mucins present in mucus. This process directly mimics the natural mechanism of secreted mucus glycoproteins which use disulphide bonds to anchor themselves within the mucus and therefore was thought to hold great potential. Indeed, thiolated polymers have shown good potential as mucoadhesives and consistently show improved mucoadhesive properties when compared to their non-thiolated counterparts [21, 24].

The mucoadhesive properties of chitosan have been modified through the production of various thiolated derivatives (Figure 6.1.). Chitosan-4-thio-butylamidine (chitosan-TBA), which is the product of a reaction between chitosan and 2-iminothiolane, has demonstrated the potential to improve mucoadhesion by up to 100-fold [25]. Chitosan-thioglycolic acid (chitosan-TGA) derivatives have also demonstrated up to 10 fold improvements in mucoadhesion in comparison with the unmodified chitosan [26]. The third type of modified chitosan, and the type adopted in the present work, are the chitosan-*N*-acetyl cysteine (chitosan-NAC) conjugates. Previous *in vitro* adhesion studies on the have reported this polymer to show a 50 fold improvement in residence time.

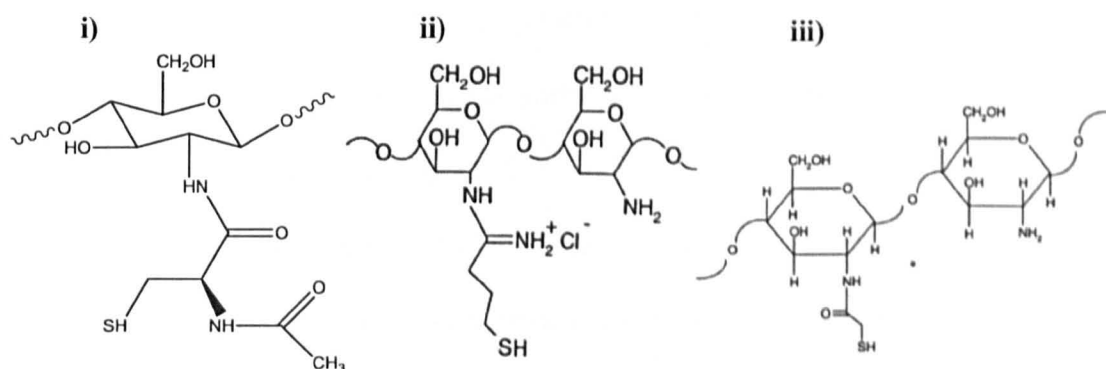


Figure 6.1 The structures of i) Chitosan-NAC ii) Chitosan-TBA and iii) Chitosan-TGA

A study comparing the mucoadhesive capacities of microspheres comprised of various bioadhesive materials demonstrated an enhancement of the retention of acyclovir at its absorption site in upper small intestine [27]. Of the various polymers tested, thiolated chitosan showed the highest mucoadhesiveness along with most improved bioavailability of the drug.

This chapter aims to augment the gastroretentive properties of a novel buoyant microparticulate system through the inclusion of the mucoadhesive polymer chitosan or its thiolated derivative chitosan-NAC. Confirmation of successful incorporation of the mucoadhesive polymers will be carried out using morphological investigations as well as spectroscopic analysis using ToF-SIMS, the novel properties bestowed upon the system will be analysed using a combination of *in vitro* techniques.

6.2 Materials and Methods

6.2.1 Materials

Low molecular weight chitosan, *N*-acetyl cysteine, *N*-(3-Dimethylaminopropyl)-*N'*-ethylcarbodiimide hydrochloride (EDAC), periodic acid 99%, porcine mucin (type III), and fluorescein isothiocyanate (FITC) were obtained from Sigma Aldrich. Basic Fuchsin was obtained from National Diagnostics. Materials used in particle preparation are as described in Chapter 3. All chemicals were used as supplied.

6.2.2 Methods

6.2.2.1 Preparation of *N*-Acetyl Cysteine Modified Chitosan (chitosan-NAC)

The chitosan-NAC conjugate was prepared by attachment of *N*-acetyl cysteine to the amine groups in the chitosan. This process is outlined in Figure 6.2 below.

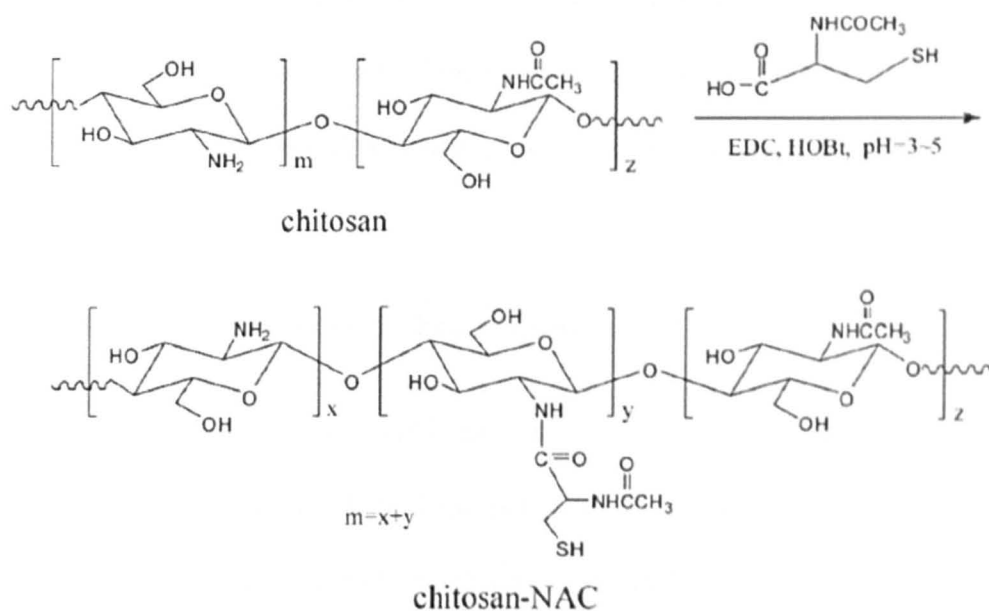


Figure 6.2 The synthesis of chitosan-NAC

The covalent attachment of *N*-acetyl cysteine (NAC) to chitosan occurs through the production of an amide group from the interaction between the primary amino group of chitosan and a carboxylic acid group of NAC [28]. The primary amino group of chitosan exhibits a pKa value of around 6.5 [29] therefore at pH 5 the amino group is protonated enabling interaction with the carboxyl group in the NAC.

The preparation of the chitosan conjugate chitosan-NAC was carried out as previously described [30]. Briefly, 1 g low molecular weight chitosan (Sigma Aldrich) was dissolved in 100 ml of acetic acid and the pH made up to 5.0 with 5 M HCl and 1 M NaOH. 6 g *N*-acetyl cysteine (NAC) and 2 g EDAC were dissolved in 100 ml dH₂O. The two solutions were then united and incubated at room temperature under constant agitation in the dark for 5 h. The solution was then dialyzed (Mw 10,000 cut off) at 10°C initially against 5 mM HCl containing 2 μ M EDTA for 3 days, followed by a further 3 days against the

same medium with the addition of 1% NaCl and a final 3 days against 1mM HCl. The resultant product was then frozen and lyophilized for a period of 3 days until product is completely dry. It is then stored in the dark at 4°C until required.

6.2.2.2 Preparation of FITC Labelled Chitosan

The synthesis of FITC labelled chitosan was based on the reaction between the isothiocyanate group of FITC and the primary amino group of chitosan [31]. Briefly, 200 mg chitosan was dissolved in 20 ml 2% acetic acid and 5 mg FITC was dissolved in 10 ml DMSO. The two solutions were united and left stirring in the dark for 12 h. Following this the solution was precipitated in an excess of acetone and dialysed against dH₂O for 3 days. The FITC-chitosan was then freeze dried for 5 days.

6.2.2.3 Nuclear Magnetic Resonance (NMR) Spectroscopy

¹H NMR spectroscopy was used to confirm the modification of chitosan with N-Acetyl-Cysteine. Samples were analysed using a Bruker Advance 600MHz spectrometer. Prior to analysis the sample was dissolved in 0.6 ml deuterated water (D₂O) containing 2 drops of deuterated hydrochloric acid (DCl) for chitosan samples and 2 drops of deuterated chloroform (CDCl₃) for polymer samples. The data was processed using TopSpin (version 2.0)

6.2.2.4 Ellman's Assay

Ellman's reagent (5,5'-dithiobis-(2-nitrobenzoic acid) or DTNB) is frequently used to quantify the sulphhydryl groups in a sample. Briefly, the reaction involves cleavage of the disulphide bond in DTNB, resulting in 2-nitro-5-

thiobenzoate (NTB⁻). In water at neutral pH NTB⁻ ionizes and the resultant NTB⁻² has a yellow colour. This reaction is dependent on the reaction pH, the pKa of the sulfhydryl group. The intensity of the yellow colour can be analysed using UV-VIS spectrophotometry and quantification of the sulfhydryl groups present may be calculated using a standard curve prepared with cysteine. Alternatively, the extinction coefficient (cited to be 14150 M⁻¹cm⁻¹ [32] at 412 nm) of the NTB⁻² may be used to calculate concentration.

The assay was carried out as follows; initially the DTNB reagent was prepared by dissolving 137 mg sodium acetate trihydrate and 15 mg DTNB in 20 ml dH₂O. Tris buffer was prepared by dissolving 121 mg Tris base in 1 litre dH₂O and made to pH8.0. The samples were prepared by dissolving 5 mg of modified chitosan in 2.5 ml dH₂O; 10µl of this was then added to 100 µl tris buffer and 50 µl DTNB and made up to 1 ml with dH₂O. The sample was then analysed for absorbance at 412 nm using UV/Vis.

6.2.2.5 Post-Processing Surface Modification of PLGA Particles

Coating microparticles for drug delivery with a polyelectrolyte has been reported to convey novel properties onto the microparticles. A common example in drug delivery is the ability to adhere to certain biological surfaces such as mucus [33, 34]. Chitosan is often the polymer of choice for mucoadhesion because of its cationic charge, biocompatibility, and strong mucoadhesive properties. The pKa (acid dissociation constant) value of chitosan is 6.5 therefore the chitosan is positively charged and soluble in acid-neutral solutions and thus in the low pH of the stomach the chitosan will be highly charged (positively), and be able to bind to negatively charged

components of mucus. The attachment of the Chitosan to the surface of PLGA particles occurs through electrostatic bonds between the protonated primary amino group of the chitosan and the negatively charged carboxyl group on the PLGA.

In this study 100 mg chitosan was dissolved in 25 ml 2% acetic acid made to pH4.5. To the chitosan solution 100 mg PLGA particles were introduced and left to stir for 1 h. Following this, the particles were filtered off the solution and washed initially with 50 ml acetic acid followed by 50 ml dH₂O and collected before freeze drying for 3 days.

6.2.2.6 Incorporation of Mucoadhesive Polymer into Formulation and Preparation of Particles using PGSS Method

Incorporating the mucoadhesive polymer during the production allows the manufacture of the system to remain a simple, one-step process. Although chitosan does not undergo plasticisation or melting it is possible to incorporate the chitosan in a similar way to the encapsulation of an active pharmaceutical ingredient. In this way the chitosan will be present throughout the polymer matrix. The particles were prepared as described in Chapter 2 (Section 2.1) with the following formulation to be weighed out and introduced to the mixing chamber:

-
- 55% PLGA ~12 KDa (w/w)
 - 20% PLGA ~25 KDa (w/w)
 - 5% Drug (w/w)
 - 5% SPAN80 (w/w)
 - 10% PEG 35 KDa (w/w)
 - 5% Low molecular weight chitosan (w/w)

6.2.2.7 Scanning Electron Microscopy

SEM was carried out as described in detail in Chapter 2 (Section 2.2).

6.2.2.8 X-ray Microtomography

microCT was carried out as described in detail in Chapter 2 (Section 2.3).

6.2.2.9 Fluorescent Microscopy

Particles were prepared for fluorescent microscopy through the addition of 0.5% w/w coumarin to the formulation. A corresponding 10 mg PLGA (Resomer RG502H) was removed from the formulation to maintain batch size. Particles were imaged using fluorescent microscopy and images analysed as described in detail in Chapter 2 (Section 2.4).

6.2.2.10 Time-of-Flight Secondary Ion Mass Spectroscopy

ToF-SIMS surface analysis was carried out as described in detail in chapter 2 (Section 2.12).

6.2.2.11 Mucous Glycoprotein Assay

A periodic acid/ Schiff reagent (PAS) colorimetric assay as previously reported [35] was utilised to determine the concentration of free mucin in a solution. This allows a value for the amount of mucin lost from a known mucin solution to be determined and therefore the amount of mucin that has adsorbed to the particle surface deduced.

This staining procedure is often employed in histological staining. Incubation with periodic acid results in oxidization of the polysaccharide which usually occurs at the vicinal diols in the compound [36]. The oxidation results in the formation of aldehydes which then react with decolourised Schiff reagent to produce a coloured product. There are two different mechanisms reported in the literature for reaction of Schiff reagent with aldehydes. The first mechanism was proposed by be decolourised by sulfonation of the central carbon atom. The mechanism of action has been proposed previously [37].

The mucin assay was carried out by incubating 10 mg PLGA particles in 1ml of a known concentration of porcine mucin for a period of 1 h in a rotamixer. Following this time the mucin solution was removed from the particles and this solution was incubated at 37°C with 100 µl 50% (w/v) periodic acid for 2 h. Once returned to room temperature 200 µl Schiff reagent was introduced and the samples were analysed for absorbance at 570 nm using UV/Vis.

6.2.2.12 Adhesion of Particles to a Mucus Producing Cell Line

Calu-3 cells were cultured to confluence in 75 cm² flasks at 5% CO₂, 37 °C. Once confluent, cells were detached from the flasks by incubating with

trypsin/EDTA solution and seeded on Transwell® permeable inserts at a density of 10^5 cells/cm². Cells were maintained at 5% CO₂, 37°C in EMEM, supplemented with FBS (10% v/v) and antibiotic/antimycotic solution, which was replaced regularly (every 48 h). Air-liquid interface (ALI) was created on day two following seeding of the cells on filters. Cell growth and tight junction formation was assessed by transepithelial electrical resistance (TEER) measurements. TEER is a measurement of resistance to ion flux across an epithelial layer and reflects the degree of confluence demonstrated by the cells. Briefly, sterilised electrodes are placed in the culture medium on the apical and basal side of the cell layer. The resulting readings were recorded and adjusted to take into account background filter resistance.

Cell monolayers were typically used for TEER and permeability experiments between days 8–10 in culture. Bioadhesive analysis was carried out by the addition of 10 mg dry particles to each transwell followed by a 30 min incubation period. Following this time the cells were thoroughly washed 3 times using PBS to remove any unadhered particles and the plate was imaged by the time elapse camera Hamamatsu 1394 ORCA-285, and the software used for video acquisition and data generation was Volocity software version 5.2.

6.3 Results

6.3.1 Preparation of NAC Modified Chitosan

The structure of the product was confirmed initially using ¹H NMR. On comparison of the spectra obtained for unmodified chitosan (Figure 6.4) and that obtained for the NAC conjugate (Figure 6.5) a large resonance peak at around 2.2 ppm is apparent. On further comparison with the spectrum

obtained for *N*-acetyl cysteine (Figure 6.3) it appears that this is the peak corresponding to the side chain which incorporates the –SH group.

The amount of thiol moieties on the chitosan conjugate was determined spectrophotometrically using the Ellman's assay. The modified polymer exhibited 4.755×10^{-4} moles thiol groups per gram of polymer.

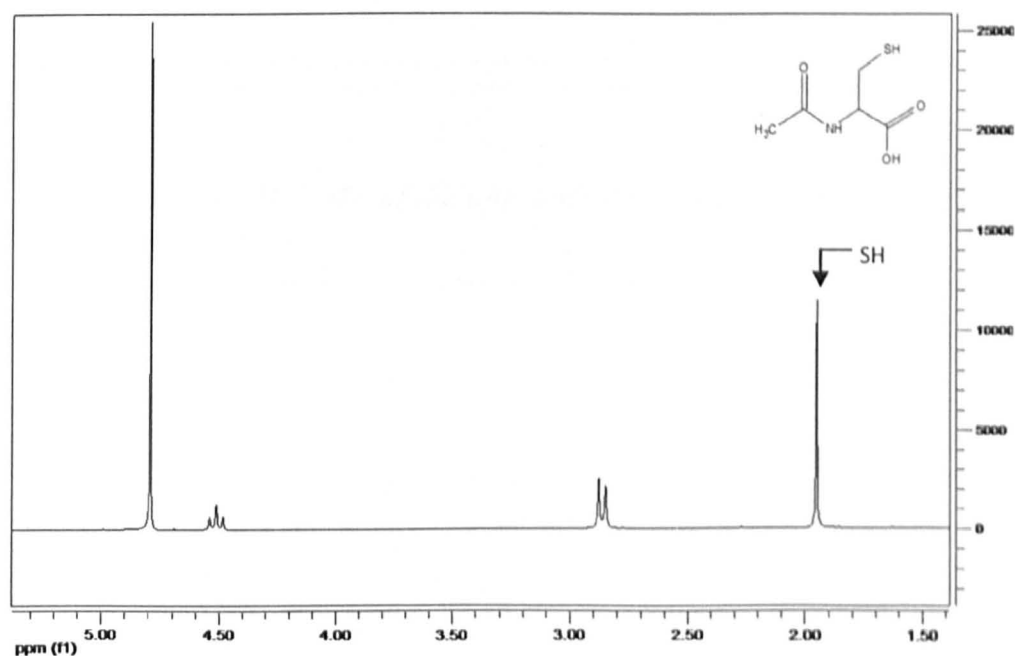


Figure 6.3 ^1H NMR spectra of *N*-acetyl cysteine in DCl

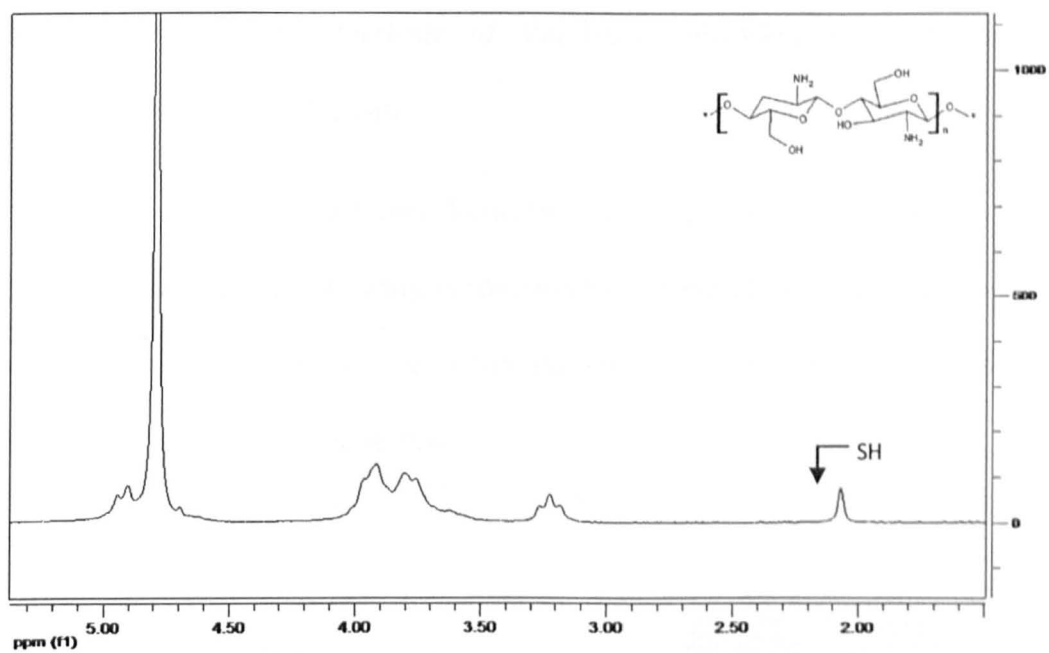


Figure 6.4 H^1 NMR of the unmodified chitosan polymer in DCl

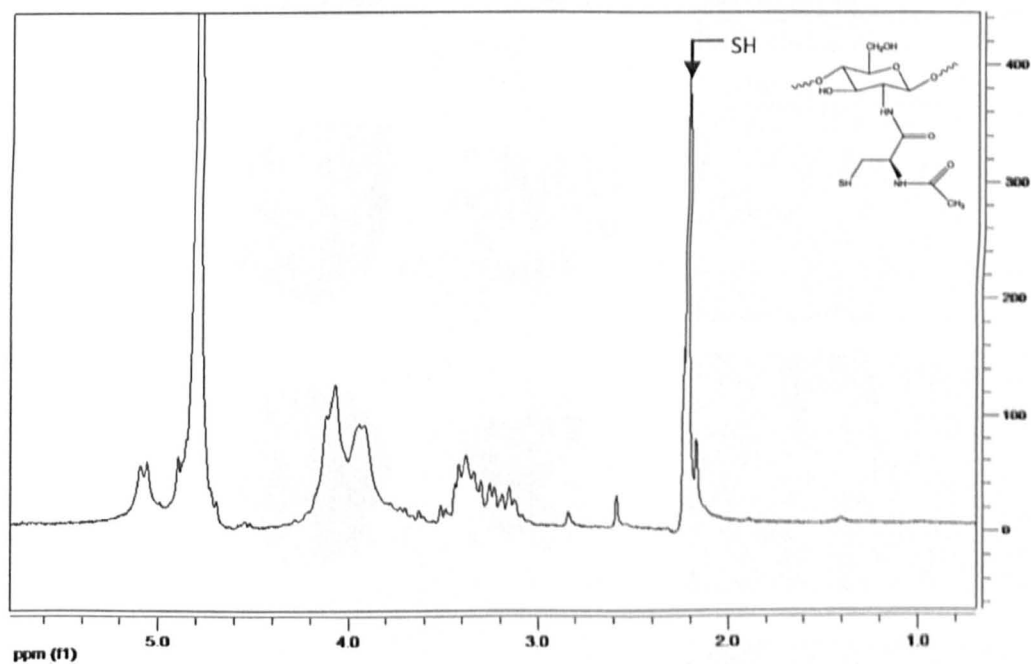


Figure 6.5 H^1 NMR spectra of the chitosan-NAC conjugate in DCl

6.3.2 Morphological Analysis of Particles Following Post-Processing Surface Modification

SEM analysis of the different formulations reveals that when the coating process is carried out following production by the PGSS method there is some disruption to the surface of the microparticles (Figure 6.6) and an increase in open pores is shown at the surface.

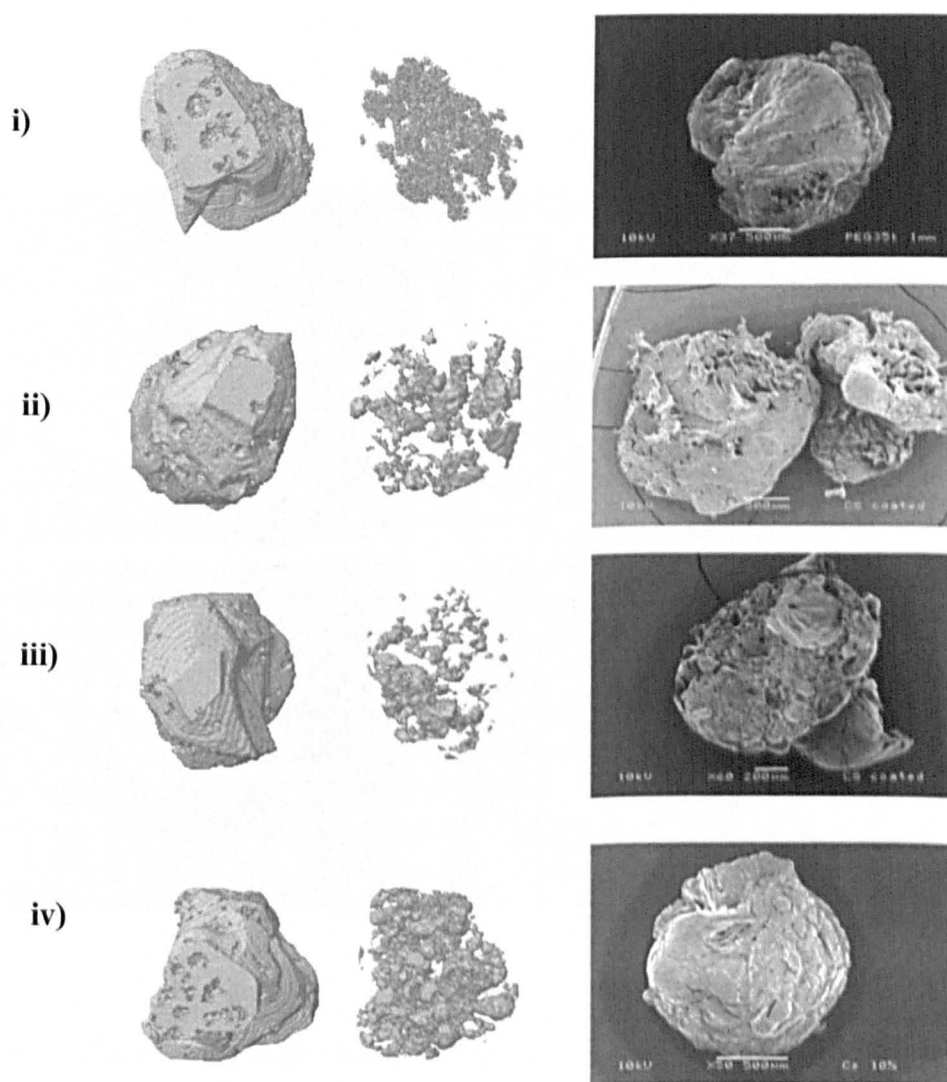


Figure 6.6 Morphological analysis of i) control (uncoated), ii) chitosan coated post processing iii) chitosan-NAC coated post processing iv) chitosan incorporated into formulation (10%(w/w)) . Both SEM and microCT images are presented.

The fluorescent images in Figure 6.7 show the difference in appearance of particles following the coating after production (i, and ii) and incorporation of chitosan during the production step (iii, and iv). Figures i) and ii) allow a detailed visualisation of the contours of the surface of the microparticles. Images corresponding to particles labelled with coumarin-6 offer an insight as to how a low molecular weight excipient may be distributed throughout the matrix. The high amount of background fluorescence in the coumarin-6 incorporated particles may prevent the defined surface contours from being apparent.

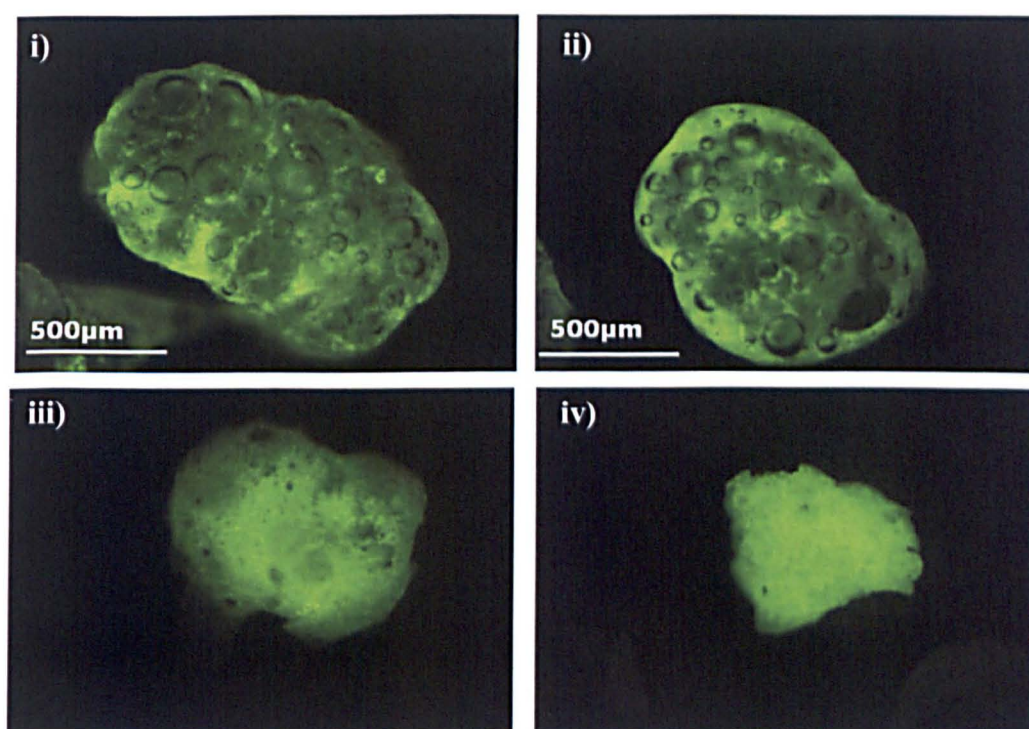


Figure 6.7 *Fluorescent images of particles containing FITC-chitosan as a post processing coating (i) and ii) alongside chitosan incorporated into coumarin-6 labelled particles (iii) iv))*

6.3.3 ToF-SIMS Surface Analysis

Although the fluorescent images provide evidence for the presence of FITC-CS on the surface of the microparticles, ToF-SIMS allows the acquisition of more detailed data including the identification and localisation of specific materials on the surface of the microparticles.

Figure 6.8 confirms that the coating process was successful and there is chitosan present on the surface of the particles. Furthermore the spectra also show how the PLGA peak decreases in the coated sample.

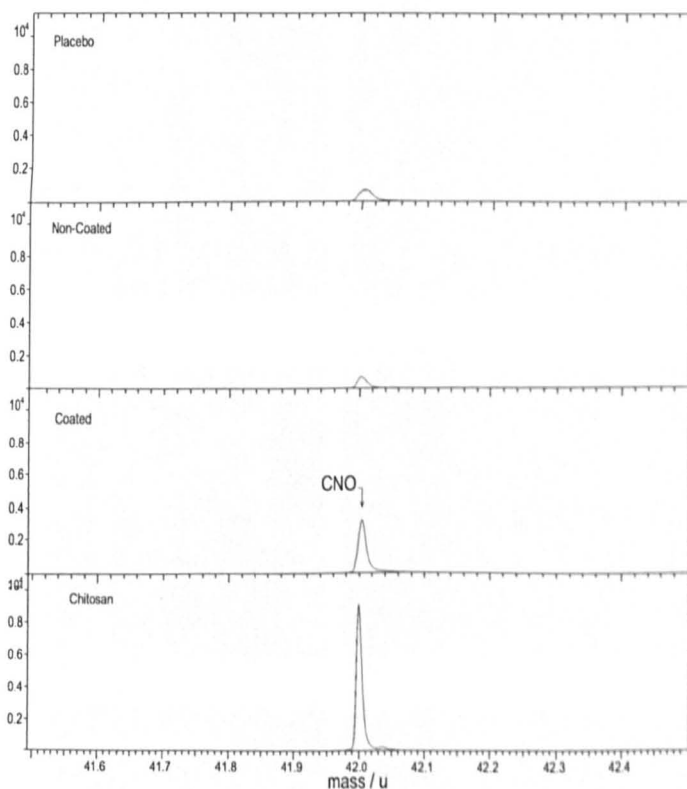


Figure 6.8 ToF-SIMS mass spectra showing the intensity of the CNO^- peak in the different formulations. The spectra confirm the increased intensity of CNO^- which is the chitosan associated ion in the coated samples.

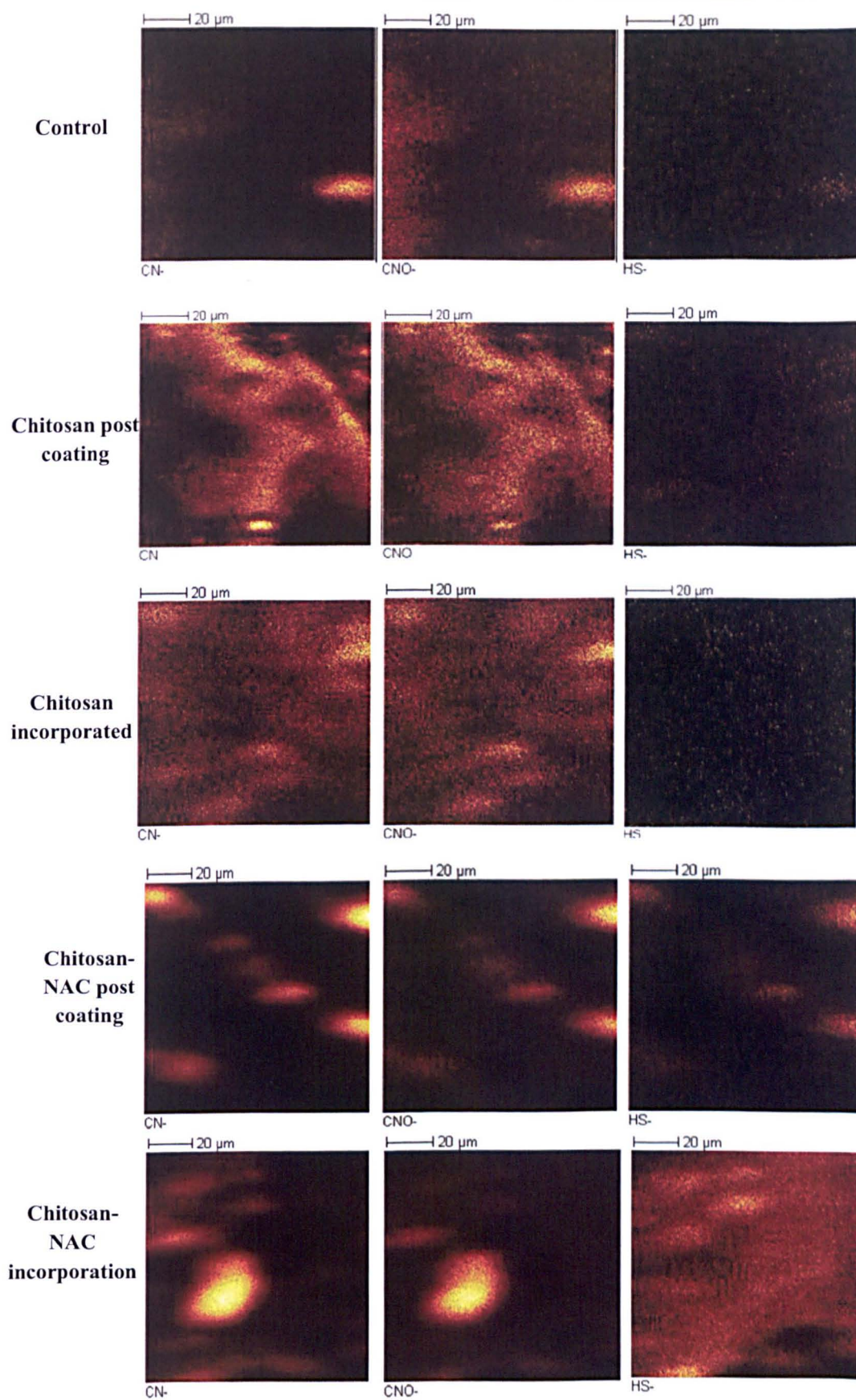


Figure 6.9 ToF-SIMS ion images demonstrating the distribution of the CN⁻, CNO⁻, and HS⁻ ions in the different formulations.

The ion images presented in Figure 6.9 demonstrate the distribution of the chitosan polymer and the chitosan-NAC in samples in both incorporation methods. In all cases the chitosan distribution is not uniform with patches of higher intensity evident for the chitosan associated peaks (CN^- , and CNO^-). The SH⁻ images show a higher intensity for the chitosan-NAC images as expected due to the presence of thiol groups in the derivative.

Following review of the individual spectra obtained for the individual components of the system, peaks were selected to represent PLGA, and chitosan in the depth profile. Peaks at m/z 73 (C_2HIO_3^-), m/z 87 ($\text{C}_3\text{H}_3\text{O}_3^-$), and m/z 89 ($\text{C}_3\text{H}_5\text{O}_3^-$) were found to be representative of PLGA with C_2HIO_3^- being selected to represent PLGA in depth profiles. Peaks which were found to be diagnostic for the presence of chitosan include m/z 26 (CN^-), m/z 42 (CNO^-), m/z 50 (C_3N^-), m/z 56 ($\text{C}_2\text{H}_2\text{NO}^-$), and m/z 82 ($\text{C}_4\text{H}_4\text{NO}^-$). The intensity of the CNO^- peak was selected to represent chitosan in depth profiling.

Figure 6.10 shows the depth profile for the microparticles coated with chitosan post-production. The depth profile confirms that on the surface there is a relatively high intensity of ions originating from the chitosan compared to PLGA, the intensity of the chitosan then decreases past these surface layers and the PLGA intensity increases. This confirms that the chitosan is confined to a shallow layer at the surface (although the actual depth cannot be quantified due to the individual nature of the sample). A different situation can be seen in Figure 6.11, where the chitosan powder was incorporated during the processing step. In this case it would be expected that the intensity of both the PLGA and the chitosan would remain almost constant through the depth of the sample. However, the intensity of chitosan is markedly higher on the surface

than through the deeper layers of the sample. This was unexpected as the chitosan is incorporated into the formulation and therefore was anticipated to be distributed homogeneously throughout the sample. During depressurisation it appears that the chitosan will locate towards the surface of the particles. The chitosan intensity past the very surface (>100 seconds) then decreases however remains higher relative to post-processing coating, indicating the presence of chitosan throughout the sample.

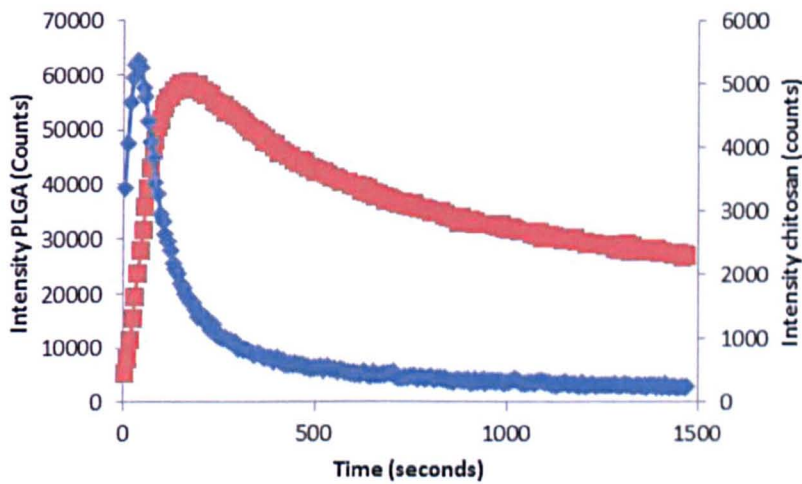


Figure 6.10 Depth profile demonstrating the intensity of the PLGA (red) ions and the chitosan ions (blue) as the analysis is carried out through the depth of the sample after post production coating.

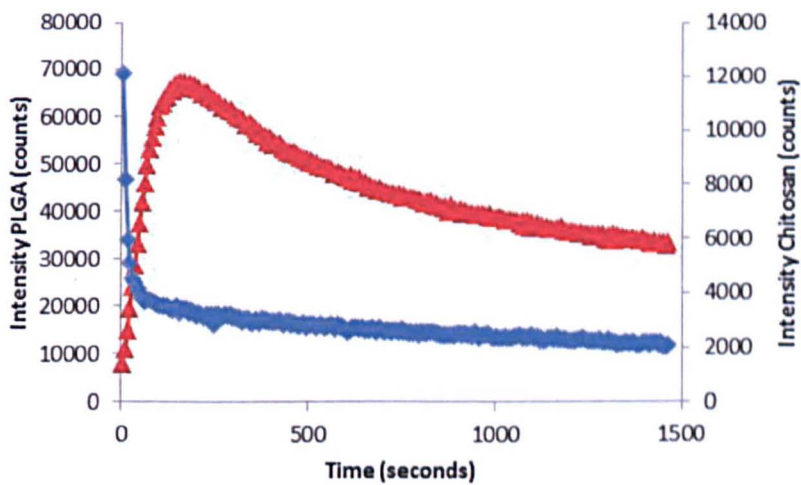


Figure 6.11 Depth profile demonstrating the intensity of the PLGA (red) ions and the chitosan ions (blue) as the analysis is carried out through the depth of the sample after the chitosan has been incorporated into the formulation.

Following the depth profiling as with the surface analysis ion images were constructed and the z view of these images is shown in Figure 6.12. The images show the high intensity of CN^- and CNO^- at the surface of the particles and interestingly for the particles coated post production this coating extends through what appears to be discrete channels into the depth of the sample. Such channels may be an indication as to the location of the pores in the system.

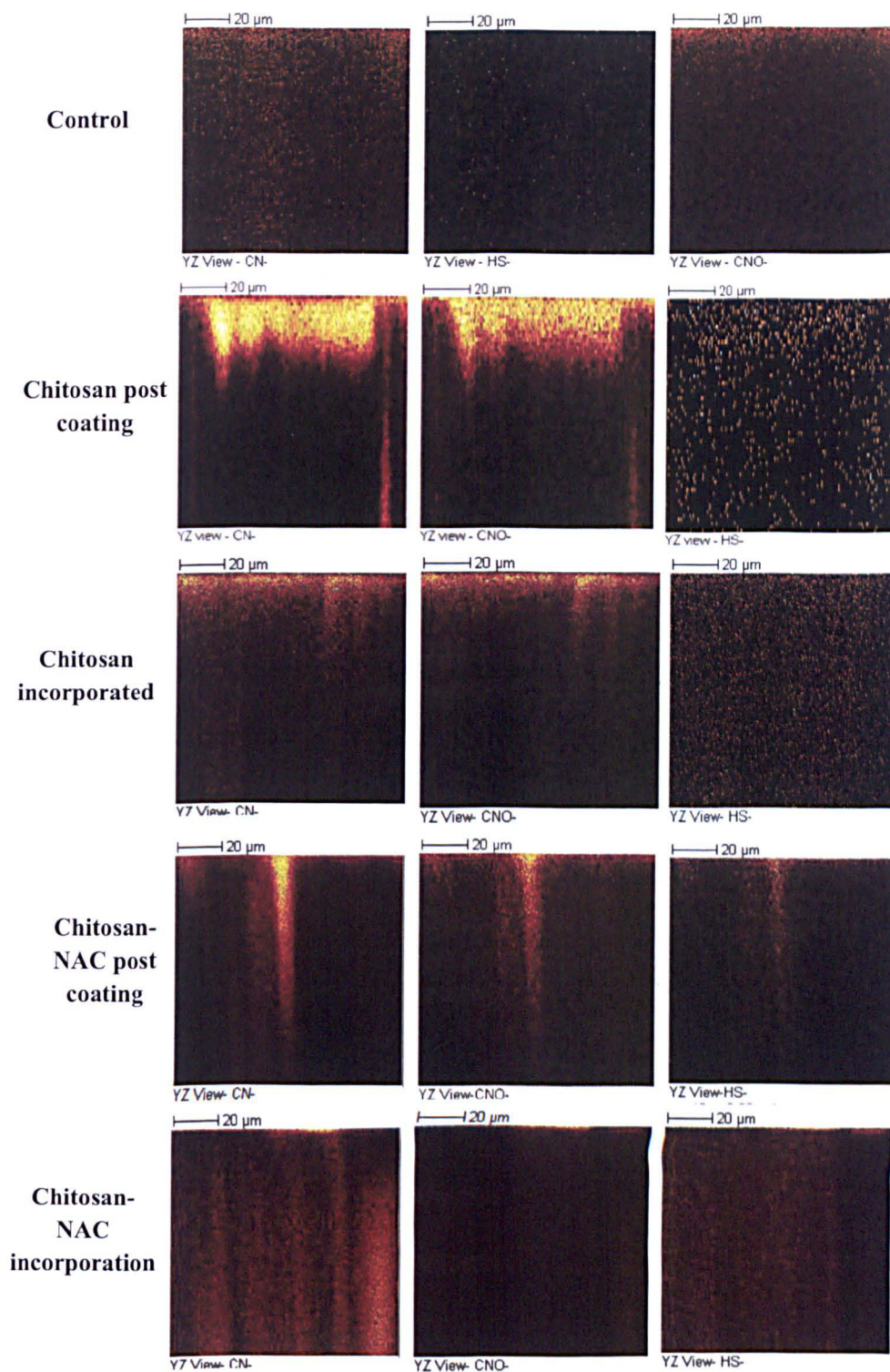


Figure 6.12 ToF-SIMS ion images demonstrating the distribution of the CN^- , CNO^- , and HS^- ions in the z view following depth profiling.

6.3.4 Mucous Glycoprotein Assay

Surface analysis confirmed the presence of chitosan at the surface of the particles. In order to investigate what mucoadhesive properties the presence of this polymer conveys on the sample, a mucin assay was carried out. Following incubation in a known concentration of mucin the colorimetric periodic acid/Schiff assay was applied to the solution to determine the end concentration. This gives an indication of the amount of mucin which has adhered to the particle surface. Figure 6.13 gives a comparison of the amount of mucin adhered to the particles for the different formulations. There is no mucin lost from the solution in the control microparticles, without the mucoadhesive polymer the microparticles do not show any mucoadhesive behaviour. Coating the microparticles with the chitosan-NAC results in the highest mucoadhesion in this assay. Whether the chitosan was incorporated post or during production did not appear to result in a difference in mucoadhesive behaviour.

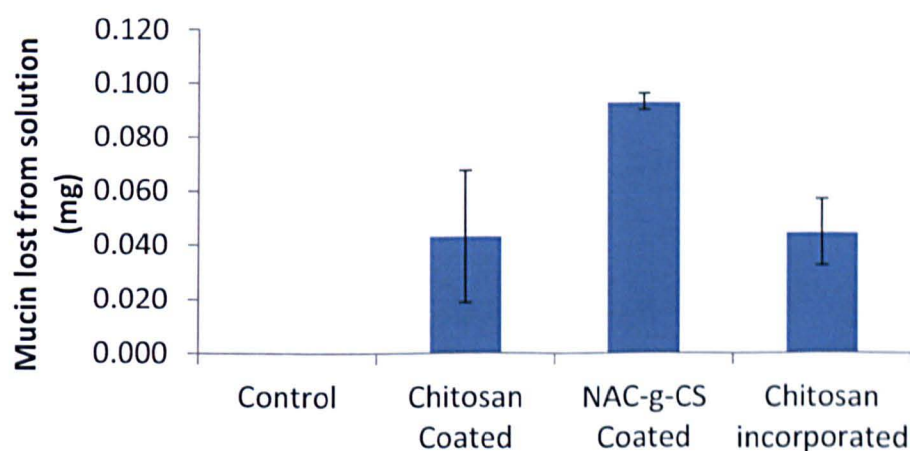


Figure 6.13 Chart comparing the amount of mucin which adheres to microparticles following incubation in a mucin solution ($n=3\pm SD$).

6.3.5 Adhesion to a Mucus Producing Cell Culture Model

The mucoadhesive properties of the chitosan containing systems were assessed using a mucus secreting cell culture model. Particles were introduced to Calu-3 cell monolayers grown on transwell supports and were then imaged prior to and following washing (Figure 6.14). This technique allows direct visual comparisons to be made of the mucoadhesion of the different samples. The images illustrate that there is no observable mucoadhesion of particles containing no mucoadhesive polymer. The presence of either chitosan, or the chitosan-NAC, results in substantial surface area of the cell monolayer covered with remaining particles. The adhesion does not appear to differ if particles were either coated with chitosan post-production or chitosan added during the production stage. Interestingly, despite higher mucin adhesion, chitosan-NAC does not appear to improve mucoadhesion in this study. On the contrary, there appears to be less particles remaining adhered to the mucus layer following washing step for the chitosan-NAC formulation, relative to the unmodified chitosan system.

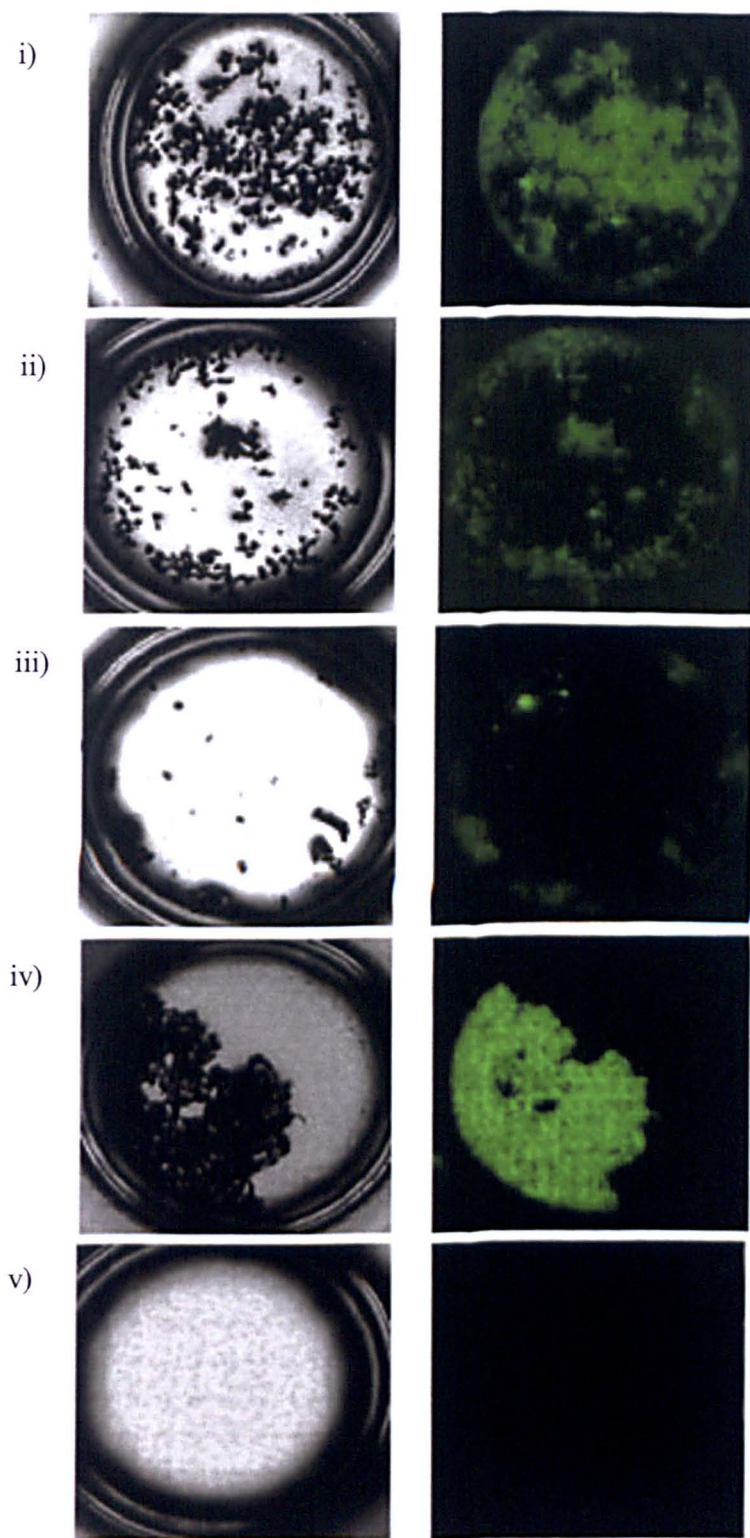


Figure 6.14 Fluorescent and bright field images showing the particles adhered to the surface of the cell monolayer i) distribution of fluorescently labelled particles prior to washing ii) FITC-chitosan coated particles iii) FITC-chitosan-NAC coated particles iv) chitosan incorporated particles labelled with coumarin-6 v) control particles labelled with coumarin-6

6.4 Discussion

In this chapter the incorporation of mucoadhesive excipients, and the introduction of novel properties to the formulation, has been explored. Chitosan was selected as the mucoadhesive polymer and has previously been widely used in drug delivery systems to improve bioavailability [38]. The PGSS method has been described as a simple, and successful, one step method towards the production of drug encapsulated microparticles [39], however chitosan does not undergo plasticisation, as the PLGA and PEG do, on exposure to the $scCO_2$. Therefore chitosan could not be incorporated in the same way PLGA and PEG are resulting in the introduction of a second step in processing with the coating being achieved through a post-processing modification. This involved the microparticles being suspended in a chitosan solution. The SEM analysis revealed that this process may cause some changes to the surface morphology of the particles, which was perhaps unsurprising due to the low pH conditions that the coating process must be carried out to ensure solubility of chitosan [40].

The pKa value of the amino group in chitosan is ~ 6.5 although this may vary depending on deacetylation degree [29], therefore at low to neutral pH level chitosan is charged. The main interaction between the positively charged chitosan and the PLGA is considered to be electrostatic. The carboxyl group in the PLGA demonstrates a pKa of 3.85 [41] and a fraction of these groups will be negatively charged allowing ionic interactions between chitosan and PLGA. It has also been reported that the coating process may continue even after a positive microparticle surface has been achieved and therefore the interactions may be in part governed by hydrogen bonding, or van der Waal's forces [42].

Detailed analysis of the internal morphology following the coating process exposed the change in the porous network which was not unlike what we have previously encountered following release studies in the low pH of SGF medium (see Chapter 4 Figure 5.5) suggesting that during the coating process there is some disruption to the structure of the microparticles.

For this reason another approach was explored to introduce chitosan during the particles formulation. The chitosan powder was added into the material mixture and, although it will not be plasticised and mixed under the sCO₂ as PLGA and PEG polymers, the chitosan particles will be expected to be distributed within the polymer matrix. This protocol does not require the suspension and exposure of particles to the chitosan coating solution. SEM and microCT analysis confirm that, as a result, there is no disruption to the surface or to the porous network in these particles. Through incorporation of the chitosan during the particles production allows a one-step process, it should be noted however the chitosan is not restricted to the surface and ToF- SIMS data indicated that it is present deeper in the matrix and should be found throughout the microparticle this may have an impact on other properties. ToF-SIMS surface analysis confirmed that the chitosan in both the post-processing coated samples is most prevalent on the surface. The depth profiles show the distribution of ions in the two coating methods, with both methods confirming the high intensity of chitosan originated ions on the surface.

By submerging the particles in the chitosan solution the coating is limited to the upper surface of the microparticles which results in this defined depth profile pattern. However, when the chitosan powder is incorporated with the molten PLGA and PEG matrix, the intensity of chitosan signal still

demonstrates a significant decrease through the layers although it does not fall as low as with post-processing coating. There is a general decrease in intensity for both ions towards the deeper layers. It has been reported that this decline in intensity maybe a result of the development of roughness in the raster area [43]. The sputter induced topography may have an impact on the depth resolution and also secondary ion yield [44].

The z view images illustrating the ion intensity through the sample (Figure 6.12) show interesting differences in chitosan distribution. The depth profile for the post-processing coating is confirmed by the ion images as the higher intensity signal from the CN^- and CNO^- ions appears towards the upper most layers with the intensity decreasing through the layers. The opposite is seen in the ion images for the PLGA ions where the upper layers are darker where the chitosan coating is located on the surface. The z view image also show that the coating penetrates into the exposed pores and this may confound the intensity data for these chitosan ions as the intensity is taken as an average of the whole area. As expected when the chitosan is incorporated during processing this high intensity is no longer restricted to the surface of the microparticles and the intensity appears to remain almost homogenous throughout the sample.

The chitosan was modified to produce the derivative chitosan-*N*-acetyl-L-cysteine. This chitosan derivative has previously demonstrated improvements in mucoadhesive properties, as the thiol group allows the formation of covalent bonds between the polymer and the mucus which results in stronger interactions [28, 45]. The modification procedure was found to be successful, with the final product containing 4.755×10^{-4} moles thiol groups per gram of

polymer. The presence of the SH⁻ is confirmed by NMR, and can also be detected in the ToF-SIMS ion images (Figures 6.9 and 6.12).

The *in vitro* mucin assay confirmed that the presence of the thiol group in the polymer increases the amount of mucin which adheres to the particles surface. This was expected due to the enhancement in the interactions as introduced by disulphide cross linking. This data however is not backed-up by the results of the cell mucoadhesion study. The images (Figure 6.14) illustrate the non modified chitosan incorporated particles demonstrate greater adhesion to the mucus following washing in comparison to the NAC modified PLGA particles. This is not in agreement with reports in the literature [45] where the modified chitosan improves the mucoadhesive properties and results in improved retention times.

Cysteine is considered to be a mucolytic and is used in therapies for respiratory conditions such as cystic fibrosis, bronchitis, and chronic obstructive pulmonary disorder. The actions of NAC as a mucolytic agent may mean that the previously reported success with mucoadhesive polymers modified with cysteine, could be a result of improved mucus penetration rather than improvements in mucoadhesion [28].

Here, the chitosan-NAC derivative may be acting as a mucolytic allowing the mucus layer, along with any adhered microparticles, to be removed during the washing steps. N-acetylcysteine has been used to remove mucus from the epithelia in an attempt to prevent mucoadhesion [46].

6.5 Conclusion

Two different methods of introducing mucoadhesive functionality to PGSS produce particles were explored in this chapter. Chitosan was either introduced post production of PLGA particles or it was incorporated into the formulation mixture and encapsulated during production. Both incorporation methods were found to successfully introduce chitosan into the system and little difference was found in mucoadhesive properties gained.

The chitosan derivative, chitosan-NAC, was also explored, as the introduction of the thiol groups in the cysteine has been reported to allow covalent interactions between the polymer and the mucins *via* disulphide bridges. Although the chitosan-NAC demonstrated better adhesion of mucin from solution, following contact with a mucus producing cell monolayer this polymer appears less mucoadhesive. An explanation for this may lie with the mucolytic actions of NAC and although the polymer is adhering to the mucins present in the mucus layer the mucolytic action cleaves the mucus allowing it to be washed away during the washing step.

This chapter concludes that the introduction of a mucoadhesive polymer into the floating particles could augment the gastroretentive behaviour of the particles.

6.6 References

1. Shaikh, R., et al., *Mucoadhesive drug delivery systems*. Journal of pharmacy & bioallied sciences, 2011. 3(1): p. 89-100.
2. Robinson, J.R., M.A. Longier, and M. Veillard, *Bioadhesive polymers for controlled drug delivery*, in Juliano, R. L. 1987. p. 307-314.

3. Morales, J.O. and J.T. McConville, *Manufacture and characterization of mucoadhesive buccal films*. European Journal of Pharmaceutics and Biopharmaceutics, 2010. **77**(2): p. 187-199.
4. Nagda, C.D., et al., *Preparation and Characterization of Spray-Dried Mucoadhesive Microspheres of Ketorolac for Nasal Administration*. Current Drug Delivery, 2011. **9**(2): p. 205-218.
5. Manca, M.L., et al., *Release of rifampicin from chitosan, PLGA and chitosan-coated PLGA microparticles*. Colloids and Surfaces B-Biointerfaces, 2008. **67**(2): p. 166-170.
6. Senel, S., *Potential applications of chitosan in oral mucosal delivery*. Journal of Drug Delivery Science and Technology, 2010. **20**(1): p. 23-32.
7. Andrews, G.P., T.P. Lavery, and D.S. Jones, *Mucoadhesive polymeric platforms for controlled drug delivery*. European Journal of Pharmaceutics and Biopharmaceutics, 2009. **71**(3): p. 505-518.
8. Carvalho, F.C., et al., *Mucoadhesive drug delivery systems*. Brazilian Journal of Pharmaceutical Sciences, 2010. **46**(1): p. 1-17.
9. Dhawan, S., A.K. Singla, and V.R. Sinha, *Evaluation of mucoadhesive properties of chitosan microspheres prepared by different methods*. AAPS PharmSciTech, 2004. **5**(4): p. e67.
10. Casettari, L., et al., *Surface Characterisation of Bioadhesive PLGA/Chitosan Microparticles Produced by Supercritical Fluid Technology*. Pharmaceutical Research, 2011. **28**(7): p. 1668-1682.
11. He, P., S.S. Davis, and L. Illum, *In vitro evaluation of the mucoadhesive properties of chitosan microspheres*. International Journal of Pharmaceutics, 1998. **166**(1): p. 75-88.
12. Lehr, C.M., et al., *Intestinal transit of bioadhesive microspheres in an in situ loop in the rat - A comparative study with copolymers and blends based on poly(acrylic acid)*. Journal of Controlled Release, 1990. **13**(1): p. 51-62.
13. Harris, D., et al., *GI transit of potential bioadhesive systems in the rat*. Journal of Controlled Release, 1990. **12**(1): p. 55-65.
14. Sakkinen, M., et al., *Are chitosan formulations mucoadhesive in the human small intestine? An evaluation based on gamma scintigraphy*. International Journal of Pharmaceutics, 2006. **307**(2): p. 285-291.
15. Lai, S.K., Y.-Y. Wang, and J. Hanes, *Mucus-penetrating nanoparticles for drug and gene delivery to mucosal tissues*. Advanced Drug Delivery Reviews, 2009. **61**(2): p. 158-171.
16. Zheng, J., et al., *Preparation and evaluation of floating-bioadhesive microparticles containing clarithromycin for the eradication of Helicobacter pylori*. Journal of Applied Polymer Science, 2006. **102**(3): p. 2226-2232.
17. Jimenez Castellanos, M.R., H. Zia, and C.T. Rhodes, *Design and testing in vitro of a bioadhesive and floating drug delivery system for oral application*. International Journal of Pharmaceutics (Amsterdam), 1994. **105**(1): p. 65-70.
18. Bansil, R. and B.S. Turner, *Mucin structure, aggregation, physiological functions and biomedical applications*. Current Opinion in Colloid & Interface Science, 2006. **11**(2-3): p. 164-170.

19. Snyder, J.D. and W.A. Walker, *Structure and function of intestinal mucin- Developmental aspects*. International Archives of Allergy and Applied Immunology, 1987. **82**(3-4): p. 351-356.
20. Jeffrey P. Pearson, A.A., David A. Hutton, *Rheology of Mucin*, in *Glycoprotein Methods and Protocols*. 2000. p. 99-109.
21. Grabovac, V., D. Guggi, and A. Bernkop-Schnurch, *Comparison of the mucoadhesive properties of various polymers*. Advanced Drug Delivery Reviews, 2005. **57**(11): p. 1713-1723.
22. Sogias, I.A., A.C. Williams, and V.V. Khutoryanskiy, *Why is chitosan mucoadhesive?* Biomacromolecules, 2008. **9**(7): p. 1837-1842.
23. Hejazi, R. and M. Amiji, *Chitosan-based gastrointestinal delivery systems*. Journal of Controlled Release, 2003. **89**(2): p. 151-165.
24. Bernkop-Schnurch, A., *Thiomers: A new generation of mucoadhesive polymers*. Advanced Drug Delivery Reviews, 2005. **57**(11): p. 1569-1582.
25. Roldo, M., et al., *Mucoadhesive thiolated chitosans as platforms for oral controlled drug delivery: synthesis and in vitro evaluation*. European Journal of Pharmaceutics and Biopharmaceutics, 2004. **57**(1): p. 115-121.
26. Kast, C.E. and A. Bernkop-Schnurch, *Thiolated polymers - thiomers: development and in vitro evaluation of chitosan-thioglycolic acid conjugates*. Biomaterials, 2001. **22**(17): p. 2345-2352.
27. Dhaliwal, S., et al., *Mucoadhesive microspheres for gastroretentive delivery of acyclovir: In vitro and in vivo evaluation*. Aaps Journal, 2008. **10**(2): p. 322-330.
28. Schmitz, T., et al., *Synthesis and characterization of a chitosan-N-acetyl cysteine conjugate*. International Journal of Pharmaceutics, 2008. **347**(1-2): p. 79-85.
29. Lopez-Leon, T., et al., *Physicochemical characterization of chitosan nanoparticles: electrokinetic and stability behavior*. Journal of Colloid and Interface Science, 2005. **283**(2): p. 344-351.
30. Wang, X., et al., *Chitosan-NAC Nanoparticles as a Vehicle for Nasal Absorption Enhancement of Insulin*. Journal of Biomedical Materials Research Part B-Applied Biomaterials, 2009. **88B**(1): p. 150-161.
31. Ge, Y., et al., *Fluorescence Modified Chitosan-Coated Magnetic Nanoparticles for High-Efficient Cellular Imaging*. Nanoscale Research Letters, 2009. **4**(4): p. 287-295.
32. Han, J.C. and G.Y. Han, *A procedure for quantitative-determination of tris(2-carboxyethyl)phosphine, an odorless reducing agent more stable and effective than dithiothreitol*. Analytical Biochemistry, 1994. **220**(1): p. 5-10.
33. Carvalho, F.C., et al., *Mucoadhesive drug delivery systems*. Brazilian Journal of Pharmaceutical Sciences. **46**(1): p. 1-17.
34. Makhlof, A., M. Werle, and H. Takeuchi, *Mucoadhesive drug carriers and polymers for effective drug delivery*. Journal of Drug Delivery Science and Technology, 2008. **18**(6): p. 375-386.
35. Mantle, M. and A. Allen, *A colorimetric assay for glyco proteins based on the periodic acid-Schiff stain*. Biochemical Society Transactions, 1978. **6**(3): p. 607-609.

36. Gilks, C.B., et al., *Simple procedure for assessing relative quantities of neutral and acidic sugars in mucin glycoproteins - Its use in assessing cyclical changes in cervical mucins*. *Journal of Clinical Pathology*, 1988. **41**(9): p. 1021-1024.
37. Keusch, P. http://www.uni-regensburg.de/Fakultaeten/nat_Fak_IV/Organische_Chemie/Didaktik/Keusch/D-ald_add-e.htm. [cited 2012 30July].
38. Luessen, H.L., et al., *Mucoadhesive polymers in peroral peptide drug delivery .1. Influence of mucoadhesive excipients on the proteolytic activity of intestinal enzymes*. *European Journal of Pharmaceutical Sciences*, 1996. **4**(2): p. 117-128.
39. SencarBozic, P., et al., *Improvement of nifedipine dissolution characteristics using supercritical CO₂*. *International Journal of Pharmaceutics*, 1997. **148**(2): p. 123-130.
40. Zolnik, B.S. and D.J. Burgess, *Effect of acidic pH on PLGA microsphere degradation and release*. *Journal of Controlled Release*, 2007. **122**(3): p. 338-344.
41. Yoo, J.-W. and S. Mitragotri, *Polymer particles that switch shape in response to a stimulus*. *Proceedings of the National Academy of Sciences of the United States of America*, 2010. **107**(25): p. 11205-11210.
42. Guo, C. and R.A. Gemeinhart, *Understanding the adsorption mechanism of chitosan onto poly(lactide-co-glycolide) particles*. *European Journal of Pharmaceutics and Biopharmaceutics*, 2008. **70**(2): p. 597-604.
43. Shard, A.G., et al., *Quantitative molecular depth profiling of organic delta-layers by C-60 ion sputtering and SIMS*. *Journal of Physical Chemistry B*, 2008. **112**(9): p. 2596-2605.
44. Cirilin, E.H., et al., *Ion-induced topography, depth resolution, and ion yield during secondary ion mass-spectrometry depth profiling of a GAAS/ALGAAS superlattice- effects of sample rotation*. *Journal of Vacuum Science & Technology a-Vacuum Surfaces and Films*, 1991. **9**(3): p. 1395-1401.
45. Mueller, C., et al., *Thiolated chitosans: In vitro comparison of mucoadhesive properties*. *Journal of Applied Polymer Science*, 2011. **124**(6): p. 5046-5055.
46. Greaves, J.L. and C.G. Wilson, *Treatment of diseases of the eye with mucoadhesive delivery systems*. *Advanced Drug Delivery Reviews*, 1993. **11**(3): p. 349-383.

Chapter 7

Pharmacokinetic Analysis of Metformin Hydrochloride Following Administration of Gastroretentive PLGA Particles

7.1 Introduction

The previous chapters compare the *in vitro* release of the two model drugs demonstrating differing solubility levels, furosemide, and riboflavin. This chapter introduces metformin; this drug is frequently reported in the literature in oral delivery systems for pharmacokinetic analysis in the rat model allowing comparisons to be made. Additionally, the high solubility of this drug will provide further information towards the characterisation of drug release behaviour. Metformin is an anti-hyperglycaemic agent and is the first-line drug of choice for type II diabetes. Although its anti-hyperglycaemic actions were characterised in the late 1920's [1], metformin was first employed in diabetes therapy only in 1957 [2]. Metformin reduces hepatic gluconeogenesis through activation of AMP-activated protein kinase (AMPK) [3]. AMPK is a multi-subunit enzyme which is involved in energy homeostasis and more specifically, it holds roles in fatty acid oxidation, muscle glucose uptake, hepatic lipogenesis. Its chronic activation may induce the expression of muscle hexokinase and glucose transporters [3].

Type II diabetes rates are rapidly increasing in line with the increasing incidence of obesity and therefore the emergence of a successful therapy is highly desired. Although metformin provides adequate therapeutic intervention [4, 5], it could be improved if the oral bioavailability (around 55%) could be further increased [6-8] and required dosing frequency reduced. Metformin therapy is also commonly associated with gastrointestinal related side effects such as gastric discomfort, nausea, and diarrhoea. Incidences of gastrointestinal related adverse effects are observed in around 30% of patients [9-11].

The biological half-life of metformin is approximately 3 h [8] and therefore by conventional delivery systems dosing is required three or four times a day [12]. There have been various attempts to decrease dosing frequency and improve the bioavailability of metformin through gastroretentive formulations [13-19]. A floating tablet formulation, prepared with sodium alginate and sodium carboxymethylcellulose as the gelling agents and Eudragit NE 30 D to provide controlled release and reduce initial burst, confirmed the system had appropriate sustained release and the gastroretentive properties suggesting its successful application in once-a-day therapy [17]. Another formulation, based on a hydrodynamically balanced system with appropriate *in vitro* buoyancy, showed prolonged gastric residence time and revealed increased AUC compared to immediate release formulations [20]. Gelucires are a family of lipid based materials which have been successfully applied in sustained drug delivery and floating times of up to 8 h have been reported for single unit Gelucire 43/01 matrices. Along with suitable controlled release of metformin over 9 h, this system holds the potential as an effective carrier for metformin

for controlled, gastroretentive release [21]. A combination of floating with bioadhesive properties in a delivery system based on PLGA, poly (acrylic acid), alginate, and pectin demonstrated good *in vitro* release of metformin and gastro-adhesive properties, although metformin drug encapsulation efficiency was relatively low at 18-54% [22]. Other systems which hold potential for controlled release and gastroretention for metformin delivery include microballoons [18], gastroretentive tablets [14] and microbeads [15].

Although these systems have shown good potential in *in vitro* release and mucoadhesion assays, replication of this success is rarely reported in *in vivo* studies. An example where this success has been reported is a mucoadhesive matrix pellet, prepared with HPMC and cellulose, revealed retention in the upper small intestine of rabbits for 10 h with metformin release being sustained over this period [13]. Extended release metformin tablets (Glumetza™) are currently available on the market and have demonstrated good efficacy [23]. This delivery system achieves improved drug bioavailability through increasing its size (up to 150% of the initial value) on contact with the gastric media, reaching the size that is preventing its emptying into the intestine.

The varied environment within the GIT is contributing to difficulties in establishing *in vitro* - *in vivo* correlation. Many factors contribute to this varied environment. One of the factors, particularly affecting mucoadhesive systems, is the high turnover rate of the mucus lining [24], as previously discussed in Chapter 1 (Section 1.4.3). Drug delivery devices designed for adhesion within GIT to this mucus lining are only as successful as the integrity of the mucus to which they are adhered [25].

The selection of an animal model for gastroretentive systems is difficult because there are significant variations in gastrointestinal physiology between species. These physiological, anatomical, and biochemical differences between species can result in significant variations in drug absorption from the oral formulations [26]. Canine models are considered to demonstrate good correlation with man for GI physiology, with similar motility patterns and pH profiles. Differences such as gastric emptying rates and intestinal transit times however may affect drug absorption, in particular for gastroretentive systems [27].

Regarding the use of rats in studies of oral formulations a comparison of the gastrointestinal physiology of that of the rat and man confirms that such small animal models are useful in the determination of bioavailability from powder and solution formulations; whereas larger animal models (dog, pig, or sheep) may be more appropriate for determination of absorption from 'larger' formulations, if only because they are easier to administer [26]. Nevertheless, the application of the rat model has been reported in pharmacokinetic studies of gastroretentive formulations of metformin as follows. A pharmacokinetic and pharmacodynamic study of the effect of controlled release formulations of metformin was carried out in diabetic rats showing gastric retention times of up to 10 h and with improvements in glucose lowering effect compared to the I.V administration [28]. Floating alginate beads loaded with metformin demonstrated significantly greater and more prolonged hypoglycaemic effect in comparison with non-floating beads in a diabetic rat model [29]. The rat model has also been applied in investigations involving mucoadhesive systems showing promise for the use of mucoadhesive excipients in the improvement

of metformin delivery [30]. The use of the rat model provides an adequate early indication of the efficacy of novel formulations; however larger animal models are usually required prior to testing in man.

7.2 Materials and Methods

7.2.1 Materials

Metformin hydrochloride (Figure 7.1) was obtained from Sigma Aldrich, Ammonium Dihydrogen Phosphate (99.9% extra pure), and phosphoric acid (85+% solution in water) were obtained from Acros Organics. Sodium alginate, acetonitrile, and HPLC grade water were obtained from Fisher Scientific. Other materials utilised in particle preparation are described in Chapters 3 and 6.

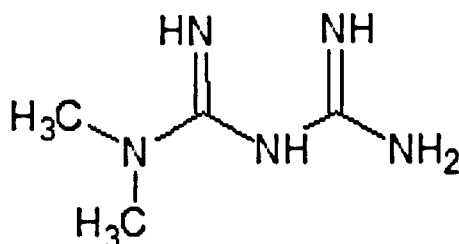


Figure 7.1 Chemical structure of metformin. (solubility >300 mg/ml)

7.2.2 Methods

7.2.2.1 Incorporation of Metformin Hydrochloride into PLGA Particles

Particles were produced using the PGSS method as described in detail in Chapter 2 (Section 2.1). The following formulation material was used weighed for a 2 g batch for buoyant particles.

-
- PLGA (RG502H ~12KDa) 55% (w/w)
 - PLGA (RG503 ~ 25 KDa) 20% (w/w)
 - PEG 35 KDa 10% (w/w)
 - SPANTM80 5% (w/w)
 - Metformin 10% (w/w)

And the following materials were weighed out for the buoyant mucoadhesive particles.

- PLGA (RG502H ~12KDa) 50% (w/w)
- PLGA(RG503 ~ 25 KDa) 20% (w/w)
- PEG 35 KDA 10% (w/w)
- SPANTM80 5% (w/w)
- Metformin 10% (w/w)
- Chitosan 5% (w/w)

7.2.2.2 Preparation of Non-Buoyant Particles

Particles were also prepared without the application of supercritical carbon dioxide technology in order to provide a non-buoyant particles control. For animal studies these particles the formulation material, as described above was heated until the PLGA polymer became molten. The mixture was then stirred for a period of 1 h before cooling at 4°C overnight. The product was then ground and sieved as described in Chapter 2 (Section 2.1).

7.2.2.3 *In Vitro* Metformin Release

In vitro release was carried out as described in Chapter 2 (Section 2.11).

7.2.2.4 High Performance Liquid Chromatography (HPLC) Analysis

Quantification of metformin HCl in rat serum samples was carried out using a high-performance liquid chromatography (HPLC) following the method modified from Wanjari et al 2008 [31] and using an Agilent HPLC 1090 HPLC system. Mobile phase was prepared by mixing 0.15 M ammonium dihydrogen phosphate (99.9% extra pure, Acros) (adjusted to pH3.0 using phosphoric acid (acid for analysis 85+% solution in water, Acros)) and 5% acetonitrile. The elution was carried out on a C18 column (250 x 4.6 mm (ACE-121-2546)) and the flow rate was maintained throughout the study at 0.5 ml/min. The presence of drug was detected using UV/Vis at 236 nm. Concentration was determined using a calibration curve.

7.2.2.5 Pharmacokinetic Analysis of Metformin in a Rat Model

All animal experimentation was carried out in compliance with current UK legislation on animal experimentation (Animals (Scientific Procedures) Act 1986) and within the requirements of Commission Directive 86/609/EEC concerning the protection of animals used for experimental and other scientific purposes Male Sprague Dawley rats (Charles River) of average weight 300 g were divided into 5 groups of 6 rats. The rats were administered a 100 mg/kg dose of metformin *via* different formulations. The different groups were as follows: i) buoyant particles ii) buoyant/mucoadhesive particles, iii) non-buoyant particles iv) oral solution of metformin v) intravenous (I.V.) solution of metformin.

The particulate formulations were administered by oral gavage suspended in 2 ml of 0.5% sodium alginate with the gavage tube washed through with a

further 1ml of sodium alginate solution. Blood samples were taken from the tail vein at 0.5, 1, 2, 4, 6, and 8 h following dosing. Blood samples were centrifuged to remove serum; serum samples were analysed using Pharmacokinetic analysis and performed on the metformin concentration versus time profile using WinNonlin (Pharsight, U.S.).

7.2.2.6 Deproteinisation of Rat Serum Samples for HPLC Analysis

In order to prepare the rat serum for HPLC analysis 200µl acetonitrile was added to 100µl serum and this was vortex-mixed for 30 seconds. The mixture was then left to stand for 10 minutes before being centrifuged at 10000 rpm for 10 mins. The upper layer was transferred to a separate tube and 20 µl used for HPLC analysis.

7.3 Results

7.3.1 Encapsulation and *In Vitro* Release of Metformin Hydrochloride

The initial loading of drug into formulation was increased from 5%, as used in Chapters 4 and 5 to 10% w/w. This was deemed necessary to provide an adequate dose of metformin in the amount of the formulation that can be administered to a small animal (rat). In order to assess possible effects of this increased loading on the drug release behaviour, *in vitro*, analysis of drug release as carried out and compared for 5% and 10% loading formulations (Figure 7.2). No significant difference was revealed for these two formulations.

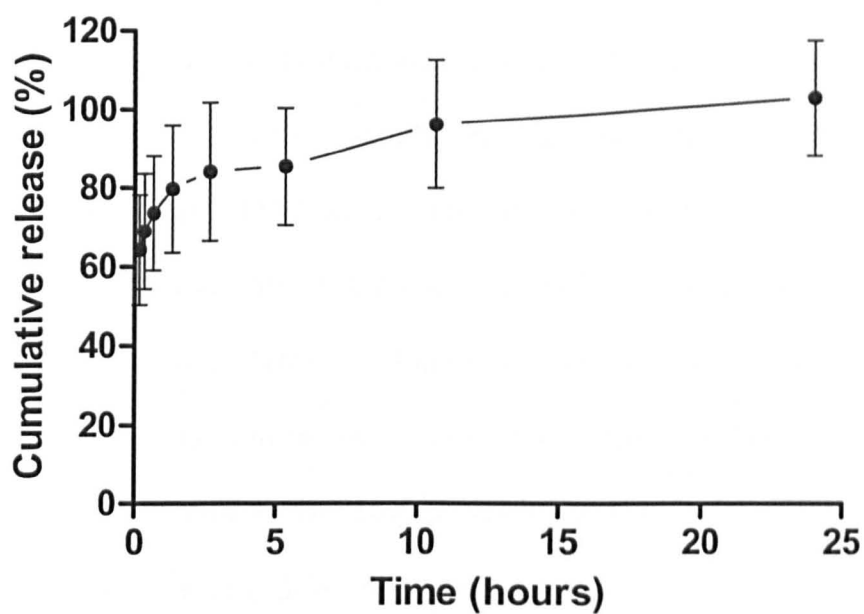


Figure 7.2 In vitro release profile of metformin hydrochloride from 250-500 μm size particles fraction for formulations with an initial drug loading of 5%. ($n=3\pm\text{SEM}$)

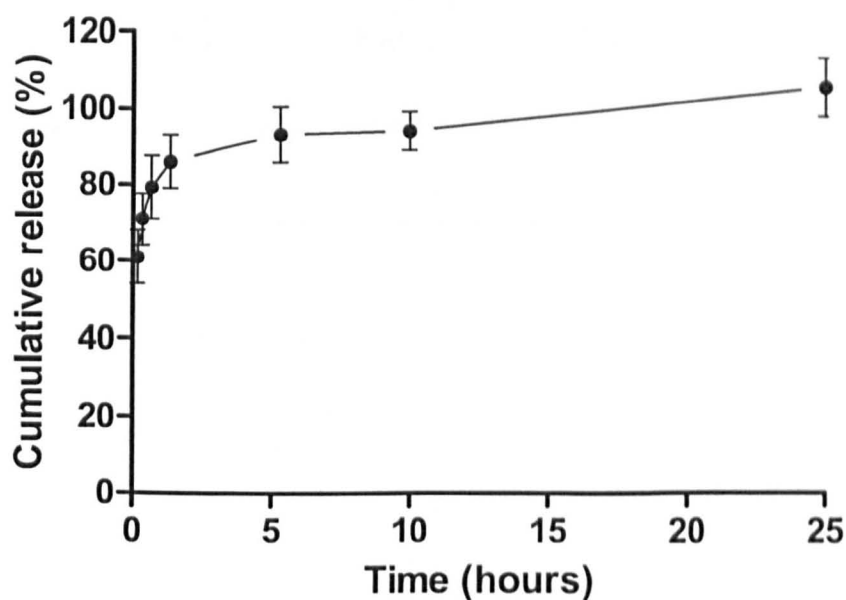


Figure 7.3 In vitro release profile of metformin hydrochloride from 250-500 μm sized particles following an initial drug loading of 10%. ($n=3\pm\text{SEM}$)

It should be noted however that the release profiles obtained for metformin (Figures 7.2 and 7.3) are dramatically different to the release profiles for he ribioflavin and furosemide formulations in previous chapters (Chapter 4 Figure 4.4). A high burst of 60% dose is revealed for both drug loadings. The release data were analysed applying the release models (as described in Chapter 5), and summarized in Table 7.1. Linearity values for metformin release appear poor in comparison to the previous results (Chapter 5 Table 5.1) for release data from this system. The Higuchi model revealed a linearity of $r^2=0.8089$ (Figure 7.4) indicating diffusion driven release.

Table 7.1 *The regression parameters obtained for release data for metformin loaded particles (10%w/w) for the different kinetic models.*

Zero-order		First-order		Higuchi		Korsemeyer-Peppas	
r^2	$K_0(\text{h}^{-1})$	r^2	$K_1(\text{h}^{-1})$	r^2	$K_H(\text{h}^{-1/2})$	r^2	n
0.6465	1.324	0.609	0.071	0.809	7.966	0.4930	0.0335

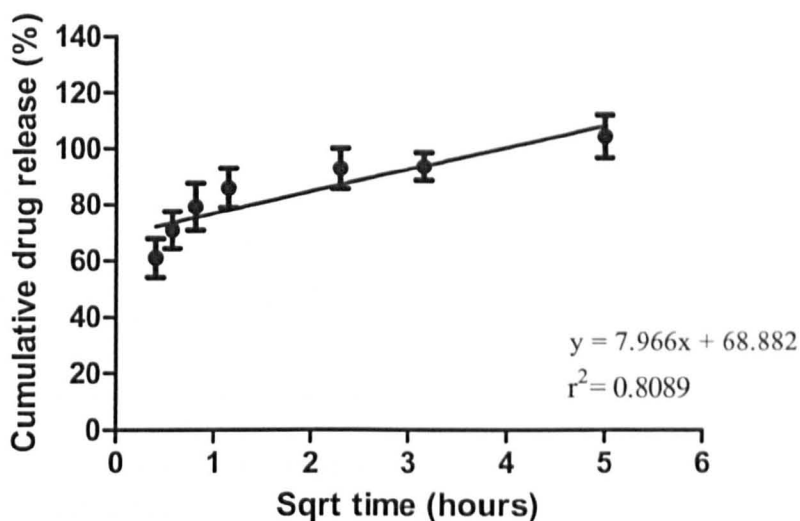


Figure 7.4 Release data applied to the Higuchi kinetic model for 10% metformin.

7.3.2 Development of HPLC Method for Quantitative Analysis of Metformin Hydrochloride in Rat Serum

Quantification of metformin in rat serum was carried out using an adapted reverse phase HPLC method [31]. Prior to analysis the HPLC method was qualified according to linearity, and system precision. All serum samples were deproteinized before analysis (Section 7.2.2.6) and recovery quantitated.

Initially two calibration curves were established using serial dilution of metformin in either mobile phase (ammonium dihydrogen phosphate (pH3.0)) or rat serum (Figure 7.5). The relationship between peak area and concentration was linear ($r^2=0.9964$ for metformin in rat serum (Figure 7.5)). Calibration curves demonstrate that the extraction step results in a loss of approximately 50% of the drug from the serum. It is possible to account for this loss when carrying out the analysis.

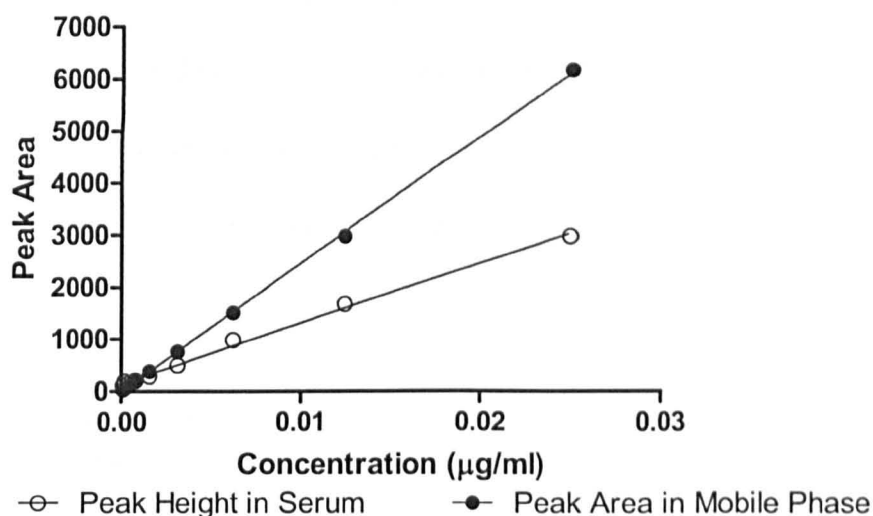


Figure 7.5 Linearity of peak area in the given concentration range for metformin in rat serum and mobile phase ($n=6 \pm SEM$)

The relative standard deviation (RSD) for peak area allows system precision to be assessed. As a biological sample the RSD values presented (Table 7.2) are considered to be low. These values provide evidence to support the precision of the method, indicating low variability in quantification.

Table 7.2 Relative Standard Deviation (RSD) values given for peak area over a large concentration range of metformin in rat serum.

Concentration (mg/ml)	Av area	SD	RSD (%)
0.1000	3924.1700	38.2048	0.9736
0.0500	1952.5290	40.3238	2.0652
0.0250	1012.9910	28.8954	2.8525
0.0125	513.3302	6.1994	1.2077
0.0063	297.5582	5.8372	1.9617
0.0031	158.7190	5.1903	3.2701
0.0016	90.4060	5.9769	6.6112
0.0008	47.6659	1.2183	2.5560
0.0004	27.7138	3.7455	13.5149

Typical chromatograms obtained for metformin in mobile phase, and rat serum are presented (Figure 7.6) alongside blank serum and a 'spiked' serum of 0.05 $\mu\text{g/ml}$. Chromatograms indicate a distinct peak corresponding to the elution of metformin at a retention time of 5.8 minutes demonstrating good resolution.

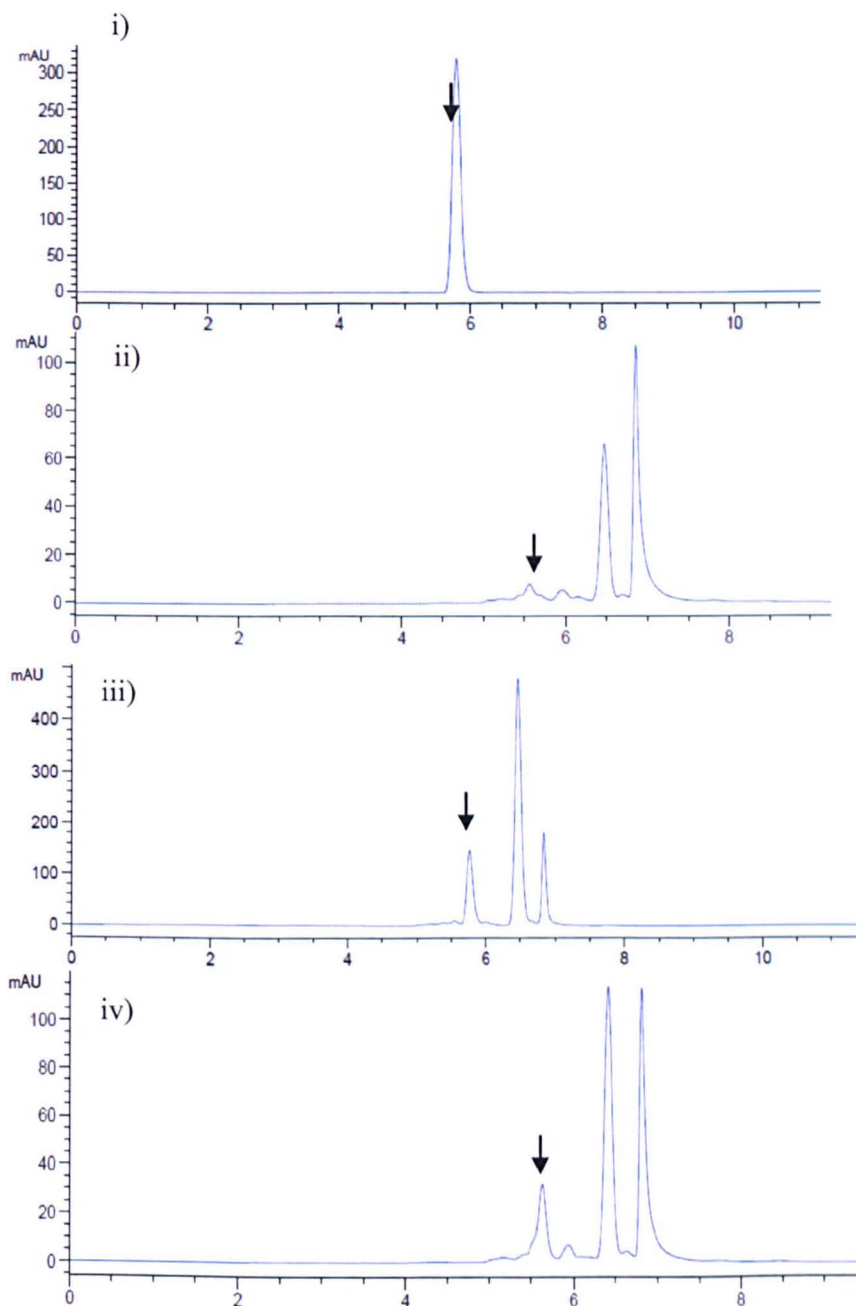


Figure 7.6 Typical chromatograms showing the resolution of the metformin peak (demonstrated by the pointer) in i) mobile phase (0.05 $\mu\text{g/ml}$) ii) blank serum iii) Spiked serum sample (0.05 $\mu\text{g/ml}$) and iv) Typical chromatogram for a group 4 animal at 60mins.

7.3.3 Analysis and Quantification of Metformin Hydrochloride in Rat Serum Following Oral Application of Different Formulations

The mean plasma concentration-time profiles of metformin following oral administration of the different formulations are presented (Figure 7.7) along with the corresponding pharmacokinetic parameters shown in Table 7.2.

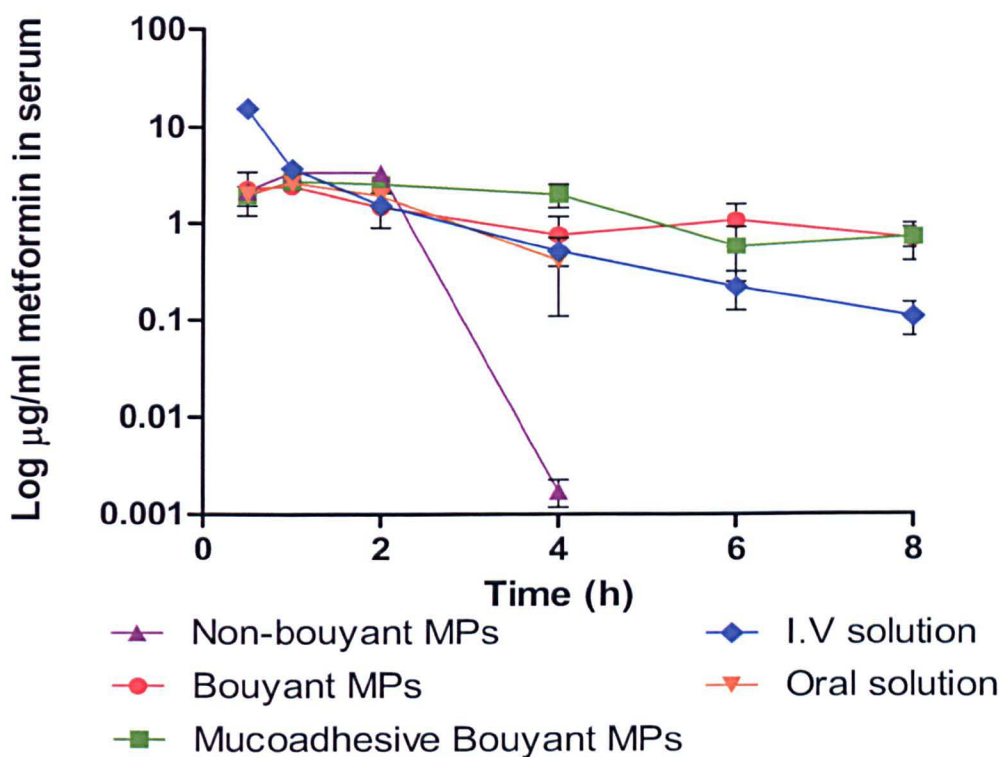


Figure 7.7 Log plasma concentration profile for metformin following oral administration of a 100 mg/kg dose from the different formulations. I.V data is also provided for absolute bioavailability calculations ($n=6\pm SEM$).

Table 7.3 Pharmacokinetic parameters of metformin following oral administration of the various metformin loaded formulations.

Parameter	Group 1		Group 2		Group 3		Group 4		Group 5	
Group	Buoyant particle		Buoyant - mucoadhesive particles		Control particles		Oral solution		I.V solution	
	Mean	SD	Mean	SD	Mean	SD	Mean	SD	Mean	SD
AUC₀₋₈ ($\mu\text{g/ml hr}$)	8.50	6.17	12.25	3.41	8.13	1.03	6.20	0.58	10.03	1.48
C_{max} ($\mu\text{g/ml}$)	3.30	2.15	3.03	0.91	3.37	0.43	2.69	0.40	15.57	1.81
T_{max} (hr)	1.67	2.14	2.00	1.10	1.00	0.00	1.00	0.00	1.00	0.00
t_{1/2} (hr)	3.24	4.05	4.32	3.99	0.34	0.01	1.17	0.54	0.58	0.21
FvsI.Oral (%)	137.02	99.54	197.53	55.04	131.09	16.63				
FvsIV (%)	84.68	61.51	122.07	34.01	81.01	10.28	61.80	5.78		

Note: AUC₀₋₈ = area under the metformin concentration-time curve from time 0 to 8 hours. F = absolute bioavailability. C_{max} = the maximum concentration of metformin achieved in the rat serum. T_{max} = the amount of time after metformin administration when the maximum plasma concentration is reached. t_{1/2} = this is the biological half life for metformin in rat serum.

Pharmacokinetic analysis demonstrates that the buoyant mucoadhesive particles formulation improves the bioavailability compared to the I.V. dose (Fvs.I.V 122.07%) and increases the T_{max} to 2.00 h. AUC is similar for the buoyant and non-buoyant particles (8.50±6.17 $\mu\text{g/ml h}$, and 8.13±1.03 $\mu\text{g/ml hr}$, respectively) whereas the introduction of the mucoadhesive chitosan increases AUC of buoyant-mucoadhesive particles to 12.25±3.4 $\mu\text{g/ml hr}$. The half life for metformin from the non-buoyant particles (0.34±0.01 h) is improved following administration of both the buoyant particles (3.24 h) and

more so for the buoyant-mucoadhesive particles (4.32 h). All particulate formulations improve bioavailability compared to the oral bolus (*FvsOral*).

7.4 Discussion

This chapter reports a pharmacokinetic investigation in the rat model of the buoyant mucoadhesive PLGA particles developed in this thesis. As a suitable candidate drug, metformin was encapsulated in the PLGA particles and release was initially assessed *in vitro*. An increase in burst release with metformin (to 60%) is revealed (Figure 7.2 and 7.3 in comparison to the release profiles for riboflavin and furosemide (Figure 4.5). This may be a consequence of the high water solubility of metformin (>300 mg/ml at 25°C [12, 32] compared to riboflavin's solubility of 0.01 mg/ml or furosemide's solubility of 0.006 mg/ml). It has been suggested that water solubility, along with the partition coefficient of drugs can influence the release, with high solubility generally leading to rapid release in aqueous media [33].

In vitro analysis provides evidence suggesting the buoyant-mucoadhesive system may demonstrate gastroretentive behaviour suitable for the improvement of the oral bioavailability of drugs including good buoyancy (Figure 3.10), and mucoadhesion (Figure 6.14). It is generally recognized that it is difficult to correlate *in vitro* with *in vivo* performance of oral delivery systems [34]. *In vitro / in vivo* correlation has been described in USP as 'the establishment of a relationship between a biological property or a parameter derived from a biological property produced by a dosage form, and a physicochemical characteristic of the same dosage form' [35]. In this study the buoyant particles, mucoadhesive buoyant particles, and non-buoyant particles were all loaded with 10% metformin hydrochloride and administered at the

same dose of 100 mg/kg. A 100 mg/kg dose was also administered by I.V. and an oral solution to allow calculation of pharmacokinetic parameters.

Pharmacokinetic analysis demonstrates that despite the poor sustained release of metformin from the system the mucoadhesive buoyant particles maintain increased drug plasma levels of the drug over a prolonged period of time in comparison to the oral solution/bolus dose. However the buoyant particles without mucoadhesive properties demonstrate similar pharmacokinetics to the oral solution/bolus dose. It should be noted that the *in vivo* evaluation of designed formulations was conducted in rats, the largest particles size which could be administered through the gavage tube effectively was the >250 μm size fraction. This fraction showed a reasonably good buoyancy in *in vitro* characterisation but larger particle sizes showed improved buoyancy potential and employing larger, more porous particles may have further enhanced bioavailability for the buoyant particles through better floating ability.

The AUC value (Table 7.3) shows the amount of metformin ($\mu\text{g}/\text{ml}$) that reached systemic circulation over the 8 h time course of the study. The similar AUC values were obtained for buoyant particles and non-buoyant particles (8.50 ± 6.17 and 8.13 ± 1.03 respectively) with an increase to a value of 12.25 $\mu\text{g}/\text{ml}\cdot\text{hr}$ upon the introduction of mucoadhesive properties. This indicates that a combination of buoyancy and mucoadhesion may enhance drug delivery in comparison to buoyancy alone. The combination of both properties has been previously evaluated *in vitro* [36-38] but how this translates *in vivo* is less widely studied.

All formulations administered *via* the oral route demonstrated similar plasma concentration values at 30 mins with T_{max} for buoyant particles, control particles and oral solution dose at 1.67, 1.00, and 1.00 h respectively. C_{max} occurs slightly later at 2.00 h following the introduction of the mucoadhesive polymer and plasma metformin concentrations are sustained for longer exhibiting a broader peak. This peak shape is comparable to the plasma concentration profile upon delivery of extended release gastric retentive tablets to healthy humans [39]. Broad, low peaks indicate sustained exposure to the drug at the absorption window with such peaks demonstrating improvements in bioavailability by 115%.

This improvement upon the introduction of the mucoadhesive property is consistent with metformin demonstrating a narrow absorption window in the upper small intestine and suggests the potential suitability of the system for once a day dosing of metformin. The application of a once-daily extended release system for metformin has demonstrated to be as effective as twice-daily immediate release dosing [23].

Orally administered metformin is subjected to high elimination values as a result of gastrointestinal first pass effects (53.8%) and demonstrated a low F value of 29.9% [40]. In the present study, the F value (vs. I.V) for oral solution administration is $61.80\% \pm 5.78$ which is improved upon encapsulation of the drug within a polymeric matrix to an average of 81.01%, 84.68%, and 122.07% for the non-buoyant, buoyant, and buoyant-mucoadhesive particles respectively. This suggests that the practice of simply encapsulating the drug may improve bioavailability. This is in contrast to previous work where a deterioration in bioavailability for two sustained release tablets compared to a

rapidly dissolving tablet and oral solution was reported [41]. This may be the case as these systems exhibit controlled release behaviour without gastroretention and the decrease in bioavailability arises from the fast gastric transit time carrying the system past the absorption window before the controlled release system has had a chance to release a significant amount of drug.

A relatively high standard deviation values obtained for pharmacokinetic parameters following administration of gastroretentive delivery system may be explained by inter-subject gastrointestinal variation. The plasma concentration profile clearly demonstrates more pronounced error bars for those formulations administered *via* the oral route in comparison with the I.V. administration. This has been reported previously [39].

The pKa of metformin is relatively high (11.5) [42], therefore in the gastrointestinal tract it is present in its ionized form. It has been reported that the positive charge of metformin results in its high affinity with the negative intestinal wall [28] this may slow down drug absorption rate and explain the similarities in pharmacokinetics between oral solution and buoyant particles.

Pharmacokinetic studies in this project used the rat as a model, although being aware that this may not be considered as suitable animal for *in vivo* testing of solid oral dosage forms due to their small size [43] and presenting difficulties in administration of devices developed for therapy in man. Prior testing in a larger animal model will be required before studies in man.

7.5 Conclusion

This chapter provides pharmacokinetic evidence to suggest that the combination of mucoadhesive and buoyant functionalities may bestow properties on the delivery system which enable an improvement in its pharmacokinetics. AUC values are improved from 6.20 $\mu\text{g/ml}$ with oral solution, and 10.03 $\mu\text{g/ml}$ for the I.V solution to 12.25 $\mu\text{g/ml}$ for the mucoadhesive buoyant particles. This demonstrates an increase in $F_{vsI.V}$ of 122.07% and in F_{vsOral} of 197.53%. There is an improvement in F_{vsOral} with all particulate formulations regardless of gastroretentive properties. This may be a result of the reduced rate of release from these formulations. An improvement in F_{vsIV} for buoyant mucoadhesive particles (122%) confirms the success of the PGSS method in the fabrication of particles suitable for enhanced delivery of metformin. The data suggests the application of the system for once-daily delivery of metformin. The system lends itself to study with other candidate drugs demonstrating a narrow absorption window in the upper small intestine.

7.6 References

1. Gottlieb, B. and W.H. Auld, *Metformin in treatment of diabetes mellitus*. British medical journal, 1962. **1**(5279): p. 680-2.
2. Emslie-Smith, A.M., et al., *Contraindications to metformin therapy in patients with Type 2 diabetes - a population-based study of adherence to prescribing guidelines*. Diabetic Medicine, 2001. **18**(6): p. 483-488.
3. Zhou, G.C., et al., *Role of AMP-activated protein kinase in mechanism of metformin action*. Journal of Clinical Investigation, 2001. **108**(8): p. 1167-1174.
4. Jackson, R.A., et al., *Mechanism of metformin action in non-insulin dependant diabetes*. Diabetes, 1987. **36**(5): p. 632-640.
5. Holmboe, E.S., *Oral anti hyperglycemic therapy for type 2 diabetes - Clinical applications*. Jama-Journal of the American Medical Association, 2002. **287**(3): p. 373-376.
6. Graham, G.G., et al., *Clinical Pharmacokinetics of Metformin*. Clinical Pharmacokinetics, 2011. **50**(2): p. 81-98.
7. Bhavesh, D., et al., *Estimation and pharmacokinetics of metformin in human volunteers*. Indian Journal of Pharmaceutical Education and Research, 2007. **41**(2): p. 135-139.
8. Pentikainen, P.J., P.J. Neuvonen, and A. Penttila, *Pharmacokinetics of metformin after intravenous and oral-administration to man*. European Journal of Clinical Pharmacology, 1979. **16**(3): p. 195-202.
9. Cubeddu, L.X., et al., *Effects of metformin on intestinal 5-hydroxytryptamine (5-HT) release and on 5-HT₃ receptors*. Naunyn-Schmiedebergs Archives of Pharmacology, 2000. **361**(1): p. 85-91.
10. Shimizu, T., et al., *Medical management of hyperglycemia in type 2 diabetes: a consensus algorithm for the initiation and adjustment of therapy: a consensus statement of the American Diabetes Association and the European Association for the Study of Diabetes*. Nihon rinsho. Japanese journal of clinical medicine, 2012. **70 Suppl 3**: p. 591-601.
11. Hoffmann, I.S., et al., *Ondansetron and metformin-induced gastrointestinal side effects*. American journal of therapeutics, 2003. **10**(6): p. 447-51.
12. Hu, L.-D., et al., *Preparation and in vitro/in vivo evaluation of sustained-release metformin hydrochloride pellets*. European Journal of Pharmaceutics and Biopharmaceutics, 2006. **64**(2): p. 185-192.
13. Ige, P.P. and S.G. Gattani, *Design and In Vitro and In Vivo Characterization of Mucoadhesive Matrix Pellets of Metformin Hydrochloride for Oral Controlled Release: A Technical Note*. Archives of Pharmacal Research, 2012. **35**(3): p. 487-498.
14. Basak, S.C., J. Rahman, and M. Ramalingam, *Design and in vitro testing of a floatable gastroretentive tablet of metformin hydrochloride*. Pharmazie, 2007. **62**(2): p. 145-148.
15. Okunlola, A., R.P. Patel, and O.A. Odcku, *Evaluation of freeze-dried pregelatinized Chinese yam (Dioscorea oppositifolia) starch as a polymer in floating gastroretentive metformin microbeads*. Journal of Drug Delivery Science and Technology, 2010. **20**(6): p. 457-465.

16. Dave, B., et al., *Fabrication of gastroretentive metformin hydrochloride tablets: application of optimised viscosity approach*. Journal of Pharmacy and Pharmacology, 2004. 56: p. S52-S53.
17. Boldhane, S.P. and B.S. Kuchekar, *Gastroretentive Drug Delivery of Metformin Hydrochloride: Formulation and In Vitro Evaluation Using 3(2) Full Factorial Design*. Current Drug Delivery, 2009. 6(5): p. 477-485.
18. Yadav, A. and D.K. Jain, *Gastroretentive microballoons of metformin: Formulation development and characterization*. Journal of advanced pharmaceutical technology & research, 2011. 2(1): p. 51-5.
19. Yadav, A. and D.K. Jain, *In-vitro characterization of gastroretentive microballoons prepared by the emulsion solvent diffusion method*. Journal of advanced pharmaceutical technology & research, 2010. 1(1): p. 56-67.
20. Ali, J., et al., *Formulation and development of hydrodynamically balanced system for metformin: In vitro and in vivo evaluation*. European Journal of Pharmaceutics and Biopharmaceutics, 2007. 67(1): p. 196-201.
21. Jain, S.K. and A. Gupta, *Development of Gelucire 43/01 Beads of Metformin Hydrochloride for Floating Delivery*. Aaps Pharmscitech, 2009. 10(4): p. 1128-1136.
22. Murphy, C., et al., *Optimization of a Dual Mechanism Gastrofloatable and Gastroadhesive Delivery System for Narrow Absorption Window Drugs*. Aaps Pharmscitech, 2011. 13(1): p. 1-15.
23. Schwartz, S., et al., *Efficacy, tolerability, and safety of a novel once-daily extended-release metformin in patients with type 2 diabetes*. Diabetes Care, 2006. 29(4): p. 759-764.
24. Lehr, C.M., et al., *An estimate of turnover time of intestinal mucus gel layer in the rat in situ loop*. International Journal of Pharmaceutics, 1991. 70(3): p. 235-240.
25. Lai, S.K., Y.-Y. Wang, and J. Hanes, *Mucus-penetrating nanoparticles for drug and gene delivery to mucosal tissues*. Advanced Drug Delivery Reviews, 2009. 61(2): p. 158-171.
26. Kararli, T.T., *Comparison of the gastrointestinal anatomy, physiology, and biochemistry of humans and commonly used laboratory-animals*. Biopharmaceutics & Drug Disposition, 1995. 16(5): p. 351-380.
27. Dressman, J.B., *Comparison of canine and human gastrointestinal physiology*. Pharmaceutical Research, 1986. 3(3): p. 123-131.
28. Stepensky, D., et al., *Preclinical evaluation of pharmacokinetic-pharmacodynamic rationale for oral CR metformin formulation*. Journal of Controlled Release, 2001. 71(1): p. 107-115.
29. Nayak, A., S.K. Jain, and R.S. Pandey, *Controlling Release of Metformin HCl through Incorporation into Stomach Specific Floating Alginate Beads*. Molecular Pharmaceutics, 2011. 8(6): p. 2273-2281.
30. Adikwu, M.U., Y. Yoshikawa, and K. Takada, *Pharmacodynamic-pharmacokinetic profiles of metformin hydrochloride from a mucoadhesive formulation of a polysaccharide with antidiabetic property in streptozotocin-induced diabetic rat models*. Biomaterials, 2004. 25(15): p. 3041-3048.

31. Wanjari, M.M., et al., *Rapid and Simple RPHPLC Method for the Estimation of Metformin in Rat Plasma*. Indian Journal of Pharmaceutical Sciences, 2008. **70**(2): p. 198-202.
32. Nanjwade, B.K., S.R. Mhase, and F.V. Manvi, *Formulation of Extended-Release Metformin Hydrochloride Matrix Tablets*. Tropical Journal of Pharmaceutical Research, 2011. **10**(4): p. 375-383.
33. Huang, X. and C.S. Brazel, *On the importance and mechanisms of burst release in matrix-controlled drug delivery systems*. Journal of Controlled Release, 2001. **73**(2-3): p. 121-136.
34. Desai, S. and S. Bolton, *A floating controlled-release drug-delivery system - In vitro-In vivo evaluation*. Pharmaceutical Research, 1993. **10**(9): p. 1321-1325.
35. Cardot, J.M. and E. Beyssac, *In vitro In vivo correlations- Scientific implications and standardization*. European Journal of Drug Metabolism and Pharmacokinetics, 1993. **18**(1): p. 113-120.
36. Gattani, S.G., P.J. Savaliya, and V.S. Belgamwar, *Floating-Mucoadhesive Beads of Clarithromycin for the Treatment of Helicobacter pylori Infection*. Chemical & Pharmaceutical Bulletin, 2010. **58**(6): p. 782-787.
37. Sahasathian, T., N. Praphairaksit, and N. Muangsin, *Mucoadhesive and Floating Chitosan-coated Alginate Beads for the Controlled Gastric Release of Amoxicillin*. Archives of Pharmacal Research, 2010. **33**(6): p. 889-899.
38. Umamaheshwari, R.B., S. Jain, and N.K. Jain, *A new approach in gastroretentive drug delivery system using cholestyramine*. Drug Delivery, 2003. **10**(3): p. 151-160.
39. Gusler, G., et al., *Pharmacokinetics of metformin gastric-retentive tablets in healthy volunteers*. Journal of Clinical Pharmacology, 2001. **41**(6): p. 655-661.
40. Choi, Y.H., S.G. Kim, and M.G. Lee, *Dose-independent pharmacokinetics of metformin in rats: Hepatic and gastrointestinal first-pass effects*. Journal of Pharmaceutical Sciences, 2006. **95**(11): p. 2543-2552.
41. Pentikainen, P.J., *Bioavailability of metformin - Comparison of solution, rapidly dissolving tablet, and 3 sustained-release products*. International Journal of Clinical Pharmacology and Therapeutics, 1986. **24**(4): p. 213-220.
42. Cheng, C.L., et al., *Biowaiver extension potential to BCS Class III high solubility-low permeability drugs: bridging evidence for metformin immediate-release tablet*. European Journal of Pharmaceutical Sciences, 2004. **22**(4): p. 297-304.
43. Saphier, S., et al., *Gastro intestinal tracking and gastric emptying of solid dosage forms in rats using X-ray imaging*. International Journal of Pharmaceutics, 2010. **388**(1-2): p. 190-195.
44. Fujioka, K., et al., *Efficacy, dose-response relationship and safety of once-daily extended-release metformin (Glucophage (R) XR) in type 2 diabetic patients with inadequate glycaemic control despite prior treatment with diet and exercise: results from two double-blind, placebo-controlled studies*. Diabetes Obesity & Metabolism, 2005. **7**(1): p. 28-39.

45. Jabbour, S. and B. Ziring, *Advantages of Extended-Release Metformin in Patients with Type 2 Diabetes Mellitus*. *Postgraduate Medicine*, 2011. **123**(1): p. 15-23.

Chapter 8

Summary and Future Directions

8.1 Overall summary

Oral drug delivery is an area of research widely investigated as a result of the good patient compliance and convenience demonstrated by this drug administration route. It is the most common and usually the preferred route of administration; however, there are various obstacles to oral drug delivery. These include the low pH levels in the stomach, rapid gastric transit times, the first-pass effect of the liver, and finally it is estimated that around one third of the population experience difficulties swallowing pills. The drugs themselves also present issues when delivered *via* the oral route as many drugs demonstrate narrow absorption windows in the upper small intestine. These drugs (which include metformin, furosemide, riboflavin, atenolol and many others) will only reach the systemic circulation if they are released from the delivery system before it passes this narrow absorption window [1].

In light of these disadvantages, various strategies have been investigated to improve oral drug delivery. The gastroretentive systems present an approach which aims to retain the delivery system in the stomach and therefore proximal to its absorption window, typically in the upper small intestine, for a prolonged period of time. There have been various attempts to achieve gastroretention

including expanding, floating, mucoadhesive, or high density systems [2, 3]. Among these technologies the floating formulations have demonstrated much promise with examples existing on the market.

The aim of this thesis was to develop a multi-unit drug delivery system demonstrating (i) density lower than the gastric fluid to enable its buoyancy, with no lag-time, and (ii) sustain drug release for the duration of the system's gastroretention. The project explored the potential of combining buoyancy with mucoadhesion in an effort to augment the gastroretentive potential. Furthermore, the application of the novel 'green' technology which produces inherently porous materials was investigated.

The production of multi-unit drug delivery systems is traditionally carried out using emulsion techniques which introduce major issues concerning the use of volatile organic solvents. A recent emergence in the field of polymer processing is the supercritical fluid technologies. In scCO_2 offers an organic solvent-free route to the production of polymeric particles at relatively low temperatures. The particles from gas saturated solutions (PGSS) method was employed in this thesis in the production of polymeric particles. This particular method exploits the ability of scCO_2 to decrease the glass transition temperature of polymers enabling drug particles to be mixed into the liquefied polymer. The presence of scCO_2 in the mixture allowed for the production of an intricate porous network as on depressurisation, this CO_2 return to the gaseous state and will diffuse out of the rapidly solidifying polymeric matrix.

The initial challenge faced in this project was the development of a suitable formulation which demonstrates a high yield and a product which

demonstrates a low density. PLGA material has been previously used in the PGSS method [4] and was therefore initially selected for processing into particles. However, the poor yield obtained with PLGA resulted in the introduction of processing aids in order to improve the processability of the liquefied mixture, improving yield and particle morphology. The incorporation of myristic acid at a relatively high content somewhat improved product yield with the density of the PLGA and myristic acid formulation was above that of the gastric contents. An *in vitro* buoyancy test was carried out verifying that the PLGA / myristic acid formulations did not reveal adequate buoyancy in a simulated gastric fluid. Various formulations were explored in an attempt to reduce the density of the product. Of the various formulations investigated a combination of PLGA (approximate molecular weight 12 KDa), PLGA (approximate molecular weight 25 KDa), and SPANTM80 in the ratio 75:20:5, respectively produced particles which demonstrated the most appropriate density (Table 3.1).

Following PGSS processing, the formulation was ground and sieved to produce discrete size fractions and allow a comparison of the density and porosity of the different size particles to be carried out. microCT porosity analysis of the different size fractions demonstrated an increase in porosity with increasing particle size from 0% with particles size < 100 μm up to over 50% for particles > 800 μm . The different size fractions were also analysed for density using helium air pycnometry with the larger and more porous particles demonstrating lower densities. The smaller size fraction (< 100 μm) demonstrated density values above reported values for gastric media with particles >250 μm demonstrating densities lower than 1.003 gcm^{-3} . Chapter 3

reported on the production of a system offering the appropriate low density to allow buoyancy in a simulated gastric fluid.

The model drugs riboflavin and furosemide were introduced into the formulation at theoretical loadings of 5%. Encapsulation efficiency was measured to be in excess of 80% for both drugs at all size fractions, with ToF-SIMS surface analysis illustrating a uniform distribution of drug across the surface of the samples with depth profiling providing data to suggest that the intensity of the drug remains constant throughout the matrix.

In vitro drug release was carried out at both pH 7.4 and in a simulated gastric fluid at pH 1.2. A size dependant release rate at pH 7.4 was revealed with larger particles demonstrating the fastest release of both drugs. In the simulated gastric fluid (pH 1.2) release was decreased from almost 80% (furosemide release from particles > 1000 μm) to under 20% for the same formulation at pH 1.2. Morphological analysis comparing particles before and after the release study confirmed that there is an increase in surface porosity creating sponge like structures for particles exposed to PBS (pH 7.4), contrasting with the smooth, less porous morphologies which are exposed following release in SGF (pH 1.2). The different morphologies offered an explanation for the different release rates in the two different media.

The hydrophilic polymer, PEG, was introduced to the formulation (10% w/w) in an attempt to increase the release over the 24 hours. The introduction of PEG (≥ 3 KDa) increases the rate of release in the PBS pH 7.4 medium. This was not the case in SGF, where the presence of PEG actually resulted in a decrease in drug release rate for system encapsulating riboflavin. MicroCT

porosity measurements showed a marked increase in porosity following exposure to PBS for particles containing PEG ≥ 3 KDa which may contribute to the increase in release for these formulations. The data demonstrated that modulation of the release rate from PLGA particles may occur through the introduction of hydrophilic excipients.

The gastroretentive behaviour of the buoyant particles was augmented through the introduction of the mucoadhesive polymer chitosan and its thiolated derivative chitosan-NAC. Previous work in the field has demonstrated that the introduction of a mucoadhesive polymer to a floating drug delivery system enables prolonged gastric residence times and may enhance performance of the drug delivery system [5, 6]. In the present study, particles were either coated with chitosan and its derivative following PGSS processing or the polymers were incorporated into the formulation and processed. ToF-SIMS surface analysis suggested both methods were successful in introducing the mucoadhesive, as judged from the increased intensity of the chitosan originated ionic species at the surface of the particles.

The mucoadhesive ability of the formulations was assessed using an *in vitro* mucin assay which confirmed that the NAC modified chitosan demonstrated the most effective adhesion to mucin; however this was not replicated when particles were introduced to a mucus producing cell line. In the cell study, chitosan incorporated particles demonstrated better adhesion following washing in comparison to the chitosan-NAC. As NAC is a well known mucolytic, the removal of these particles following washing may be a result of the mucus cleaving actions of NAC allowing the mucus to be washed away during the washing step.

Finally, this thesis assesses the success of the system in an *in vivo* model. The anti-diabetic drug metformin was loaded into the PLGA particles at an increased loading of 10% to achieve appropriate drug dose within the administered amount of the particles. A comparison of pharmacokinetic parameter for the buoyant particles, buoyant-mucoadhesive particles, and non-buoyant particles, with I.V. and orally applied drug solution illustrates that the combination of buoyancy and mucoadhesion improve bioavailability to 122.07% (AUC value of 12.25 $\mu\text{g/ml.hr}$) with the buoyant particles revealing a bioavailability of 84.68% (AUC value of 8.50 $\mu\text{g/ml.hr}$). The data obtained from the *in vivo* rat study suggests that the gastroretentive system developed in this thesis may hold promise in the improvement of oral drug delivery, in particular for drugs exhibiting narrow absorption windows in the upper small intestine.

8.2 Future Directions

Overcoming the obstacles presented by oral drug delivery, in particular for drugs exhibiting narrow absorption windows in the upper small intestine is currently an area which is being widely researched. Although these systems often demonstrate the appropriate characteristics in the *in vitro* setting they are not as yet widely available on the market. This thesis provides a foundation for the manufacture of a system which demonstrates prolonged gastric residence times and therefore improved pharmacokinetics over a conventional delivery system. However, it would be naive to suggest that good performance in the rat model is indicative of success in man and therefore further *in vivo* analysis

would be required in a larger animal model before eventual studies in man in order to confirm the success of the system.

Pharmacokinetic analysis does not enable conclusions to be drawn on the ability of the gastroretentive system to remain in the stomach for prolonged periods of time. In order to acquire this data the use of gamma scintigraphy [7] or MRI [8] studies could follow the transit of the delivery system through the GIT.

In this thesis it was shown that changes in the formulation may be used to modulate drug release characteristics, in this way, additional modifications could be explored to further improve release characteristics. Pharmacokinetic analysis illustrates improvements in bioavailability on the introduction of chitosan-NAC to the formulation. Various modified chitosans have been reported in the literature with different levels of mucoadhesion being achieved. In particular Chitosan-TBA has demonstrated 100 fold increase in mucoadhesion in comparison to an unmodified chitosan [9]. A comparison of mucoadhesive properties following incorporation of some alternative mucoadhesive polymers may increase gastroretention further.

8.3 References

1. Davis, S.S., *Formulation strategies for absorption windows*. Drug Discovery Today, 2005. **10**(4): p. 249-257.
2. Garg, R. and G.D. Gupta, *Progress in Controlled Gastroretentive Delivery Systems*. Tropical Journal of Pharmaceutical Research, 2008. **7**(3): p. 1055-1066.
3. Streubel, A., J. Siepmann, and R. Bodmeier, *Drug delivery to the upper small intestine window using gastroretentive technologies*. Current Opinion in Pharmacology, 2006. **6**(5): p. 501-508.
4. Jordan, F., et al., *Sustained release hGH microsphere formulation produced by a novel supercritical fluid technology: In vivo studies*. Journal of Controlled Release, 2010. **141**(2): p. 153-160.

-
5. Jimenez Castellanos, M.R., H. Zia, and C.T. Rhodes, *Design and testing in vitro of a bioadhesive and floating drug delivery system for oral application*. International Journal of Pharmaceutics (Amsterdam), 1994. **105**(1): p. 65-70.
 6. Zheng, J., et al., *Preparation and evaluation of floating-bioadhesive microparticles containing clarithromycin for the eradication of Helicobacter pylori*. Journal of Applied Polymer Science, 2006. **102**(3): p. 2226-2232.
 7. Pund, S., et al., *Gastroretentive delivery of rifampicin: In vitro mucoadhesion and in vivo gamma scintigraphy*. International Journal of Pharmaceutics, 2011. **411**(1-2): p. 106-112.
 8. Kremser, C., et al., *In vivo determination of the time and location of mucoadhesive drug delivery systems disintegration in the gastrointestinal tract*. Magnetic Resonance Imaging, 2008. **26**(5): p. 638-643.
 9. Roldo, M., et al., *Mucoadhesive thiolated chitosans as platforms for oral controlled drug delivery: synthesis and in vitro evaluation*. European Journal of Pharmaceutics and Biopharmaceutics, 2004. **57**(1): p. 115-121.